

A Floating Ball and Two Asymptotic Problems in Capillarity

by

Hanzhe Chen

A thesis
presented to the University of Waterloo
in fulfillment of the
thesis requirement for the degree of
Doctor of Philosophy
in
Applied Mathematics

Waterloo, Ontario, Canada, 2021

© Hanzhe Chen 2021

Examining Committee Membership

The following served on the Examining Committee for this thesis. The decision of the Examining Committee is by majority vote.

External Examiner: Thomas I. Vogel
Associate Professor Emeritus, Dept. of Mathematics,
Texas A&M University

Supervisor(s): David Siegel
Professor Emeritus, Dept. of Applied Mathematics,
University of Waterloo

Internal Member: Sander Rhebergen
Assistant Professor, Dept. of Applied Mathematics,
University of Waterloo

Marek Stastna
Professor, Dept. of Applied Mathematics,
University of Waterloo

Internal-External Member: Spiro Karigiannis
Associate Professor, Dept. of Pure Mathematics,
University of Waterloo

Author's Declaration

I hereby declare that I am the sole author of this thesis. This is a true copy of the thesis, including any required final revisions, as accepted by my examiners.

I understand that my thesis may be made electronically available to the public.

Abstract

The study of capillary phenomena can be traced back to the age of Aristotle. In this thesis, a floating ball and two asymptotic problems in capillarity are considered, all of which include surface tension and gravity.

The first problem, the ascent of fluid surface outside a narrow vertical circular tube has been studied for decades. Lo obtained a five-term asymptotic expansion of the fluid height near the boundary for the small Bond number using the method of matched asymptotic expansions. Miersemann gave a rigorous proof of a two-term asymptotic expansion but the error bound he obtained is inferior to Lo's. We reconsider this problem and our goal is to establish a rigorous approach to improve Miersemann's error bound. We construct two piecewise smooth approximate solutions. Each approximate solution consists of an inner solution and an outer solution. The first approximate solution with its inner solution having zero mean curvature is shown as an upper bound. The second approximate solution with its inner solution having constant mean curvature is shown as a lower bound. The approximations are optimized in terms of the transition radius q by use of Olver's theorem. This establishes the two-term asymptotic expansion. Its error bound is an improvement of Miersemann's but is inferior to Lo's. A modification of the outer solution helps improve our error bound. However, we did not achieve Lo's error bound.

Interest in floating objects goes back to antiquity. In recent research, many examples of multiple equilibrium configurations have been found with or without surface tension and gravity. We consider a ball floating on an unbounded reservoir. The floating configuration is assumed to be radially symmetric. By a result of Elcrat, Neel and Siegel, the fluid interface is determined by the attachment radius r_0 and inclination angle ψ_0 . Both of these are given in terms of the attachment angle ϕ_0 . However, the zero solution is not included in the parametric solution. So, the graph description of the fluid height is considered, as well. We develop C^1 smoothness of the attachment height u_0 with respect to ϕ_0 . This requires an extension of Vogel's description of solutions and monotonicity results. As a by-product, Vogel's conjecture on the smoothness of the envelope of exterior solutions is shown. In the study of the number of equilibria and their stability, both force and energy approaches are considered. We classify forces and energies and establish a relation between the total force and the total energy. This requires determining the asymptotic expansion of the interface as the inclination angle tends to zero, which is achieved through the use of Levinson's theorem. A critical point of the total energy can be either a force balanced point or a critical point of the height of the center. Both the total force and the center

height contain u_0 , which has to be found numerically by the shooting method. In order to understand the behavior of the total force and the height curves, both asymptotic analysis and numerical tests are employed. We investigate the limiting behavior of the total force and the height curves for small and large Bond number or when the attachment angle tends to its end points. We perform thousands of numerical tests with different values of Bond numbers and contact angles. Combined with the numerical observations and the results from the asymptotic analysis, we conjecture that there are at most two force balanced points. If there is only one force balanced point, it must be stable. If there are two force balanced points, the one with smaller attachment angle must be stable and the other one with larger attachment angle can be either stable or unstable. For a given contact angle, the information on the number of equilibria and their stability for the floating ball system are illustrated in Bond number versus density ratio figures. We give several such figures with typical contact angles. Finally, two examples are presented. One admits two stable equilibrium configurations. Another example shows a case with no force balanced point where there is an energy minimizer. This prompts discussion of the necessary condition for the floating configuration and a modification of changing topological structure for the floating configurations in this example.

For the second asymptotic problem, an unbounded capillary surface in a vertical wedge domain near the corner is considered. We are interested in whether the unboundedness holds if the wedge is tilted by an angle from the vertical axis. Euler's angles are used to describe the tilted coordinate system. A tilted capillary equation is obtained using the invariance of mean curvature under rotation. We apply Miersemann's idea to construct both a sub-solution and a super-solution near the corner. With the comparison principle, unboundedness of the titled capillary surface is shown and its the bound estimate is analyzed, as well.

Acknowledgements

First, I would like to express my deepest gratitude to my supervisor Professor David Siegel. Thank you for your support, guidance, opportunities and encouragement during my master's and doctoral study in mathematics.

I would like to thank my PhD thesis defence committee members, Thomas I. Vogel, Spiro Karigiannis, Marek Stastna, Sander Rhebergen and David Siegel for your suggestions and time.

Furthermore, I would like to thank Sander Rhebergen and his students Abdullah Ali Sivas, Giselle Sosa Jones, Keegan Kirk and Greg Wang. They help me discover many interesting problems in numerical analysis. I would like to thank my office mates Kamran Akbari, Lindsey Daniels and Keenan Lyon for creating the harmonious working environment. I would like to thank my department colleagues Yangang Chen and Yinan Li for many enlightened discussions.

Finally, I would like to thank my family for the continued support and unconditional love. In particular, my girlfriend Baobao Zhang, will you marry me?

Dedication

To my parents and my grandma.

Table of Contents

List of Figures	xi
List of Symbols	xvi
1 Introduction	1
1.1 Background	1
1.2 Motivation and Thesis Outline	3
2 The Asymptotic Expansion of the Capillary Surface for a Needle Cylindrical Tube	11
2.1 Introduction	11
2.2 Preliminaries	14
2.3 First Approximate Solution: $u_1(r)$	18
2.3.1 First Approximate Inner Solution: $u_1^{\text{in}}(r)$	19
2.3.2 First Approximate Outer Solution: $u_1^{\text{out}}(r)$	21
2.3.3 C^1 First Approximate Solution: $u_1(r)$	21
2.3.4 Asymptotic Expansion of the First Approximate Solution $u_1(r)$ as $\epsilon \rightarrow 0$	22
2.3.5 Optimal Choice of q	24
2.4 Second Approximate Solution: $u_2(r)$	29
2.4.1 One-step Iteration for the Inner Solution: $\underline{u}_2^{\text{in}}(r)$	30
2.4.2 Constant Mean Curvature Solution: $u_2^{\text{in}}(r)$	31
2.4.3 Choice of $u_2^{\text{in}}(q)$	34
2.4.4 Asymptotic Expansion of the Second Approximate Inner Solution: $u_2^{\text{in}}(r)$	36
2.4.5 Second Approximate Outer Solution: $u_2^{\text{out}}(r)$	41
2.4.6 Another Choice of $u_2^{\text{in}}(q)$	51

2.4.7	Asymptotic Expansion of the Second Approximation Solution: $u_2(r)$	52
2.5	Improved Bound Estimate for the Asymptotic Expansion of $u(r)$	53
2.5.1	Modified Outer Solutions u_i^{out}	54
2.5.2	Asymptotic Expansion of u_3^{in}	58
2.5.3	Choice of $u_4^{\text{in}}(q)$ and the Asymptotic Expansion of $u_4^{\text{in}}(r)$	62
2.6	Conclusion	67
3	A Floating Ball on an Unbounded Bath	69
3.1	Introduction	69
3.2	Various Forms of the Capillary Equation	74
3.3	Preliminaries	77
3.4	Differentiable Dependence of Solutions on ϕ_0	78
3.4.1	Profile Curve $\bar{r}(\psi; \sigma)$ and $\bar{u}(\psi; \sigma)$	79
3.4.2	Profile Curve $w(\bar{r}; r_w, \bar{u})$	81
3.4.3	Smooth Dependence of Solutions on ϕ_0	90
3.4.4	The Envelope of the Profile Curves	93
3.5	Asymptotic Analysis of Solutions as $\psi \rightarrow 0$	94
3.5.1	Asymptotic Forms of $\bar{r}(\psi; \phi_0)$ and $\bar{u}(\psi; \phi_0)$ as $\psi \rightarrow 0$	94
3.5.2	Limiting Behavior of $\dot{w}(\bar{r}; r_w, \xi)$ as $\bar{r} \rightarrow \infty$	97
3.5.3	Limiting Behavior of $\dot{\bar{r}}(\psi; \phi_0)$ and $\dot{\bar{u}}(\psi; \phi_0)$ as $\psi \rightarrow 0$	100
3.5.4	Relation between \dot{w} , $\dot{\bar{r}}$ and $\dot{\bar{u}}$	103
3.5.5	Improved Error Bounds for $\dot{\bar{r}}(t; \phi_0)$ and $\dot{\bar{u}}(t; \phi_0)$ as $t \rightarrow \infty$	105
3.6	Total Energy, Total Force and Their Relation	106
3.6.1	Decomposition of Total Energy E_T	107
3.6.2	Decomposition of Total Force F_T	109
3.6.3	Relation Between Total Energy \hat{E}_T and Total Force \hat{F}_T	111
3.6.4	Stability Criterion	121
3.7	Shooting Method	123
3.8	Behavior of the Total Force $\hat{F}_T(\phi_0)$ and Height $\hat{h}(\phi_0)$ Curves	126
3.8.1	Asymptotic Expansion of the fluid interface as $B \rightarrow 0$	130
3.8.2	Behavior of $\hat{h}(\phi_0)$ and $\hat{F}_T(\phi_0)$ As $B \rightarrow 0$	141
3.8.3	Behavior of $\hat{h}(\phi_0)$ and $\hat{F}_T(\phi_0)$ as $\phi_0 \rightarrow 0$ or π	147
3.8.4	Behavior of $\hat{h}(\phi_0)$ and $\hat{F}_T(\phi_0)$ As $B \rightarrow \infty$	154
3.8.5	Numerical Observation of the Total Force $\hat{F}_T(\phi_0)$ and Height $\hat{h}(\phi_0)$ Curves	167
3.9	Illustrating the Number of Equilibria and their Stability	173
3.10	Numerical Results	178
3.10.1	An Example with Two Stable Equilibria	179

3.10.2	An Example with No Force Balanced Point	181
3.11	Conclusion	184
4	The Capillary Surface in a Tilted Wedge	186
4.1	Introduction	186
4.1.1	A Wedge Domain in Cylindrical Coordinates	187
4.1.2	Tilted Capillary Equation	189
4.2	Approximate Solution $v(r, \theta)$	191
4.3	Error Bounds on the Tilted Capillary Surface	195
4.3.1	Sub-solution and Super-solution in Ω_{r_0}	196
4.3.2	Conditions on Boundary Σ_{r_0}	198
4.3.3	Conditions on Boundary Γ_{r_0}	201
4.3.4	Results	205
4.4	Improved Error Bounds on u	207
4.4.1	Sub-solution and Super-solution in Ω_{r_0}	208
4.4.2	Conditions on Boundary Σ_{r_0}	212
4.4.3	Conditions on Boundary Γ_{r_0}	215
4.4.4	Results	216
4.5	Conclusion	217
5	Conclusion	219
	References	222
	APPENDICES	227
A		228
A.1	Asymptotic Expansions of Some Functions	228
A.2	Asymptotic Expansions of p_3, k_3, p_4 and k_4	229
B		233
B.1	Transformation $T(t)$	233
B.2	Numerical Differentiation	236
B.3	Iterative Method	241
C		245
C.1	Tilting Coordinates Using Euler's Angles	245
C.2	Calculation of Nw , where $w(r, \theta) = v(r, \theta) + Aq(\theta)r^\lambda$	246
C.3	Computation of $\nu \cdot Tw$ on the Boundary Σ_{r_0} , where $w(r, \theta) = v(r, \theta) + Aq(\theta)r^\lambda$	263

List of Figures

1.1	The simple case: a capillary tube, it forms a three-phase system.	2
1.2	A wedge domain.	6
1.3	A floating ball on an unbounded bath.	9
2.1	The comparison among $w(q)$, $u(q)$ and $u_2^{\text{in}}(q)$	35
2.2	The comparison among $u_1^{\text{in}}(r)$, $u_2^{\text{in}}(r)$ and $u(r)$ in the inner region with $\epsilon = \sqrt{0.001}$, $\gamma = \frac{\pi}{4}$ and $q = 10$	35
2.3	The comparison among $u_1(r)$, $u_2(r)$ and $u(r)$ in the inner region with $\epsilon = 0.001$, $\gamma = \frac{\pi}{4}$ and $q = 10$	52
3.1	(a) The cross-sectional configuration of the ball floating on the liquid, (b) the measurement of the inclination angle ψ for both positive and negative fluid heights.	71
3.2	The contact point (r_0, u_0) and the height of the center h	73
3.3	The figure illustrates W_2 region, the upper dashed curve represents the profile with $\sigma = 1$ and the lower dashed curve represents the profile with $\bar{r}(\pi/2) = 2$	82
3.4	\bar{u}_0 versus ϕ_0 with $\gamma = \frac{\pi}{3}$ and $B = 1$	92
3.5	A family of profile curves with $B = 1$, $\psi \in (-\pi, 0)$ and $\sigma \in (0, 1)$	93
3.6	(a) The contact point (r_0, u_0) and the height of the center h ; (b) Computation of the fluid potential energy F_F	108
3.7	The gravitational, surface tension and buoyant forces.	111
3.8	(a) The shooting method algorithm; (b) the numerical result for the fluid height $\bar{u}(\bar{r})$	125
3.9	The non-monotone relation between ϕ_0 and $h(\phi_0)$. Given $h = 1.3$, there are two corresponding ϕ_0 values: $\phi_0 = 0.1028$ and $\phi_0 = 0.6805$	126

3.10	(a) The configuration with $\phi_0 = 0.1028$, $h = 1.3$, $a = 1$, $\gamma = \frac{\pi}{2}$, (b) another configuration with the same height $h = 1.3$ and $\phi_0 = 0.6805$	126
3.11	A comparison between the numerical result and the asymptotic expansion with data $\gamma = \frac{\pi}{8}$, $\phi_0 = \frac{\pi}{8}$ and $B = 0.01$	140
3.12	(a) The comparison between the numerical solution and the asymptotic expansion of $\hat{h}(\phi_0)$ with $B = 0.01$, $\gamma = \frac{\pi}{3}$; (b) the comparison between the numerical solution and the asymptotic expansion of $\hat{F}_T(\phi_0)$ with the same data and $\alpha = 0$	142
3.13	The comparison between the numerical solution by the five-point method and the asymptotic expansion of $\frac{d\hat{u}_0}{d\phi_0}$ with $B = 0.01$ and $\gamma = \frac{\pi}{3}$	144
3.14	(a) The comparison between the asymptotic expansion of \hat{u}_0 and the numerical result near $\phi_0 = 0$ with $\gamma = 0$; (b) the comparison near $\phi_0 = \pi$ with $\gamma = \pi$	148
3.15	(a) The comparison between the asymptotic expansion of $\frac{d\hat{u}_0}{d\phi_0}$ and the numerical results by the five-point method near $\phi_0 = 0$ with $B = 1$, $\gamma = \frac{\pi}{3}$, and uniform step size $\Delta\phi_0 = \frac{\pi}{N}$, $N = 500, 1000$; (b) the comparison near $\phi_0 = \pi$ with the same data.	150
3.16	(a) The comparison between the asymptotic expansion of $\frac{d\hat{u}_0}{d\phi_0}$ and the numerical results by the five-point method near $\phi_0 = 0$ with $B = 1$, $\gamma = 0$, and uniform step size $\Delta\phi_0 = \frac{\pi}{N}$, $N = 500, 1000$; (b) the comparison near $\phi_0 = \pi$ with the same data.	151
3.17	(a) The comparison between the asymptotic expansion of $\frac{d\hat{u}_0}{d\phi_0}$ and the numerical results by the five-point method near $\phi_0 = 0$ with $B = 1$, $\gamma = \pi$, and uniform step size $\Delta\phi_0 = \frac{\pi}{N}$, $N = 500, 1000$; (b) the comparison near $\phi_0 = \pi$ with the same data.	151
3.18	(a) The comparison between the numerical solution and the approximate form with $B = 1000$ and $\gamma = \frac{\pi}{3}$; (b) the comparison between the numerical solution and the approximate form with $B = 1000$ and $\gamma = 0$	157

3.19	(a) The comparison between the numerical solution and the limiting case of the height curve with $B = 1000$, $\gamma = \frac{\pi}{3}$; (b) the comparison between the numerical solution and the limiting case of the total force curve with the same data and $\alpha = 0$.	166
3.20	(a) The comparison between the numerical solution and the limiting case of the height curve with $B = 5000$, $\gamma = \frac{\pi}{3}$; (b) the comparison between the numerical solution and the limiting case of the total force curve with the same data and $\alpha = 0$.	166
3.21	(a) The height curve with $B = 5$, $\gamma = \frac{\pi}{2}$; (b) the total force curve with the same data and $\alpha = 0$.	168
3.22	(a) The height curve with $B = 0.0001$, $\gamma = \frac{\pi}{2}$; (b) the total force curve with the same data and $\alpha = 0$.	169
3.23	(a) The height curve with $B = 50$, $\gamma = \frac{\pi}{2}$; (b) the total force curve with the same data and $\alpha = 0$.	169
3.24	(a) The height curve with $B = 1$, $\gamma = 0$; (b) the total force curve with the same data and $\alpha = 0$.	170
3.25	(a) The height curve with $B = 1$, $\gamma = \pi$; (b) the total force curve with the same data and $\alpha = 0$.	171
3.26	(a) The comparison between the numerical solution and the limiting case of the height curve with $B = 0.001$, $\gamma = 0$; (b) the comparison between the numerical solution and the limiting case of the total force curve with the same data and $\alpha = 0$.	172
3.27	(a) The comparison between the numerical solution and the limiting case of the height curve with $B = 0.001$, $\gamma = \pi$; (b) the comparison between the numerical solution and the limiting case of the total force curve with the same data and $\alpha = 0$.	172
3.28	B versus α : the $\gamma = 0$ case. \mathcal{R}_1 region represents there is only one equilibrium point, which is stable. \mathcal{R}_0 is the region with no equilibrium point.	175
3.29	B versus α : the $\gamma = \frac{\pi}{10}$ case.	175
3.30	B versus α : the $\gamma = \frac{\pi}{4}$ case.	176
3.31	B versus α : the $\gamma = \frac{\pi}{2}$ case.	176
3.32	B versus α : the $\gamma = \frac{3\pi}{4}$ case.	177
3.33	(a) B versus α : the $\gamma = \pi$ case; (b) the zoomed in region.	177
3.34	B versus α : the $\gamma = \pi$ case.	178

3.35	The comparison between the numerical \mathcal{C}_3 curve and the approximated \mathcal{C}_3 curve for the $\gamma = \frac{3\pi}{4}$ case	179
3.36	Given the density ratio 1.4, there are four critical points for \hat{E}_T : $\phi_0 = 0.3551$ and $\phi_0 = 2.7865$ (in black squares), and $\phi_0 = 1.9262$ and $\phi_0 = 2.8791$ (in black circles).	180
3.37	(a) There are two critical points of height $\hat{h}(\phi_0)$, the smaller one $\phi_0 = 0.3551$ and the larger one $\phi_0 = 2.7865$. Those two extreme points are shown in the black squares; (b) two force balanced points $\phi_0 = 1.9262$ and $\phi_0 = 2.8791$	180
3.38	The zoomed in figure for \hat{E}_T with the density ratio 1.4, the critical point $\phi_0 = 2.7865$ (in black square) is the critical point of $\hat{h}(\phi_0)$ and the critical point $\phi_0 = 2.8791$ (in black circle) is the force balanced point.	181
3.39	(a) Given the density ratio 2.2, there is no force balanced point, (b) the corresponding \hat{E}_T has two critical points: $\phi_0 = 0.3551$ and $\phi_0 = 2.7865$ (in black squares), which are related with the critical points of $\hat{h}(\phi_0)$	182
3.40	(a) The configuration for $\hat{h} = \hat{h}_{\min}$, (b) a different topological structure for $\hat{h} = \hat{h}_{\min}$	183
3.41	(a) \hat{E}_T vs \hat{h} with data: $\gamma = \frac{\pi}{2}$, $B = 1$ and $\alpha = 2.2$, (b) the modified \hat{E}_T vs \hat{h} with the same data.	183
4.1	(a) A bounded wedge domain; (b) a tilted wedge along the negative x axis with an angle $\tau \in \left(0, \frac{\pi}{2}\right)$	188
4.2	The level curve of $v(r, \theta) = C$	192
4.3	The bound of u in B_{δ_0}	202
B.1	the case $\phi_0 \in (0, \pi)$, $B = 0.01$, $\gamma = \frac{\pi}{4}$, and uniform step size $\Delta\phi_0 = \frac{\pi}{N}$, $N = 100$	238
B.2	The five-point method for $\frac{d\hat{u}_0}{d\phi_0}$ with data: $B = 1$, $\gamma = \frac{\pi}{3}$, and uniform step size $\Delta\phi_0 = \frac{\pi}{N}$, $N = 500, 1000$	239
B.3	(a) The height curve with $B = 1$, $\gamma = \frac{\pi}{3}$, the local minimum point is $(2.8879, -1.2835)$; (b) The corresponding zoomed in figure shows the Lagrange interpolation polynomial is used to find the local minimum of the height.	240

B.4	(a) The total force curve with $B = 1$, $\gamma = \frac{\pi}{3}$, $\alpha = 0$, the local maximum point is $(2.6108, 1.8885)$; (b) The corresponding zoomed in figure shows the Lagrange interpolation polynomial is used to find the local maximum of the total force.	240
B.5	The comparison between the shooting method result and the iterative solution \tilde{v}_2 with data: $B = 1$, $\gamma = \frac{\pi}{4}$, $\bar{r}_0 = \frac{\sqrt{3}}{2}$ and $\psi_0 = -\frac{5\pi}{12}$	244
C.1	Euler's angles with "ZYZ" convention.	246

List of Symbols

- (ϕ, τ, ψ) Euler's angles used to describe a rotation of coordinates in Chapter 4
- A_i Coefficient of the outer solution u_i^{out} , $i = 1, 2, 3, 4$
- B Bond number
- $D(\epsilon, q)$ Constant mean curvature of u_2^{in}
- E_T Total energy of the floating ball system. \hat{E}_T is its dimensionless form
- F_T Total force of the floating ball system. \hat{F}_T is its dimensionless form
- I_i Modified Bessel function of the first kind of order i
- K_i Modified Bessel function of the second kind of order i
- R Outer variable defined as $R = \epsilon r$ in Chapter 2
- $T(\sigma)$ Corresponding fluid height at radial distance σ
- $\tilde{\kappa}$ Capillary constant defined as $\tilde{\kappa} = \tilde{\kappa} \tilde{r} \left(-\frac{\pi}{2}\right)$, where $\tilde{r} = \frac{r}{r_0}$, where r_0 is the dimensional radial distance at the contact point
- \tilde{r} Radial distance defined as $\tilde{r} = \frac{\tilde{r}}{l_c}$, where $l_c = \tilde{r} \left(-\frac{\pi}{2}\right)$
- \tilde{u} Fluid height defined as $\tilde{u} = \frac{\tilde{u}}{l_c}$, where $l_c = \tilde{r} \left(-\frac{\pi}{2}\right)$
- α Density ratio of the floating ball compared to the liquid in Chapter 3. The opening angle of the wedge in Chapter 4.
- $\bar{D}(\epsilon, q)$ Constant mean curvature of u_4^{in}
- $\bar{\kappa}$ New capillary constant for the tilted capillary equation
- $\bar{\phi}_0$ Force balanced point

\bar{r} Scaled radial distance $\bar{r} = \frac{\sqrt{B}}{a}r$

\bar{u} Scaled fluid height $\bar{u} = \frac{\sqrt{B}}{a}u$

\bar{u}_L Solution of the scaled linearized capillary equation in Chapter 3

$\dot{r}(\psi; \phi_0)$ Derivative of r with respect to ϕ_0 , $\dot{r}(\psi; \phi_0) = \frac{\partial}{\partial \phi_0}r(\psi; \phi_0)$

$\dot{r}(\psi; \sigma)$ Derivative of r with respect to σ , $\dot{r}(\psi; \sigma) = \frac{\partial}{\partial \sigma}r(\psi; \sigma)$

$\dot{u}(\psi; \phi_0)$ Derivative of u with respect to ϕ_0 , $\dot{u}(\psi; \phi_0) = \frac{\partial}{\partial \phi_0}u(\psi; \phi_0)$

$\dot{u}(\psi; \sigma)$ Derivative of u with respect to σ , $\dot{u}(\psi; \sigma) = \frac{\partial}{\partial \sigma}u(\psi; \sigma)$

$\dot{w}(r; r_w, u)$ Derivative of w with respect to u , $\dot{w}(r; r_w, u) = \frac{\partial}{\partial u}w(r; r_w, u)$

ϵ Square root of Bond number, $\epsilon = \sqrt{B}$

γ Contact angle

γ_e Euler's constant

\hat{r} Dimensionless radial distance $\hat{r} = \frac{r}{a}$, where a is the radius of the ball

\hat{u} Dimensionless fluid height $\hat{u} = \frac{u}{a}$, where a is the radius of the ball

κ Capillary constant

\mathcal{C}_i Boundary curve in B versus α region, $i = 1, 2, 3$

\mathcal{R}_0 Region with no equilibrium point in B versus α figure

\mathcal{R}_1 Region with one equilibrium point in B versus α figure

$\mathcal{R}_{2,1}$ Region with two equilibrium points and the smaller one is stable and the larger one is unstable in B versus α figure

$\mathcal{R}_{2,2}$ Region with two equilibrium points and two of which are stable in B versus α figure

ϕ_0 Attachment angle

ϕ_0^* Critical point of $\hat{F}_T(\phi_0)$

ϕ_0^{**} Critical point of $\hat{h}(\phi_0)$

- ψ Inclination angle of the fluid interface
- ψ_0 Inclination angle at the contact point
- ψ_i^{in} Inclination angle of the i th approximate inner solution u_i^{in}
- σ Radial distance when the slope of the profile curve becomes vertical
- σ Surface tension along the fluid interface. It is used in the capillary constant κ and calculation of the buoyant force F_B
- $\tilde{\kappa}$ Capillary constant $\tilde{\kappa} = B \sin^2(\phi_0)$ when the floating ball problem is fitted into the needle problem
- \tilde{r} Radial distance of the fluid interface when $\tilde{\kappa}$ is used as the capillary constant
- \tilde{u} Fluid height when $\tilde{\kappa}$ is used as the capillary constant
- a Radius of a cylindrical tube in Chapter 2. Radius of a ball in Chapter 3
- g Gravitational acceleration
- h Height of the center of the floating ball to the reference level in Chapter 3. $\hat{h} = \frac{h}{a}$ is its dimensionless form, a is the radius of the ball
- $h(\theta)$ Angle function in approximate solution $v(r, \theta)$ in Chapter 4
- $p(r, u)$ Slope function in the graph case. u is considered as a parameter
- q Transition variable between the inner region and the outer region
- q^* Optimal choice of q to obtain the optimal error bound of the two-term asymptotic expansion of u
- q^{**} Optimal choice of q to obtain the improved error bound of the two-term asymptotic expansion of u
- $r(\psi; \phi_0)$ Parametric description of radial distance with the attachment angle ϕ_0 as a parameter when the profile curve is fitted into the floating ball problem
- $r(\psi; \sigma)$ Parametric description of radial distance. ψ is the inclination angle and σ is the radial distance when the slope of the profile curve becomes vertical
- r_0 Radial distance at the contact point
- u Fluid height of a capillary surface
- $u(\psi; \phi_0)$ Parametric description of fluid height with the attachment angle ϕ_0 as a parameter when the profile curve is fitted into the floating ball problem

- $u(\psi; \sigma)$ Parametric description of fluid height. ψ is the inclination angle and σ is the radial distance when the slope of the profile curve becomes vertical
- $u(r; r_0, u_0)$ Graph description of fluid height with (r_0, u_0) as the initial data when the profile curve is fitted into the floating ball problem
- u_0 Fluid height at the contact point
- u_1 First approximate solution of u . It consists an inner solution and an outer solution
- u_2 Second approximate solution of u . It consists an inner solution and an outer solution
- u_i^{in} Inner solution of u_i , $i = 1, 2, 3, 4$
- u_i^{out} Outer solution of u_i , $i = 1, 2, 3, 4$
- $v(r, \theta)$ Approximate solution $v(r, \theta) = \frac{h(\theta)}{r}$ in Chapter 4
- $w'(r; r_w, u)$ Derivative of w with respect to r , $\frac{\partial}{\partial r} w(r; r_w, u)$
- $w(r; r_w, u)$ Graph description of fluid height with (r_w, u) as the initial data
- $w_{\pm}(r, \theta)$ Choices of sub and super-solutions of u in Chapter 4

Chapter 1

Introduction

1.1 Background

Capillary phenomena have been quantitatively studied since the early nineteenth century, introduced by Young [65], Laplace [10] and Gauss [26]. In Young's celebrated work in 1805 [65], he was the first to present the relation between the pressure change δp across the surface formed by two different fluids and the surface tension σ . Laplace reintroduced Young's results with formal mathematical notation a year later [10]. In modern mathematical language, the relation can be expressed as

$$\delta p = 2\sigma H, \tag{1.1}$$

where σ is known as the surface tension and H represents the mean curvature of the surface.

In 1830, Gauss considered the problem from an energy point of view [26], seeking the configuration that minimizes the total energy. The method is presented in a general framework by Finn in his monograph [18]. Here, we present a simple case, a vertical open tube immersed in an infinite bath, see Fig. 1.1. It forms a three-phase system (two fluids: the air and the liquid, and the solid: the tube). Suppose $u(x)$ is the fluid height over the domain $\Omega \subset \mathbb{R}^2$, the air-liquid interface meets the tube (solid) with the contact angle γ , the surface tension along the fluid interface is σ . β denotes the adhesion coefficient (it can be shown that $\beta = \cos \gamma$). In Gauss' framework, the contact angle γ is assumed to be a unique constant. However, the measurement and properties of contact angle are not trivial, see [9]. In general, contact angle is not necessarily unique, there is contact angle hysteresis. We are

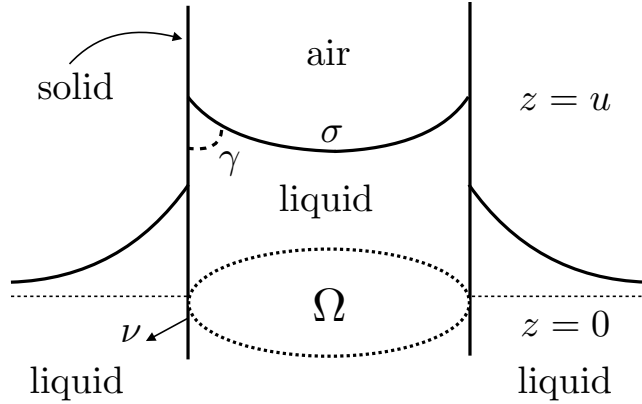


Figure 1.1: The simple case: a capillary tube, it forms a three-phase system.

interested in the model under the idealized conditions (i.e. perfectly smooth objects and homogeneous solid, liquid and air). So, the assumption of unique constant contact angle γ is applied throughout the thesis. ρ represents the density difference of the fluid and the air. With the downward pointing gravitational acceleration g , the energy functional can be expressed as

$$\mathcal{E}[u] = \sigma \int_{\Omega} \sqrt{1 + |\nabla u|^2} dx - \beta \sigma \int_{\partial\Omega} u ds + \rho g \int_{\Omega} \frac{u^2}{2} dx. \quad (1.2)$$

The first variation of $\mathcal{E}[u]$ gives the corresponding Euler-Lagrange equation (also known as the capillary equation) and the boundary condition

$$Nu = \kappa u \quad \text{in } \Omega, \quad (1.3)$$

$$Tu \cdot \nu = \cos \gamma \quad \text{on } \partial\Omega, \quad (1.4)$$

where $Nu = \text{div}Tu$, $Tu = \frac{\nabla u}{\sqrt{1 + |\nabla u|^2}}$, $\kappa = \frac{\rho g}{\sigma} \geq 0$ is known as the capillary constant

and ν denotes the outward unit normal of $\partial\Omega$. Moreover, $\left(Tu, \frac{-1}{\sqrt{1 + |\nabla u|^2}}\right)$ represents the downward unit normal of the surface. Nu has the geometric interpretation of twice the mean curvature of the surface. If there is a volume constraint, the extra term λ would be

added on the right-hand side of (1.3), which is to be determined by the constraint. (1.4) is known as the contact angle condition.

1.2 Motivation and Thesis Outline

The boundary value problem (BVP) in (1.3) and (1.4) can be applied to study the behavior of capillary surfaces in many applications, see the comprehensive monograph by Finn [18]. However, due to the non-linearity of the capillary equation, there is no explicit solution in general. One powerful tool that can be applied to study the capillary equation is the comparison principle, see Concus and Finn [7]. We restate the comparison principle for a bounded domain from [48], shown as follows.

Theorem 1. (*Comparison Principle for a Bounded Domain*) Suppose $\kappa > 0$. Let $\Omega \in \mathbb{R}^2$ be a bounded connected domain and its boundary Σ admits a decomposition $\Sigma = \Sigma_\alpha \cup \Sigma_\beta \cup \Sigma_0$ such that Σ_0 can be covered, for any $\epsilon > 0$, by a countable number of disks B_{δ_i} of radius δ_i , such that $\sum \delta_i < \epsilon$, that is, the one-dimensional Hausdorff measure of Σ_0 is zero. Σ_α is Lipschitz and Σ_β is C^1 . Let $u, v \in C^2(\Omega) \cap C^1(\Omega \cup \Sigma_\alpha)$ and suppose

(i) $N(u - v) \geq \kappa(u - v)$ in Ω ,

(ii) $u \leq v$ on Σ_α ,

(iii) $\nu \cdot Tu \leq \nu \cdot Tv$ on Σ_β where ν is the outward unit normal of Σ_β ,

then $u \leq v$ in Ω . If $u(x_0) = v(x_0)$ at $x_0 \in \Omega$, then $u \equiv v$.

A useful alternative condition (i)' which implies (i) in the comparison principle is that $Nu \geq \kappa u$ and $Nv \leq \kappa v$ in Ω . $Nu \geq \kappa u$ is called a sub-solution condition (or we say u is a sub-solution) and $Nv \leq \kappa v$ is called a super-solution condition (or we say v is a super-solution). The comparison principle is also valid for an unbounded domain with no condition required at infinity, see Finn and Hwang [22]. A proof of the comparison principle for a radial unbounded domain is given in Chapter 2.

A classic example is the vertical circular open capillary tube with radius a immersed in an infinite bath, see Fig. 1.1. Assume the capillary surface is radially symmetric. Let $r = |x|$ be a radial distance, $x \in \mathbb{R}^2$ and $|\cdot|$ represents the Euclidean norm. Capillary surfaces in both interior ($0 \leq r \leq a$) and exterior ($r \geq a$) domains have been studied. Siegel [56]

studied the problem and gave the estimates of the fluid height in both interior and exterior domains of the capillary tube. We are interested in the exterior problem. The capillary equation can be reduced to

$$\frac{u_{rr}}{(1+u_r^2)^{3/2}} + \frac{u_r}{r\sqrt{1+u_r^2}} = \kappa u, \quad \text{for } r > a, \quad (1.5)$$

$u = u(r)$ can be understood as the fluid height. Geometrically,

$$\frac{1}{r}(r \sin \psi)_r = \kappa u, \quad \text{for } r > a, \quad (1.6)$$

if the inclination angle ψ of the capillary surface $u(r)$ is introduced. The boundary conditions are

$$\sin(\psi(a)) = -\cos(\gamma) \quad \text{and} \quad \lim_{r \rightarrow \infty} u(r) = 0. \quad (1.7)$$

A more detailed description of the radially symmetric capillary equation can be seen in Chapter 2. A dimensionless constant $B = \kappa a^2$ is introduced, which is known as the Bond number (sometimes, $\epsilon = \sqrt{B}$ is used). Physically, B is a dimensionless ratio of gravitational to capillary forces. The asymptotic expansion of the fluid height $u(r)$ as $B \rightarrow 0$ or $B \rightarrow \infty$ has been investigated. Geometrically, for a large Bond number, the problem can be considered a wide tube. When the Bond number is small, the tube becomes a needle. Laplace [10] and Rayleigh [53] first studied these problems. Concus [5] found the asymptotic solutions for the large and the small B near the tube in the interior domain. In the exterior domain, the asymptotic expansion near the circular needle has been widely studied, see Turkington [59], Lo [41], Miersemann [47], Siegel [57] and Lagerstrom [38]. Lo [41] obtained a five-term asymptotic expansion by the matched asymptotic expansions method (see [11, 24, 32, 60]). Lo's result is broadly accepted as the correct asymptotic expansion for the needle problem. We truncate Lo's expansion up to $\mathcal{O}(\epsilon^2 \ln^2(\epsilon))$, then, as $\epsilon \rightarrow 0$,

$$u(r) = c \ln(\epsilon) + c(\gamma_e - 2 \ln 2) + c \ln\left(r + \sqrt{r^2 - c^2}\right) + \mathcal{O}(\epsilon^2 \ln^2(\epsilon)), \quad (1.8)$$

where $c = -\cos(\gamma)$ and γ_e is known as Euler's constant. However, Lo's result has not been rigorously proven. Miersemann [47] proved the correctness of its first two terms with error bound $\mathcal{O}(\epsilon^{2/5} \ln^2(\epsilon))$. His error bound is inferior to Lo's.

We study this problem in Chapter 2. The domain is separated into an inner and an outer regions by $r = q$. We construct two C^1 , piecewise C^2 , approximate solutions over the whole domain. One can be shown as an upper bound of the fluid height $u(r)$ and the other is a lower bound of $u(r)$ based on the comparison principle. Each approximate solution consists of an inner solution and an outer solution. Geometrically, the upper bound inner solution has zero mean curvature and the lower bound inner solution has constant mean curvature. As $\epsilon \rightarrow 0$, both approximate solutions have the same two-term asymptotic expansion which is the two-term expansion of $u(r)$. We apply Olver's theorem [49] to determine the choice of q to optimize the error bound. With the optimal choice of q , the error bound of the two-term asymptotic expansion is obtained, $\mathcal{O}(\epsilon(-\ln \epsilon)^{3/2})$. The error bound can be improved by considering a modified outer solution. Our error bound $\mathcal{O}(\epsilon^{4/3}(-\ln \epsilon)^{5/3})$ is an improvement from Miersemann's [47] but is inferior to Lo's [41].

Another interesting application is the capillary surface in a wedge. Consider a vertical wedge domain with a vertex at the origin. The x -axis bisects the wedge with the opening angle 2α , $0 < \alpha < \frac{\pi}{2}$, see Fig. 1.2. Concus and Finn [6] showed that the capillary surface is bounded if $\alpha + \gamma \geq \frac{\pi}{2}$. When $0 < \alpha + \gamma < \frac{\pi}{2}$, the capillary surface is unbounded near the corner. They constructed an approximate solution of the form

$$v_1(r, \theta) = \frac{h_1(\theta)}{r}, \quad (1.9)$$

where $h_1(\theta) = \frac{\cos \theta - \sqrt{k^2 - \sin^2 \theta}}{k\kappa}$ and $k = \frac{\sin \alpha}{\cos \gamma}$. Near the corner, the error bound $u = v_1 + \mathcal{O}(1)$ is established. Miersemann [45, 46] studied the $0 < \alpha + \gamma < \frac{\pi}{2}$ case and gave an improved error bound $\mathcal{O}(r^3)$ near the corner. More related work can be seen in Finn [18], Lancaster and Siegel [39] and Aoki and Siegel [2].

In Chapter 4, a wedge with $0 < \alpha + \gamma < \frac{\pi}{2}$ is considered. We are interested in whether the capillary surface is still unbounded if the wedge is tilted from the vertical axis. Euler's angles (ϕ, ψ, τ) are used to describe the tilting. A tilted capillary equation can be obtained in the tilted coordinates (r, θ, z) , shown as follows,

$$Nu = \bar{\kappa}u + f(\theta; \kappa, \phi, \tau)r \quad (1.10)$$

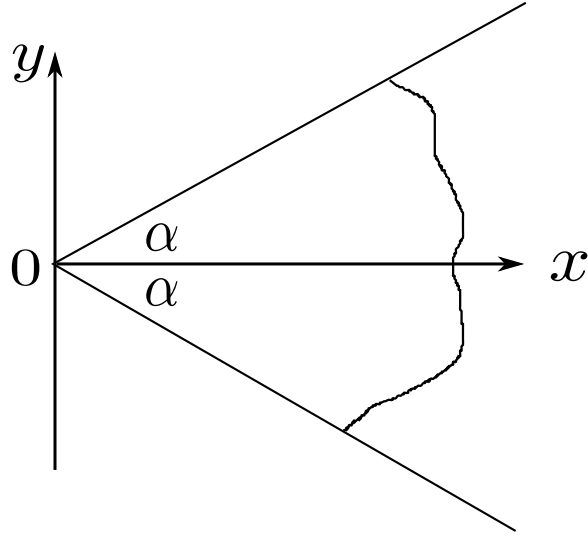


Figure 1.2: A wedge domain.

with boundary condition on the tilted wall

$$\nu \cdot Tu = \cos \gamma, \quad (1.11)$$

where $u = u(r, \theta)$ is the tilted capillary surface, $\bar{\kappa} = \kappa \cos(\tau) > 0$, $\tau \in \left(0, \frac{\pi}{2}\right)$. $\bar{\kappa}$ can be treated as the new capillary constant.

$$f(\theta; \kappa, \phi, \tau) = -\kappa \sin \tau \cos(\theta + \phi). \quad (1.12)$$

$f(\theta; \kappa, \phi, \tau)$ is smooth and $|f| \leq \kappa$ and ν is the outward normal of the tilted wall, see Chapter 4 for more details. v_1 in (1.9) can be applied in analysis of the tilted capillary equation with κ replacing by $\bar{\kappa}$. So, we define

$$v(r, \theta) = \frac{h(\theta)}{r}, \quad (1.13)$$

where $h(\theta) = \frac{\cos \theta - \sqrt{k^2 - \sin^2 \theta}}{k\bar{\kappa}}$. Moreover, v is the solution of an approximate equation

$$\operatorname{div} \left(\frac{\nabla v}{|\nabla v|} \right) = \bar{\kappa} v \quad (1.14)$$

with the same boundary condition in (1.11), see Ron [28] and King and Ockendon [35].

The approximate solution v can be applied to construct sub-solutions and super-solutions of u . We employ Miersemann's choices [45, 46] and examine conditions of the comparison principle. Finally, $|u - v| = \mathcal{O}(r)$ can be established near the corner.

Floating objects have captured people's attention since the age of Archimedes. Archimedes's principle states that a body immersed in a fluid is buoyed up by a force which is equal to the weight of the displaced fluid. However, Archimedes's principle is not correct in general due to the presence of surface tension, see McCuan and Treinen [43] and Vella [61]. Especially, for small particles, surface tension cannot be neglected. In recent research, many examples of multiple equilibrium configurations have been found with or without surface tension and gravity. Erdős, Schibler and Herndon [15, 16] considered floating objects with different shapes without surface tension. They found multiple equilibrium configurations of floating prisms of square and equilateral triangular cross-section, cube, octahedron and tetrahedron. Even asymmetric floating configurations of symmetric objects have been found. Raphaël, di Meglio, Berger and Calabi [52] considered a long prismatic particle with smooth strictly convex cross-section. Multiple stable equilibrium configurations can be found. Kemp and Siegel [34] gave the stability analysis of the prisms with elliptical or polygonal cross-section. In presence of both gravity and surface tension, the situation becomes more complicated. So, symmetric objects have received more attention. Bhatnagar and Finn [3] studied a horizontal circular cylinder floating on an unbounded bath and gave the first example where a floating cylinder admits two equilibrium positions. Chen and Siegel [4] gave a full stability analysis of the problem. They concluded that there exist at most two equilibrium configurations. One of them is stable. Vella, Lee and Kim [62] applied the floating cylinder to study the load-bearing capacity of water strider legs. Similar results are also obtained in Liu et al [40] and Zheng et al [66]. McCuan and Treinen [44] considered a floating cylinder in a laterally finite container. They gave an example with three equilibrium configurations, two of which are stable.

In three dimensions, a floating ball is the simplest case and its floating configuration is assumed to be radially symmetric. The capillary surface can be either a graph or a non-graph. When the fluid interface is a non-graph, parametric equations have been employed,

shown as follows,

$$\frac{dr}{d\psi} = \frac{r \cos \psi}{\kappa r u - \sin \psi} \quad \text{and} \quad \frac{du}{d\psi} = \frac{r \sin \psi}{\kappa r u - \sin \psi}. \quad (1.15)$$

with boundary conditions

$$r(\psi_0) = r_0 \quad \text{and} \quad \lim_{\psi \rightarrow 0} u(\psi) = 0, \quad (1.16)$$

where ψ_0 and r_0 are the inclination angle and the radial distance at the contact point, respectively. Parametric solutions have also been studied in many other applications, see Concus and Finn [8] for a pendant drop, Finn [17] for the sessile drop, Vogel [63] for a liquid bridge and Elcrat, Neel and Siegel for a floating drop [13].

To the best of our knowledge, the earliest work on the equilibrium configuration of a floating ball including the consideration of surface tension was done by Rapacchietta, Neumann and Omeyi [51]. They discussed both the force and energy analysis. Due to the difficulty of the computation, they only applied force analysis to determine the equilibrium configuration. The stability of the equilibrium configurations is unknown. McCuan and Treinen [43] considered a floating ball in a finite container or an unbounded bath. They derived additional necessary condition for the floating configuration, which is force balance. They gave an example of two equilibrium configurations of a floating ball on an unbounded bath, one of which admits a lower energy. However, the number of equilibria and their stability for a floating ball has not been well studied.

In Chapter 3, we consider a floating ball on an unbounded bath, see Fig. 1.3. The fluid interface can be either a graph or a non-graph. So, both graph and parametric descriptions of the fluid height are considered. At the contact point, a geometric relation is obtained among the attachment angle ϕ_0 , the contact angle γ and the inclination angle ψ_0 ,

$$\psi_0 = \phi_0 + \gamma - \pi. \quad (1.17)$$

Therefore, the uniqueness argument from Elcrat, Neel and Siegel [13] can be applied to the floating ball problem and we conclude that the fluid interface can be uniquely determined by an attachment angle ϕ_0 . Therefore, we can write the parametric solutions as

$$r = r(\psi; \phi_0) \quad \text{and} \quad u = u(\psi; \phi_0). \quad (1.18)$$

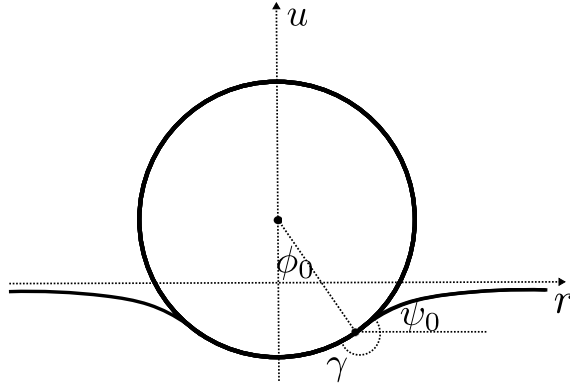


Figure 1.3: A floating ball on an unbounded bath.

The zero solution $u = 0$ is not contained in the parametric form so the graph description of the form

$$u = u(r; r_0, u_0) \quad (1.19)$$

is considered as in Vogel [63]. The initial values (r_0, u_0) determine a unique solution by the comparison theorem. We are also interested in the behavior of the fluid height at the contact point and at infinity. The study of the C^1 smoothness of the fluid height at the contact point u_0 is built on the work of Vogel [63]. Both forms in (1.18) and (1.19) are discussed. As a by-product, we prove Vogel's conjecture on the C^1 smoothness of the envelope of the exterior solutions. Olver's theorem [49] and Levinson's theorem [12] are used in analysis of the limiting behavior of solutions at infinity. The asymptotic forms of parametric solutions $r(\psi; \phi_0)$ and $u(\psi; \phi_0)$ are obtained as $\psi \rightarrow 0$. The limiting behavior of $\dot{r}(\psi; \phi_0)$ and $\dot{u}(\psi; \phi_0)$ is investigated, as well. \dot{r} and \dot{u} mean $\frac{\partial}{\partial \phi_0} r(\psi; \phi_0)$ and $\frac{\partial}{\partial \phi_0} u(\psi; \phi_0)$, respectively. The asymptotic behavior of solutions and their rate of change with respect to the parameter ϕ_0 are then used for analysis of the total force F_T and the total energy E_T . To study the number of equilibrium points and their stability, both force and energy approaches are considered. Forces and energies are classified, see the detailed description in Chapter 3. We establish the relation between the total energy and the total force,

$$\frac{dE_T}{d\phi_0} = -F_T h'(\phi_0), \quad (1.20)$$

where $h(\phi_0) = \cos(\phi_0) + u_0$ is defined as the height of the center. The relation in (1.20) helps us to formulate a stability criterion. To understand the behavior of the total force

and the height curves, both asymptotic analysis and numerical tests are considered. The asymptotic forms of $F_T(\phi_0)$ and $h(\phi_0)$ are investigated for $B \rightarrow 0$, $B \rightarrow \infty$ or $\phi_0 \rightarrow 0, \pi$. In numerical observation, we perform a series of numerical tests with different values of Bond numbers and contact angles. The asymptotic forms are validated, as well. The following conjecture is proposed:

Conjecture. *In the floating ball system, there are at most two force balanced points. If there is only one force balanced point, it is stable. If there are two force balanced points, the one with smaller attachment angle must be stable and the one with larger attachment angle can be either stable or unstable.*

For a given contact angle, the information on the number of equilibria and their stability can be illustrated in a Bond number versus density ratio figure. Several figures with typical contact angles are presented. Finally, we give two examples. One shows a case with two stable equilibrium configurations. Another example shows a case with no force balanced point but there is an energy minimizer. This prompts discussion of the necessary condition of the floating configuration and a modification of changing topological structure for the floating configurations to this example.

In this thesis, the floating ball and two asymptotic problems are studied. The thesis is organized as follows: in Chapter 2, the asymptotic expansion of the capillary surface around a needle cylindrical tube is discussed. In Chapter 3, the floating ball on an unbounded bath is studied. In Chapter 4, we discuss the behavior of the capillary surface in a tilted wedge. Conclusions and future work are summarized in Chapter 5.

Chapter 2

The Asymptotic Expansion of the Capillary Surface for a Needle Cylindrical Tube

2.1 Introduction

In this chapter, we focus on a radially symmetric capillary surface around a cylindrical tube with radius $a > 0$. Let $r = |x|$ be the radial distance, $x \in \Omega = \{(x_1, x_2) \in \mathbb{R}^2, x_1^2 + x_2^2 \geq a^2\}$. Suppose a capillary surface has the form $z = u(r)$ (by symmetry, $u(r)$ can also be treated as the fluid height at r) with the inclination angle ψ satisfying $\sin(\psi) = \frac{u_r}{\sqrt{1 + u_r^2}}$. So, twice the mean curvature of the surface has the form

$$Nu = \frac{u_{rr}}{(1 + u_r^2)^{3/2}} + \frac{u_r}{r\sqrt{1 + u_r^2}} \quad (2.1)$$

or geometrically, if ψ is treated as a function of r , $\psi = \psi(r)$,

$$Nu = \frac{1}{r} (r \sin(\psi(r)))_r. \quad (2.2)$$

Hence, the BVP in (1.3) and (1.4) turns into

$$Nu = \kappa u \quad \text{for } r > a, \quad (2.3)$$

$$\sin(\psi(a)) = -\cos(\gamma) \quad \text{and} \quad \lim_{r \rightarrow \infty} u(r) = 0. \quad (2.4)$$

When $\gamma = \frac{\pi}{2}$, then the fluid height is identically zero, $u = 0$. The $\gamma \in \left(\frac{\pi}{2}, \pi\right]$ case can be converted to the $\gamma \in \left[0, \frac{\pi}{2}\right)$ case through simply replacing u by $-u$. Hence, in this chapter, we restrict

$$\gamma \in \left[0, \frac{\pi}{2}\right). \quad (2.5)$$

By introducing the characteristic length $l_c = a$, we define the dimensionless radial distance and fluid height as $\hat{r} = \frac{r}{a}$ and $\hat{u} = \frac{u}{a}$, respectively. We obtain the dimensionless BVP, as follows,

$$N\hat{u} = B\hat{u} \quad \text{for } \hat{r} > 1, \quad (2.6)$$

$$\sin(\psi(1)) = -\cos(\gamma), \quad (2.7)$$

$$\lim_{\hat{r} \rightarrow \infty} \hat{u}(\hat{r}) = 0, \quad (2.8)$$

where $N\hat{u}$ takes the same form in (2.1) or (2.2), the only difference is the dimensionless variables are being used. $B = \kappa a^2$ is Bond number. (2.7) is known as the contact angle condition.

By scaling, the boundary of the tube becomes $\hat{r} = 1$. A needle tube means the radius of the cylindrical tube $a \rightarrow 0$, equivalently, it implies $B \rightarrow 0$. In the rest of this chapter, we focus on the dimensionless form in (2.6) - (2.8). For simplicity, we define $\epsilon = \sqrt{B}$, rewrite \hat{r} and \hat{u} as r and u , respectively.

The asymptotic expansion of $u(r)$ near the boundary as $\epsilon \rightarrow 0$ has been discussed for decades. The fluid height behaves quite differently near the boundary and far away from the tube. A popular approach is the matched asymptotic expansions method. In this method, the inner expansion (near the boundary) and the outer expansion (far away from the tube) are considered. Two expansions are matched in some overlapped region, see Derjaguin [11], Fraenkel [24], James [32], Van Dyke [60] and Lo [41]. However, Fraenkel [24] pointed out that the matching principle may fail in some cases. Lo [41] remedied Fraenkel's warning in the needle problem by adding a switchback term of order $\mathcal{O}(\epsilon^2 \ln \epsilon)$. She obtained a five-term asymptotic expansion of $u(r)$ up to $\mathcal{O}(\epsilon^2)$. It is accepted as a correct expansion. We truncate her expansion up to $\mathcal{O}(\epsilon^2 \ln^2 \epsilon)$, shown as follows,

$$u(r) = c \ln(\epsilon) + c(\gamma_e - 2 \ln 2) + c \ln \left(r + \sqrt{r^2 - c^2} \right) + \mathcal{O}(\epsilon^2 \ln^2(\epsilon)), \quad (2.9)$$

where γ_e is known as Euler's constant¹ and

$$c = -\cos \gamma. \quad (2.10)$$

$c \in [-1, 0)$ since $\gamma \in \left[0, \frac{\pi}{2}\right)$. In the rest of the chapter, c is defined in (2.10).

Remark 1. We call (2.9) the two-term asymptotic expansion of $u(r)$. $c \ln(\epsilon)$ is the leading term and $c(\gamma_e - 2 \ln 2) + c \ln \left(r + \sqrt{r^2 - c^2} \right)$ is considered as the $\mathcal{O}(1)$ term.

However, Lo's result has not been rigorously proven. Turkington [59] showed $u(1) \sim c \ln(\epsilon)$ as $\epsilon \rightarrow 0$. Siegel [57] modified Turkington's conclusion to $u(1) = c \ln(\epsilon) + \mathcal{O}(1)$. Miersemann [47] proved the expansion in (2.9) with a different bound $\mathcal{O}(\epsilon^{2/5} \ln^2(\epsilon))$ at $r = 1$.

In this chapter, we construct two C^1 , piecewise C^2 , approximate solutions of $u(r)$, $u_1(r)$ and $u_2(r)$. Each of them consists of an inner solution on $[1, q]$ and an outer solution on $[q, \infty)$. q is the transition radius which separates the inner and outer regions. The approximate solution has the form

$$u_i(r) = \begin{cases} u_i^{\text{in}}(r), & 1 \leq r \leq q, \\ u_i^{\text{out}}(r), & r \geq q, \end{cases} \quad (2.11)$$

where $i \in \{1, 2\}$, u_i^{in} is denoted as the inner solution and u_i^{out} is denoted as the outer solution. For inner solutions, u_1^{in} is defined with zero mean curvature and u_2^{in} is defined with constant mean curvature. For outer solutions, u_1^{out} is chosen as the solution of the linearized capillary equation. u_2^{out} is constructed such that it becomes a sub-solution of $u(r)$ in outer region. Both $u_1(r)$ and $u_2(r)$ can be made to be C^1 over the whole domain by matching the conditions at $r = q$,

$$u_i^{\text{in}}(q) = u_i^{\text{out}}(q), \quad (2.12)$$

$$\frac{du_i^{\text{in}}}{dr}(q) = \frac{du_i^{\text{out}}}{dr}(q), \quad (2.13)$$

¹Euler's constant $\gamma_e \approx 0.5772156649$.

where (2.12) is known as the height condition and (2.13) is known as the slope condition. Moreover, we show that $u_1(r)$ is an upper bound and $u_2(r)$ is a lower bound of $u(r)$ on $[1, \infty)$.

We are interested in the asymptotic expansion of $u(r)$ in the inner region as $\epsilon \rightarrow 0$. Two different choices of $u_2^{\text{in}}(q)$ are considered. One of which only makes $u_2^{\text{in}}(r)$ a lower bound of u in the inner region. The other, $u_2(q)$, makes a lower bound for the whole region. We show the inner approximate solutions have the same two-term asymptotic expansion which is the two-term expansion of $u(r)$ but their error bounds are different from Lo's in (2.9). By controlling q , we achieve the optimized error bound, which is equal to $\mathcal{O}(\epsilon(-\ln \epsilon)^{3/2})$. With a modified outer solution, the error bound is improved to $\mathcal{O}(\epsilon^{4/3}(-\ln(\epsilon))^{5/3})$. Comparing with Lo and Miersemann's results, our error bound is better than Miersemann's, $\mathcal{O}(\epsilon^{2/5} \ln^2(\epsilon))$ while it is inferior to Lo's, $\mathcal{O}(\epsilon^2 \ln^2(\epsilon))$, see Lo [41] and Miersemann [47].

Under the construction of the approximate solutions and in analysis of the error bound of the asymptotic expansions, two main tools will be employed. A theorem from Olver [49] is used to determine the optimal choice of q for the error bound. Another is the comparison principle, which is widely used in capillary problems, see [18] and [22]. Two theorems are presented in Section 2.2. The construction of approximate solutions, their asymptotic expansions and error bounds are discussed in Sec. 2.3 and Sec. 2.4. The improved error bound is discussed in Sec. 2.5. The conclusion is made in Sec. 2.6.

2.2 Preliminaries

In this section, we state two theorems which will be used in later analysis. To describe limiting behavior of functions, the following notations are often used, see Olver [49].

- (i) Asymptotic notation \sim . We write $f(x) \sim g(x)$ as $x \rightarrow \alpha$ (or $\alpha = \infty$) if $\lim_{x \rightarrow \alpha} \frac{f(x)}{g(x)} = 1$. In words, f is asymptotic to g .
- (ii) Little o notation. We write $f(x) = o(g(x))$ as $x \rightarrow \alpha$ (or $\alpha = \infty$) if $\lim_{x \rightarrow \alpha} \frac{f(x)}{g(x)} = 0$. In words, f is of order less than g .
- (iii) Big \mathcal{O} notation. We write $f(x) = \mathcal{O}(g(x))$ as $x \rightarrow \alpha$ (or $\alpha = \infty$) if $\left| \frac{f(x)}{g(x)} \right|$ is bounded. In words, f is of order not exceeding g .

We summarize the properties of above notations as follows,

Property 1. If $f_1 \sim g_1$ and $f_2 \sim g_2$ as $x \rightarrow \alpha$ (or $\alpha = \infty$), then

- (i) $f_1 = (1 + o(1))g_1$.
- (ii) $f_1 f_2 \sim g_1 g_2$.
- (iii) If f_2 and g_2 are non-zero in a neighborhood of α , except possibly at α , then $\frac{f_1}{f_2} \sim \frac{g_1}{g_2}$.
- (iv) If $f_1, g_1 > 0$, then $f_1^\beta \sim g_1^\beta$ for $\beta \in \mathbb{R}$.
- (v) If $f_1, g_1 > 0$ and $\lim_{x \rightarrow \alpha} g_1(x) \neq 1$, then $\ln(f_1) \sim \ln(g_1)$.
- (vi) If $\lim_{x \rightarrow \alpha} (f_1 - g_1) = 0$, then $\exp(f_1) \sim \exp(g_1)$.

Olver's theorem [49] is a powerful tool for solving for the root of an equation asymptotically. It will be applied to find the optimal q such that the error bound of the asymptotic expansion is optimized. We restate Olver's theorem in Theorem 2.

Theorem 2 (Olver [49]). *Let $f(\xi)$ be continuous and strictly increasing in an interval $m < \xi < \infty$, and*

$$f(\xi) \sim \xi \quad (\xi \rightarrow \infty).$$

Denote by $\xi(z)$ the root of the equation

$$f(\xi) = z,$$

which lies in (m, ∞) when $z > f(m)$. Then

$$\xi(z) \sim z \quad (z \rightarrow \infty).$$

Another powerful tool is the comparison principle. The comparison principle of Concus and Finn [7] is widely used in study of the behavior of the capillary surfaces. The principle is also valid in an unbounded domain with no condition required at infinity, see Finn and Hwang [22]. We give a proof of the version of the comparison principle for the unbounded domain that fits our problem in Theorem 3.

Theorem 3 (Comparison Principle for the Needle Problem). *Suppose u, v are C^2 functions on $\mathcal{I} = (1, q) \cup (q, \infty)$, $q > 1$ and are C^1 at $r = q$. If*

1. $Nu \geq \epsilon^2 u$ (sub-solution) and $Nv \leq \epsilon^2 v$ (super-solution) on \mathcal{I} .
2. $\sin \psi_v(1) \leq \sin \psi_u(1)$, assume $\psi_v(r)$ and $\psi_u(r)$ are continuous at $r = 1$ or $u(1) \leq v(1)$, assume $u(r)$ and $v(r)$ are continuous at $r = 1$.

then $u \leq v$ on $(1, \infty)$.

Proof. We are going to prove this by contradiction. Suppose there exists some point $p \in (1, \infty)$ such that $u(p) > v(p)$. Let $w(r) = u(r) - v(r)$. So, $w(p) > 0$. Let $\mathcal{S} = (a, b)$ be a maximal interval containing p such that $w(r) > 0$ for all $r \in \mathcal{S}$. In detail, we define

$$b = \sup\{b' \mid w(r) > 0 \text{ on } [p, b']\}. \quad (2.14)$$

If b is finite, then $\forall \delta > 0$, there exists a c_δ , $b < c_\delta < b + \delta$, with $w(c_\delta) \leq 0$. So, $w(b) = \lim_{\delta \rightarrow 0} w(c_\delta) \leq 0$. In addition, $w(b) = \lim_{r \rightarrow b^-} w(r) \geq 0$. It follows that $w(b) = 0$. For a , we define

$$a = \inf\{a' \geq 1 \mid w(r) > 0 \text{ on } (a', p]\}. \quad (2.15)$$

A similar argument gives that if $a > 1$, then $w(a) = 0$ and if $a = 1$, then $w(a) \geq 0$. Next, we will show that such \mathcal{S} cannot exist. So, consider the following possibilities.

- (i) Case 1: $a > 1$ and $b < \infty$. $w > 0$ on \mathcal{S} and $w = 0$ at both a and b . By assumption,

$$Nu - Nv \geq \epsilon^2(u - v). \quad (2.16)$$

Hence,

$$r(u - v)(Nu - Nv) \geq r\epsilon^2(u - v)^2 = \epsilon^2 r w^2 > 0. \quad (2.17)$$

If $q \notin \mathcal{S}$, we integrate from a to b and apply integration by parts,

$$\begin{aligned} 0 &< \int_a^b (u - v) [(r \sin \psi_u)_r - (r \sin \psi_v)_r] dr = - \int_a^b r(u_r - v_r) (\sin \psi_u - \sin \psi_v) dr \\ &= - \int_a^b r \left(\frac{\sin \psi_u}{\sqrt{1 - \sin^2 \psi_u}} - \frac{\sin \psi_v}{\sqrt{1 - \sin^2 \psi_v}} \right) (\sin \psi_u - \sin \psi_v) dr \\ &\leq 0. \end{aligned}$$

If $q \in \mathcal{S}$,

$$\begin{aligned}
0 < \int_a^b (u - v) [(r \sin \psi_u)_r - (r \sin \psi_v)_r] dr &= \int_a^q (u - v) [(r \sin \psi_u)_r - (r \sin \psi_v)_r] dr \\
&\quad + \int_q^b (u - v) [(r \sin \psi_u)_r - (r \sin \psi_v)_r] dr \\
&= - \int_a^q r(u_r - v_r) [\sin \psi_u - \sin \psi_v] dr \\
&\quad - \int_q^b r(u_r - v_r) [\sin \psi_u - \sin \psi_v] dr \\
&\leq 0.
\end{aligned}$$

So, in this case, we cannot have $w > 0$ on \mathcal{S} .

- (ii) Case 2: $a = 1$ and $b < \infty$. $w > 0$ on \mathcal{S} , $w \geq 0$ at a and $w = 0$ at b . From case 1, we can see that the results are the same if q is contained in \mathcal{S} or not. Without loss of generality, we consider $q \notin \mathcal{S}$,

$$\begin{aligned}
\int_a^b (u - v) [(r \sin \psi_u)_r - (r \sin \psi_v)_r] dr &= - (u - v) [r \sin(\psi_u) - r \sin(\psi_v)] |_{a_i=1} \\
&\quad - \int_a^b r(u_r - v_r) [\sin(\psi_u) - \sin(\psi_v)] dr \\
&\leq 0,
\end{aligned}$$

where $-r(u - v) [\sin(\psi_u) - \sin(\psi_v)] |_{a=1} \leq 0$ since, by assumption, we have either case $\sin \psi_v(1) - \sin \psi_u(1) \leq 0$ and $w(1) \geq 0$ or $w(1) = u(1) - v(1) \leq 0$ (which implies $w(1) = 0$). So, in this case, we cannot have $w > 0$ on \mathcal{S} .

- (iii) Case 3: $a \geq 1$ and $b = \infty$. Let $I(\beta) = \epsilon^2 \int_a^\beta r w^2 dr$. So, $I'(\beta) = \epsilon^2 \beta w^2(\beta)$ and from (2.17), it gives

$$\begin{aligned}
I(\beta) &< \int_a^\beta (u-v) [(r \sin \psi_u)_r - (r \sin \psi_v)_r] dr = w(\beta) \beta (\sin \psi_u(\beta) - \sin \psi_v(\beta)) \\
&\quad - (u-v) [r \sin(\psi_u) - r \sin(\psi_v)] \Big|_a \\
&\quad - \int_a^\beta (u_r - v_r) [r \sin(\psi_u) - r \sin(\psi_v)] dr \\
&\leq w(\beta) \beta (\sin \psi_u(\beta) - \sin \psi_v(\beta)) \\
&\leq 2\beta w(\beta) = \frac{2}{\epsilon} \sqrt{\beta} \sqrt{I'(\beta)}.
\end{aligned}$$

Thus,

$$\frac{4}{\epsilon^2} \beta I'(\beta) \geq I^2(\beta). \quad (2.18)$$

After some arrangement,

$$\frac{\epsilon^2}{4} \ln \left(\frac{\beta}{\beta_0} \right) \leq \int_{\beta_0}^\beta \frac{I'(s)}{I^2(s)} ds, \quad (2.19)$$

where $\beta_0 > a$. Therefore, as $\beta \rightarrow \infty$,

$$\infty \leftarrow \frac{\epsilon^2}{4} \ln(\beta) - \frac{\epsilon^2}{4} \ln(\beta_0) \leq -\frac{1}{I(\beta)} + \frac{1}{I(\beta_0)} \leq \frac{1}{I(\beta_0)}. \quad (2.20)$$

So, in this case, we cannot have $w > 0$ on \mathcal{S} .

In summary, there is no such \mathcal{S} exists. So, $u \leq v$ on $(1, \infty)$.

□

2.3 First Approximate Solution: $u_1(r)$

In this section, our aim is to construct a first approximate solution $u_1(r)$ on $[1, \infty)$, which consists of the inner solution $u_1^{\text{out}}(r)$ and the outer solution $u_1^{\text{in}}(r)$, shown as follows,

$$u_1(r) = \begin{cases} u_1^{\text{in}}(r), & 1 \leq r \leq q, \\ u_1^{\text{out}}(r), & r \geq q, \end{cases} \quad (2.21)$$

where q is to be determined. $u_1^{\text{out}}(r)$ and $u_1^{\text{in}}(r)$ are constructed such that both are super-solutions of $u(r)$, see Sec. 2.3.1 and Sec. 2.3.2. $u_1(r)$ can be made to be C^1 over $[1, \infty)$ by matching the conditions at $r = q$.

$$u_1^{\text{in}}(q) = u_1^{\text{out}}(q), \quad (2.22)$$

$$u_{1r}^{\text{in}}(q) = u_{1r}^{\text{out}}(q), \quad (2.23)$$

where (2.22) is known as the height condition and (2.23) is known as the slope condition. Such $u_1(r)$ also gives an upper bound of $u(r)$ on $[1, \infty)$, see Sec. 2.3.3.

In Sec. 2.3.4, we obtain the asymptotic expansion of $u_1(r)$ as $\epsilon \rightarrow 0$, which is the same as the two-term asymptotic expansion of $u(r)$, see [41] and [47]. In Sec. 2.3.5, the choice of q is discussed, which leads to the optimal error bound of the two-term asymptotic expansion of $u_1(r)$. Our optimal error bound is better than Miersemann's while it is inferior to Lo's.

2.3.1 First Approximate Inner Solution: $u_1^{\text{in}}(r)$

Let us start with the geometric form

$$\frac{1}{r} (r \sin \psi)_r = \epsilon^2 u. \quad (2.24)$$

As $\epsilon \rightarrow 0$, the solution $u(r)$ behaves like zero mean curvature solution near the boundary ($r = 1$). Therefore, we consider the zero mean curvature solution as the first approximate inner solution $u_1^{\text{in}}(r)$ on $r \in [1, q]$,

$$Nu_1^{\text{in}} = 0 \quad \Leftrightarrow \quad \frac{1}{r} (r \sin \psi_1^{\text{in}})_r = 0. \quad (2.25)$$

where $\psi_1^{\text{in}} = \psi_1^{\text{in}}(r)$ is the inclination angle of $u_1^{\text{in}}(r)$ and satisfies the inclination angle condition at $r = 1$, see (2.7). Since $Nu_1^{\text{in}} = 0 \leq \epsilon^2 u_1^{\text{in}}$, u_1^{in} satisfies the super-solution condition. Solving (2.25) for $\sin \psi_1^{\text{in}}$, we obtain

$$\sin \psi_1^{\text{in}}(r) = \frac{c}{r}, \quad (2.26)$$

The inclination angle $\psi_1^{\text{in}}(r)$ and the exact inclination angle $\psi(r)$ are comparable. It is showed in Lemma 1.

Lemma 1. *The inclination angle $\psi_1^{\text{in}}(r)$ of the first approximate inner solution and the exact inclination angle $\psi(r)$ are comparable, that is,*

$$\sin \psi_1^{\text{in}}(r) < \sin \psi(r), \quad (2.27)$$

equivalently, $\psi_1^{\text{in}}(r) < \psi(r)$ for $r \in (1, q]$. And at $r = 1$, $\psi_1^{\text{in}}(1) = \psi(1)$.

Proof. With $Nu_1^{\text{in}} = 0 < \epsilon^2 u = Nu$, that is,

$$\frac{1}{r} (r \sin \psi_1^{\text{in}}(r))_r = 0 < \epsilon^2 u = \frac{1}{r} (r \sin \psi(r))_r. \quad (2.28)$$

We multiply r on both sides of (2.28), and integrate from 1 to r , it gives

$$\sin \psi_1^{\text{in}}(r) < \sin \psi(r). \quad (2.29)$$

Equivalently, we have $\psi_1^{\text{in}}(r) < \psi(r)$. At $r = 1$, $\psi_1^{\text{in}}(1) = \psi(1)$ is directly from the contact angle condition. □

Besides the inclination angle ψ_1^{in} , the inner solution $u_1^{\text{in}}(r)$ can be constructed as follows.

(2.26) implies $u_{1r}^{\text{in}}(r) = \tan(\psi_1^{\text{in}}) = \frac{\sin \psi_1^{\text{in}}}{\sqrt{1 - \sin^2 \psi_1^{\text{in}}}}$, thus,

$$u_{1r}^{\text{in}}(r) = \frac{c}{\sqrt{r^2 - c^2}}. \quad (2.30)$$

By integrating from r to q ,

$$u_1^{\text{in}}(q) - u_1^{\text{in}}(r) = \int_r^q \frac{c}{\sqrt{s^2 - c^2}} ds. \quad (2.31)$$

After some calculation, we have

$$u_1^{\text{in}}(r) = c \ln \left(r + \sqrt{r^2 - c^2} \right) + u_1^{\text{in}}(q) - c \ln \left(q + \sqrt{q^2 - c^2} \right), \quad (2.32)$$

where $1 \leq r \leq q$ and $u_1^{\text{in}}(q)$ is to be determined based on the height condition in (2.22).

2.3.2 First Approximate Outer Solution: $u_1^{\text{out}}(r)$

Following Lo [41], the outer variable $R = \epsilon r$ is considered. The capillary equation becomes

$$u_{RR} + \frac{1}{R}u_R(1 + \epsilon^2 u_R^2) = u(1 + \epsilon^2 u_R^2)^{\frac{3}{2}}, \quad (2.33)$$

where $u = u(R)$ and $u_R = \frac{du}{dR}$. As $\epsilon \rightarrow 0$, the solution behaves like the linearized solution. Therefore, we consider the first approximate outer solution $u_1^{\text{out}}(R)$ as the solution of the linearized equation. So,

$$u_{1RR}^{\text{out}} + \frac{1}{R}u_{1R}^{\text{out}} - u_1^{\text{out}} = 0. \quad (2.34)$$

Fortunately, the linearized equation can be solved exactly, combined with the boundary condition $\lim_{R \rightarrow \infty} u_1^{\text{out}}(R) = 0$, we obtain

$$u_1^{\text{out}}(R) = A_1 K_0(R), \quad (2.35)$$

where $K_0(R)$ is known as the modified Bessel function of the second kind of order 0. The coefficient A_1 is to be determined by the slope condition in (2.23). Moreover, u_1^{out} is a super-solution of u , see Siegel [57].

Remark 2. Since $R = \epsilon r$, we also write $u_1^{\text{out}}(r) = A_1 K_0(\epsilon r)$.

2.3.3 C^1 First Approximate Solution: $u_1(r)$

In this section, the C^1 first approximate solution $u_1(r)$ is constructed by matching the inner $u_1^{\text{in}}(r)$ and the outer $u_1^{\text{out}}(r)$ solutions at $r = q$ with two conditions in (2.22) and (2.23). Combining $u_1^{\text{in}}(r)$ and $u_1^{\text{out}}(r)$ together, (2.21) gives

$$u_1(r) = \begin{cases} c \ln(r + \sqrt{r^2 - c^2}) + u_1^{\text{in}}(q) - c \ln(q + \sqrt{q^2 - c^2}), & \text{if } 1 \leq r \leq q, \\ A_1 K_0(\epsilon r), & \text{if } r \geq q. \end{cases} \quad (2.36)$$

With conditions in (2.22) and (2.23), A_1 and $u_1^{\text{in}}(q)$ can be determined. In particular, the slope condition gives

$$\frac{c}{\sqrt{q^2 - c^2}} = -A_1 \epsilon K_1(\epsilon q). \quad (2.37)$$

Thus,

$$A_1 = -\frac{c}{\epsilon K_1(\epsilon q) \sqrt{q^2 - c^2}}. \quad (2.38)$$

Moreover, by matching the height at $r = q$,

$$u_1^{\text{in}}(q) = A_1 K_0(\epsilon q). \quad (2.39)$$

Therefore, with the choice of $u_1^{\text{in}}(q)$ in (2.39), $u_1(r)$ in (2.36) gives a C^1 first approximate solution over $[1, \infty)$.

Since $u_1(r)$ satisfies the conditions on Theorem 3 (comparison principle), we address the following Theorem 4,

Theorem 4. $u_1(r)$ defined in (2.36) is an upper bound of $u(r)$ on $[1, \infty)$.

2.3.4 Asymptotic Expansion of the First Approximate Solution $u_1(r)$ as $\epsilon \rightarrow 0$

In this section, we are interested in the asymptotic expansion of $u_1(r)$ near the boundary as $\epsilon \rightarrow 0$, $q \rightarrow \infty$ and $\epsilon q \rightarrow 0$. Since we focus on the inner region, $r \in [1, q]$,

$$u_1(r) = u_1^{\text{in}}(r). \quad (2.40)$$

When $u_1(r)$ is expanded, the following Lemma 2 is useful.

Lemma 2. With $\epsilon \rightarrow 0$, $q \rightarrow \infty$ and $\epsilon q \rightarrow 0$, A_1 and $u_1^{\text{in}}(q)$, defined in (2.38) and (2.39), respectively, can be expanded as follows,

$$A_1 = -c + \frac{c}{2}(\epsilon q)^2 \ln(\epsilon q) - \frac{c^3}{2q^2} + \mathcal{O}(\epsilon^2 \ln(\epsilon q)), \quad (2.41)$$

$$u_1^{\text{in}}(q) = c \ln(\epsilon q) + c(\gamma_e - \ln 2) + \mathcal{O}(\Delta), \quad (2.42)$$

where γ_e is known as Euler's constant and

$$\Delta = (\epsilon q)^2 \ln^2(\epsilon q) - \frac{1}{q^2} \ln(\epsilon q). \quad (2.43)$$

Proof. $u_1^{\text{in}}(q)$ can be written down as

$$u_1^{\text{in}}(q) = A_1 K_0(\epsilon q) = -c \left(\frac{K_0(\epsilon q)}{\epsilon q K_1(\epsilon q)} \right) \left(\frac{q}{\sqrt{q^2 - c^2}} \right).$$

And the asymptotic expansions of A_1 and $u_1^{\text{in}}(q)$ are straightforward based on Appendix A.1. Moreover, the error bound of $u_1^{\text{in}}(q)$ in (2.42) is $\mathcal{O}\left(-\frac{c}{2}(\epsilon q)^2 \ln^2(\epsilon q) + \frac{c^3}{2q^2} \ln(\epsilon q)\right)$. Since the worst case occurs when $c = -1$, therefore, the error bound can be simplified to $\mathcal{O}(\Delta)$. \square

Therefore, combined with Lemma 2 and Appendix A.1, the asymptotic expansion of the first approximate solution $u_1(r)$ in the inner region has the form

$$\begin{aligned} u_1(r) &= c \ln\left(r + \sqrt{r^2 - c^2}\right) + u_1^{\text{in}}(q) - c \ln\left(q + \sqrt{q^2 - c^2}\right) \\ &= c \ln(\epsilon) + c(\gamma_e - 2 \ln 2) + c \ln\left(r + \sqrt{r^2 - c^2}\right) + \mathcal{O}(\Delta), \end{aligned} \quad (2.44)$$

where Δ is defined in (2.43). The asymptotic expansion of $u_1(r)$ gives the same two-term asymptotic expansion of $u(r)$ as $\epsilon \rightarrow 0$, see [41] and [47]. Moreover, the error bound Δ defined in (2.43) is unspecified. The optimal error bound $\mathcal{O}(\Delta)$ can be obtained by choosing q . The details will be discussed in Section 2.3.5.

2.3.5 Optimal Choice of q

In this section, we discuss the optimal error bound $\mathcal{O}(\Delta)$ as $\epsilon \rightarrow 0$, $q \rightarrow \infty$ and $\epsilon q \rightarrow 0$. Our idea is to find the best choice of q , say q^* , which leads to the optimal error bound $\mathcal{O}(\Delta)$. Two approaches will be presented. The main tool employed is Theorem 2 (Olver [49]).

One of our approaches is to minimize Δ with respect to q . Let $x = \frac{1}{\epsilon q}$, Δ can be converted to

$$\Delta = \frac{1}{x^2} \ln^2(x) + \epsilon^2 x^2 \ln(x). \quad (2.45)$$

We differentiate Δ with respect to x , denoted as Δ' ,

$$\Delta' = -\frac{1}{x^3} (2 \ln^2(x) - 2 \ln(x) - 2\epsilon^2 x^4 \ln(x) - \epsilon^2 x^4). \quad (2.46)$$

Since $\epsilon q \rightarrow 0$ implies $x \rightarrow \infty$, we are interested in the root of Δ' for the large x . With ϵ fixed and small, there is exactly one root, say x^* . Moreover, suppose x is near x^* , when $x < x^*$, $\Delta' < 0$ and when $x > x^*$, $\Delta' > 0$. Hence, x^* minimizes Δ . To find x^* , we require

$$2 \ln^2(x) - 2 \ln(x) - 2\epsilon^2 x^4 \ln(x) - \epsilon^2 x^4 = 0. \quad (2.47)$$

Let $\xi = \ln(x)$, hence, $\xi \rightarrow \infty$ as $x \rightarrow \infty$. Thus, (2.47) becomes

$$\frac{2\xi(\xi - 1)}{e^{4\xi}(2\xi + 1)} = \epsilon^2. \quad (2.48)$$

Rearranging (2.48),

$$f_1(\xi) = z_1, \quad (2.49)$$

where

$$f_1(\xi) = \xi - \frac{1}{4} \ln \left(\frac{2\xi(\xi - 1)}{2\xi + 1} \right), \quad (2.50)$$

$$z_1 = -\frac{1}{2} \ln(\epsilon). \quad (2.51)$$

In addition, $f_1(\xi)$ is continuous and strictly increasing on $2 < \xi < \infty$, and $f_1(\xi) \sim \xi$ as $\xi \rightarrow \infty$. Hence, Theorem 2 can be applied to (2.49), we have

$$\xi(z_1) \sim z_1. \quad (2.52)$$

Equivalently, we have $\xi(z_1) = (1 + o(1))z_1$. In detail, (2.49) and (2.52) give

$$\begin{aligned} \xi(z_1) &= z_1 + \frac{1}{4} \ln \left(\frac{2\xi(\xi - 1)}{2\xi + 1} \right) \\ &= z_1 + \frac{1}{4} \ln \left(\frac{2z_1(z_1 - 1)}{2z_1 + 1} \right) + o(1). \end{aligned} \quad (2.53)$$

Transforming back to x , we have

$$x = e^{z_1} e^{\frac{1}{4} \ln \left(\frac{2z_1(z_1 - 1)}{2z_1 + 1} \right)} (1 + o(1)). \quad (2.54)$$

Transforming back to ϵq , we obtain the optimal q , denoted as q^* ,

$$q^* = \frac{1}{\sqrt{\epsilon}} \left(z_1 - \frac{3z_1}{2z_1 + 1} \right)^{-1/4} (1 + o(1)), \quad (2.55)$$

where $z_1 = -\frac{1}{2} \ln(\epsilon)$.

Asymptotically, we have

$$\begin{aligned}
q^* &\sim \frac{1}{\sqrt{\epsilon}} \left(-\frac{1}{2} \ln(\epsilon) - \frac{3}{2} \right)^{-1/4} \\
&\sim \frac{1}{\sqrt{\epsilon}} \left(-\frac{1}{2} \ln(\epsilon) \right)^{-1/4},
\end{aligned} \tag{2.56}$$

$$\epsilon q^* \sim \sqrt{\epsilon} \left(-\frac{1}{2} \ln(\epsilon) \right)^{-1/4} \tag{2.57}$$

and

$$\begin{aligned}
\ln(\epsilon q^*) &\sim \frac{1}{2} \ln(\epsilon) - \frac{1}{4} \ln \left(-\frac{1}{2} \ln \epsilon \right) \\
&\sim \frac{1}{2} \ln(\epsilon).
\end{aligned} \tag{2.58}$$

Combining (2.56) - (2.58), with the optimal q^* , we have

$$\Delta \sim \epsilon \left(-\frac{1}{2} \ln \epsilon \right)^{3/2}. \tag{2.59}$$

Therefore, the optimal error bound becomes

$$\mathcal{O}(\Delta) = \mathcal{O} \left(\epsilon (-\ln \epsilon)^{3/2} \right), \tag{2.60}$$

where the coefficient $\left(\frac{1}{2} \right)^{3/2}$ is absorbed in big \mathcal{O} notation.

Another approach is to consider the same asymptotic order of both terms in Δ , since we are interested in $\mathcal{O}(\Delta)$. Neglecting the constant coefficients, it leads to the following transcendental (2.61) for q , by solving that can be treated as the best choice of q .

$$-(\epsilon q)^2 \ln(\epsilon q) = \frac{1}{q^2}. \tag{2.61}$$

Using the similar change of variable, let $x = \frac{1}{\epsilon q}$, (2.61) can be converted to

$$\ln(x) = \epsilon^2 x^4. \quad (2.62)$$

If ϵ is fixed, (2.62) has two roots. One is near $x = 1$, but we are interested in the root for large x , since we require $\epsilon q \rightarrow 0$. Therefore, we take $\ln(\cdot)$ and substitute $\xi = \ln(x)$ in (2.62), it leads

$$f_2(\xi) = z_2. \quad (2.63)$$

where

$$f_2(\xi) = \xi - \frac{1}{4} \ln(\xi), \quad (2.64)$$

$$z_2 = -\frac{1}{2} \ln(\epsilon). \quad (2.65)$$

$f_2(\xi)$ is continuous and strictly increasing on $(e^{\frac{1}{4}}, \infty)$. Moreover, with $\xi \rightarrow \infty$ and $z_2 \rightarrow \infty$ (since $x \rightarrow \infty$ and $\epsilon \rightarrow 0$), (2.63) satisfies the conditions for Theorem 2, thus,

$$\xi \sim z_2. \quad (2.66)$$

Equivalently, we have $\xi(z_2) = (1 + o(1))z_2$. In detail,

$$\xi(z_2) = z_2 + \frac{1}{4} \ln(z_2) + o(1). \quad (2.67)$$

(2.67) implies,

$$x = e^{\xi(z_2)} = z_2^{\frac{1}{4}} e^{z_2} e^{o(1)}, \quad (2.68)$$

where $e^{o(1)} = 1 + o(1)$. Moreover, transforming back to ϵq ,

$$\begin{aligned} \epsilon q^* &= \frac{1}{x} = e^{-\xi(z_2)} \\ &= \sqrt{\epsilon} \left(-\frac{1}{2} \ln(\epsilon) \right)^{-\frac{1}{4}} (1 + o(1)), \end{aligned} \quad (2.69)$$

Therefore, the optimal q^* is chosen as

$$q^* = \frac{1}{\sqrt{\epsilon}} \left(-\frac{1}{2} \ln(\epsilon) \right)^{-\frac{1}{4}} (1 + o(1)). \quad (2.70)$$

With the best choice q^* , we have

$$\begin{aligned} \ln(\epsilon q^*) &= \ln \left(\sqrt{\epsilon} \left(-\frac{1}{2} \ln(\epsilon) \right)^{-\frac{1}{4}} (1 + o(1)) \right) \\ &= \frac{1}{2} \ln(\epsilon) - \frac{1}{4} \ln \left(-\frac{1}{2} \ln(\epsilon) \right) + o(1). \end{aligned} \quad (2.71)$$

Asymptotically,

$$\epsilon q^* \sim \sqrt{\epsilon} \left(-\frac{1}{2} \ln(\epsilon) \right)^{-\frac{1}{4}} \quad \text{and} \quad \ln(\epsilon q^*) \sim \frac{1}{2} \ln(\epsilon). \quad (2.72)$$

Thus, the optimal error bound becomes

$$\mathcal{O}(\Delta) = \mathcal{O} \left(\epsilon (-\ln \epsilon)^{3/2} \right), \quad (2.73)$$

which is the same as the error bound in (2.60). Hence, two approaches give the same optimal error bound.

Therefore, we can summarize the above results in Theorem 5.

Theorem 5. *With the optimal choice of q ,*

$$q^* = \frac{1}{\sqrt{\epsilon}} \left(-\frac{1}{2} \ln(\epsilon) \right)^{-\frac{1}{4}} (1 + o(1)), \quad (2.74)$$

then the optimal error bound $\mathcal{O}(\Delta)$ becomes $\mathcal{O} \left(\epsilon (-\ln \epsilon)^{3/2} \right)$.

With the optimal error bound $\mathcal{O}(\Delta)$, the asymptotic expansion of $u_1(r)$ becomes

$$u_1(r) = c \ln(\epsilon) + c(\gamma_e - 2 \ln 2) + c \ln \left(r + \sqrt{r^2 - c^2} \right) + \mathcal{O} \left(\epsilon (-\ln(\epsilon))^{\frac{3}{2}} \right) \quad (2.75)$$

as $\epsilon \rightarrow 0$.

2.4 Second Approximate Solution: $u_2(r)$

In this section, similar to the first approximate solution $u_1(r)$, we construct a second approximate solution $u_2(r)$ on $[1, \infty)$, which consists of an inner solution and an outer solution. However, the construction of the second approximate solution $u_2(r)$ is more complicated. One potential inner solution, denoted as $\underline{u}_2^{\text{in}}$, is obtained from the one-step iteration based on the first inner solution,

$$N\underline{u}_2^{\text{in}} = \epsilon^2 u_1^{\text{in}}. \quad (2.76)$$

While the form of $\underline{u}_2^{\text{in}}$ makes it difficult to analyze, see Sec. 2.4.1. Another choice has a simpler form, denoted as u_2^{in} . Motivated from (2.76), instead of taking all values of u_1^{in} , only $u_1^{\text{in}}(1)$ is used,

$$Nu_2^{\text{in}} = \epsilon^2 u_1^{\text{in}}(1), \quad (2.77)$$

Hence, u_2^{in} has constant mean curvature, see Sec. 2.4.2. In Section 2.4.3, we discuss choice of height of u_2^{in} at $r = q$ such that the second inner solution u_2^{in} becomes a lower bound of $u(r)$ on $[1, q]$. Moreover, with such choice of $u_2^{\text{in}}(q)$, the second inner solution $u_2^{\text{in}}(r)$ gives the same two-term asymptotic expansion which is the two-term expansion of $u(r)$ and its error bound is the same as the error bound of u_1^{in} , see Sec. 2.4.4.

We define a second approximate solution

$$u_2(r) = \begin{cases} u_2^{\text{in}}(r), & 1 \leq r \leq q, \\ u_2^{\text{out}}(r), & r \geq q. \end{cases} \quad (2.78)$$

The outer solution, denoted as $u_2^{\text{out}}(r)$, is determined by the sub-solution condition, see Sec. 2.4.5. In section 2.4.6, another $u_2^{\text{in}}(q)$ is discussed. With a new height and the slope

conditions at $r = q$, $u_2(r)$ becomes a C^1 , piecewise C^2 , lower bound of $u(r)$ over $[1, \infty)$. In Sec. 2.4.7, we show the two-term asymptotic expansions of $u_1(r)$ and $u_2(r)$ are the same which is the two-term expansion of $u(r)$. The error bound we obtained is better than Miersemann's while it is inferior to Lo's.

2.4.1 One-step Iteration for the Inner Solution: $\underline{u}_2^{\text{in}}(r)$

The iterative procedure has been discussed in capillary problems. Gordon and Siegel [29] applied the iterative procedure to approximate the solution for the annular problem. The iteration is also used to study the asymptotic behavior of the exterior capillary surface for the needle problem, see Siegel [57] and Miersemann [47].

A potential second approximate inner solution is defined based on a one-step iterative procedure, denoted as $\underline{u}_2^{\text{in}}(r)$, shown as follows,

$$N\underline{u}_2^{\text{in}} = \epsilon^2 u_1^{\text{in}} \quad \text{for } 1 \leq r \leq q. \quad (2.79)$$

We denote $\underline{\psi}_2^{\text{in}}(r)$ as the inclination angle of $\underline{u}_2^{\text{in}}(r)$, (2.79) becomes

$$\frac{1}{r} \left(r \sin \underline{\psi}_2^{\text{in}} \right)_r = \epsilon^2 u_1^{\text{in}}, \quad (2.80)$$

where $\underline{\psi}_2^{\text{in}}(1)$ is chosen to satisfy the contact angle condition in (2.7).

(2.80) implies

$$\sin \underline{\psi}_2^{\text{in}}(r) = \frac{c}{r} + \frac{\epsilon^2}{r} \int_1^r s u_1^{\text{in}}(s) ds. \quad (2.81)$$

The integral term in (2.81) can be calculated explicitly. Therefore,

$$\begin{aligned}
\sin \underline{\psi}_2^{\text{in}}(r) &= \frac{c}{r} - \frac{\epsilon^2 c}{4} \left(\sqrt{r^2 - c^2} + \frac{(c^2 - 2r^2)}{r} \ln \left(r + \sqrt{r^2 - c^2} \right) \right) \\
&\quad + \frac{\epsilon^2 c}{4} \left(\sqrt{1 - c^2} + (c^2 - 2) \ln \left(1 + \sqrt{1 - c^2} \right) \right) \left(\frac{1}{r} \right) \\
&\quad + \frac{\epsilon^2}{2} \left(u_1^{\text{in}}(q) - c \ln \left(q + \sqrt{q^2 - c^2} \right) \right) \left(\frac{r^2 - 1}{r} \right). \tag{2.82}
\end{aligned}$$

Moreover,

$$\underline{u}_{2r}^{\text{in}}(r) = \tan \underline{\psi}_2^{\text{in}}(r) = \frac{\sin \underline{\psi}_2^{\text{in}}(r)}{\sqrt{1 - \sin^2 \underline{\psi}_2^{\text{in}}(r)}}. \tag{2.83}$$

Therefore, we obtain the integral representation of $\underline{u}_2^{\text{in}}(r)$,

$$\underline{u}_2^{\text{in}}(r) = \underline{u}_2^{\text{in}}(q) - \int_r^q \frac{\sin \underline{\psi}_2^{\text{in}}(s)}{\sqrt{1 - \sin^2 \underline{\psi}_2^{\text{in}}(s)}} ds, \tag{2.84}$$

where the choice of $\underline{u}_2^{\text{in}}(q)$ will be discussed in Section 2.4.3.

However, due to the complicated expression of $\sin \underline{\psi}_2^{\text{in}}(r)$, it is challenging to analyze the asymptotic expansion of $\underline{u}_2^{\text{in}}(r)$ for small Bond number. We come up with a simpler choice of the second approximate inner solution, shown below in Section 2.4.2.

2.4.2 Constant Mean Curvature Solution: $u_2^{\text{in}}(r)$

The consideration of a constant mean curvature equation is motivated by the inner solution $\underline{u}_2^{\text{in}}(r)$ based on the one-step iterative procedure discussed in Section 2.4.1. Instead of using all values of u_1^{in} , only its maximum is considered, that is $u_1^{\text{in}}(1)$. We denote $\epsilon^2 u_1^{\text{in}}(1)$ as $D(\epsilon, q^*)$, where the optimal q^* is used, see Theorem 5. We construct a second approximate inner solution $u_2^{\text{in}}(r)$,

$$Nu_2^{\text{in}} = \epsilon^2 u_1^{\text{in}}(1) = D(\epsilon, q^*). \tag{2.85}$$

u_2^{in} is defined with constant mean curvature $D(\epsilon, q^*)$. We denote the inclination angle of $u_2^{\text{in}}(r)$ as ψ_2^{in} , where ψ_2^{in} satisfies the contact angle condition in (2.7), as well. Solving (2.85), we have

$$\sin \psi_2^{\text{in}}(r) = \frac{c}{r} + D(\epsilon, q^*) \frac{r^2 - 1}{2r} \quad \text{for } 1 \leq r \leq q^*. \quad (2.86)$$

Moreover, we can solve for $u_2^{\text{in}}(r)$. With

$$u_{2r}^{\text{in}} = \tan \psi_2^{\text{in}}(r) = \frac{\sin \psi_2^{\text{in}}(r)}{\sqrt{1 - \sin^2 \psi_2^{\text{in}}(r)}}, \quad (2.87)$$

we have

$$u_2^{\text{in}}(r) = u_2^{\text{in}}(q) - \int_r^q \frac{\sin \psi_2^{\text{in}}(s)}{\sqrt{1 - \sin^2 \psi_2^{\text{in}}(s)}} ds, \quad (2.88)$$

where $q = q^*$ and $u_2^{\text{in}}(q)$ has two different choices, which will be discussed in Section 2.4.3 and Section 2.4.6.

The following Lemma 3 shows the relation between the inclination angle $\psi_2^{\text{in}}(r)$ of the inner solution $\underline{u}_2^{\text{in}}(r)$, the inclination angle $\psi_2^{\text{in}}(r)$ of the inner solution $u_2^{\text{in}}(r)$, and the exact inclination angle $\psi(r)$. Lemma 3 also illustrates the comparability among $u(r)$, $\underline{u}_2^{\text{in}}(r)$ and $u_2^{\text{in}}(r)$.

Lemma 3. *For $r \in [1, q]$, the inclination angle $\psi_2^{\text{in}}(r)$ of the inner solution $\underline{u}_2^{\text{in}}(r)$, the inclination angle $\psi_2^{\text{in}}(r)$ of the inner solution $u_2^{\text{in}}(r)$, and the exact inclination angle $\psi(r)$ are comparable, shown below*

$$\sin \psi(r) < \sin \underline{\psi}_2^{\text{in}}(r) < \sin \psi_2^{\text{in}}(r), \quad (2.89)$$

where $r \in (1, q]$. And at $r = 1$, $\underline{\psi}_2^{\text{in}}(1) = \psi_2^{\text{in}}(1) = \psi(1)$. Moreover,

$$u(q) - u(r) < \underline{u}_2^{\text{in}}(q) - \underline{u}_2^{\text{in}}(r). \quad (2.90)$$

$\underline{u}_2^{\text{in}}(r)$ and $u_2^{\text{in}}(r)$ are comparable if we assume $\underline{u}_2^{\text{in}}(q) = u_2^{\text{in}}(q)$, then

$$u_2^{\text{in}}(r) < \underline{u}_2^{\text{in}}(r). \quad (2.91)$$

Proof. At $r = 1$, inclination angles are required to satisfy the contact angle condition. Hence,

$$\underline{\psi}_2^{\text{in}}(1) = \psi_2^{\text{in}}(1) = \psi(1).$$

For $r \in (1, q]$, from (2.76),

$$N\underline{u}_2^{\text{in}} = \epsilon^2 u_1^{\text{in}} > \epsilon^2 u(r) = Nu$$

and (2.85) gives

$$Nu_2^{\text{in}} = \epsilon^2 u_1^{\text{in}}(1) > \epsilon^2 u_1^{\text{in}} = N\underline{u}_2^{\text{in}}.$$

Similar to Lemma 1, the above two inequalities lead to

$$\sin \psi(r) < \sin \underline{\psi}_2^{\text{in}}(r) < \sin \psi_2^{\text{in}}(r).$$

To show (2.91), we make use of the result in (2.89),

$$\tan(\psi(r)) < \tan(\psi_2^{\text{in}}(r)).$$

It is equivalent to

$$u_r(r) < u_{2r}^{\text{in}}(r).$$

Integrating from r to q ,

$$u(q) - u(r) < u_2^{\text{in}}(q) - u_2^{\text{in}}(r).$$

A similar argument leads to (2.91). □

We cannot compare $u(r)$ and $u_2^{\text{in}}(r)$ in (2.90) without the choice of $u_2^{\text{in}}(q)$. In the next section, the choice of $u_2^{\text{in}}(q)$ is presented in order to make $u_2^{\text{in}}(r)$ as a lower bound of $u(r)$ over $r \in [1, q]$.

2.4.3 Choice of $u_2^{\text{in}}(q)$

In this section, our goal is to define $u_2^{\text{in}}(q)$ such that $u_2^{\text{in}}(r)$ becomes a lower bound of $u(r)$ over $r \in [1, q]$. Recall the inequality in (2.89) of Lemma 3, at $r = q$,

$$\sin \psi(q) < \sin \psi_2^{\text{in}}(q). \quad (2.92)$$

In the outer region $r \in [q, \infty)$, based on the argument from Siegel [57], let $w(r) = A_{\text{vol}} K_0(\epsilon r)$ and $A_{\text{vol}} = \frac{-\sin \psi(q)}{\epsilon K_1(\epsilon q)}$, where A_{vol} is chosen such that $w(r)$ admits the correct volume² as $u(r)$ over $r \in [q, \infty)$, that is,

$$\int_q^\infty r w(r) dr = \int_q^\infty r u(r) dr = -\frac{1}{\epsilon^2} q \sin \psi(q). \quad (2.93)$$

Moreover, $w(r)$ is a super-solution of $u(r)$ in the outer region. $w(r)$ satisfies $w(q) < u(q)$ and intersects with $u(r)$ at the exactly one point, see Siegel [57].

We choose $u_2^{\text{in}}(q)$ by replacing $\sin \psi(q)$ by $\sin \psi_2^{\text{in}}(q)$ in A_{vol} and denote the expression as $v_1(q)$,

$$u_2^{\text{in}}(q) = \frac{-\sin \psi_2^{\text{in}}(q)}{\epsilon K_1(\epsilon q)} K_0(\epsilon q) = v_1(q), \quad (2.94)$$

and therefore $u_2^{\text{in}}(q) < w(q) < u(q)$, see Fig. 2.1.

In Fig. 2.1, it shows the comparison among $w(q)$, $u(q)$ and $u_2^{\text{in}}(q)$.

Therefore, with such choice of $u_2^{\text{in}}(q)$, we obtain a lower bound inner solution based on (2.90), shown in the following Lemma 4.

Lemma 4. *With the choice $u_2^{\text{in}}(q) = v_1(q)$ defined in (2.94), the second approximate inner solution $u_2^{\text{in}}(r)$ defined in (2.88) gives a lower bound of $u(r)$ on $r \in [1, q]$.*

$$u_2^{\text{in}}(r) < u(r). \quad (2.95)$$

²The volume means the liquid volume lifted up or pushed down from the reference level.

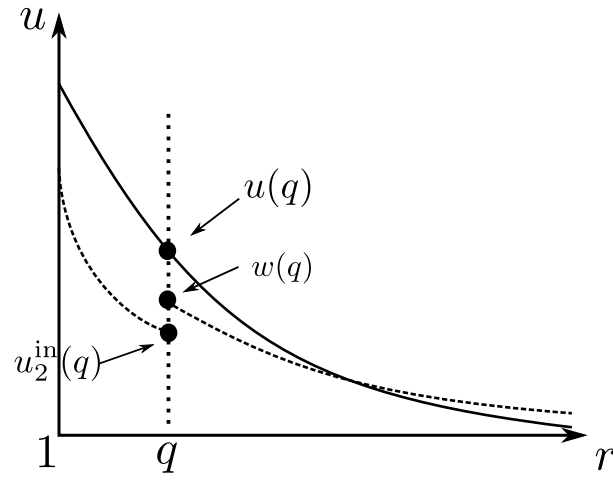


Figure 2.1: The comparison among $w(q)$, $u(q)$ and $u_2^{\text{in}}(q)$.

The following Fig. 2.2 shows the comparison among $u_1^{\text{in}}(r)$, $u_2^{\text{in}}(r)$ and $u(r)$ in the inner region.

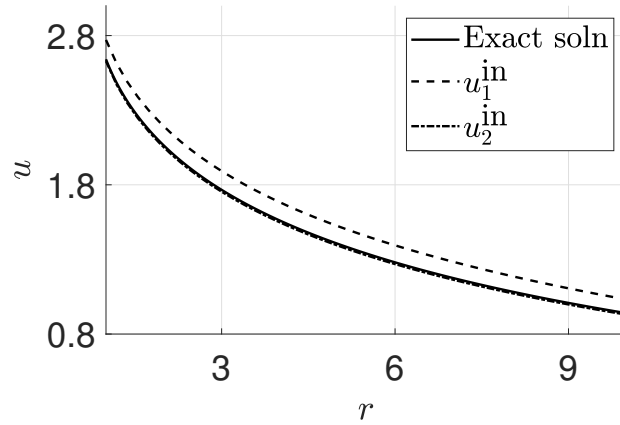


Figure 2.2: The comparison among $u_1^{\text{in}}(r)$, $u_2^{\text{in}}(r)$ and $u(r)$ in the inner region with $\epsilon = \sqrt{0.001}$, $\gamma = \frac{\pi}{4}$ and $q = 10$.

2.4.4 Asymptotic Expansion of the Second Approximate Inner Solution: $u_2^{\text{in}}(r)$

Similar to the work in Section 2.3.4, we investigate the asymptotic expansion of the second approximate inner solution $u_2^{\text{in}}(r)$ as $\epsilon \rightarrow 0$, $q \rightarrow \infty$ and $\epsilon q \rightarrow 0$, where the optimal q is chosen, see (2.74) in Theorem 5 and $u_2^{\text{in}}(q)$ defined in Lemma 4. Recall the expression of $u_2^{\text{in}}(r)$,

$$u_2^{\text{in}}(r) = u_2^{\text{in}}(q) - \int_r^q \frac{\sin \psi_2^{\text{in}}(s)}{\sqrt{1 - \sin^2 \psi_2^{\text{in}}(s)}} ds. \quad (2.96)$$

At first, we analyze the asymptotic expansion of $u_2^{\text{in}}(q)$, which contains $\sin \psi_2^{\text{in}}(q)$ defined in (2.86), see Lemma 5.

Lemma 5. *With the optimal choice of q defined in (2.74) in Theorem 5 and $u_2^{\text{in}}(q)$ defined in Lemma 4, as $\epsilon \rightarrow 0$, we have*

$$\sin \psi_2^{\text{in}}(q) = \frac{c}{q} + \mathcal{O}\left(\epsilon^{3/2} (-\ln(\epsilon))^{3/4}\right), \quad (2.97)$$

$$u_2^{\text{in}}(q) = c \ln(\epsilon q) + c(\gamma_e - \ln 2) + \mathcal{O}\left(\epsilon (-\ln \epsilon)^{3/2}\right). \quad (2.98)$$

Proof. With $q = q^*$ in (2.74), we have $q = \frac{1}{\sqrt{\epsilon}} \left(-\frac{1}{2} \ln(\epsilon)\right)^{-1/4} (1 + o(1))$. Recall that $\sin \psi_2^{\text{in}}(q)$ in (2.86),

$$\sin \psi_2^{\text{in}}(q) = \frac{c}{q} + D(\epsilon, q^*) \frac{q^2 - 1}{2q},$$

where $D(\epsilon, q^*) = \epsilon^2 u_1^{\text{in}}(1)$. Asymptotically, we have

$$D(\epsilon, q^*) \sim c\epsilon^2 \ln(\epsilon), \quad (2.99)$$

$$D(\epsilon, q^*) \frac{q^2 - 1}{2q} \sim -c\epsilon^{3/2} \left(-\frac{1}{2} \ln(\epsilon)\right)^{3/4}. \quad (2.100)$$

Hence, we have

$$\sin \psi_2^{\text{in}}(q) = \frac{c}{q} + \mathcal{O}\left(\epsilon^{3/2}(-\ln(\epsilon))^{3/4}\right).$$

$u_2^{\text{in}}(q)$ can be separated into

$$\begin{aligned} u_2^{\text{in}}(q) &= \frac{-\sin \psi_2^{\text{in}}(q)}{\epsilon K_1(\epsilon q)} K_0(\epsilon q) \\ &= -\left(c + D(\epsilon, q^*) \frac{q^2 - 1}{2}\right) \frac{K_0(\epsilon q)}{\epsilon q K_1(\epsilon q)}. \end{aligned} \quad (2.101)$$

Combined with Appendix A.1, we obtain

$$u_2^{\text{in}}(q) = c \ln(\epsilon q) + c(\gamma_\epsilon - \ln 2) + \mathcal{O}\left(\epsilon(-\ln \epsilon)^{3/2}\right).$$

□

In order to analyze the integral part of (2.96), we consider the Taylor expansion of a function $\frac{x}{\sqrt{1-x^2}}$ about $x = x_0$:

$$\frac{x}{\sqrt{1-x^2}} = \frac{x_0}{\sqrt{1-x_0^2}} + \frac{x-x_0}{(1-x_0^2)^{3/2}} + \mathcal{O}\left((x-x_0)^2\right). \quad (2.102)$$

In our case, we expand $\sin \psi_2^{\text{in}}(r)$ around $\frac{c}{r}$,

$$\frac{\sin \psi_2^{\text{in}}(r)}{\sqrt{1 - \sin^2 \psi_2^{\text{in}}(r)}} = \frac{c/r}{\sqrt{1 - (c/r)^2}} + \frac{1}{(1 - (c/r)^2)^{3/2}} D(\epsilon, q^*) \frac{r^2 - 1}{2r} + \mathcal{O}\left(\left(D(\epsilon, q^*) \frac{r^2 - 1}{2r}\right)^2\right). \quad (2.103)$$

Therefore, we expand the integral part of (2.96),

$$\begin{aligned} \int_r^q \frac{\sin \psi_2^{\text{in}}(s)}{\sqrt{1 - \sin^2 \psi_2^{\text{in}}(s)}} ds &= \int_r^q \frac{c}{\sqrt{s^2 - c^2}} ds + D(\epsilon, q^*) g(r; c) \\ &\quad + \mathcal{O}\left(\int_r^q \left(D(\epsilon, q^*) \frac{s^2 - 1}{2s}\right)^2 ds\right), \end{aligned} \quad (2.104)$$

where

$$\int_r^q \frac{c}{\sqrt{s^2 - c^2}} ds = -c \ln \left(r + \sqrt{r^2 - c^2} \right) + c \ln \left(q + \sqrt{q^2 - c^2} \right), \quad (2.105)$$

$$g(r; c) = \int_r^q \left(\frac{s^2 - 1}{2s} \right) \left(\frac{1}{(1 - (c/s)^2)^{3/2}} \right) ds \quad (2.106)$$

and

$$\begin{aligned} \mathcal{O} \left(\int_r^q \left(D(\epsilon, q^*) \frac{s^2 - 1}{2s} \right)^2 ds \right) &= \mathcal{O} \left(\int_1^q \left(D(\epsilon, q^*) \frac{s^2 - 1}{2s} \right)^2 ds \right) \\ &= \mathcal{O} \left(D^2(\epsilon, q^*) \frac{(q^* - 1)^3 (q^* + 3)}{12q^*} \right) \\ &= \mathcal{O} \left(\epsilon^{5/2} (-\ln \epsilon)^{5/4} \right). \end{aligned} \quad (2.107)$$

Hence, (2.96) becomes

$$\begin{aligned} u_2^{\text{in}}(r) &= c \ln \left(r + \sqrt{r^2 - c^2} \right) + u_2^{\text{in}}(q) - c \ln \left(q + \sqrt{q^2 - c^2} \right) - D(\epsilon, q^*) g(r; c) \\ &\quad + \mathcal{O} \left(\epsilon^{5/2} (-\ln \epsilon)^{5/4} \right). \end{aligned} \quad (2.108)$$

Moreover, with Lemma 5,

$$u_2^{\text{in}}(q) - c \ln \left(q + \sqrt{q^2 - c^2} \right) = c \ln(\epsilon) + c(\gamma_e - 2 \ln 2) + \mathcal{O} \left(\epsilon (-\ln \epsilon)^{3/2} \right). \quad (2.109)$$

To find the error bound of $D(\epsilon, q^*)g(r; c)$, we need the following Lemma 6,

Lemma 6. *With the optimal choice of q defined in (2.74) in Theorem 5, as $\epsilon \rightarrow 0$, we have*

$$\mathcal{O} \left(D(\epsilon, q^*) g(r; c) \right) = \mathcal{O} \left(\epsilon (-\ln \epsilon)^{1/2} \right). \quad (2.110)$$

Proof. We first note that $g(r; c)$ has the explicit expression.

$$\begin{aligned}
g(r; c) &= \int_r^q \left(\frac{s^2 - 1}{2s} \right) \left(\frac{1}{(1 - (c/s)^2)^{3/2}} \right) ds \\
&= \frac{1}{2} \int_r^q \frac{s^4}{(s^2 - c^2)^{3/2}} - \frac{s^2}{(s^2 - c^2)^{3/2}} ds \\
&= g_1(r; c) + g_2(q; c),
\end{aligned} \tag{2.111}$$

where

$$g_1(r; c) = \left(\frac{1}{2} - \frac{3}{4}c^2 \right) \ln \left(r + \sqrt{r^2 - c^2} \right) - \frac{\frac{r^3}{4} + \left(\frac{1}{2} - \frac{3}{4}c^2 \right) r}{\sqrt{r^2 - c^2}} \tag{2.112}$$

and

$$g_2(q; c) = \left(\frac{q^2}{4} + \frac{1}{2} - \frac{3}{4}c^2 \right) \frac{q}{\sqrt{q^2 - c^2}} - \left(\frac{1}{2} - \frac{3}{4}c^2 \right) \ln \left(q + \sqrt{q^2 - c^2} \right). \tag{2.113}$$

We notice that

$$0 \leq g(r; c) \leq g(r; -1), \tag{2.114}$$

where the upper bound is the $\gamma = 0$ case. Luckily, $g_1(r; -1)$ does not blow up at $r = 1$, since

$$\lim_{r \rightarrow 1^+} g_1(r; -1) = 0. \tag{2.115}$$

And asymptotically,

$$g_2(q; -1) \sim \frac{q^2}{4} + \frac{1}{4} \ln(2q). \tag{2.116}$$

Therefore,

$$\begin{aligned}
\mathcal{O}(D(\epsilon, q^*)g(r; c)) &= \mathcal{O}(D(\epsilon, q^*)g(1; -1)) \\
&= \mathcal{O}(D(\epsilon, q^*)g_2(q; -1)) \\
&= \mathcal{O}(\epsilon(-\ln \epsilon)^{1/2}).
\end{aligned} \tag{2.117}$$

□

Therefore, with (2.109) and Lemma 6, (2.108) turns into

$$\begin{aligned}
u_2^{\text{in}}(r) &= c \ln(\epsilon) + c(\gamma_e - 2 \ln 2) + c \ln \left(r + \sqrt{r^2 - c^2} \right) + \mathcal{O}(\epsilon(-\ln \epsilon)^{3/2}) \\
&\quad + \mathcal{O}(\epsilon(-\ln \epsilon)^{1/2}) + \mathcal{O}(\epsilon^{5/2}(-\ln \epsilon)^{5/4}).
\end{aligned} \tag{2.118}$$

Comparing the error bounds in $u_2^{\text{in}}(r)$, we have

$$\epsilon^{5/2}(-\ln \epsilon)^{5/4} \ll \epsilon(-\ln \epsilon)^{1/2} \ll \epsilon(-\ln \epsilon)^{3/2}, \tag{2.119}$$

as $\epsilon \rightarrow 0$.

Combining the above results, the asymptotic expansion of $u_2^{\text{in}}(r)$ becomes

$$u_2^{\text{in}}(r) = c \ln(\epsilon) + c(\gamma_e - 2 \ln 2) + c \ln \left(r + \sqrt{r^2 - c^2} \right) + \mathcal{O} \left(\epsilon(-\ln(\epsilon))^{\frac{3}{2}} \right). \tag{2.120}$$

Therefore, $u_2^{\text{in}}(r)$ is a lower bound of $u(r)$ in the inner region and has the same two-term asymptotic expansion as that of $u_1(r)$ in (2.75). We conclude

Theorem 6. *With the optimal choice of q defined in (2.74) in Theorem 5, for $r \in [1, q]$, $u_1(r)$ and $u_2^{\text{in}}(r)$ are the upper and lower bounds of $u(r)$, respectively. As $\epsilon \rightarrow 0$, both $u_1(r)$ and $u_2^{\text{in}}(r)$ have the same two-term asymptotic expansions and error bound as well. Therefore,*

$$u(r) = c \ln(\epsilon) + c(\gamma_e - 2 \ln 2) + c \ln \left(r + \sqrt{r^2 - c^2} \right) + \mathcal{O} \left(\epsilon(-\ln(\epsilon))^{\frac{3}{2}} \right). \tag{2.121}$$

From the study of Lo's in [41], she obtained a five-term asymptotic expansion of $u(r)$ as $\epsilon \rightarrow 0$ by the method of matched asymptotic expansions. Her result is accepted as the correct asymptotic expansion. However, the rigorous proof has not been established. If we truncate her asymptotic expansion to the first two terms and we obtain the error bound $\mathcal{O}(\epsilon^2 \ln^2 \epsilon)$. Miersemann [47] rigorously showed the two-term expansion with the error bound $\mathcal{O}(\epsilon^{\frac{2}{5}} \ln^2 \epsilon)$. (2.121) in Theorem 6 gives the same two-term asymptotic expansion as Lo and Miersemann's results but with a different error bound. Compared with the error bound $\mathcal{O}(\epsilon^2 \ln^2 \epsilon)$ in Lo [41] and $\mathcal{O}(\epsilon^{\frac{2}{5}} \ln^2 \epsilon)$ in Miersemann [47], the error bound we obtained is better than Miersemann's while it is inferior to Lo's.

2.4.5 Second Approximate Outer Solution: $u_2^{\text{out}}(r)$

We attempt to construct a C^1 , piecewise C^2 , approximate solution $u_2(r)$, which is a lower bound of $u(r)$ over the whole region. We address a question how to construct a second approximate outer solution $u_2^{\text{out}}(r)$ in outer region, $r \in [q, \infty)$, such that it is a lower bound of $u(r)$. We cannot simply define $u_2^{\text{out}}(r) = A_2 K_0(\epsilon r)$ for some constant A_2 . Since $A_2 K_0(\epsilon r)$ is a super-solution, the comparison principle is not suitable to show a super-solution which gives a lower bound.

Instead, we define $u_2^{\text{out}}(r)$ in the following way based on the work from Siegel [56],

$$u_2^{\text{out}}(r) = A_2 K_0(\epsilon r) (1 + \eta K_0^2(\epsilon r)) \quad \text{for } r \in [q, \infty), \quad (2.122)$$

where $0 < \eta \ll 1$ and the term $\eta K_0^2(\epsilon r)$ is considered to be a small perturbation.

Our aim is to find A_2 and η such that $u_2^{\text{out}}(r)$ also satisfies the sub-solution condition, that is,

$$N u_2^{\text{out}} \geq \epsilon^2 u_2^{\text{out}} \quad \text{for } r \in [q, \infty). \quad (2.123)$$

At $r = q$, we need the slope condition, $u_{2r}^{\text{in}}(q) = u_{2r}^{\text{out}}(q)$, where $u_{2r}^{\text{in}}(q)$ is determined by (2.86) in Sec. 2.4.2,

$$u_{2r}^{\text{out}}(q) = u_{2r}^{\text{in}}(q) = \frac{\sin \psi_2^{\text{in}}(q)}{\sqrt{1 - \sin^2 \psi_2^{\text{in}}(q)}} = \beta, \quad (2.124)$$

where β is considered as known in this section.

Differentiating (2.122) gives

$$u_{2r}^{\text{out}}(r) = -A_2 \epsilon K_1(\epsilon r) (1 + 3\eta K_0^2(\epsilon r)). \quad (2.125)$$

With the condition in (2.124), η can be expressed in terms of A_2 . Combining (2.125) with the condition in (2.124), we have

$$\eta = -\frac{1}{3K_0^2(\epsilon q)} \left(1 + \frac{\beta}{A_2 \epsilon K_1(\epsilon q)} \right). \quad (2.126)$$

Remark 3. We do not impose the height condition with

$$u_2^{\text{in}}(q) = v_1(q) = u_2^{\text{out}}(q), \quad (2.127)$$

based on (2.94) in Section 2.4.3. Only the slope condition is imposed in (2.124). The reason is that if both the height and the slope conditions are imposed, the exact expression of A_2 and η , denoted as \tilde{A}_2 and $\tilde{\eta}$, respectively, can be obtained, as follows,

$$\tilde{A}_2 = -\frac{\beta}{2} \left(\frac{3}{\sqrt{1+\beta^2}} - 1 \right) \frac{1}{\epsilon K_1(\epsilon q)}, \quad (2.128)$$

$$\tilde{\eta} = \left(\frac{2}{3 - \sqrt{1+\beta^2}} - 1 \right) \frac{1}{K_0^2(\epsilon q)}. \quad (2.129)$$

Unfortunately, equipped with \tilde{A}_2 and $\tilde{\eta}$, such $u_2^{\text{out}}(r)$ defined in (2.122) cannot guarantee to satisfy the sub-solution condition.

With β in (2.124) and η in (2.126), to find the condition on A_2 such that u_2^{out} becomes a sub-solution, we require the inequality holds in (2.123), that is,

$$u_{2rr}^{\text{out}} + \frac{1}{r} u_{2r}^{\text{out}} \left(1 + (u_{2r}^{\text{out}})^2 \right) \geq \epsilon^2 u_2^{\text{out}} \left(1 + (u_{2r}^{\text{out}})^2 \right)^{3/2} \quad \text{for } r \in [q, \infty), \quad (2.130)$$

where

$$u_{2rr}^{\text{out}} = A_2 \epsilon^2 \left[K_0(\epsilon r) + 3\eta K_0^3(\epsilon r) + \frac{1}{\epsilon r} K_1(\epsilon r) + \frac{3\eta}{\epsilon r} K_1(\epsilon r) K_0^2(\epsilon r) \right] + 6A_2 \epsilon^2 \eta K_1^2(\epsilon r) K_0(\epsilon r) \quad (2.131)$$

and

$$u_{2rr}^{\text{out}} + \frac{1}{r} u_{2r}^{\text{out}} = A_2 \epsilon^2 K_0(\epsilon r) + 3A_2 \epsilon^2 \eta K_0^3(\epsilon r) + 6A_2 \epsilon^2 \eta K_1^2(\epsilon r) K_0(\epsilon r). \quad (2.132)$$

Instead of the condition in (2.130), a stronger condition is imposed,

$$\frac{1}{\epsilon^2 u_2^{\text{out}}} \left(u_{2rr}^{\text{out}} + \frac{1}{r} u_{2r}^{\text{out}} \right) + \frac{1}{\epsilon^2 r u_2^{\text{out}}} (u_{2r}^{\text{out}})^3 \geq 1 + c_1 (u_{2r}^{\text{out}})^2 > \left(1 + (u_{2r}^{\text{out}})^2 \right)^{3/2}, \quad (2.133)$$

where c_1 is chosen such that

$$\frac{\left(1 + (u_{2r}^{\text{out}})^2 \right)^{3/2} - 1}{(u_{2r}^{\text{out}})^2} < \frac{(1 + \beta^2)^{3/2} - 1}{\beta^2} = c_1, \quad \text{since } |u_{2r}^{\text{out}}(r)| < |\beta|. \quad (2.134)$$

With

$$\frac{1}{\epsilon^2 u_2^{\text{out}}} \left(u_{2rr}^{\text{out}} + \frac{1}{r} u_{2r}^{\text{out}} \right) = 1 + \frac{2\eta (K_0^2(\epsilon r) + 3K_1^2(\epsilon r))}{1 + \eta K_0^2(\epsilon r)} \quad (2.135)$$

and

$$\frac{1}{\epsilon^2 r u_2^{\text{out}}} (u_{2r}^{\text{out}})^3 = -\frac{K_1(\epsilon r) (1 + 3\eta K_0^2(\epsilon r))}{(\epsilon r) K_0(\epsilon r) (1 + \eta K_0^2(\epsilon r))} (u_{2r}^{\text{out}})^2, \quad (2.136)$$

(2.133) becomes

$$\frac{2\eta (K_0^2(\epsilon r) + 3K_1^2(\epsilon r))}{1 + \eta K_0^2(\epsilon r)} \geq \left(\frac{K_1(\epsilon r) (1 + 3\eta K_0^2(\epsilon r))}{(\epsilon r) K_0(\epsilon r) (1 + \eta K_0^2(\epsilon r))} + c_1 \right) (u_{2r}^{\text{out}})^2, \quad (2.137)$$

where $r \in [q, \infty)$.

After multiplying $1 + \eta K_0^2(\epsilon r)$ on both sides, then

$$2\eta (K_0^2(\epsilon r) + 3K_1^2(\epsilon r)) \geq \left(\frac{K_1(\epsilon r) (1 + 3\eta K_0^2(\epsilon r))}{(\epsilon r)K_0(\epsilon r)} + c_1 (1 + \eta K_0^2(\epsilon r)) \right) (u_{2r}^{\text{out}})^2. \quad (2.138)$$

Since $\eta K_0^2(\epsilon r) > 0$, then $1 + 3\eta K_0^2(\epsilon r) > 1 + \eta K_0^2(\epsilon r)$, we can impose a stronger condition compared than the condition in (2.137),

$$2\eta (K_0^2(\epsilon r) + 3K_1^2(\epsilon r)) \geq \left(\frac{K_1(\epsilon r) (1 + 3\eta K_0^2(\epsilon r))}{(\epsilon r)K_0(\epsilon r)} + c_1 (1 + 3\eta K_0^2(\epsilon r)) \right) (u_{2r}^{\text{out}})^2. \quad (2.139)$$

After some arrangement, we obtain

$$\frac{2\eta}{A_2^2 \epsilon^2} \geq \left(\frac{K_1(\epsilon r)}{(\epsilon r)K_0(\epsilon r)} + c_1 \right) \left(\frac{K_1^2(\epsilon r) (1 + 3\eta K_0^2(\epsilon r))^3}{K_0^2(\epsilon r) + 3K_1^2(\epsilon r)} \right), \quad (2.140)$$

where $r \in [q, \infty)$.

It's easy to see the right-handed side of (2.140) is a decreasing function in terms of r (with fixed ϵ and η). It's equivalent to satisfy

$$\frac{2\eta}{A_2^2 \epsilon^2} \geq \left(\frac{K_1(\epsilon q)}{(\epsilon q)K_0(\epsilon q)} + c_1 \right) \left(\frac{K_1^2(\epsilon q) (1 + 3\eta K_0^2(\epsilon q))^3}{K_0^2(\epsilon q) + 3K_1^2(\epsilon q)} \right), \quad (2.141)$$

Combined with $1 + 3\eta K_0^2(\epsilon q) = -\frac{\beta}{A_2 \epsilon K_1(\epsilon q)}$ from (2.126), we have

$$\begin{aligned} \frac{2\eta}{A_2^2 \epsilon^2} &\geq \left(\frac{K_1(\epsilon q)}{(\epsilon q)K_0(\epsilon q)} + c_1 \right) \left(\frac{1 + 3\eta K_0^2(\epsilon q)}{K_0^2(\epsilon q) + 3K_1^2(\epsilon q)} \right) \left(K_1^2(\epsilon q) (1 + 3\eta K_0^2(\epsilon q))^2 \right) \\ &\geq \left(\frac{K_1(\epsilon q)}{(\epsilon q)K_0(\epsilon q)} + c_1 \right) \left(\frac{1 + 3\eta K_0^2(\epsilon q)}{K_0^2(\epsilon q) + 3K_1^2(\epsilon q)} \right) \left(\frac{\beta^2}{A_2^2 \epsilon^2} \right). \end{aligned} \quad (2.142)$$

(2.142) gives

$$2\eta \geq \alpha \left(\frac{1 + 3\eta K_0^2(\epsilon q)}{K_0^2(\epsilon q) + 3K_1^2(\epsilon q)} \right), \quad (2.143)$$

where

$$\alpha = \left(\frac{K_1(\epsilon q)}{\epsilon q K_0(\epsilon q)} + c_1 \right) \beta^2. \quad (2.144)$$

The following Lemma 7 shows the properties of α ,

Lemma 7. *As α defined above, we have*

$$(i) \quad \alpha > \left(\frac{K_1(\epsilon q)}{\epsilon q K_0(\epsilon q)} + \frac{3}{2} \right) \beta^2.$$

(ii) *As $\epsilon \rightarrow 0$, with the choice of $q = q^*$, defined in (2.74) in Theorem 5, we have*

$$\alpha \sim c^2. \quad (2.145)$$

Proof. (i) is straightforward. To show (ii), with the choice of $q = q^*$, as $\epsilon \rightarrow 0$, then $\epsilon q \rightarrow 0$, combined with Lemma 5, we have

$$\beta = \frac{\sin \psi_2^{\text{in}}(q)}{\sqrt{1 - \sin^2 \psi_2^{\text{in}}(q)}} \sim \frac{c}{q}, \quad (2.146)$$

$$c_1 = \frac{(1 + \beta^2)^{3/2} - 1}{\beta^2} \sim \frac{3}{2}, \quad (2.147)$$

$$\frac{K_1(\epsilon q)}{\epsilon q K_0(\epsilon q)} \sim -\frac{1}{(\epsilon q)^2 \ln(\epsilon q)}. \quad (2.148)$$

Thus, $c_1 \ll \frac{K_1(\epsilon q)}{\epsilon q K_0(\epsilon q)}$. Based on the optimal condition of q in (2.61), that is,

$$-(\epsilon q)^2 \ln(\epsilon q) = \frac{1}{q^2}, \quad (2.149)$$

it leads to $\alpha = \left(\frac{K_1(\epsilon q)}{\epsilon q K_0(\epsilon q)} + c_1 \right) \beta^2 \sim \frac{q^2 c^2}{q^2} = c^2$.

□

Lemma 7 implies that with ϵ small enough and $q = q^*$, α is close to $c^2 \in (0, 1]$. We solve the inequality in (2.143) and obtain

$$\eta \geq \eta_0, \quad (2.150)$$

where

$$\eta_0 = \alpha \left[2 \left(K_0^2(\epsilon q) + 3K_1^2(\epsilon q) \right) - 3\alpha K_0^2(\epsilon q) \right]^{-1}. \quad (2.151)$$

Moreover, with ϵ small enough, η_0 can be shown that $\eta_0 > 0$.

With (2.126) and (2.150), we have

$$\begin{aligned} A_2 &\leq -\frac{\beta}{\epsilon K_1(\epsilon q)} \left(\frac{1}{1 + 3K_0^2(\epsilon q)\eta_0} \right) \\ &= -\frac{\beta}{\epsilon K_1(\epsilon q)} \left[1 - \frac{3\alpha K_0^2(\epsilon q)}{2(K_0^2(\epsilon q) + 3K_1^2(\epsilon q))} \right]. \end{aligned} \quad (2.152)$$

Moreover, if we replace α by $\left(\frac{K_1(\epsilon q)}{\epsilon q K_0(\epsilon q)} + \frac{3}{2} \right) \beta^2$ from Lemma 7, we obtain a stronger condition for A_2 ,

$$A_2 \leq -\frac{\beta}{\epsilon K_1(\epsilon q)} Q = A_{\text{crit}}, \quad (2.153)$$

where $Q = 1 - \left(\frac{K_1(\epsilon q)}{\epsilon q K_0(\epsilon q)} + \frac{3}{2} \right) \left(\frac{3K_0^2(\epsilon q)}{2(K_0^2(\epsilon q) + 3K_1^2(\epsilon q))} \right) \beta^2$.

Therefore, we summarize the above analysis to the following Theorem 7,

Theorem 7. *With the choice $A_2 = A_{\text{crit}}$ shown in (2.153),*

$$u_2^{\text{out}}(r) = A_2 K_0(\epsilon r) (1 + \eta K_0^2(\epsilon r)) \quad (2.154)$$

satisfies the sub-solution condition $Nu_2^{\text{out}} \geq \epsilon^2 u_2^{\text{out}}$ for $r \in [q, \infty)$, where

$$\eta = -\frac{1}{3K_0^2(\epsilon q)} \left(1 + \frac{\beta}{A_2 \epsilon K_1(\epsilon q)} \right), \quad (2.155)$$

where $\frac{\beta}{A_2 \epsilon K_1(\epsilon q)} = -Q^{-1}$ and $1 + \frac{\beta}{A_2 \epsilon K_1(\epsilon q)} < 0$.

We are also interested in the asymptotic behavior of A_2 and η defined in Theorem 7, see Lemma 8,

Lemma 8. *As $\epsilon \rightarrow 0$, with the choice $q = q^*$, defined in (2.74) in Theorem 5, we have*

$$A_2 = A_{crit} = -c + \mathcal{O}\left(\epsilon(-\ln(\epsilon))^{1/2}\right), \quad (2.156)$$

$$\eta \sim \mathcal{O}\left(\epsilon(-\ln(\epsilon))^{-1/2}\right). \quad (2.157)$$

Proof. With the choice $q = q^*$ and the results in (2.146) and (2.148),

$$\begin{aligned} \left(\frac{K_1(\epsilon q)}{\epsilon q K_0(\epsilon q)} + \frac{3}{2}\right) \left(\frac{3K_0^2(\epsilon q)}{2(K_0^2(\epsilon q) + 3K_1^2(\epsilon q))}\right) \beta^2 &\sim \left(-\frac{1}{(\epsilon q)^2 \ln(\epsilon q)}\right) \left(\frac{1}{2}(\epsilon q)^2 \ln^2(\epsilon q)\right) \left(\frac{c^2}{q^2}\right) \\ &\sim \frac{c^2}{2}(\epsilon q)^2 \ln^2(\epsilon q) \\ &\sim \frac{c^2}{2}\epsilon \left(-\frac{1}{2}\ln(\epsilon)\right)^{3/2}. \end{aligned} \quad (2.158)$$

Hence, we obtain $Q \sim 1$. Moreover, with $\beta = \frac{c}{q} + \mathcal{O}\left(\epsilon^{3/2}(-\ln(\epsilon))^{3/4}\right)$ and $\frac{1}{\epsilon K_1(\epsilon q)} = q(1 + \mathcal{O}((\epsilon q)^2 \ln(\epsilon q)))$ based on Appendix A.1,

$$\begin{aligned} \frac{\beta}{\epsilon K_1(\epsilon q)} &= c + c\mathcal{O}((\epsilon q)^2 \ln(\epsilon q)) + q\mathcal{O}\left(\epsilon^{3/2}(-\ln(\epsilon))^{3/4}\right) \\ &= c + \mathcal{O}\left(\epsilon(-\ln(\epsilon))^{1/2}\right), \end{aligned} \quad (2.159)$$

where $q = q^* \sim \frac{1}{\sqrt{\epsilon}} \left(-\frac{1}{2}\ln(\epsilon q)\right)^{-1/4}$ from (2.70) and $-(\epsilon q)^2 \ln(\epsilon q) = \frac{1}{q^2}$, according to the optimal condition of q .

Therefore, we have

$$A_2 = A_{\text{crit}} = -c + \mathcal{O}\left(\epsilon(-\ln(\epsilon))^{1/2}\right). \quad (2.160)$$

As for η , we find

$$1 + \frac{\beta}{A_2 \epsilon K_1(\epsilon q)} = \frac{Q-1}{Q} \sim \mathcal{O}\left(\epsilon(-\ln(\epsilon))^{3/2}\right), \quad (2.161)$$

$$\frac{1}{K_0^2(\epsilon q)} \sim \frac{1}{\ln^2(\epsilon q)} \sim \mathcal{O}\left((-\ln(\epsilon))^{-2}\right). \quad (2.162)$$

Thus,

$$\eta \sim \mathcal{O}\left(\epsilon(-\ln(\epsilon))^{-1/2}\right). \quad (2.163)$$

□

The comparison principle can be applied to show $u_2^{\text{out}}(r)$ defined in (2.154) in Theorem 7 is a lower bound of $u(r)$ on $[q, \infty)$. A height condition at $r = q$ is needed. We first notice that $u_2^{\text{out}}(q)$ is comparable to $v_1(q)$ in (2.94), which is constructed in Sec. 2.4.3, see Lemma 9.

Lemma 9. *If ϵq is sufficiently small, then $u_2^{\text{out}}(q) < v_1(q)$, where $u_2^{\text{out}}(q)$ is defined in (2.154) in Theorem 7 and $v_1(q)$ is defined in (2.94) in Sec. 2.4.3.*

Proof.

$$\begin{aligned} u_2^{\text{out}}(q) - v_1(q) &= A_2 K_0(\epsilon q) (1 + \eta K_0^2(\epsilon q)) - \frac{-\sin \psi_2^{\text{in}}(q)}{\epsilon K_1(\epsilon q)} K_0(\epsilon q) \\ &= -\frac{A_2}{3} K_0(\epsilon q) \left(\frac{\beta}{A_2 \epsilon K_1(\epsilon q)} - 2 \right) - \left(-\frac{\beta}{\sqrt{1+\beta^2}} \right) \left(\frac{1}{\epsilon K_1(\epsilon q)} \right) K_0(\epsilon q) \\ &< -\frac{1}{3} \frac{\beta}{\epsilon K_1(\epsilon q)} K_0(\epsilon q) + \frac{2}{3} A_{\text{crit}} K_0(\epsilon q) - (\beta^2 - 1) \left(\frac{\beta}{\epsilon K_1(\epsilon q)} \right) K_0(\epsilon q) \\ &= -\frac{\beta}{\epsilon K_1(\epsilon q)} K_0(\epsilon q) \left(\frac{1}{3} + \frac{2}{3} Q + \beta^2 - 1 \right) \\ &= -\frac{\beta^3}{\epsilon K_1(\epsilon q)} K_0(\epsilon q) \bar{Q}(\epsilon q), \end{aligned} \quad (2.164)$$

where the inequality $\frac{1}{\sqrt{1+\beta^2}} > 1 - \beta^2$ is applied and

$$\bar{Q}(\epsilon q) = 1 - \left(\frac{K_1(\epsilon q)}{\epsilon q K_0(\epsilon q)} + \frac{3}{2} \right) \left(\frac{K_0^2(\epsilon q)}{K_0^2(\epsilon q) + 3K_1^2(\epsilon q)} \right).$$

Moreover, $\bar{Q}(\epsilon q)$ is a monotone increasing function in terms of ϵq . Numerically, when $\epsilon q < 0.05$, we have $\bar{Q}(\epsilon q) < 0$. Thus, when ϵq is sufficiently small, then $u_2^{\text{out}}(q) < v_1(q)$. \square

Remark 4. $\epsilon q < 0.05$ is a rough choice. If we solve $\bar{Q}(\epsilon q) = 0$ in terms of ϵq numerically, a better choice can be imposed, $\epsilon q < 0.0579356$.

Thus, based on Lemma 4 and Lemma 9, we have

$$u_2^{\text{out}}(q) < v_1(q) < u(q). \quad (2.165)$$

With the sub-solution condition $Nu_2^{\text{out}} \geq Bu_2^{\text{out}}$ and (2.165), Theorem 3 (comparison principle) gives the following Lemma 10

Lemma 10. *For $r \geq q$, the second approximate outer solution $u_2^{\text{out}}(r)$ gives a lower bound of $u(r)$,*

$$u_2^{\text{out}}(r) < u(r). \quad (2.166)$$

Therefore, in outer region $r \geq q$,

$$u_2^{\text{out}}(r) \leq u(r) \leq u_1^{\text{out}}(r). \quad (2.167)$$

Siegel [56] showed that there exists a constant μ which depends on ϵ and γ such that

$$\lim_{r \rightarrow \infty} \frac{u(r)}{K_0(\epsilon r)} = \mu(\epsilon, \gamma). \quad (2.168)$$

The inequality in (2.167) can be applied to find the bounds of μ and evaluate a limit of μ when ϵ is small, see Theorem 8.

Theorem 8.

$$A_2 \leq \mu \leq A_1, \quad (2.169)$$

where A_1 is defined in (2.38) and A_2 is defined in Theorem 7. Recall that,

$$A_1 = -\frac{c}{\epsilon K_1(\epsilon q) \sqrt{q^2 - c^2}},$$

$$A_2 = -\frac{\beta}{\epsilon K_1(\epsilon q)} \left[1 - \left(\frac{K_1(\epsilon q)}{\epsilon q K_0(\epsilon q)} + \frac{3}{2} \right) \left(\frac{3K_0^2(\epsilon q)}{2(K_0^2(\epsilon q) + 3K_1^2(\epsilon q))} \right) \beta^2 \right].$$

As $\epsilon \rightarrow 0$, then $\mu(\epsilon, \gamma) \rightarrow -c$.

Proof. From (2.167),

$$A_2 \leq A_2 (1 + \eta K_0^2(\epsilon r)) \leq \frac{u(r)}{K_0(\epsilon r)} \leq A_1, \quad (2.170)$$

where

$$A_1 = -\frac{c}{\epsilon K_1(\epsilon q) \sqrt{q^2 - c^2}},$$

$$A_2 = -\frac{\beta}{\epsilon K_1(\epsilon q)} \left[1 - \left(\frac{K_1(\epsilon q)}{\epsilon q K_0(\epsilon q)} + \frac{3}{2} \right) \left(\frac{3K_0^2(\epsilon q)}{2(K_0^2(\epsilon q) + 3K_1^2(\epsilon q))} \right) \beta^2 \right].$$

Hence, we can show μ is bounded,

$$A_2 \leq \mu \leq A_1. \quad (2.171)$$

Moreover, as $\epsilon \rightarrow 0$,

$$\mu \rightarrow -c, \quad (2.172)$$

since

$$\begin{aligned} A_1 &= -c + \mathcal{O}(\epsilon(-\ln \epsilon)^{1/2}), \\ A_2 &= -c + \mathcal{O}(\epsilon(-\ln \epsilon)^{1/2}). \end{aligned}$$

□

2.4.6 Another Choice of $u_2^{\text{in}}(q)$

We have explained that the choice $u_2^{\text{in}}(q) = v_1(q)$ defined in (2.94) in Section 2.4.3 is not appropriate in the construction of a lower bound $u_2(r)$ over the whole region, see Remark 3. In this section, we consider another choice of $u_2^{\text{in}}(q)$ such that $u_2(r)$ becomes a C^1 , piecewise C^2 , function and a lower bound of $u(r)$ over $[1, \infty)$.

From Lemma 10, we impose the height condition at $r = q$ for $u_2(r)$ as

$$u_2^{\text{in}}(q) = u_2^{\text{out}}(q), \tag{2.173}$$

where $u_2^{\text{out}}(r)$ is defined in Theorem 7.

With such height condition, $u_2^{\text{in}}(r)$ is a lower bound of $u(r)$ in inner region, see the following Lemma 11,

Lemma 11. *With the choice $u_2^{\text{in}}(q)$ defined in (2.173), the second approximate inner solution in (2.88) in Sec. 2.4.2 gives a lower bound of $u(r)$ on $[1, q]$, that is,*

$$u_2^{\text{in}}(r) < u(r). \tag{2.174}$$

Combined with Lemma 10 and Lemma 11, we conclude the following Theorem 9,

Theorem 9. *The second approximate solution $u_2(r)$ defined in (2.78) is a lower bound of $u(r)$ on the whole interval $[1, \infty)$,*

$$u_2(r) < u(r). \tag{2.175}$$

The following Fig. 2.3 shows the comparison among $u_1(r)$, $u_2(r)$ and $u(r)$ over the whole region.

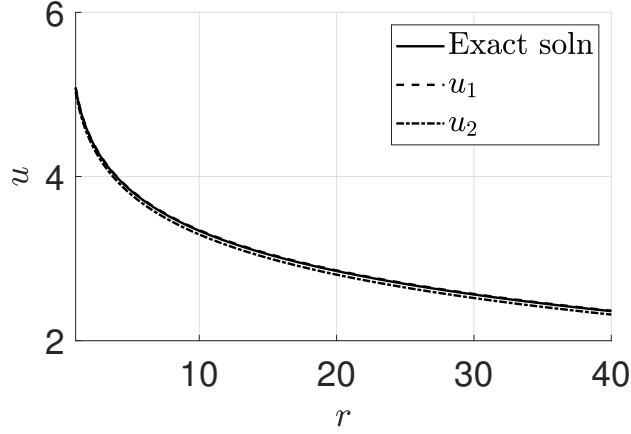


Figure 2.3: The comparison among $u_1(r)$, $u_2(r)$ and $u(r)$ in the inner region with $\epsilon = 0.001$, $\gamma = \frac{\pi}{4}$ and $q = 10$.

2.4.7 Asymptotic Expansion of the Second Approximation Solution: $u_2(r)$

Similar to the work in Section 2.4.4, we investigate the asymptotic expansion of $u_2(r)$ near the wall as $\epsilon \rightarrow 0$, $q \rightarrow \infty$ and $\epsilon q \rightarrow 0$, where the optimal q is defined in (2.74) in Theorem 5. The only difference in this section is the choice of $u_2^{\text{in}}(q)$. The height condition in (2.173) is used. Near the boundary, $u_2(r) = u_2^{\text{in}}(r)$, shown as follows,

$$u_2(r) = u_2^{\text{in}}(q) - \int_r^q \frac{\sin \psi_2^{\text{in}}(s)}{\sqrt{1 - \sin^2 \psi_2^{\text{in}}(s)}} ds. \quad (2.176)$$

Since $u_2^{\text{in}}(q) = u_2^{\text{out}}(q)$, we make use of the results from Lemma 8 and Appendix A.1, thus,

$$u_2^{\text{in}}(q) = c \ln(\epsilon q) - c(-\gamma_e + \ln 2) + \mathcal{O}(\epsilon(-\ln \epsilon)^{3/2}). \quad (2.177)$$

With the similar argument in Section 2.4.4, asymptotically, we have

$$\begin{aligned}
u_2(r) &= u_2^{\text{in}}(q) + c \ln \left(r + \sqrt{r^2 - c^2} \right) - c \ln \left(q + \sqrt{q^2 - c^2} \right) \\
&\quad - D(\epsilon, q^*)g(r) + \mathcal{O} \left(\int_r^q \left(D(\epsilon, q^*) \frac{s^2 - 1}{2s} \right)^2 ds \right) \\
&= c \ln(\epsilon) + c(\gamma_e - 2 \ln 2) + c \ln \left(r + \sqrt{r^2 - c^2} \right) + \mathcal{O} \left(\epsilon (-\ln \epsilon)^{3/2} \right). \tag{2.178}
\end{aligned}$$

The error bound of $u_2(r)$ is identical to the error bound of $u_2^{\text{in}}(r)$ in Section 2.4.4. Two different choices of $u_2^{\text{in}}(q)$ in Sec. 2.4.3 and Sec. 2.4.6 give the same error bound of $u_2^{\text{in}}(r)$. Therefore, we summarize the results as follows,

Theorem 10. *As $\epsilon \rightarrow 0$, $u_2(r)$ defined in (2.176) gives the same two-term asymptotic expansion of $u(r)$ with error bound $\mathcal{O} \left(\epsilon (-\ln \epsilon)^{3/2} \right)$. Therefore, the results of Theorem 6 are still valid if we use $u_2(r)$ as a lower bound.*

2.5 Improved Bound Estimate for the Asymptotic Expansion of $u(r)$

In Sec. 2.3 and Sec. 2.4, we constructed two approximate solutions $u_1(r)$ and $u_2(r)$, which become an upper bound and a lower bound of $u(r)$ over $[1, \infty)$, respectively. Asymptotically, as $\epsilon \rightarrow 0$, with the optimal choice of q defined in (2.74) in Theorem 5, $u_1(r)$, $u_2(r)$ and $u(r)$ share the same two-term asymptotic expansion with the bound $\mathcal{O} \left(\epsilon (-\ln(\epsilon))^{\frac{3}{2}} \right)$ near the wall. In this section, we consider modified outer solutions of the form

$$u_i^{\text{out}}(R) = u_{i1}^{\text{out}}(R) + u_{i2}^{\text{out}}(R), \tag{2.179}$$

where $R = \epsilon r$, $r \in [q, \infty)$, $i \in \{3, 4\}$ and assume $u_{i2}^{\text{out}}(R) \ll u_{i1}^{\text{out}}(R)$ and $|u_{i2}^{\text{out}}(R)| \ll |u_{i1}^{\text{out}}(R)|$. $u_i^{\text{out}}(R)$ is defined and showed that it satisfies the super-solution condition. The details are discussed in Sec. 2.5.1.

The forms of inner solutions remain unchanged except the choice of q . $u_3^{\text{in}}(r)$ is defined as a zero mean curvature solution, see Sec. 2.3.1 and $u_4^{\text{in}}(r)$ is defined as a constant mean

curvature solution with twice the mean curvature being equal to $\bar{D}(\epsilon, q) = \epsilon^2 u_3^{\text{in}}(1)$, see Sec. 2.4.2. Similar to the discussion in Sec. 2.3 and Sec. 2.4, we construct $u_3(r)$ as

$$u_3(r) = \begin{cases} c \ln(r + \sqrt{r^2 - c^2}) + u_3^{\text{in}}(q) - c \ln(q + \sqrt{q^2 - c^2}), & \text{if } 1 \leq r \leq q, \\ u_3^{\text{out}}, & \text{if } r \geq q. \end{cases} \quad (2.180)$$

By matching the height and the slope conditions in (2.22) and (2.23) at $r = q$, $u_3^{\text{in}}(q)$ and the coefficient of u_3^{out} will be determined. Moreover, $u_3(r)$ can be made to be C^1 and an upper bound of $u(r)$ over $[1, \infty)$, see Sec. 2.5.2. In analysis of the coefficient of u_3^{out} , denoted as A_3 , another optimal choice of q , denoted as q^{**} is derived, see (2.213). Such optimal choice of q is applied to achieve the improved error bound for the asymptotic expansion of $u(r)$.

Similar to $u_2^{\text{in}}(r)$ defined in (2.88) in Sec. 2.4.2, we construct $u_4^{\text{in}}(r)$ as

$$u_4^{\text{in}}(r) = u_4^{\text{in}}(q) - \int_r^q \frac{\sin \psi_4^{\text{in}}(s)}{\sqrt{1 - \sin^2 \psi_4^{\text{in}}(s)}} ds, \quad (2.181)$$

where $\sin \psi_4^{\text{in}}$ is similar to $\sin \psi_2^{\text{in}}$ except the usage of different mean curvature $\bar{D}(\epsilon, q)$,

$$\sin \psi_4^{\text{in}}(r) = \frac{c}{r} + \bar{D}(\epsilon, q) \frac{r^2 - 1}{2r} \quad \text{for } 1 \leq r \leq q. \quad (2.182)$$

With a proper choice of $u_4^{\text{in}}(q)$, see Sec. 2.5.3, similar to $u_2^{\text{in}}(q)$ in Sec. 2.4.3, $u_4^{\text{in}}(r)$ is shown to be a lower bound of $u(r)$ on $[1, q)$, see Sec. 2.5.3.

As $\epsilon \rightarrow 0$, with the optimal choice of q , $q = q^{**}$, both u_3^{in} and u_4^{in} are shown to share the same two-term asymptotic expansion of $u(r)$ with the error bound $\mathcal{O}\left(\epsilon^{4/3} (-\ln(\epsilon))^{5/3}\right)$, which is an improvement of the error bound we obtained in Sec. 2.3 and Sec. 2.4.

2.5.1 Modified Outer Solutions u_i^{out}

In this section, we construct modified outer solutions $u_i^{\text{out}}(R)$ with the form in (2.179) and show it satisfies the super-solution condition. Recall that,

$$u_i^{\text{out}}(R) = u_{i1}^{\text{out}}(R) + u_{i2}^{\text{out}}(R),$$

where $R = \epsilon r$, $r \in [q, \infty)$, $i \in \{3, 4\}$. We define

$$u_{i1}^{\text{out}}(R) = A_i K_0(R), \quad (2.183)$$

where $A_i > 0$ is to be determined. u_{i1}^{out} has the same form of $u_1^{\text{out}}(r)$ and is a solution of the linearized capillary equation, see (2.34) in Sec. 2.3.2. With the assumption $u_{i2}^{\text{out}}(R) \ll u_{i1}^{\text{out}}(R)$ and $|u_{i2}^{\text{out}'}(R)| \ll |u_{i1}^{\text{out}'}(R)|$, when $u_i^{\text{out}}(R)$ is substituted into the capillary equation, $u_{i2}^{\text{out}}(R)$ is suggested to be defined as a particular solution of

$$u_{i2}^{\text{out}''} + \frac{1}{R}u_{i2}^{\text{out}'} - u_{i2}^{\text{out}} = Q(R), \quad (2.184)$$

where $u_{i2}^{\text{out}'} = \frac{d}{dR}u_{i2}^{\text{out}}$ and

$$Q(R) = -\frac{\epsilon^2}{R}(u_{i1}^{\text{out}'})^3 + \frac{3}{2}\epsilon^2 u_{i1}^{\text{out}}(u_{i1}^{\text{out}'})^2. \quad (2.185)$$

(2.184) is the same as Lo's in her second approximate solution, see [41]. $u_{i2}^{\text{out}}(R)$ can be solved by the variation of parameters. The two linearly independent solutions of the homogeneous equation of (2.184) are $K_0(R)$ and $I_0(R)$ with Wronskian $\frac{1}{R}$. Therefore,

$$u_{i2}^{\text{out}}(R) = \epsilon^2 A_i^3 \bar{u}_2^{\text{out}}(R), \quad (2.186)$$

where

$$\bar{u}_2^{\text{out}}(R) = K_0(R)f_1(R) - I_0(R)f_2(R) \quad (2.187)$$

with

$$f_1(R) = \int_R^\infty I_0 K_1^3 + \frac{3}{2}s I_0 K_0 K_1^2 ds, \quad (2.188)$$

$$f_2(R) = \int_R^\infty K_0 K_1^3 + \frac{3}{2}s K_0^2 K_1^2 ds. \quad (2.189)$$

Moreover, differentiating \bar{u}_2^{out} , we have

$$\frac{d\bar{u}_2^{\text{out}}}{dR}(R) = -K_0(R)f_1(R) - I_1(R)f_2(R). \quad (2.190)$$

Next, we show that $u_i^{\text{out}}(R)$ is a super-solution on $R \in [\epsilon q, \infty)$. It requires

$$u_i^{\text{out}''} + \frac{1}{R}u_i^{\text{out}'} \left(1 + \epsilon^2(u_i^{\text{out}'})^2\right) \leq u_i^{\text{out}} \left(1 + \epsilon^2(u_i^{\text{out}'})^2\right)^{3/2}. \quad (2.191)$$

With the inequality

$$1 + \frac{3}{2}\epsilon^2(u_i^{\text{out}'})^2 \leq \left(1 + \epsilon^2(u_i^{\text{out}'})^2\right)^{3/2}, \quad (2.192)$$

we impose the stronger condition

$$u_i^{\text{out}''} + \frac{1}{R}u_i^{\text{out}'} \left(1 + \epsilon^2(u_i^{\text{out}'})^2\right) - u_i^{\text{out}} \leq \frac{3}{2}u_i^{\text{out}}\epsilon^2(u_i^{\text{out}'})^2. \quad (2.193)$$

Adding DE of u_{i1}^{out} , see (2.34) and DE of u_{i2}^{out} , see (2.184), we have

$$u_{i1}^{\text{out}''} + \frac{1}{R}u_{i1}^{\text{out}'} - u_{i1}^{\text{out}} + u_{i2}^{\text{out}''} + \frac{1}{R}u_{i2}^{\text{out}'} - u_{i2}^{\text{out}} = Q. \quad (2.194)$$

After some rearrangement,

$$\left(u_{i1}^{\text{out}''} + u_{i2}^{\text{out}''}\right) + \frac{1}{R} \left(u_{i1}^{\text{out}'} + u_{i2}^{\text{out}'}\right) + \frac{1}{R}\epsilon^2 \left(u_{i1}^{\text{out}'} + u_{i2}^{\text{out}'}\right)^3 - \left(u_{i1}^{\text{out}} + u_{i2}^{\text{out}}\right) = \frac{1}{R}\epsilon^2 \left(u_{i1}^{\text{out}'} + u_{i2}^{\text{out}'}\right)^3 + Q. \quad (2.195)$$

With (2.193) and (2.195), we require

$$\frac{1}{R}\epsilon^2 \left(u_{i1}^{\text{out}'} + u_{i2}^{\text{out}'}\right)^3 + Q - \frac{3}{2}\epsilon^2 \left(u_{i1}^{\text{out}} + u_{i2}^{\text{out}}\right) \left(u_{i1}^{\text{out}'} + u_{i2}^{\text{out}'}\right)^2 \leq 0. \quad (2.196)$$

Since $u_{i1}^{\text{out}} > 0$, $u_{i2}^{\text{out}} > 0$ and $u_{i1}^{\text{out}'} < 0$, $u_{i2}^{\text{out}'} < 0$, we have

$$\begin{aligned}
& \frac{1}{R}\epsilon^2 \left(u_{i1}^{\text{out}'} + u_{i2}^{\text{out}'} \right)^3 + Q - \frac{3}{2}\epsilon^2 \left(u_{i1}^{\text{out}} + u_{i2}^{\text{out}} \right) \left(u_{i1}^{\text{out}'} + u_{i2}^{\text{out}'} \right)^2 \\
&= \frac{1}{R}\epsilon^2 \left[\left(u_{i1}^{\text{out}'} + u_{i2}^{\text{out}'} \right)^3 - \left(u_{i1}^{\text{out}'} \right)^3 \right] + \frac{3}{2}\epsilon^2 \left[u_{i1}^{\text{out}} \left(u_{i1}^{\text{out}'} \right)^2 - \left(u_{i1}^{\text{out}} + u_{i2}^{\text{out}} \right) \left(u_{i1}^{\text{out}'} + u_{i2}^{\text{out}'} \right)^2 \right] \\
&\leq 0.
\end{aligned} \tag{2.197}$$

Hence, (2.191) is satisfied. Therefore, we summarize the above analysis to the following Theorem 11,

Theorem 11. $u_i^{\text{out}}(R)$, $i \in \{3, 4\}$, satisfies the super-solution condition in (2.191) on $R \in [\epsilon q, \infty)$.

As $R \rightarrow 0$, the following asymptotic expansions of the integrals are obtained by L'Hopital's rule and are used for the expansions of $f_1(R)$, $f_2(R)$, $\bar{u}_2^{\text{out}}(R)$ and $\frac{d\bar{u}_2^{\text{out}}}{dR}(R)$.

$$\begin{aligned}
(1) \quad & \int_R^\infty I_0 K_1^3 ds \sim \frac{1}{2R^2} - \frac{3}{4} \ln^2(R) + \left(\frac{1}{2} + \frac{3a}{2} \right) \ln(R). \\
(2) \quad & \int_R^\infty \frac{3}{2} s I_0 K_0 K_1^2 ds \sim \frac{3}{4} \ln^2(R) - \frac{3a}{2} \ln(R). \\
(3) \quad & \int_R^\infty K_0 K_1^3 ds \sim -\frac{\ln(R)}{2R^2} + \left(-\frac{1}{4} + \frac{a}{2} \right) \frac{1}{R^2} + \frac{\ln^3(R)}{2} - \left(\frac{1}{4} + \frac{3a}{2} \right) \ln^2(R) \\
& \quad \quad \quad + \left(-\frac{1}{4} + \frac{a}{2} + \frac{3a^2}{2} \right) \ln(R). \\
(4) \quad & \int_R^\infty \frac{3}{2} s K_0^2 K_1^2 ds \sim -\frac{\ln^3(R)}{2} + \frac{3a}{2} \ln^2(R) - \frac{3a^2}{2} \ln(R),
\end{aligned}$$

where $a = \ln 2 - \gamma_e$. Hence,

$$f_1(R) \sim \frac{1}{2R^2} + \frac{1}{2} \ln(R), \tag{2.198}$$

$$f_2(R) \sim -\frac{\ln(R)}{2R^2} + \left(-\frac{1}{4} + \frac{a}{2} \right) \frac{1}{R^2} - \frac{1}{4} \ln^2(R) - \left(\frac{1}{4} + \frac{3a}{2} \right) \ln(R). \tag{2.199}$$

Therefore,

$$\bar{u}_2^{\text{out}}(R) \sim \frac{1}{4R^2} - \frac{1}{4} \ln^2(R) + \frac{1}{4} \ln(R), \quad (2.200)$$

which agrees with Lo's expansion, see [41]. Moreover,

$$\frac{d\bar{u}_2^{\text{out}}}{dR}(R) \sim -\frac{1}{2R^3} - \frac{\ln(R)}{2R} + \frac{1}{4R}. \quad (2.201)$$

Remark 5. In Lo's work [41], she just stated the expansion of her second approximate solution. We present the expansions with detailed calculation.

2.5.2 Asymptotic Expansion of u_3^{in}

We write u_3^{out} as a function of inner variable r ,

$$u_3^{\text{out}}(r) = A_3 K_0(\epsilon r) + \epsilon^2 A_3^3 \bar{u}_2^{\text{out}}(\epsilon r). \quad (2.202)$$

Both $u_3^{\text{in}}(r)$ and $u_3^{\text{out}}(r)$ can be determined with the height and the slope conditions at $r = q$.

$$u_3^{\text{in}}(q) = u_3^{\text{out}}(q), \quad (2.203)$$

$$\frac{du_3^{\text{in}}}{dr}(q) = \frac{du_3^{\text{out}}}{dr}(q), \quad (2.204)$$

where $\frac{du_3^{\text{in}}}{dr}(q) = \frac{c}{\sqrt{q^2 - c^2}}$ and

$$\frac{du_3^{\text{out}}}{dr}(q) = -A_3 \epsilon K_1(\epsilon q) + \epsilon^3 A_3^3 \frac{d\bar{u}_2^{\text{out}}}{dR}(\epsilon q). \quad (2.205)$$

The slope condition in (2.204) leads a cubic equation for coefficient A_3 , which can be shown with a unique root and determined by the cubic formula, see (2.210). Therefore, u_3 defined in (2.180) can be determined and is C^1 . The comparison principle shows that u_3 is an upper bound of $u(r)$ over $[1, \infty)$. In analysis of the asymptotic expansion of A_3 , another

optimal choice of q , say q^{**} , is discussed. With $q = q^{**}$, the error bound of the two-term asymptotic expansion of u_3^{in} can be shown as $\mathcal{O}\left(\epsilon^{4/3}(-\ln(\epsilon))^{5/3}\right)$.

From

$$\frac{c}{\sqrt{q^2 - c^2}} = -A_3 \epsilon K_1(\epsilon q) + \epsilon^3 A_3^3 \frac{d\bar{u}_2^{\text{out}}}{dR}(\epsilon q), \quad (2.206)$$

where

$$\frac{d\bar{u}_2^{\text{out}}}{dR}(\epsilon q) = -K_0(\epsilon q) f_1(\epsilon q) - I_1(\epsilon q) f_2(\epsilon q), \quad (2.207)$$

(2.206) gives a cubic equation of A_3 .

$$A_3^3 + p_3 A_3 + k_3 = 0, \quad (2.208)$$

where

$$p_3 = -\frac{\epsilon q K_1(\epsilon q)}{\epsilon^3 q \frac{d\bar{u}_2^{\text{out}}}{dR}(\epsilon q)} > 0 \quad \text{and} \quad k_3 = -\frac{\frac{cq}{\sqrt{q^2 - c^2}}}{\epsilon^3 q \frac{d\bar{u}_2^{\text{out}}}{dR}(\epsilon q)} < 0. \quad (2.209)$$

The cubic equation for A_3 satisfies the condition $\left(\frac{k_3}{2}\right)^2 + \left(\frac{p_3}{3}\right)^3 > 0$. Hence, there is a unique root for A_3 . The cubic formula gives

$$A_3 = \sqrt[3]{-\frac{k_3}{2} - \sqrt{\left(\frac{k_3}{2}\right)^2 + \left(\frac{p_3}{3}\right)^3}} + \sqrt[3]{-\frac{k_3}{2} + \sqrt{\left(\frac{k_3}{2}\right)^2 + \left(\frac{p_3}{3}\right)^3}} \quad (2.210)$$

Moreover, let $F_3(A_3) = A_3^3 + p_3 A_3 + k_3$, $F_3(0) = k_3 < 0$ and $F_3(b) > 0$, for some large value $b > A_3$. Therefore, the intermediate value theorem implies $A_3 > 0$.

To investigate the asymptotic expansion of A_3 as $\epsilon \rightarrow 0$, $q \rightarrow \infty$ and $\epsilon q \rightarrow 0$. We first have

$$p_3 = 2q^2 + (\epsilon q)^2 q^2 \ln(\epsilon q) + o((\epsilon q)^2 q^2 \ln(\epsilon q)), \quad (2.211)$$

$$k_3 \sim 2cq^2 + c^3 + \frac{3c^5}{4q^2} - 2c(\epsilon q)^2 q^2 \ln(\epsilon q), \quad (2.212)$$

where the details can be seen in Appendix A.2. There are two terms appearing in the expansions of k_3 , $\frac{3c^5}{4q^2}$ and $2c(\epsilon q)^2 q^2 \ln(\epsilon q)$. As we did in Sec. 2.3.5, we consider the same asymptotic order of both terms, which can be treated as the optimal choice of q . It leads to the following transcendental equation for q ,

$$-(\epsilon q)^2 q^2 \ln(\epsilon q) = \frac{1}{q^2}. \quad (2.213)$$

This equation is similar to (2.61) considered in Sec. 2.3.5. Hence, Theorem 2 (Olver [49]) can be applied. After an analogous argument to Sec. 2.3.5, we obtain the solution q^{**} for (2.213), considered as the optimal choice of q ,

$$q^{**} = \epsilon^{-1/3} \left(-\frac{2}{3} \ln(\epsilon) \right)^{-1/6} (1 + o(1)). \quad (2.214)$$

Remark 6. For later use, we set q as q^{**} defined in (2.214).

Let

$$m_3 = -\frac{k_3}{2} - \sqrt{\left(\frac{k_3}{2}\right)^2 + \left(\frac{p_3}{3}\right)^3}, \quad (2.215)$$

$$n_3 = -\frac{k_3}{2} + \sqrt{\left(\frac{k_3}{2}\right)^2 + \left(\frac{p_3}{3}\right)^3}, \quad (2.216)$$

where $m_3 \sim -\left(\frac{2}{3}\right)^{3/2} q^3$ and $n_3 \sim \left(\frac{2}{3}\right)^{3/2} q^3$. Thus, the asymptotics of $A_3 = m_3^{1/3} + n_3^{1/3}$ is inconclusive if we apply the asymptotics of m_3 and n_3 directly. Then, we consider an identity $m_3 + n_3 = \left(m_3^{1/3} + n_3^{1/3}\right) \left(m_3^{2/3} - m_3^{1/3} n_3^{1/3} + n_3^{2/3}\right)$, then

$$A_3 = m_3^{1/3} + n_3^{1/3} = \frac{m_3 + n_3}{m_3^{2/3} - m_3^{1/3} n_3^{1/3} + n_3^{2/3}}, \quad (2.217)$$

where $m_3 + n_3 = -k_3$ and $m_3 n_3 = \left(-\frac{p_3}{3}\right)^3$. Thus,

$$m_3 + n_3 \sim -2cq^2, \quad (2.218)$$

$$m_3^{2/3} - m_3^{1/3} n_3^{1/3} + n_3^{2/3} \sim \frac{2}{3}q^2 + \frac{2}{3}q^2 + \frac{2}{3}q^2 = 2q^2. \quad (2.219)$$

Therefore,

$$A_3 \sim -c \quad \Leftrightarrow \quad A_3 = -c + o(1). \quad (2.220)$$

Let $A_3 = -c + \eta_3$, where $\eta_3 = o(1)$. To see the leading term of η_3 , we consider

$$\eta_3 = A_3 + c = \frac{(m_3 + n_3) + c \left(m_3^{2/3} - m_3^{1/3} n_3^{1/3} + n_3^{2/3}\right)}{m_3^{2/3} - m_3^{1/3} n_3^{1/3} + n_3^{2/3}}. \quad (2.221)$$

With the identity $m_3^{2/3} + n_3^{2/3} = \left(m_3^{1/3} + n_3^{1/3}\right)^2 - 2m_3^{1/3} n_3^{1/3} = A_3^2 + \frac{2}{3}p_3$, we have

$$\eta_3 = \frac{-k_3 + c(A_3^2 + p_3)}{A_3^2 + p_3}, \quad (2.222)$$

where $A_3^2 \ll p_3$, in detail,

$$-k_3 + c(A_3^2 + p_3) \sim -\frac{3c^5}{4q^2} + 3c(\epsilon q)^2 q^2 \ln(\epsilon q), \quad (2.223)$$

$$A_3^2 + p_3 \sim 2q^2, \quad (2.224)$$

where the expansions can be seen in Appendix A.2. With q^{**} in (2.214),

$$\begin{aligned} \eta_3 &= \mathcal{O}\left((\epsilon q)^2 \ln(\epsilon q)\right) \\ &= \mathcal{O}\left(\epsilon^{4/3} (-\ln(\epsilon))^{2/3}\right), \end{aligned} \quad (2.225)$$

where the coefficient is absorbed in the big- \mathcal{O} .

Remark 7. Theorem 2 (Olver [49]) gives another approach to achieve the leading order behavior of η_3 . With $A_3 \sim -c$, and the asymptotic expansions of p_3 and k_3 in (2.211) and (2.212), the cubic term A_3^3 is negligible compared with other two terms in (2.208). Hence, we rearrange the cubic equation and obtain

$$A_3 = -\frac{1}{p_3} (k_3 + A_3^3). \quad (2.226)$$

Therefore, with $q = q^{**}$,

$$\eta_3 = -\frac{1}{p_3} (k_3 + A_3^3 - cp_3) = \mathcal{O}((\epsilon q)^2 \ln(\epsilon q)), \quad (2.227)$$

which is the same as that in (2.225).

Therefore, near $r = 1$, with $A_3 = -c + \eta_3$, where η_3 is defined in (2.225),

$$u_3^{\text{in}}(r) = c \ln(\epsilon) + c \ln(r + \sqrt{r^2 - c^2}) + c(\gamma_\epsilon - 2 \ln 2) + \mathcal{O}(\eta_3 \ln(\epsilon q)), \quad (2.228)$$

where $\mathcal{O}(\eta_3 \ln(\epsilon q)) = \mathcal{O}(\epsilon^{4/3} (-\ln(\epsilon))^{5/3})$.

2.5.3 Choice of $u_4^{\text{in}}(q)$ and the Asymptotic Expansion of $u_4^{\text{in}}(r)$

Although we cannot construct a new lower bound of u in the whole domain, we can still find a lower bound of u in the inner solution. The inner solution $u_4^{\text{in}}(r)$ has the form

$$u_4^{\text{in}}(r) = u_4^{\text{in}}(q) - \int_r^q \frac{\sin \psi_4^{\text{in}}(s)}{\sqrt{1 - \sin^2 \psi_4^{\text{in}}(s)}} ds, \quad (2.229)$$

where $\sin \psi_4^{\text{in}}$ is similar to $\sin \psi_2^{\text{in}}$ except the usage of different mean curvature $\bar{D}(\epsilon, q)$,

$$\sin \psi_4^{\text{in}}(r) = \frac{c}{r} + \bar{D}(\epsilon, q) \frac{r^2 - 1}{2r} \quad \text{for } 1 \leq r \leq q, \quad (2.230)$$

where $\bar{D}(\epsilon, q) = \epsilon^2 u_3^{\text{in}}(1)$. Similar to the work in Sec. 2.4.2, the construction of $u_4^{\text{in}}(r)$ is based on one-step iteration $Nu_4^{\text{in}} = \bar{D}(\epsilon, q)$. Similar to the choice of $u_2^{\text{in}}(q)$ in Sec. 2.4.3, we define the height of u_4^{in} at $r = q$ as

$$u_4^{\text{in}}(q) = u_4^{\text{out}}(\epsilon q), \quad (2.231)$$

where the coefficient of u_4^{out} , A_4 , will be determined such that $u_4^{\text{in}}(q) < u(q)$. Recall that,

$$u_4^{\text{out}}(R) = u_{41}^{\text{out}}(R) + u_{42}^{\text{out}}(R) \quad (2.232)$$

where $u_{41}^{\text{out}} = A_4 K_0(R)$ and $u_{42}^{\text{out}} = \epsilon^2 A_4^3 \bar{u}_2^{\text{out}}(R)$, $\bar{u}_2^{\text{out}}(R)$ is defined in (2.187). A_4 will be determined by

$$\int_{\epsilon q}^{\infty} R u_4^{\text{out}}(R) dR = -q \sin \psi_4^{\text{in}}(q), \quad (2.233)$$

where

$$\sin \psi_4^{\text{in}}(q) = \frac{c}{q} + \bar{D}(\epsilon, q) \frac{q^2 - 1}{2q}, \quad (2.234)$$

which is similar to $\sin \psi_2^{\text{in}}(q)$ defined in Sec. 2.4.2 and $\bar{D}(\epsilon, q) = \epsilon^2 u_3^{\text{in}}(1)$, $q = q^{**}$ defined in (2.214). With the similar argument in Sec. 2.4.3, $u_4^{\text{out}}(R)$ in (2.232) gives the lower bound at $R = \epsilon q$. Therefore, $u_4^{\text{in}}(r)$ can be shown to be a lower bound of $u(r)$ in $r \in [1, q]$.

The left hand side of (2.233), $\int_{\epsilon q}^{\infty} R u_4^{\text{out}}(R) dR$, can be simplified. With the identity $RK_0(R) = (-RK_1(R))'$,

$$\int_{\epsilon q}^{\infty} R u_{41}^{\text{out}}(R) dR = \int_{\epsilon q}^{\infty} A_4 R K_0(R) dR = A_4 \epsilon q K_1(\epsilon q). \quad (2.235)$$

And with

$$\int_{\epsilon q}^{\infty} R u_{42}^{\text{out}}(R) dR = \int_{\epsilon q}^{\infty} R \epsilon^2 A_4^3 \bar{u}_2^{\text{out}}(R) dR, \quad (2.236)$$

(2.233) also gives a cubic equation for A_4 ,

$$A_4^3 + p_4 A_4 + k_4 = 0, \quad (2.237)$$

where

$$p_4 = \frac{\epsilon q K_1(\epsilon q)}{\epsilon^2 \int_{\epsilon q}^{\infty} R \bar{u}_2(R) dR} > 0 \quad \text{and} \quad k_4 = \frac{q \sin \psi_4^{\text{in}}(q)}{\epsilon^2 \int_{\epsilon q}^{\infty} R \bar{u}_2(R) dR} < 0. \quad (2.238)$$

The cubic equation for A_4 satisfies the condition $\left(\frac{k_4}{2}\right)^2 + \left(\frac{p_4}{3}\right)^3 > 0$. Hence, there is a unique root for A_4 . The cubic formula gives

$$A_4 = \sqrt[3]{-\frac{k_4}{2} - \sqrt{\left(\frac{k_4}{2}\right)^2 + \left(\frac{p_4}{3}\right)^3}} + \sqrt[3]{-\frac{k_4}{2} + \sqrt{\left(\frac{k_4}{2}\right)^2 + \left(\frac{p_4}{3}\right)^3}} \quad (2.239)$$

The analysis of the asymptotic expansion for A_4 is similar to A_3 . We first notice that $\int_{\epsilon q}^{\infty} R \bar{u}_2(R) dR$ can be simplified using integration by parts. With the identities $RK_0(R) = (-RK_1(R))'$ and $RI_0(R) = (RI_1(R))'$,

$$\begin{aligned} \int_R^{\infty} s \bar{u}_2^{\text{out}}(s) ds &= \int_R^{\infty} s K_0(s) f_1(s) - s I_0(s) f_2(s) ds \\ &= RK_1(R) f_1(R) + RI_1(R) f_2(R) \\ &\quad - \int_R^{\infty} s I_0 K_1^4 + \frac{3}{2} s^2 I_0 K_0 K_1^3 ds \\ &\quad - \int_R^{\infty} s K_0 I_0 K_1^3 + \frac{3}{2} s^2 I_1 K_0^2 K_1^2 ds. \end{aligned} \quad (2.240)$$

Asymptotically, as $R \rightarrow 0$,

$$\begin{aligned} RK_1(R) f_1(R) + RI_1(R) f_2(R) &\sim \frac{1}{2R^2} + \frac{1}{2} \ln(R) - \frac{1}{4}, \\ - \int_R^{\infty} s I_0 K_1^4 + \frac{3}{2} s^2 I_0 K_0 K_1^3 ds - \int_R^{\infty} s K_0 I_0 K_1^3 + \frac{3}{2} s^2 I_1 K_0^2 K_1^2 ds &\sim -\frac{1}{2R^2} - \frac{3}{4} \ln(R). \end{aligned}$$

Thus,

$$\int_R^\infty s \bar{u}_2^{\text{out}}(s) ds \sim -\frac{1}{4} \ln(R) - \frac{1}{4}. \quad (2.241)$$

We define

$$m_4 = -\frac{k_4}{2} - \sqrt{\left(\frac{k_4}{2}\right)^2 + \left(\frac{p_4}{3}\right)^3}, \quad (2.242)$$

$$n_4 = -\frac{k_4}{2} + \sqrt{\left(\frac{k_4}{2}\right)^2 + \left(\frac{p_4}{3}\right)^3}, \quad (2.243)$$

where

$$p_4 \sim -\frac{4}{\epsilon^2 \ln(\epsilon q)} + \frac{4}{\epsilon^2 \ln^2(\epsilon q)} - 2q^2, \quad (2.244)$$

$$k_4 \sim -\frac{4c}{\epsilon^2 \ln(\epsilon q)} + \frac{4c}{\epsilon^2 \ln^2(\epsilon q)} - 2c \frac{\ln(\epsilon)(q^2 - 1)}{\ln(\epsilon q)}, \quad (2.245)$$

see Appendix A.2.

$$m_4 \sim -\left(\frac{4}{3}\right)^{3/2} \left(-\frac{1}{\epsilon^2 \ln(\epsilon q)}\right)^{3/2} \text{ and } n_4 \sim -m_4. \text{ Then}$$

$$A_4 = m_4^{1/3} + n_4^{1/3} = \frac{m_4 + n_4}{m_4^{2/3} - m_4^{1/3} n_4^{1/3} + n_4^{2/3}}, \quad (2.246)$$

where $m_4 + n_4 = -k_4$ and $m_4 n_4 = \left(-\frac{p_4}{3}\right)^3$. Thus,

$$m_4 + n_4 \sim \frac{4c}{\epsilon^2 \ln(\epsilon q)}, \quad (2.247)$$

$$m_4^{2/3} - m_4^{1/3} n_4^{1/3} + n_4^{2/3} \sim -\frac{4c}{\epsilon^2 \ln(\epsilon q)}. \quad (2.248)$$

Therefore,

$$A_4 \sim -c. \quad (2.249)$$

Let $A_4 = -c + \eta_4$, where $\eta_4 = o(1)$. To see the leading term of η_4 , we have

$$\eta_4 = \frac{-k_4 + c(A_4^2 + p_4)}{A_4^2 + p_4}, \quad (2.250)$$

where $A_4^2 \ll p_4$, in details,

$$cp_4 - k_4 + cA_4^2 \sim -2cq^2 + \frac{2c \ln(\epsilon)(q^2 - 1)}{\ln(\epsilon q)}, \quad (2.251)$$

$$A_4^2 + p_4 \sim -\frac{4}{\epsilon^2 \ln(\epsilon q)}, \quad (2.252)$$

where the expansions can be seen in Appendix [A.2](#).

Thus, with $q = q^{**}$,

$$\begin{aligned} \eta_4 &= \mathcal{O}((\epsilon q)^2 \ln(\epsilon q)) \\ &= \mathcal{O}\left(\epsilon^{4/3} (-\ln(\epsilon))^{2/3}\right), \end{aligned} \quad (2.253)$$

which has the same order as η_3 .

Recall that,

$$u_4^{\text{in}}(r) = u_4^{\text{in}}(q) - \int_r^\infty \frac{\sin \psi_4^{\text{in}}}{\sqrt{1 - \sin^2 \psi_4^{\text{in}}}} ds, \quad (2.254)$$

where $u_4^{\text{in}}(q) = u_4^{\text{out}}(\epsilon q)$. Asymptotically,

$$\int_r^q \frac{\sin \psi_4^{\text{in}}(s)}{\sqrt{1 - \sin^2 \psi_4^{\text{in}}(s)}} ds = \int_r^q \frac{c}{\sqrt{s^2 - c^2}} ds + \bar{D}(\epsilon, q)g(r; c) + \mathcal{O}\left(\bar{D}^2(\epsilon, q)\frac{(q-1)^3(q+3)}{12q}\right), \quad (2.255)$$

where $g(r; c)$ is defined in (2.106) in Sec. 2.4.4 with $\mathcal{O}(g(r; c)) = \mathcal{O}(q^2)$ and $\bar{D}(\epsilon, q) = \epsilon^2 u_3^{\text{in}}(1) \sim c\epsilon^2 \ln(\epsilon)$. Thus, $\bar{D}(\epsilon, q)g(r) = \mathcal{O}((\epsilon^2 q) \ln(\epsilon))$. With $q = q^{**}$, we have

$$\int_r^q \frac{\sin \psi_4^{\text{in}}(s)}{\sqrt{1 - \sin^2 \psi_4^{\text{in}}(s)}} ds = -c \ln\left(r + \sqrt{r^2 - c^2}\right) + c \ln\left(q + \sqrt{q^2 - c^2}\right) + \mathcal{O}\left(\epsilon^{5/3} (-\ln(\epsilon))^{5/6}\right). \quad (2.256)$$

Thus, near $r = 1$, with $A_4 = -c + \eta_4$, where η_4 is defined in (2.225),

$$u_4^{\text{in}}(r) = c \ln(\epsilon) + c \ln\left(r + \sqrt{r^2 - c^2}\right) + c(\gamma_e - 2 \ln 2) + \mathcal{O}\left(\epsilon^{4/3} (-\ln(\epsilon))^{5/3}\right). \quad (2.257)$$

Therefore, we conclude

Theorem 12. *With the optimal choice of q , $q = q^{**}$, for $r \in [1, q]$, $u_3^{\text{in}}(r)$ and $u_4^{\text{in}}(r)$ are upper and lower bounds of $u(r)$, respectively. As $\epsilon \rightarrow 0$, both $u_3^{\text{in}}(r)$ and $u_4^{\text{in}}(r)$ have the same two-term asymptotic expansions and error bound as well. Therefore,*

$$u(r) = c \ln(\epsilon) + c(\gamma_e - 2 \ln 2) + c \ln\left(r + \sqrt{r^2 - c^2}\right) + \mathcal{O}\left(\epsilon^{4/3} (-\ln(\epsilon))^{5/3}\right). \quad (2.258)$$

So, we improve the error bound to $\mathcal{O}\left(\epsilon^{4/3} (-\ln(\epsilon))^{5/3}\right)$.

2.6 Conclusion

In this chapter, we constructed two C^1 , piecewise C^2 approximate solutions of $u(r)$ over $[1, \infty)$. The first approximate solution $u_1(r)$ consists of an inner solution, which has zero

mean curvature and an outer solution, which is a solution of the linearized capillary equation. By Theorem 3 (the comparison principle), $u_1(r)$ gives an upper bound of $u(r)$ over the whole domain. The second approximate solution $u_2(r)$ consists of an inner solution, which has constant mean curvature and an outer solution, which is constructed as a subsolution of u (in outer region). $u_2(r)$ gives a lower bound of $u(r)$ over the whole domain.

Near the boundary $r = 1$, $u_1(r)$ and $u_2(r)$ have the same two-term asymptotic expansion which is the two-term asymptotic expansion of $u(r)$ as $\epsilon \rightarrow 0$. Their error bound is optimized by the choice of a transition radius q , which is obtained based on Theorem 2 (Olver [49]). We achieve the error bound $\mathcal{O}(\epsilon(-\ln \epsilon)^{3/2})$. This error bound is improved when we apply a modified outer solution. Therefore, we obtain the two-term asymptotic expansion of $u(r)$ with error bound $\mathcal{O}(\epsilon^{4/3}(-\ln(\epsilon))^{5/3})$. Compared with Lo and Miersemann's results, our error bound is better than Miersemann's, $O(\epsilon^{2/5} \ln^2(\epsilon))$ while it is inferior to Lo's, $\mathcal{O}(\epsilon^2 \ln^2(\epsilon))$.

Unfortunately, we cannot improve the error bound up to $\mathcal{O}(\epsilon^2 \ln^2(\epsilon))$, which is obtained by Lo through matched asymptotic expansions. In Lo's study, a more complicated form of inner solution is considered. However, in our study, zero mean curvature and constant mean curvature inner solutions are used. Therefore, a more complicated form of inner solution is suggested for future work. Moreover, Miersemann [47] conjectured a full asymptotic expansion for the needle problem. A proof of the conjecture is anticipated in the future.

Chapter 3

A Floating Ball on an Unbounded Bath

3.1 Introduction

The study of the floating objects with surface tension has attracted many physicists' and mathematicians' interests. General discussion can be found in Vella's survey paper [61] or in Finn's paper [21] with more mathematical treatment. Floating ability can be influenced by many factors such as surface tension, the shape of the object, the density of the object, gravity, contact angle and so on. People study floating objects and the conditions of their stable configurations in various scenarios. Two-dimensional floating objects are not physically realizable but have lots of interests. Erdős, Schibler and Herndon [15] considered floating objects with different shapes without surface tension. They found multiple equilibrium configurations of floating prisms of square and equilateral triangular cross-section. Even asymmetric floating configurations of symmetric objects have been found. Raphaël, di Meglio, Berger and Calabi [52] considered a long prismatic particle with smooth strictly convex cross-section. They showed there are at least four equilibrium configurations obeying the contact angle condition. Among those positions, half of them are stable. Kemp and Siegel [34] studied the prisms with elliptical or polygonal cross-section. They concluded that a body cannot float in a stable equilibrium with the fluid interface intersecting the interior of a straight side in a single point. Bhatnagar and Finn [3], Chen and Siegel [4] considered a two-dimensional cylinder horizontally floating on an unbounded bath. At most two equilibrium configurations (force balanced) can be found. Chen and Siegel [4] concluded that one of them is stable and the other is unstable by applying both the energy and the force approaches. McCuan and Treinen [44] studied the floating cylinder in

the laterally finite container and gave one example of three equilibrium configurations and two of them are stable. So, the existence of multiple equilibrium configurations has been found in many applications. In three dimensions, the floating problem is more physically familiar but more challenging. Finn and Vogel [23] gave the floating criteria of the general convex objects in both zero gravity and positive gravity situations. McCuan and Treinen derived additional necessary condition for the floating problem, see [43]. The forces and torques conditions appeared as well in the derivation of equilibrium configurations of a floating particle, see Miersemann [48]. The floating ball is the simplest case in three dimensions. The floating configuration is assumed to be radially symmetric. In McCuan and Treinen [43], they considered a floating ball in both a finite container and an unbounded bath. They gave an example of two equilibrium configurations of a floating ball on an unbounded bath, one of which admits a lower energy. More related work can be seen in [27, 31, 16, 19, 62, 40, 66, 58, 48].

In this chapter, we study a homogeneous ball with radius a floating on a unbounded reservoir. Suppose this unbounded reservoir of fluid has its interface with the air at the zero level. In the presence of surface tension, the fluid interface will be lifted up or pushed down to the fluid height u and is tending to the zero level at infinity. The floating configurations are assumed to be radially symmetric. We set the center of the ball on the vertical axis. By symmetry, we introduce the radial distance r as we did in Chapter 2 and $r > 0$ in this case. The inclination angle ψ is measured counterclockwise from the positive direction, see Fig. 3.1b. The fluid interface meets the ball at a contact point with an attachment angle ϕ_0 , a contact angle γ and a inclination angle ψ_0 , see the configuration in Fig. 3.1a. Based on Bhatnagar and Finn [3] and Chen and Siegel [4], we have a geometric constraint,

$$\psi_0 = \phi_0 + \gamma - \pi, \quad (3.1)$$

where $\psi_0 \in (-\pi, \pi)$, $\phi_0 \in (0, \pi)$ and $\gamma \in [0, \pi]$. And we denote the horizontal distance of the contact point as r_0 ,

$$r_0 = a \sin(\phi_0). \quad (3.2)$$

The fluid interface $u(r)$ will be determined by the following BVP,

$$Nu = \kappa u \quad \text{for } r > r_0, \quad (3.3)$$

$$\psi(r_0) = \psi_0 \quad \text{and} \quad \lim_{r \rightarrow \infty} u(r) = 0. \quad (3.4)$$

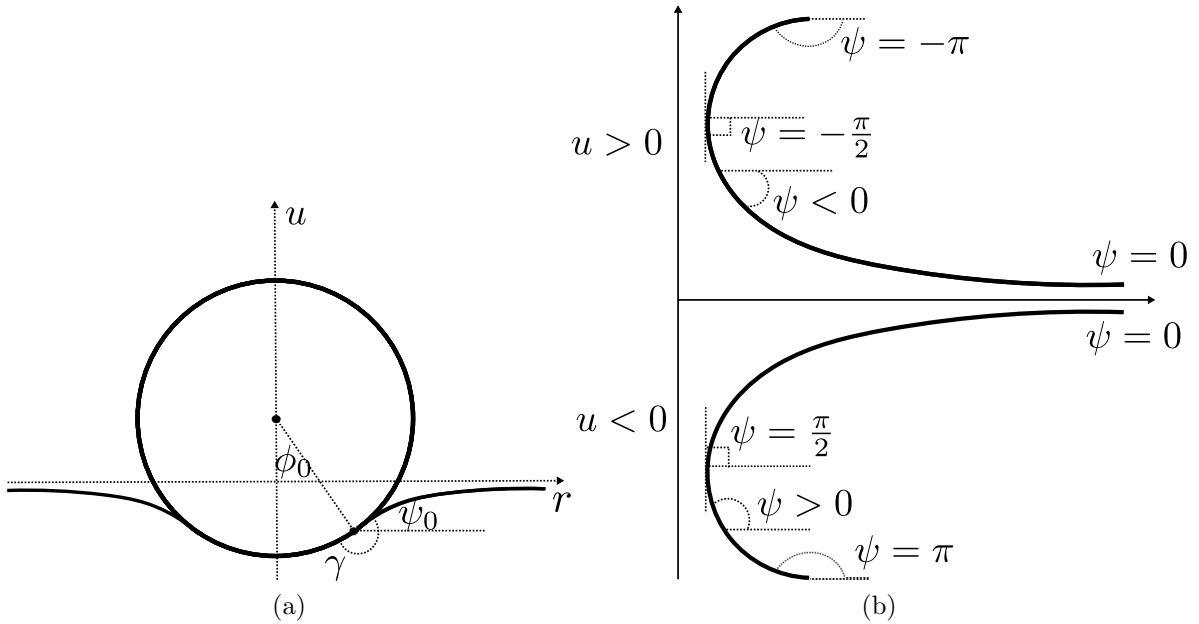


Figure 3.1: (a) The cross-sectional configuration of the ball floating on the liquid, (b) the measurement of the inclination angle ψ for both positive and negative fluid heights.

Various forms of the capillary equation will be discussed in Sec. 3.2. The fluid interface u can be either a graph or a non-graph. So, both graph and parametric descriptions of the fluid interface are considered. When u is not a graph, the solution can be parametrized by the inclination angle ψ , denoted as $r = r(\psi)$ and $u = u(\psi)$. Vogel [63] and Elcrat, Neel and Siegel [13] studied the parametric solution $r = r(\psi; \sigma)$ and $u = u(\psi; \sigma)$ with parameter σ , where σ is the radial distance when the slope of the fluid interface becomes vertical. Vogel [63] noticed that a family of the profile curves forms an envelope. The envelope was used to study the stability of the liquid bridge by Vogel [63] and developed the floating criteria by Finn and Vogel [23]. The uniqueness argument from Elcrat, Neel and Siegel [13] can be applied to the floating ball problem. The fluid interface can be uniquely determined by ϕ_0 . Therefore, we can write the parametric solution as $r = r(\psi; \phi_0)$ and $u = u(\psi; \phi_0)$. The zero solution $u = 0$ is not contained in the parametric description, so a graph description $u = u(r)$ is considered. Following Vogel [63], we write $u = u(r; r_0, u_0)$, where r_0 and $u_0 = u(r_0; r_0, u_0)$ are the radial distance and the fluid height at the contact point, respectively, see Fig. 3.2. The initial values (r_0, u_0) determine a unique solution by the comparison principle. We develop C^1 smoothness of u_0 with respect to ϕ_0 . This requires an extension of Vogel's description of solutions and monotonicity results. As a

by-product, Vogel’s conjecture [63] on the smoothness of the envelope of exterior solutions is shown, see Sec. 3.4.

Levinson’s theorem [12] is a powerful technique to determine the limiting property of a linear dynamical system, see Sec. 3.3. In Sec. 3.5, Theorem 2 (Olver [49]) and Theorem 16 (Levinson’s Theorem [12]) are applied to explore the limiting behavior of solutions, which is used for later analysis of the total force and the total energy. The asymptotic forms of parametric solutions $r(\psi; \phi_0)$ and $u(\psi; \phi_0)$ are obtained as $\psi \rightarrow 0$. The limiting behavior of $\dot{r}(\psi; \phi_0)$ and $\dot{u}(\psi; \phi_0)$ is investigated as well, where $\dot{r} = \frac{\partial}{\partial \phi_0} r(\psi; \phi_0)$ and $\dot{u} = \frac{\partial}{\partial \phi_0} u(\psi; \phi_0)$.

Bhatnagar and Finn [3] and Chen and Siegel [4] apply both energy and force analysis to study the number of equilibria and their stability for the floating cylinder problem. The similar work is done for the floating ball problem. In Sec. 3.6, we apply both energy and force approaches and establish a relation between the total energy E_T and the total force F_T , shown as follows,

$$\frac{dE_T}{d\phi_0} = -F_T h'(\phi_0), \quad (3.5)$$

where $h'(\phi_0)$ is the derivative of the height of the center, which is defined as

$$h(\phi_0) = \cos(\phi_0) + u_0, \quad (3.6)$$

see Fig. 3.2. (3.5) shows a critical point of the total energy can be either a force balanced point or a critical point of the height. From McCuan and Treinen [43] and [44], they argue that the force balance condition should be a necessary condition for equilibrium when a floating object is considered. In the derivation of the equilibrium configuration of a floating particle with only vertical movement, Miersemann [48] argued that the vertical force balance should be satisfied. Thus, we are more interested in the equilibrium point which is the force balanced point.

The fluid height at the contact point u_0 appears in both total energy and total force equations, which has to be found numerically. The shooting method algorithm is introduced to determine the fluid interface, see Sec. 3.7. In Sec. 3.8, several limiting cases of the total force F_T and the height h are discussed. For small Bond number, the asymptotic expansion of $u(r)$ obtained in Chapter 2 can be fitted into the floating ball problem and we extend

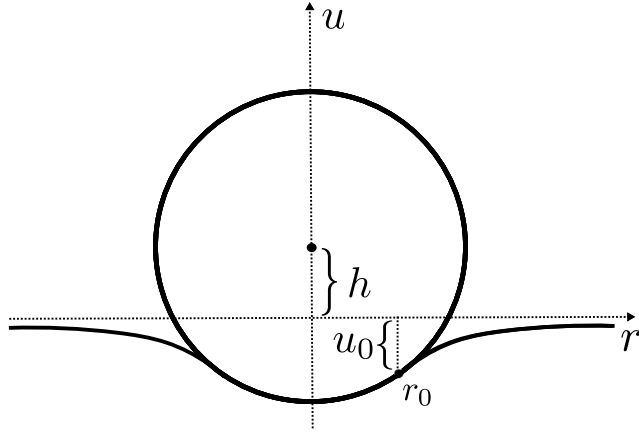


Figure 3.2: The contact point (r_0, u_0) and the height of the center h .

it to the non-graph case. The asymptotic forms of F_T and h are obtained based on the asymptotic forms of u_0 . The asymptotic behavior of F_T and h is developed for large Bond number and $\phi_0 \rightarrow 0, \pi$, too. In numerical observation, we perform a series of numerical tests with different values of Bond numbers and contact angles. We conjecture on the number of equilibria and their stability for the floating ball system. The most important conjecture is stated as follows,

Conjecture. *In the floating ball system, there are at most two force balanced points. If there is only one force balanced point, it is stable. If there are two force balanced points, the one with smaller attachment angle must be stable and the one with larger attachment angle can be either stable or unstable.*

The values of Bond number B , the density ratio α and the contact angle γ play important roles on determining the number of equilibria and their stability. We illustrate the information in B versus α figures with given contact angles. Examples with typical contact angles will be discussed, sec. 3.9. In Sec. 3.10, two examples are presented. We give an example of two stable equilibrium configurations. Another example shows a case with no force balanced point where there is an energy minimizer. This prompts discussion of the necessary condition for the floating configuration and a modification of changing topological structure for the floating configurations in this example. The conclusion is made in Sec. 3.11.

3.2 Various Forms of the Capillary Equation

In this section, we consider various forms of capillary equation, which will be discussed throughout the chapter. As discussed, the floating configurations are assumed to be radially symmetric about the vertical axis. The fluid interface can be either a graph or a non-graph. Both graph and parametric descriptions of solutions are considered. If the fluid interface is a graph, denoted as $u = u(r)$, it satisfies the following BVP,

$$\frac{u_{rr}}{(1 + u_r^2)^{3/2}} + \frac{u_r}{r\sqrt{1 + u_r^2}} = \kappa u \quad \text{for } r > r_0, \quad (3.7)$$

$$\psi(r_0) = \psi_0 \quad \text{and} \quad \lim_{r \rightarrow \infty} u(r) = 0, \quad (3.8)$$

where $r_0 = a \sin(\phi_0)$, known as the radial distance of the contact point and ψ_0 is the inclination angle at the contact point, which satisfies a geometric constraint in (3.1). Based on Johnson and Perko [33], there is a unique solution satisfying the above BVP.

By introducing the characteristic length $l_c = a$, we define the dimensionless radial distance \hat{r} and fluid height \hat{u} as $\hat{r} = \frac{r}{a}$ and $\hat{u} = \frac{u}{a}$, respectively. Thus, the radius of the ball is scaled to 1 and we obtain the dimensionless BVP,

$$\frac{\hat{u}''}{(1 + \hat{u}'^2)^{3/2}} + \frac{\hat{u}'}{\hat{r}\sqrt{1 + \hat{u}'^2}} = B\hat{u}, \quad \text{for } \hat{r} > \hat{r}_0, \quad (3.9)$$

$$\psi(\hat{r}_0) = \psi_0 \quad \text{and} \quad \lim_{\hat{r} \rightarrow \infty} \hat{u}(\hat{r}) = 0, \quad (3.10)$$

where $\hat{u}' = \frac{d\hat{u}}{d\hat{r}}$, $\hat{r}_0 = \sin(\phi_0)$ and $B = \kappa a^2$, known as Bond number.

Bond number B can be scaled to 1 by $\bar{r} = \sqrt{B}\hat{r}$ and $\bar{u} = \sqrt{B}\hat{u}$ (instead, B appears in the boundary condition). Therefore, the scaled BVP is

$$\frac{\bar{u}''}{(1 + \bar{u}'^2)^{3/2}} + \frac{\bar{u}'}{\bar{r}\sqrt{1 + \bar{u}'^2}} = \bar{u}, \quad \text{for } \bar{r} > \bar{r}_0, \quad (3.11)$$

$$\psi(\bar{r}_0) = \psi_0 \quad \text{and} \quad \lim_{\bar{r} \rightarrow \infty} \bar{u}(\bar{r}) = 0, \quad (3.12)$$

where $\bar{u}' = \frac{d\bar{u}}{d\bar{r}}$ and $\bar{r}_0 = \sqrt{B} \sin(\phi_0)$.

The fluid interface can also be a non-graph. The geometric form is considered. Thus, the dimensionless DE is shown as follows,

$$\frac{1}{\hat{r}} (\hat{r} \sin \psi)_{\hat{r}} = B\hat{u}, \quad (3.13)$$

where ψ is the inclination angle of the fluid interface, see Fig. 3.1b. The solutions \hat{r} and \hat{u} can be parametrized by ψ , see Finn [18]. From (3.13),

$$\sin(\psi) + \hat{r} \cos(\psi) \frac{d\psi}{d\hat{r}} = B\hat{r}\hat{u}, \quad (3.14)$$

combined with $\frac{d\hat{u}}{d\hat{r}} = \tan(\psi)$, we obtain

$$\frac{d\hat{r}}{d\psi} = \frac{\hat{r} \cos \psi}{B\hat{r}\hat{u} - \sin \psi} \quad \text{and} \quad \frac{d\hat{u}}{d\psi} = \frac{\hat{r} \sin \psi}{B\hat{r}\hat{u} - \sin \psi}. \quad (3.15)$$

The boundary conditions become

$$\hat{r}(\psi_0) = \hat{r}_0 \quad \text{and} \quad \lim_{\psi \rightarrow 0} \hat{u}(\psi) = 0, \quad (3.16)$$

where $\hat{r}_0 = \sin(\phi_0)$. Based on Elcrat, Neel and Siegel [13], with the prescribed initial data: the inclination angle ψ_0 and the radial distance \hat{r}_0 , there exists a unique solution for the above BVP. Therefore, we write

$$\hat{r} = \hat{r}(\psi; \hat{r}_0, \psi_0) \quad \text{and} \quad \hat{u} = \hat{u}(\psi; \hat{r}_0, \psi_0). \quad (3.17)$$

From the geometric constraint in (3.1), there is one-to-one correspondence between ψ_0 and ϕ_0 . So, the fluid interface can be uniquely determined by the attachment angle ϕ_0 . So, we define

$$\hat{r}_c(\psi; \phi_0) = \hat{r}(\psi; \sin(\phi_0), \phi_0 + \gamma - \pi) \quad \text{and} \quad \hat{u}_c(\psi; \phi_0) = \hat{u}(\psi; \sin(\phi_0), \phi_0 + \gamma - \pi). \quad (3.18)$$

where c stands for composition. In later discussion, we ignore the subscript c for simplicity.

Moreover, the scaled system of DEs are

$$\frac{d\bar{r}}{d\psi} = \frac{\bar{r} \cos \psi}{\bar{r}\bar{u} - \sin \psi}, \quad \frac{d\bar{u}}{d\psi} = \frac{\bar{r} \sin \psi}{\bar{r}\bar{u} - \sin \psi}, \quad (3.19)$$

and the boundary conditions become

$$\bar{r}(\psi_0) = \bar{r}_0 \quad \text{and} \quad \lim_{\psi \rightarrow 0} \bar{u}(\psi) = 0, \quad (3.20)$$

where $\bar{r}_0 = \sqrt{B} \sin \phi_0$. As discussed, the solutions can be written as $\bar{r} = \bar{r}(\psi; \phi_0)$ and $\bar{u} = \bar{u}(\psi; \phi_0)$.

Remark 8. Vogel [63] and Elcrat, Neel and Siegel [13] studied the solutions with the form

$$\bar{r} = \bar{r}(\psi; \sigma) \quad \text{and} \quad \bar{u} = \bar{u}(\psi; \sigma), \quad (3.21)$$

where σ is the radial distance of the profile curve when the slope becomes vertical. Based on Vogel [63], both \bar{r} and \bar{u} are C^1 and monotonic in σ . In Sec. 3.4, we develop the smoothness of solutions with respect to ϕ_0 . This requires the extension of Vogel's smoothness and monotonicity results.

The parametric solution in (3.17) is also valid when the fluid interface is a graph. However, the zero solution ($\hat{u} = 0$) is not contained. It is included in (3.11), instead. Therefore, both graph and parametric descriptions are considered in discussion of the differentiable dependence of solutions on ϕ_0 (see Sec. 3.4) and the relation between the total force and the total energy (see Sec. 3.6).

Remark 9. When we analyze the behavior of solutions or apply the shooting method, the scaled capillary equation is considered. Since the Bond number can be scaled to 1 in the capillary equation, it becomes more convenient in analysis and numerical computation, see Sec. 3.7.

3.3 Preliminaries

In this section, we state the dependence of solutions on initial data from ODE theory, see [55] and Levinson's theorem, which will be used for later analysis. Consider the following IVP,

$$x' = f(t, x), \tag{3.22}$$

$$x(t_0) = x_0, \tag{3.23}$$

where $(t, x), (t_0, x_0) \in \mathbb{R} \times \mathbb{R}^n$. Suppose the system has a solution $x = x(t; t_0, x_0)$.

Theorem 13. (*Continuous Dependence on Initial Data*) Let $U \subset \mathbb{R} \times \mathbb{R}^n$ be an open bounded set and the closure $\bar{U} \subset \mathbb{R} \times \mathbb{R}^n$ and $(t_0, x_0) \in U$. Assume that $f(t, x)$ is Lipschitz in x on U . Then the unique solution $x(t) = x(t; t_0, x_0)$ is a continuous function of (t_0, x_0) .

We also state the smooth dependence on initial data for the $n = 1$ case.

Theorem 14. (*Smooth Dependence on (t_0, x_0)*) Let $f, \frac{\partial f}{\partial x}$ are both continuous on U and $x(t) = x(t; t_0, x_0)$ is the unique solution of IVP, then $\frac{\partial x}{\partial t_0}(t; t_0, x_0)$ exists and satisfies

$$\frac{\partial x}{\partial t_0}(t; t_0, x_0) = -\frac{\partial x}{\partial x_0}(t; t_0, x_0)f(t_0, x_0). \tag{3.24}$$

Theorem 15. (*One-dimensional Maximum Principle [50]*) Suppose $y = y(x)$ satisfies

$$y'' + g(x)y' + h(x)y \geq 0 \tag{3.25}$$

for $x \in (a, b)$ with $h(x) \leq 0$. If both $g(x)$ and $h(x)$ are bounded functions, and if the non-negative maximum M of y is attained at an interior point $c \in (a, b)$, then $y \equiv M$.

Levinson's theorem is a powerful technique to determine the limiting property of a linear dynamical system, see Eastham [12]. We restate Levinson's theorem for the 2×2 diagonal system case.

Theorem 16. (Levinson's Theorem [12]) Let $\Lambda(t)$ be an 2×2 matrix,

$$\Lambda(t) = \text{diag}(\lambda_1(t), \lambda_2(t)),$$

which satisfies either of the following conditions L (known as the dichotomy condition):

$$(i) \int_s^t \text{Re} \{ \lambda_1(\xi) - \lambda_2(\xi) \} d\xi \leq K_1,$$

$$(ii) \int_s^t \text{Re} \{ \lambda_1(\xi) - \lambda_2(\xi) \} d\xi \geq K_2,$$

for all $t_0 \leq s \leq t < \infty$. K_1 and K_2 are constants. Let the 2×2 matrix $R(t)$ satisfy

$$\int_{t_0}^{\infty} |R(t)| dt < \infty \quad (3.26)$$

((3.26) means each entry in $R(t)$, $R_{i,j}$, satisfies $\int_{t_0}^{\infty} |R_{i,j}(t)| dt < \infty$ for $i, j = 1, 2$). Then, as $t \rightarrow \infty$, the system

$$Y'(t) = \{ \Lambda(t) + R(t) \} Y(t) \quad (3.27)$$

has solutions $Y_i(t)$, $i \in \{1, 2\}$ with the asymptotic forms

$$Y_1(t) = \left\{ \begin{pmatrix} 1 \\ 0 \end{pmatrix} + o(1) \right\} \exp \left(\int_{t_0}^t \lambda_1(\xi) d\xi \right), \quad (3.28)$$

$$Y_2(t) = \left\{ \begin{pmatrix} 0 \\ 1 \end{pmatrix} + o(1) \right\} \exp \left(\int_{t_0}^t \lambda_2(\xi) d\xi \right). \quad (3.29)$$

3.4 Differentiable Dependence of Solutions on ϕ_0

In this section, we develop C^1 smoothness of solutions with respect to ϕ_0 . We study both parametric and graph descriptions of solutions based on Vogel [63]. In Sec. 3.4.1, the profile curve of the form $\bar{r}(\psi; \sigma)$ and $\bar{u}(\psi; \sigma)$ is studied. The inclination angle ψ is extended to $-\pi$ or π . $\sigma > 0$ is the radial distance when the slope of the profile curve becomes vertical, which is used as a parameter. However, the zero solution is not contained in parametric solutions. We consider the graph description of the profile curve, $w(\bar{r}; r_w, \bar{u})$, where (r_w, \bar{u}) are initial values. \bar{u} is considered as a parameter. In Sec. 3.4.2, the properties of $w(\bar{r}; r_w, \bar{u})$ are studied. In Sec. 3.4.3, we fit the profile curve to the floating ball problem. Both the non-graph and graph cases are considered. Smooth dependence of solutions on ϕ_0 is shown. As a by-product, we prove Vogel's conjecture on the smoothness of the envelope of exterior solutions, see Sec. 3.4.4.

3.4.1 Profile Curve $\bar{r}(\psi; \sigma)$ and $\bar{u}(\psi; \sigma)$

In this section, the parametric profile curve $\bar{r}(\psi; \sigma)$ and $\bar{u}(\psi; \sigma)$ is considered, where $\sigma > 0$ is the radial distance of which the slope of the profile curve becomes vertical and the inclination angle ψ is extended to $-\pi$ or π . Suppose $\psi \in [-\pi, 0)$, hence, $\bar{u} > 0$ (the $\psi \in (0, \pi]$ case is similar). Vogel [63] and Elcrat, Neel and Siegel [13] study the properties of the profile curve depending on σ . Let $(\sigma, T(\sigma))$ be the point of the profile curve, where the slope becomes vertical ($\psi = -\frac{\pi}{2}$). Hence,

$$\bar{r}\left(-\frac{\pi}{2}\right) = \sigma \quad \text{and} \quad \bar{u}\left(-\frac{\pi}{2}\right) = T(\sigma). \quad (3.30)$$

From Vogel [63], for any given $\sigma > 0$, there is a unique solution passing through $(\sigma, T(\sigma))$. He also showed $T(\sigma)$ is C^1 for $\sigma \in (0, \infty)$. Based on smooth dependence of solutions on initial data in (3.30), \bar{r} and \bar{u} are C^1 in σ .

Remark 10. The property of $T(\sigma)$ has been studied. Siegel [56] showed $T(\sigma)$ is strictly increasing in σ . Turkington [59] showed $T(\sigma) \sim \sigma \ln\left(\frac{1}{\sigma}\right)$ as $\sigma \rightarrow 0$. Vogel [63] also showed $\bar{u}(\psi; \sigma) < 2T(\sigma)$ for all $\psi \in [-\pi, 0)$ and $\sigma > 0$. And $\bar{r}(-\pi; \sigma) = \mathcal{O}\left(\frac{1}{\sqrt{\ln(1/\sigma)}}\right)$ as $\sigma \rightarrow 0$. More discussion of $T(\sigma)$ can be found in Heartland and Hartley [30], Elcrat, Neel and Siegel [13] and Elcrat and Treinen [14].

In the following Lemma 12 and Lemma 13, the monotonicity of \bar{r} and \bar{u} with respect to the parameter σ is investigated.

Lemma 12. *For $\psi \in [-\pi, 0)$, \bar{r} and \bar{u} are both strictly increasing in σ . Hence, $\dot{\bar{r}} \geq 0$ and $\dot{\bar{u}} \geq 0$.*

Proof. Let $0 < \sigma_1 < \sigma_2$, we define $f(\psi) = \bar{r}(\psi; \sigma_2) - \bar{r}(\psi; \sigma_1)$ and $g(\psi) = \bar{u}(\psi; \sigma_2) - \bar{u}(\psi; \sigma_1)$. We have $f\left(-\frac{\pi}{2}\right) = \sigma_2 - \sigma_1 > 0$ and $g\left(-\frac{\pi}{2}\right) > 0$ from Siegel [56]. We claim that $f(\psi) > 0$ and $g(\psi) > 0$ on $[-\frac{\pi}{2}, 0)$. If not, there is a smallest $\psi_1 \in (-\frac{\pi}{2}, 0)$ so that either

- (i) $f(\psi_1) = 0$ and $g(\psi_1) > 0$;
- (ii) $f(\psi_1) > 0$ and $g(\psi_1) = 0$;

(iii) $f(\psi_1) = 0$ and $g(\psi_1) = 0$.

From Elcrat, Neel and Siegel [13], $f(\psi_1) = 0$ implies that the solutions are the same giving $f = g = 0$ for all $\psi \in [-\frac{\pi}{2}, 0)$. By Vogel [63], $g(\psi_1) = 0$ implies that the solutions are the same giving $f = g = 0$ for all $\psi \in [-\frac{\pi}{2}, 0)$. Thus, (i), (ii) or (iii) lead to a contradiction. A similar argument shows $f(\psi) > 0$ and $g(\psi) > 0$ on $[-\pi, -\frac{\pi}{2}]$. □

Let

$$\dot{r} = \frac{\partial}{\partial \sigma} \bar{r}(\psi; \sigma) \quad \text{and} \quad \dot{u} = \frac{\partial}{\partial \sigma} \bar{u}(\psi; \sigma). \quad (3.31)$$

We differentiate the scaled capillary equation in (3.19) with respect to σ ,

$$\frac{d\dot{r}}{d\psi} = -\frac{\cos \psi (\bar{r}^2 \dot{u} + \dot{r} \sin \psi)}{(\bar{r}\bar{u} - \sin \psi)^2}, \quad (3.32)$$

$$\frac{d\dot{u}}{d\psi} = -\frac{\sin \psi (\bar{r}^2 \dot{u} + \dot{r} \sin \psi)}{(\bar{r}\bar{u} - \sin \psi)^2}. \quad (3.33)$$

Lemma 12 gives $\dot{r} \geq 0$ and $\dot{u} \geq 0$ for $\psi \in [-\pi, 0)$. Lemma 13 improves Lemma 12 such that $\dot{r} > 0$ for $\psi \in (-\pi, 0)$ and $\dot{u} > 0$ for $\psi \in [-\pi, 0)$.

Lemma 13. $\dot{r} > 0$ for $\psi \in (-\pi, 0)$ and $\dot{u} > 0$ for $\psi \in [-\pi, 0)$.

Proof. We first show both $\dot{r} > 0$ and $\dot{u} > 0$ for $\psi \in (-\pi, 0)$. Suppose either \dot{r} or \dot{u} are not strictly greater than 0, there is $\psi_2 \in (-\pi, 0)$ such that $\dot{r}(\psi_2; \sigma) = 0$ or $\dot{u}(\psi_2; \sigma) = 0$. Without loss of generality, suppose the first of these, combined with $\dot{r} \geq 0$, it gives $\frac{d\dot{r}}{d\psi}(\psi_2; \sigma) = 0$. At $\psi = \psi_2$, (3.32) implies $\dot{u}(\psi_2; \sigma) = 0$ or $\psi_2 = -\frac{\pi}{2}$. But $\dot{r}(-\frac{\pi}{2}; \sigma) = 1$, which rules out the $\psi_2 = -\frac{\pi}{2}$ case. Then, $\dot{u}(\psi_2; \sigma) = 0$. By the uniqueness theorem of IVP, $\dot{r}(\psi; \sigma)$ and $\dot{u}(\psi; \sigma)$ are identically zero on $(-\pi, 0)$ which contradicts $\dot{r}(-\frac{\pi}{2}; \sigma) = 1$. The other case is similar. At $\psi = -\pi$, we follow Vogel's idea [63] and consider two possibilities:

- (i) $\dot{r}(-\pi; \sigma) = 0$ and $\dot{u}(-\pi; \sigma) = 0$. It is impossible. The above uniqueness argument rules out this case.
- (ii) $\dot{r}(-\pi; \sigma) > 0$ and $\dot{u}(-\pi; \sigma) = 0$. It implies $\frac{d\dot{u}}{d\psi}(-\pi; \sigma) = 0$. By L'Hopital's rule, we obtain

$$\lim_{\psi \rightarrow -\pi} \frac{\dot{u}(\psi; \sigma)}{\psi + \pi} = 0. \quad (3.34)$$

Then

$$\lim_{\psi \rightarrow -\pi} \frac{\bar{r}^2 \dot{u} + \dot{r} \sin \psi}{\psi + \pi} < 0. \quad (3.35)$$

Therefore, there exists a small $\eta > 0$ such that $\bar{r}^2 \dot{u} + \dot{r} \sin \psi < 0$ on $(-\pi, -\pi + \eta)$. It implies $\frac{d\dot{r}}{d\psi}(\psi; \sigma) < 0$ on $(-\pi, -\pi + \eta)$. Then, we must have $\dot{r}(-\pi + \eta; \sigma) < 0$, which contracts with our previous result. □

3.4.2 Profile Curve $w(\bar{r}; r_w, \bar{u})$

The zero solution $\bar{u} = 0$ is not included in the parametric solution (\bar{r}, \bar{u}) but is contained in the graph case. Suppose $\bar{r} = r_w > 0$ is fixed and consider the corresponding fluid height $\bar{u} \in (-T(r_w), T(r_w))$ as a parameter. According to Johnson and Perko [33] and Vogel [63], we write the profile curve as $w(\bar{r}; r_w, \bar{u})$, $\bar{r} \geq r_w$. $w(\bar{r}; r_w, \bar{u})$ satisfies

$$w'' = w(1 + w'^2)^{3/2} - \frac{w'}{\bar{r}}(1 + w'^2) \quad (3.36)$$

with boundary conditions

$$w(r_w; r_w, \bar{u}) = \bar{u}, \quad (3.37)$$

$$\lim_{\bar{r} \rightarrow \infty} w(\bar{r}; r_w, \bar{u}) = 0 \quad (3.38)$$

$$w'(r_w; r_w, \bar{u}) = p(r_w, \bar{u}), \quad (3.39)$$

where $w' = \frac{\partial}{\partial \bar{r}} w(\bar{r}; r_w, \bar{u})$. From Johnson and Perko [33] and Vogel [63], there is a unique solution of $w(\bar{r}; r_w, \bar{u})$ which satisfies (3.37) and (3.38). Moreover, (3.39) defines a slope

function $p(r_w, \bar{u})$, which is continuous in parameter \bar{u} .

Consider a region, defined as follows,

$$W_2 = \{(\bar{r}, \bar{u}) : \bar{r} > 0 \text{ and } -T(\bar{r}) < \bar{u} < T(\bar{r})\}, \quad (3.40)$$

which is swept out by the solutions which are graphs, not including the vertical points, see Fig. 3.3.

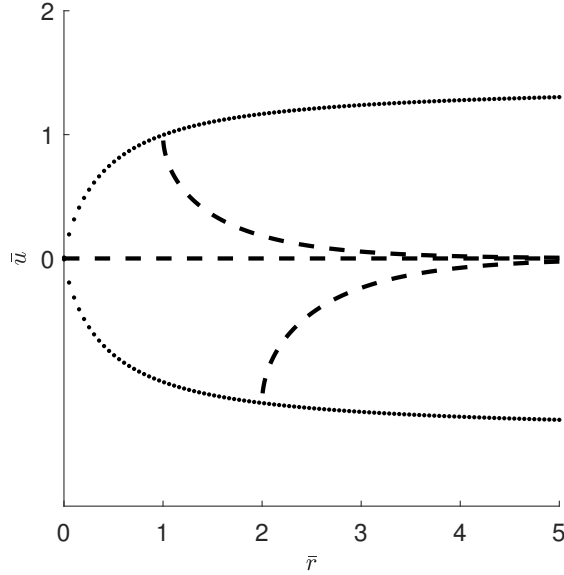


Figure 3.3: The figure illustrates W_2 region, the upper dashed curve represents the profile with $\sigma = 1$ and the lower dashed curve represents the profile with $\bar{r}(\pi/2) = 2$.

Property 2 summarizes the properties of $w(\bar{r}; r_w, \bar{u})$, see Johnson and Perko [33], Siegel [56] and Vogel [63].

Property 2. Fixed $r_w > 0$, let $\bar{r} \geq r_w$, $\bar{u}, \bar{u}_i \in (-T(r_w), T(r_w))$, and $\bar{u}_1 < \bar{u}_2$, then

- (i) if $\bar{u} > 0$, then $w(\bar{r}; r_w, \bar{u}) > 0$, $w'(\bar{r}; r_w, \bar{u}) < 0$ and $w''(\bar{r}; r_w, \bar{u}) > 0$; if $\bar{u} < 0$, then $w(\bar{r}; r_w, \bar{u}) < 0$, $w'(\bar{r}; r_w, \bar{u}) > 0$ and $w''(\bar{r}; r_w, \bar{u}) < 0$; if $\bar{u} = 0$, then $w(\bar{r}; r_w, \bar{u}) = w'(\bar{r}; r_w, \bar{u}) = w''(\bar{r}; r_w, \bar{u}) = 0$.

- (ii) $w(\bar{r}; r_w, \bar{u}_1) < w(\bar{r}; r_w, \bar{u}_2)$, $w'(\bar{r}; r_w, \bar{u}_2) < w'(\bar{r}; r_w, \bar{u}_1)$ and $w''(\bar{r}; r_w, \bar{u}_1) < w''(\bar{r}; r_w, \bar{u}_2)$.
- (iii) If $\bar{u} \neq 0$, then $w(\bar{r}; r_w, \bar{u})$, $w'(\bar{r}; r_w, \bar{u})$ and $w''(\bar{r}; r_w, \bar{u})$ are of order $\mathcal{O}\left(\frac{e^{-\bar{r}}}{\sqrt{\bar{r}}}\right)$ as $\bar{r} \rightarrow \infty$. In detail, $w \sim cK_0(\bar{r})$, $w' \sim -cK_1(\bar{r})$ and $w'' \sim cK_1'(\bar{r}) = \frac{c}{2}(K_0 + K_2)$, for some c .

Vogel [63] proved $p(r_w, \bar{u})$ is C^1 in \bar{u} for r_w sufficiently large. We follow Vogel's recipe and modify the result to any $r_w > 0$.

We define

$$v_\delta(\bar{r}) = \frac{w(\bar{r}; r_w, \bar{u} + \delta) - w(\bar{r}; r_w, \bar{u})}{\delta} \quad (3.41)$$

for small $\delta \neq 0$ and $(r_w, \bar{u} + \delta), (r_w, \bar{u}) \in W_2$. Hence,

$$v'_\delta(\bar{r}) = \frac{w'(\bar{r}; r_w, \bar{u} + \delta) - w'(\bar{r}; r_w, \bar{u})}{\delta}. \quad (3.42)$$

To study $v_\delta(\bar{r})$, we first show $v_\delta(\bar{r})$ satisfies a BVP. Suppose $w_1(\bar{r})$ and $w_2(\bar{r})$ are two graph solutions of the scaled capillary equation. Thus,

$$\frac{d}{d\bar{r}} \left(\bar{r} \frac{w_{1\bar{r}}}{\sqrt{1 + w_{1\bar{r}}^2}} \right) = \bar{r}w_1 \quad \text{and} \quad \frac{d}{d\bar{r}} \left(\bar{r} \frac{w_{2\bar{r}}}{\sqrt{1 + w_{2\bar{r}}^2}} \right) = \bar{r}w_2. \quad (3.43)$$

Subtract the two equations above, then

$$\frac{d}{d\bar{r}} \left(\bar{r} \left(\frac{w_{1\bar{r}}}{\sqrt{1 + w_{1\bar{r}}^2}} - \frac{w_{2\bar{r}}}{\sqrt{1 + w_{2\bar{r}}^2}} \right) \right) = \bar{r}(w_1 - w_2). \quad (3.44)$$

Let $f(x) = \frac{x}{\sqrt{1 + x^2}}$. We apply the fundamental theorem of calculus on $f(x)$,

$$f(b) - f(a) = \int_a^b g(\varphi) d\varphi. \quad (3.45)$$

where $g(x) = f'(x) = \frac{1}{(1 + x^2)^{3/2}}$. By changing the variable, $\varphi = a + \tau(b - a)$,

$$f(b) - f(a) = (b - a) \int_0^1 g(a + \tau(b - a)) d\tau. \quad (3.46)$$

So, choose $a = w_{2\bar{r}}$ and $b = w_{1\bar{r}}$, we obtain

$$\frac{w_{1\bar{r}}}{\sqrt{1 + w_{1\bar{r}}^2}} - \frac{w_{2\bar{r}}}{\sqrt{1 + w_{2\bar{r}}^2}} = (w_{1\bar{r}} - w_{2\bar{r}})q_d(\bar{r}),$$

where

$$q_d(\bar{r}) = \int_0^1 g(w_{2\bar{r}} + \tau(w_{1\bar{r}} - w_{2\bar{r}})) d\tau.$$

Set $w_d(\bar{r}) = w_1(\bar{r}) - w_2(\bar{r})$, (3.44) gives

$$\frac{d}{d\bar{r}} (\bar{r}w'_d(\bar{r})q_d(\bar{r})) = \bar{r}w_d. \quad (3.47)$$

After some arrangement, we obtain a linear DE for $w_d(r)$,

$$w_d'' + \left(\frac{1}{\bar{r}} + \frac{q'_d}{q_d} \right) w_d' = \frac{1}{q_d} w_d, \quad (3.48)$$

where

$$q_d(\bar{r}) = \int_0^1 [1 + (w_{2\bar{r}} + \tau(w_{1\bar{r}} - w_{2\bar{r}}))^2]^{-3/2} d\tau. \quad (3.49)$$

Since the DE in (3.48) is linear, replacing w_1 and w_2 by $w(\bar{r}; r_w, \bar{u} + \delta)$ and $w(\bar{r}; r_w, \bar{u})$, respectively, thus, $v_\delta(\bar{r})$ solves the following BVP:

$$v_\delta'' + \left(\frac{1}{\bar{r}} + \frac{q'_\delta}{q_\delta} \right) v_\delta' = \frac{1}{q_\delta} v_\delta \quad (3.50)$$

for $\bar{r} \geq r_w$, with boundary conditions

$$v_\delta(r_w) = 1 \quad \text{and} \quad \lim_{\bar{r} \rightarrow \infty} v_\delta(\bar{r}) = 0, \quad (3.51)$$

and $q_\delta(\bar{r})$ is defined as

$$q_\delta(\bar{r}) = \int_0^1 [1 + (w'(\bar{r}; r_w, \bar{u}) + \tau(w'(\bar{r}; r_w, \bar{u} + \delta) - w'(\bar{r}; r_w, \bar{u})))^2]^{-3/2} d\tau. \quad (3.52)$$

Remark 11. The construction of $v_\delta(\bar{r})$ and the BVP of $v_\delta(\bar{r})$ in (3.50) - (3.52) are both considered by Vogel [63]. If we can show $\lim_{\delta \rightarrow 0} v'_\delta(r_w)$ exists, it is equivalent to show $p_{\bar{u}}(r_w, \bar{u})$ exists. The DE of w_d in (3.48) is first seen in Siegel [56], he applied w_d to study the limiting behavior of the difference of solutions as $\bar{r} \rightarrow \infty$.

The following Lemma 14 shows the bounds of $q_\delta(\bar{r})$ and $q'_\delta(\bar{r})$,

Lemma 14. *For $\delta \neq 0$ small enough and $\bar{r} \geq r_w$, there exist $d_1, d_2 > 0$ such that*

$$d_1 \leq q_\delta(\bar{r}) < 1, \quad (3.53)$$

$$0 < q'_\delta(\bar{r}) \leq d_2. \quad (3.54)$$

Proof. Let $w'_1 = w'(\bar{r}; r_w, \bar{u} + \delta)$ and $w'_2 = w'(\bar{r}; r_w, \bar{u})$. Given $\delta \neq 0$ small enough, from Property 2, if $\bar{u} > 0$, then $w'_1 < 0$ ($w''_1 > 0$) and $w'_2 < 0$ ($w''_2 > 0$). If $\bar{u} < 0$, then $w'_1 > 0$ ($w''_1 < 0$) and $w'_2 > 0$ ($w''_2 < 0$). If $\bar{u} = 0$, then $w'_2 = 0$ ($w''_2 = 0$). So, we cannot have $w'_2 + \tau(w'_1 - w'_2) = 0$ for all $\tau \in [0, 1]$. Hence, $q_\delta(\bar{r}) < 1$. By boundedness of w'_1 and w'_2 , let $|w'_2 + \tau(w'_1 - w'_2)| \leq m_1$ for some $m_1 > 0$. Thus, $q_\delta(\bar{r}) \geq (1 + m_1^2)^{-3/2} = d_1 > 0$.

For $q'_\delta(\bar{r})$,

$$q'_\delta(\bar{r}) = -3 \int_0^1 \frac{(w'_2 + \tau(w'_1 - w'_2))(w''_2 + \tau(w''_1 - w''_2))}{[1 + (w'_2 + \tau(w'_1 - w'_2))^2]^{5/2}} d\tau. \quad (3.55)$$

By noting that $w'_2 + \tau(w'_1 - w'_2)$ and $w''_2 + \tau(w''_1 - w''_2)$ have different signs, thus, $q'_\delta(\bar{r}) > 0$.

Let $\left| 3 \frac{w'_2 + \tau(w'_1 - w'_2)}{[1 + (w'_2 + \tau(w'_1 - w'_2))^2]^{5/2}} \right| \leq m_2$ and $|w''_2 + \tau(w''_1 - w''_2)| \leq m_3$ for some $m_2 > 0$ and $m_3 > 0$. Hence,

$$q'_\delta(\bar{r}) \leq \int_0^1 m_2 m_3 d\tau = m_2 m_3 = d_2 < \infty.$$

□

We construct both sub-solution and super-solution of $v_\delta(\bar{r})$ in Lemma 15.

Lemma 15. For $\bar{r} \in [r_w, \infty)$, let $U(\bar{r}) = A_1 e^{-\omega \bar{r}}$ for $A_1, \omega > 0$ and $V(\bar{r}) = A_2 K_0(\bar{r})$ for $A_2 > 0$. $A_1 = e^{\omega r_w}$ and $A_2 = \frac{1}{K_0(r_w)}$ are chosen such that both $U(\bar{r})$ and $V(\bar{r})$ satisfying boundary conditions of v_δ in (3.51). If ω satisfies the condition

$$\omega^2 - \left(\frac{1}{r_w} + \frac{d_2}{d_1} \right) \omega - \frac{1}{d_1} > 0, \quad (3.56)$$

where $d_1, d_2 > 0$ satisfy the inequalities in Lemma 14, then $U(\bar{r})$ is a sub-solution of v_δ ,

$$U'' + \left(\frac{1}{\bar{r}} + \frac{q'_\delta}{q_\delta} \right) U' > \frac{1}{q_\delta} U, \quad (3.57)$$

and $V(\bar{r})$ is a super-solution of v_δ ,

$$V'' + \left(\frac{1}{\bar{r}} + \frac{q'_\delta}{q_\delta} \right) V' < \frac{1}{q_\delta} V. \quad (3.58)$$

Proof. When $\omega > 0$ is chosen large enough, (3.56) is satisfied. From Lemma 14, there exist $d_1, d_2 > 0$ such that $d_1 \leq q_\delta < 1$ and $0 < q'_\delta \leq d_2$. Hence,

$$\omega^2 - \omega \left(\frac{1}{r_w} + \frac{q'_\delta}{q_\delta} \right) - \frac{1}{q_\delta} \geq \omega^2 - \omega \left(\frac{1}{r_w} + \frac{d_2}{d_1} \right) - \frac{1}{d_1}.$$

Therefore,

$$\begin{aligned} U'' + \left(\frac{1}{\bar{r}} + \frac{q'_\delta}{q_\delta} \right) U' - \frac{1}{q_\delta} U &= A_1 e^{-\omega \bar{r}} \left(\omega^2 - \omega \left(\frac{1}{r_w} + \frac{q'_\delta}{q_\delta} \right) - \frac{1}{q_\delta} \right) \\ &\geq A_1 e^{-\omega \bar{r}} \left(\omega^2 - \omega \left(\frac{1}{r_w} + \frac{d_2}{d_1} \right) - \frac{1}{d_1} \right) \\ &> 0, \end{aligned}$$

and

$$\begin{aligned}
V'' + \left(\frac{1}{\bar{r}} + \frac{q'_\delta}{q_\delta}\right) V' - \frac{1}{q_\delta} V &= A_2 K_0(\bar{r}) + \frac{1}{\bar{r}} A_2 K_1(\bar{r}) - \left(\frac{1}{\bar{r}} + \frac{q'_\delta}{q_\delta}\right) A_2 K_1(\bar{r}) - \frac{1}{q_\delta} A_2 K_0(\bar{r}) \\
&= A_2 K_0(\bar{r}) \left(\frac{q_\delta - 1}{q_\delta}\right) - A_2 K_1(\bar{r}) \frac{q'_\delta}{q_\delta} \\
&< 0.
\end{aligned}$$

Hence, $U(\bar{r})$ becomes a sub-solution of v_δ and $V(\bar{r})$ becomes a super-solution of v_δ . Moreover, $A_1 = e^{\omega r_w}$ and $A_2 = \frac{1}{K_0(r_w)}$ can be determined by $U(r_w) = V(r_w) = 1$. As $\bar{r} \rightarrow \infty$, $\lim_{\bar{r} \rightarrow \infty} U(\bar{r}) = \lim_{\bar{r} \rightarrow \infty} V(\bar{r}) = 0$. Hence, boundary conditions of v_δ are satisfied.

□

With the sub-solution $U(\bar{r})$ and the super-solution $V(\bar{r})$ in Lemma 15, we construct the inequalities of $v_\delta(\bar{r})$ based on the maximum principle, see Theorem 15 (Protter and Weinberger [50]). Let $U_d(\bar{r}) = U(\bar{r}) - v_\delta(\bar{r})$ and $V_d(\bar{r}) = v_\delta(\bar{r}) - V(\bar{r})$. Hence,

$$U_d'' + \left(\frac{1}{\bar{r}} + \frac{q'_\delta}{q_\delta}\right) U_d' - \frac{1}{q_\delta} U_d > 0, \quad (3.59)$$

$$V_d'' + \left(\frac{1}{\bar{r}} + \frac{q'_\delta}{q_\delta}\right) V_d' - \frac{1}{q_\delta} V_d > 0. \quad (3.60)$$

With $U_d(r_w) = V_d(r_w) = 0$ and $\lim_{\bar{r} \rightarrow \infty} U_d(\bar{r}) = \lim_{\bar{r} \rightarrow \infty} V_d(\bar{r}) = 0$, the maximum principle implies $U_d(\bar{r}) \leq 0$ and $V_d(\bar{r}) \leq 0$ for $\bar{r} \in [r_w, \infty)$, therefore,

$$U(\bar{r}) \leq v_\delta(\bar{r}) \leq V(\bar{r}) \quad (3.61)$$

for $\bar{r} \in [r_w, \infty)$. Moreover, with $U(r_w) = V(r_w) = 1$, we have

$$-\omega = U'(r_w) \leq v'_\delta(r_w) \leq V'(r_w) = -A_2 K_1(r_w) < 0. \quad (3.62)$$

(3.62) gives the boundedness of $v'_\delta(r_w)$. For any sequence $\{\delta_i\} \rightarrow 0$, there exists a subsequence $\{\bar{\delta}_i\} \rightarrow 0$ such that

$$\lim_{i \rightarrow \infty} v'_{\delta_i}(r_w) = L, \quad (3.63)$$

where $L < 0$.

Therefore, when $\bar{r} \geq r_w$, the following initial value problem of $v(\bar{r}; \bar{u})$ is constructed,

$$v'' + \left(\frac{1}{\bar{r}} + \frac{q'}{q} \right) v' = \frac{1}{q} v, \quad (3.64)$$

where v' means $\frac{\partial}{\partial \bar{r}} v(\bar{r}; \bar{u})$, with initial conditions

$$v(r_w; \bar{u}) = 1 \quad \text{and} \quad v'(r_w; \bar{u}) = L, \quad (3.65)$$

where

$$q(\bar{r}) = \left(1 + (w'(\bar{r}; r_w, \bar{u}))^2 \right)^{-3/2} \quad (3.66)$$

and L is defined in (3.63).

The above IVP has a unique solution $v(\bar{r}; \bar{u})$. And From Property 2, both $q_\delta(\bar{r}) \rightarrow q(\bar{r})$ and $q'_\delta(\bar{r}) \rightarrow q'(\bar{r})$ uniformly as $\delta \rightarrow 0$ for $\bar{r} \in [r_w, \infty)$. Hence, $v_\delta(\bar{r})$ converges almost uniformly to $v(\bar{r}; \bar{u})$ as $\delta \rightarrow 0$ for $\bar{r} \in [r_w, r_1)$, r_1 can be extended to $+\infty$, see Vogel [63]. Vogel also argued that $v(\bar{r}; \bar{u}) > 0$, $v'(\bar{r}; \bar{u}) < 0$ and $v''(\bar{r}; \bar{u}) > 0$. Moreover, $\lim_{\bar{r} \rightarrow \infty} v(\bar{r}; \bar{u}) = 0$. Therefore, the limit L does not depend on the sequence chosen. We have

$$p_{\bar{u}}(r_w, \bar{u}) = \lim_{\delta \rightarrow 0} v'_\delta(r_w) = v'(r_w; \bar{u}) = L. \quad (3.67)$$

And the continuity of $p_{\bar{u}}(r_w, \bar{u})$ is directly from the continuous dependence of $v'(\bar{r}; \bar{u})$ on parameter \bar{u} .

Therefore, we can state the differentiability of $p(r_w, \bar{u})$ in the following Lemma 16.

Lemma 16. For any $r_w > 0$, $\bar{u} \in (-T(r_w), T(r_w))$, then $p(r_w, \bar{u})$ is C^1 in \bar{u} such that

$$p_{\bar{u}}(r_w, \bar{u}) = v'(r_w; \bar{u}) < 0. \quad (3.68)$$

Remark 12. Lemma 16 modifies Lemmas 3.3 of Vogel [63], where he proved $p(r_w, \bar{u})$ is differentiable in \bar{u} for sufficiently large r_w . We extend his result to any $r_w > 0$, $\bar{u} \in (-T(r_w), T(r_w))$, which contains the $\bar{u} = 0$ case.

Lemma 16 shows $p(r_w, \bar{u})$ is C^1 in \bar{u} . To show $p(\bar{r}, \bar{u})$ is C^1 in W_2 , we replace \bar{u} by a parameter $\xi \in (-T(r_w), T(r_w))$, based on the smooth dependence of $w(\bar{r}; r_w, \xi)$ on the initial condition ξ , $w(\bar{r}; r_w, \xi)$ and $w'(\bar{r}; r_w, \xi)$ are both C^1 in ξ ($w(\bar{r}; r_w, \xi)$ and $w'(\bar{r}; r_w, \xi)$ are both C^1 in \bar{r} , as well). Choose $(\bar{r}, \bar{u}) \in W_2$ and r_w such that $\bar{r} \geq r_w > 0$. Consider

$$\bar{u} = w(\bar{r}; r_w, \xi), \quad (3.69)$$

where $w(\bar{r}; r_w, \xi)$ satisfies (3.36) with initial conditions defined in (3.37) and (3.39), recall that,

$$w(r_w; r_w, \xi) = \xi, \quad (3.70)$$

$$w'(r_w; r_w, \xi) = p(r_w, \xi). \quad (3.71)$$

To apply the implicit function theorem on (3.69), we differentiate equation of w with respect to ξ and denote $\frac{\partial}{\partial \xi} w(\bar{r}; r_w, \xi)$ as \dot{w} . Hence, \dot{w} satisfies

$$\dot{w}'' = (1 + w'^2)^{1/2}(\dot{w} + \dot{w}(w')^2 + 3ww'(\dot{w}')) - \frac{\dot{w}'}{\bar{r}}(1 + 3w'^2), \quad (3.72)$$

with initial conditions

$$\dot{w}(r_w; r_w, \xi) = 1, \quad (3.73)$$

$$\dot{w}'(r_w; r_w, \xi) = p_{\bar{u}}(r_w, \xi). \quad (3.74)$$

The properties of \dot{w} are shown in the following Property 3.

Property 3. Given $r_w > 0$, for any $\bar{r} > r_w$, we have $0 < \dot{w}(\bar{r}; r_w, \xi) < 1$ and $\dot{w}'(\bar{r}; r_w, \xi) < 0$. Moreover, if $\bar{r} \rightarrow \infty$, then $\dot{w}(\bar{r}; r_w, \xi) = \mathcal{O}\left(\frac{e^{-\bar{r}}}{\sqrt{\bar{r}}}\right)$.

Proof. From Property 2, we have $\dot{w}(\bar{r}; r_w, \xi) \geq 0$ and $\dot{w}'(\bar{r}; r_w, \xi) \leq 0$. Suppose there exists $r_4 > r_w$ such that $\dot{w}(r_4; r_w, \xi) = \dot{w}'(r_4; r_w, \xi) = 0$. The uniqueness of the IVP tells $\dot{w}(\bar{r}; r_w, \xi) = 0$ for $\bar{r} \geq r_4$, a contradiction. Thus, $\dot{w}(\bar{r}; r_w, \xi)$ and $\dot{w}'(\bar{r}; r_w, \xi)$ cannot be zero simultaneously. Furthermore, suppose we have either of the cases:

1. there exists $r_5 > r_w$ so that $\dot{w}(r_5; r_w, \xi) = 0$ and $\dot{w}'(r_5; r_w, \xi) < 0$;
2. there exists $r_6 > r_w$ so that $\dot{w}(r_6; r_w, \xi) > 0$ and $\dot{w}'(r_6; r_w, \xi) = 0$.

In case 1, consider $\dot{w}'(\bar{r}; r_w, \xi) < 0$ on some interval (r_5, η_1) . Integrating $\dot{w}'(\bar{r}; r_w, \xi)$ from r_5 to η_1 , we must have $\int_{r_5}^{\eta_1} \dot{w}'(t; r_w, \xi) dt < 0$. But $\int_{r_5}^{\eta_1} \dot{w}'(t; r_w, \xi) dt = \dot{w}(\eta_1; r_w, \xi) - \dot{w}(r_5; r_w, \xi) \geq 0$, a contradiction. In case 2, at $\bar{r} = r_6$, (3.72) gives $\dot{w}''(r_6; r_w, \xi) > 0$. Suppose $\dot{w}''(\bar{r}; r_w, \xi) > 0$ on some interval (r_6, η_2) . Integrating $\dot{w}''(\bar{r}; r_w, \xi)$ from r_6 to η_2 , we must have $\int_{r_6}^{\eta_2} \dot{w}''(t; r_w, \xi) dt > 0$. But $\int_{r_6}^{\eta_2} \dot{w}''(t; r_w, \xi) dt = \dot{w}'(\eta_2; r_w, \xi) - \dot{w}'(r_6; r_w, \xi) \leq 0$, a contradiction. Therefore, $\dot{w}(\bar{r}; r_w, \xi) > 0$ and $\dot{w}'(\bar{r}; r_w, \xi) < 0$. In addition, with $\dot{w}(r_w; r_w, \xi) = 1$, we have $\dot{w}(\bar{r}; r_w, \xi) < 1$.

From (3.61), as $\delta \rightarrow 0$, then $0 < \dot{w}(\bar{r}; r_w, \xi) \leq V(\bar{r})$. Hence, $V(\bar{r}) = \mathcal{O}\left(\frac{e^{-\bar{r}}}{\sqrt{\bar{r}}}\right)$. We obtain $\dot{w}(\bar{r}; r_w, \xi) = \mathcal{O}\left(\frac{e^{-\bar{r}}}{\sqrt{\bar{r}}}\right)$ as $\bar{r} \rightarrow \infty$. □

Since $0 < \dot{w}(\bar{r}; r_w, \xi) < 1$, the implicit function theorem gives that $\xi = \xi(\bar{r}, \bar{u})$ is C^1 in both \bar{r} and \bar{u} . Therefore, we conclude

Theorem 17. $p(\bar{r}, \bar{u}) = w'(\bar{r}; r_w, \xi(\bar{r}, \bar{u}))$ is C^1 in W_2 .

3.4.3 Smooth Dependence of Solutions on ϕ_0

In this section, we fit the profile curves obtained in Sec. 3.4.1 and Sec. 3.4.2 into the fluid interface of the floating ball using the geometric constraint, $\psi_0 = \phi_0 + \gamma - \pi$ with $\phi_0 \in (0, \pi)$

and $\gamma \in [0, \pi]$. Hence, $\psi_0 \in (-\pi, \pi)$. We are able to show the smooth dependence of solutions on ϕ_0 using the implicit function theorem. Both the graph and the non-graph cases are considered.

Suppose $\psi_0 \in (-\pi, 0) \cup (0, \pi)$. The parametric solution $\bar{r}(\psi; \sigma)$ and $\bar{u}(\psi; \sigma)$ discussed in Sec. 3.4.1 is considered. We have the following Lemma 17,

Lemma 17. *For any $\psi_0 \in (-\pi, 0)$, with the geometric constraint $\psi_0 = \phi_0 + \gamma - \pi$, γ is restricted to $\gamma \in [0, \pi)$, we denote $\bar{u}_0(\phi_0) = \bar{u}(\psi_0; \sigma)$, then $\bar{u}_0(\phi_0)$ is C^1 in $\phi_0 \in (0, \pi - \gamma)$.*

Proof. For a $\psi_0 \in (-\pi, 0)$, with the geometric constraint $\psi_0 = \phi_0 + \gamma - \pi$, γ is restricted to $\gamma \in [0, \pi)$, we have $\phi_0 \in (0, \pi - \gamma)$. Since $\bar{r}(\psi_0; \sigma) = \sqrt{B} \sin \phi_0$ is C^1 in ψ_0 and $\dot{r} > 0$ from Lemma 13, by the implicit function theorem, $\bar{r}(\psi_0; \sigma) = \sqrt{B} \sin(\phi_0)$ has a C^1 solution $\sigma = \sigma(\psi_0)$, so $\sigma = \sigma(\phi_0)$ is C^1 , where $\phi_0 \in (0, \pi - \gamma)$. This gives $\bar{u}_0(\phi_0) = \bar{u}(\psi_0; \sigma(\phi_0))$ is C^1 for $\phi_0 \in (0, \pi - \gamma)$. \square

Replacing \bar{u} by $-\bar{u}$, we address the result for the $\psi \in (0, \pi)$ case.

Lemma 18. *For any $\psi_0 \in (0, \pi)$, and $\gamma \in (0, \pi]$, $\bar{u}_0(\phi_0)$ is C^1 in $\phi_0 \in (\pi - \gamma, \pi)$.*

The only case left is when $\psi_0 = 0$ or $\phi_0 = \pi - \gamma$. To show the C^1 behavior of $\bar{u}_0(\phi_0)$ near $\phi_0 = \pi - \gamma$, we consider the profile curve $w(\bar{r}; r_w, \xi)$ in W_2 , see Sec. 3.4.2. With the geometric constraint,

$$p(\bar{r}_0, \bar{u}) = \tan(\psi_0), \tag{3.75}$$

where $(\bar{r}_0, \bar{u}) \in W_2$, $\bar{r}_0 = \sqrt{B} \sin(\phi_0) = \sqrt{B} \sin(\psi_0 - \gamma + \pi)$, and $\psi_0 \in \left(-\frac{\pi}{2}, \frac{\pi}{2}\right)$. Since p is C^1 in W_2 and $p_{\bar{u}} < 0$, the implicit function theorem gives \bar{u} is C^1 in ψ_0 , equivalently, $\bar{u}_0 = \bar{u}(\phi_0)$ is C^1 in ϕ_0 , $\phi_0 \in \left(\frac{\pi}{2} - \gamma, \frac{3\pi}{2} - \gamma\right)$, if $\gamma \in \left[0, \frac{\pi}{2}\right]$ or $\phi_0 \in \left[0, \frac{3\pi}{2} - \gamma\right)$, if $\gamma \in \left(\frac{\pi}{2}, \pi\right]$, both of which contain the case $\phi_0 = \pi - \gamma$. Thus, the following Lemma 19 states this result.

Lemma 19. For any $\psi_0 \in \left(-\frac{\pi}{2}, \frac{\pi}{2}\right)$ and $\gamma \in [0, \pi]$, $\bar{u}_0(\phi_0)$ is C^1 in ϕ_0 . Moreover, if $\gamma \in \left[0, \frac{\pi}{2}\right]$, then $\phi_0 \in \left(\frac{\pi}{2} - \gamma, \frac{3\pi}{2} - \gamma\right)$. If $\gamma \in \left(\frac{\pi}{2}, \pi\right]$, then $\phi_0 \in \left[0, \frac{3\pi}{2} - \gamma\right)$.

With Lemma 17 - Lemma 19, we summarize

Theorem 18. $\bar{u}_0(\phi_0)$ is C^1 for $\phi_0 \in (0, \pi)$.

Fig. 3.4 shows \bar{u}_0 versus ϕ_0 . As we can see, $\bar{u}_0(\phi_0)$ curve is consistent with Theorem 18. In addition, by smooth dependence on initial data, $w(\bar{r}; r_w, \xi)$ is C^1 in r_w , as well. Since $w(\bar{r}, r_w, \xi) = w(\bar{r}; \tau, w(\tau; r_w, \xi))$ by uniqueness, we differentiate the equation with respect to τ and set $\tau = r_w$, then

$$\frac{\partial}{\partial r_w} w(\bar{r}; r_w, \xi) = -\dot{w}(\bar{r}; r_w, \xi) p(r_w, \xi). \quad (3.76)$$

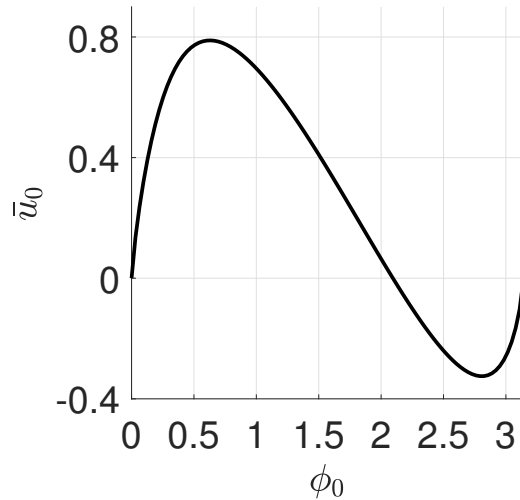


Figure 3.4: \bar{u}_0 versus ϕ_0 with $\gamma = \frac{\pi}{3}$ and $B = 1$.

Therefore, when the profile curves are fitted into the floating ball problem, we can write the solution as $\bar{r} = \bar{r}(\psi; \phi_0)$ and $\bar{u} = \bar{u}(\psi; \phi_0)$ in the non-graph case. In the graph case, we have $\bar{u} = \bar{u}(\bar{r}; \bar{r}_0, \bar{u}_0)$. In both graph and parametric descriptions, solutions are C^1 for $\phi_0 \in (0, \pi)$.

3.4.4 The Envelope of the Profile Curves

From Finn [18] and Vogel [63], the envelope of the profile curves satisfies

$$\begin{vmatrix} \frac{d\bar{u}}{d\psi}(\psi; \sigma) & \frac{d\bar{r}}{d\psi}(\psi; \sigma) \\ \dot{\bar{u}}(\psi; \sigma) & \dot{\bar{r}}(\psi; \sigma) \end{vmatrix} = 0 \quad (3.77)$$

or

$$F(\psi, \sigma) \equiv \dot{\bar{u}}(\psi; \sigma) \cos(\psi) - \dot{\bar{r}}(\psi; \sigma) \sin(\psi) = 0. \quad (3.78)$$

Fig. 3.5 shows a family of profile curves. As we can see, the profile curves form an envelope. Vogel [63] has a conjecture that the envelope is a C^1 curve. In this section, we are able to show it by applying the implicit function theorem.

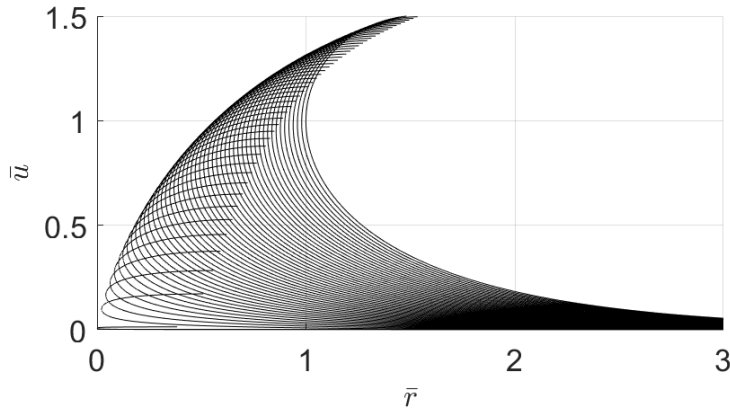


Figure 3.5: A family of profile curves with $B = 1$, $\psi \in (-\pi, 0)$ and $\sigma \in (0, 1)$.

Consider

$$\frac{dF}{d\psi} = -(\dot{\bar{u}}(\psi; \sigma) \sin(\psi) + \dot{\bar{r}}(\psi; \sigma) \cos(\psi)). \quad (3.79)$$

From Lemma 13, $\dot{u}(\psi; \sigma) > 0$ and $\dot{r}(\psi; \sigma) > 0$ for $\psi \in (-\pi, 0)$ and $\sigma > 0$. When $\psi \in \left[-\frac{\pi}{2}, 0\right)$, we have $F(\psi, \sigma) > 0$. Thus, F has no solution if $\psi \in \left[-\frac{\pi}{2}, 0\right)$. Hence, ψ must lie on $\left(-\pi, -\frac{\pi}{2}\right)$. In addition, $\frac{dF}{d\psi} > 0$ if $\psi \in \left(-\pi, -\frac{\pi}{2}\right)$. Hence, F is a monotone increasing function with respect to ψ . $F(-\pi, \sigma) = -\dot{u}(-\pi; \sigma) < 0$ and $F(-\frac{\pi}{2}, \sigma) = 1 > 0$. Thus, there is a unique $\psi \in \left(-\pi, -\frac{\pi}{2}\right)$ such that $F(\psi, \sigma) = 0$. Therefore, the implicit function theorem gives there is a unique C^1 function $\psi = \psi(\sigma)$ such that $F(\psi(\sigma), \sigma) = 0$. We address the following Theorem 19,

Theorem 19. *When $\psi \in (-\pi, 0)$ and $\sigma > 0$, there is a unique envelope and it is a C^1 curve, which can be described by $(\bar{r}(\psi(\sigma); \sigma), \bar{u}(\psi(\sigma); \sigma))$, where $\psi(\sigma)$ is a C^1 function on $(0, \infty)$.*

3.5 Asymptotic Analysis of Solutions as $\psi \rightarrow 0$

The limiting behavior of solutions is of our interest and will be applied in derivation of the relation between the total force and the total energy. In Sec. 3.5.1, the asymptotic expansions of $\bar{r}(\psi; \phi_0)$ and $\bar{u}(\psi; \phi_0)$ as $\psi \rightarrow 0$ are obtained by applying Theorem 2 (Olver [49]). From Lemma 3 in Sec. 3.4, $\dot{w}(\bar{r}; r_w, \xi) = \mathcal{O}\left(\frac{e^{-\bar{r}}}{\sqrt{\bar{r}}}\right)$ as $\bar{r} \rightarrow \infty$ is achieved. Equipped with Theorem 16 (Levinson's Theorem [12]), the leading order of \dot{w} as $\bar{r} \rightarrow \infty$ is found in Sec. 3.5.2. Levinson's Theorem can be applied to find the limiting behavior of \dot{r} and \dot{u} as $\psi \rightarrow 0$, as well. It is different from the notations used in Sec. 3.4. For the rest of the chapter, $\dot{r} = \frac{\partial}{\partial \phi_0} \bar{r}(\psi; \phi_0)$ and $\dot{u} = \frac{\partial}{\partial \phi_0} \bar{u}(\psi; \phi_0)$ are redefined. When the connection between the graph case and the non-graph case is considered, the limiting behavior of \dot{r} and \dot{u} is improved. The error bounds of \dot{r} and \dot{u} are improved as well when Picard's iterative method is used, see Sec. 3.5.3 - Sec. 3.5.5.

3.5.1 Asymptotic Forms of $\bar{r}(\psi; \phi_0)$ and $\bar{u}(\psi; \phi_0)$ as $\psi \rightarrow 0$

In this section, we discuss the asymptotic forms of $\bar{r}(\psi; \phi_0)$ and $\bar{u}(\psi; \phi_0)$ as $\psi \rightarrow 0$. We consider the $\psi < 0$ case (the $\psi > 0$ case is similar). As ψ is getting small ($\bar{r} \rightarrow \infty$), the

fluid interface becomes a graph and recall from Siegel [56],

$$\bar{u}(\bar{r}) = AK_0(\bar{r}) (1 + \mathcal{O}(K_0^2(\bar{r}))), \quad (3.80)$$

$$\bar{u}'(\bar{r}) = -AK_1(\bar{r}) (1 + \mathcal{O}(K_0^2(\bar{r}))), \quad (3.81)$$

where $A > 0$ depends on the boundary condition \bar{r}_0 and the contact angle γ and $\bar{u}'(\bar{r}) = \tan(\psi(\bar{r}))$ as well.

Taking the ratio of (3.80) and (3.81), we have

$$\frac{\bar{u}}{\tan \psi} = -\frac{K_0(\bar{r})}{K_1(\bar{r})} (1 + \mathcal{O}(K_0^2(\bar{r}))) \quad (3.82)$$

as $\bar{r} \rightarrow \infty$. Moreover, with $\frac{K_0(\bar{r})}{K_1(\bar{r})} \sim 1$ and $\tan(\psi) \sim \psi$, we have

$$\bar{u} \sim -\psi \quad (3.83)$$

as $\psi \rightarrow 0$.

To explore the asymptotic form of \bar{r} , from (3.81), we have

$$-\ln(-\tan(\psi)) = -\ln(AK_1(\bar{r})) - \ln(1 + \mathcal{O}(K_0^2(\bar{r}))). \quad (3.84)$$

We define RHS of (3.84) as $f(\bar{r})$,

$$f(\bar{r}) = -\ln(AK_1(\bar{r})) - \ln(1 + \mathcal{O}(K_0^2(\bar{r}))).$$

$f(\bar{r})$ is continuous and strictly increasing on an interval $a < \bar{r} < \infty$ for some $a > 0$. As $\bar{r} \rightarrow \infty$, we have $K_1(\bar{r}) \sim \sqrt{\frac{\pi}{2}} \frac{e^{-\bar{r}}}{\sqrt{\bar{r}}}$, and

$$f(\bar{r}) \sim \bar{r}.$$

From (3.84),

$$f(\bar{r}) = \xi, \quad (3.85)$$

where $\xi = -\ln(-\tan(\psi))$. Note that, $\xi \rightarrow \infty$ as $\bar{r} \rightarrow \infty$ (or $\psi \rightarrow 0$), as well.

Therefore, Theorem 2 (Olver [49]) from Chapter 2 can be applied to (3.85). It follows,

$$\bar{r}(\xi) \sim \xi, \quad (3.86)$$

as $\xi \rightarrow \infty$. Moreover,

$$f(\bar{r}) = \bar{r} + \frac{1}{2} \ln(\bar{r}) - \ln\left(\sqrt{\frac{\pi}{2}}A\right) + o(1). \quad (3.87)$$

Combined (3.87) and $\bar{r} \sim \xi$, (3.85) gives

$$\begin{aligned} \bar{r} &= \xi - \frac{1}{2} \ln(\bar{r}) + \ln\left(\sqrt{\frac{\pi}{2}}A\right) + o(1) \\ &= \xi - \frac{1}{2} \ln(\xi) + \ln\left(\sqrt{\frac{\pi}{2}}A\right) + o(1). \end{aligned} \quad (3.88)$$

Plugging $\xi = -\ln(-\tan \psi)$ and $\tan(\psi) \sim \psi$ into above equation, with L'Hopital's rule, we have

$$\bar{r} = -\ln(-\psi) - \frac{1}{2} \ln(-\ln(-\psi)) + \ln\left(\sqrt{\frac{\pi}{2}}A\right) + o(1) \quad (3.89)$$

as $\psi \rightarrow 0$ ($\xi \rightarrow \infty$).

To explore the higher order terms of the asymptotic forms of \bar{u} , we reconsider (3.82), with $\frac{K_0(\bar{r})}{K_1(\bar{r})} = 1 - \frac{1}{2\bar{r}} + \frac{3}{8\bar{r}^2} + \mathcal{O}\left(\frac{1}{\bar{r}^3}\right)$ for large \bar{r} , then

$$\bar{u} = -(\psi + \mathcal{O}(\psi^3)) \left(1 - \frac{1}{2\bar{r}} + \frac{3}{8\bar{r}^2} + \mathcal{O}\left(\frac{1}{\bar{r}^3}\right)\right) (1 + \mathcal{O}(K_0^2(\bar{r}))). \quad (3.90)$$

With (3.89), after some simplification, we obtain,

$$\bar{u} = -\psi - \frac{\psi}{2\ln(-\psi)} + \mathcal{O}\left(-\frac{\psi}{\ln^2(-\psi)}\right), \quad (3.91)$$

In conclusion, when $\psi < 0$, as $\psi \rightarrow 0$, we have

$$\bar{r} = -\ln(-\psi) - \frac{1}{2} \ln(-\ln(-\psi)) + \ln\left(\sqrt{\frac{\pi}{2}}A\right) + o(1), \quad (3.92)$$

$$\bar{u} = -\psi - \frac{\psi}{2\ln(-\psi)} + \mathcal{O}\left(-\frac{\psi}{\ln^2(-\psi)}\right). \quad (3.93)$$

3.5.2 Limiting Behavior of $\dot{w}(\bar{r}; r_w, \xi)$ as $\bar{r} \rightarrow \infty$

From Lemma 3 in Sec. 3.4, we conclude that $\dot{w}(\bar{r}; r_w, \xi) = \mathcal{O}\left(\frac{e^{-\bar{r}}}{\sqrt{\bar{r}}}\right)$ as $\bar{r} \rightarrow \infty$. In this section, we apply Theorem 16 (Levinson's Theorem [12]) to find the leading order of \dot{w} as $\bar{r} \rightarrow \infty$. Recall DE of \dot{w} in (3.72) in Sec. 3.4,

$$\dot{w}'' = (1 + w'^2)^{1/2}(\dot{w} + \dot{w}(w')^2 + 3ww'(\dot{w}')) - \frac{\dot{w}'}{\bar{r}}(1 + 3w'^2), \quad (3.94)$$

Consider $\mathbf{w}(\bar{r}) = (\dot{w}, \dot{w}')^T$, we rewrite DE of \dot{w} into a system of DEs,

$$\mathbf{w}'(\bar{r}) = J(\bar{r})\mathbf{w}(\bar{r}), \quad (3.95)$$

where \mathbf{w}' denotes the derivative of \mathbf{w} with respect to \bar{r} , $\bar{r} \in [r_1, \infty)$ for $r_1 \geq r_w$ and

$$J(\bar{r}) = \begin{pmatrix} 0 & 1 \\ j_{21}(\bar{r}) & j_{22}(\bar{r}) \end{pmatrix}, \quad (3.96)$$

in detail,

$$j_{21}(\bar{r}) = (1 + (w')^2)^{3/2} > 0, \quad (3.97)$$

$$j_{22}(\bar{r}) = 3ww'(1 + (w')^2)^{1/2} - \frac{1}{\bar{r}}(1 + 3(w')^2). \quad (3.98)$$

$J(\bar{r})$ has two distinct real eigenvalues $\lambda_1(\bar{r}) > 0$ and $\lambda_2(\bar{r}) < 0$, where

$$\lambda_1 = \frac{j_{22} + \sqrt{j_{22}^2 + 4j_{21}}}{2} \quad \text{and} \quad \lambda_2 = \frac{j_{22} - \sqrt{j_{22}^2 + 4j_{21}}}{2}, \quad (3.99)$$

with corresponding eigenvectors

$$\mathbf{v}_1 = \begin{pmatrix} 1 \\ \lambda_1 \end{pmatrix} \quad \text{and} \quad \mathbf{v}_2 = \begin{pmatrix} 1 \\ \lambda_2 \end{pmatrix} \quad (3.100)$$

Asymptotically, as $\bar{r} \rightarrow \infty$, $w \sim c_1 \frac{e^{-\bar{r}}}{\sqrt{\bar{r}}}$ and $w' \sim c_2 \frac{e^{-\bar{r}}}{\sqrt{\bar{r}}}$, see Property 2 in Sec. 3.4 and

$$j_{21} = 1 + \mathcal{O}\left(\frac{e^{-2\bar{r}}}{\bar{r}}\right) \quad \text{and} \quad j_{22} = -\frac{1}{\bar{r}} + \mathcal{O}\left(\frac{e^{-2\bar{r}}}{\bar{r}}\right). \quad (3.101)$$

Therefore,

$$\lambda_1 = \frac{-\frac{1}{\bar{r}} + \sqrt{\frac{1}{\bar{r}^2} + 4}}{2} + \mathcal{O}\left(\frac{e^{-\bar{r}}}{\bar{r}}\right) \quad \text{and} \quad \lambda_2 = \frac{-\frac{1}{\bar{r}} - \sqrt{\frac{1}{\bar{r}^2} + 4}}{2} + \mathcal{O}\left(\frac{e^{-\bar{r}}}{\bar{r}}\right). \quad (3.102)$$

Consider the transformation $\mathbf{w} = P(t)\mathbf{u}$, where

$$P(t) = \begin{pmatrix} 1 & 1 \\ \lambda_1 & \lambda_2 \end{pmatrix}, \quad (3.103)$$

then (3.95) turns into

$$\mathbf{u}' = M\mathbf{u}, \quad (3.104)$$

where

$$M(\bar{r}) = \Lambda(\bar{r}) + R(\bar{r}), \quad (3.105)$$

in details,

$$\Lambda(\bar{r}) = P^{-1}(\bar{r})J(\bar{r})P(\bar{r}) = \text{diag}(\lambda_1, \lambda_2), \quad (3.106)$$

$$R(\bar{r}) = -P^{-1}(\bar{r})P'(\bar{r}) = \frac{1}{\lambda_1 - \lambda_2} \begin{pmatrix} -\lambda_1' & -\lambda_2' \\ \lambda_1' & \lambda_2' \end{pmatrix}. \quad (3.107)$$

To show $R(\bar{r}) \in L^1([r_1, \infty))$, we notice that

$$\frac{\lambda'_1}{\lambda_1 - \lambda_2} = \frac{j'_{22}}{2\sqrt{j_{22}^2 + 4j_{21}}} + \frac{j_{22}j'_{22} + 2j_{21}j'_{21}}{2(j_{22}^2 + 4j_{21})}, \quad (3.108)$$

$$\frac{\lambda'_2}{\lambda_1 - \lambda_2} = \frac{j'_{22}}{2\sqrt{j_{22}^2 + 4j_{21}}} - \frac{j_{22}j'_{22} + 2j_{21}j'_{21}}{2(j_{22}^2 + 4j_{21})} \quad (3.109)$$

since with (3.101), and

$$j'_{21} = 3w'w'' (1 + (w')^2)^{1/2} = \mathcal{O}\left(\frac{e^{-2\bar{r}}}{\bar{r}}\right), \quad (3.110)$$

$$\begin{aligned} j'_{22} &= 3((w')^2 + ww'') (1 + (w')^2)^{1/2} + 3w(w')^2w'' (1 + (w')^2)^{-1/2} \\ &\quad - \left(\frac{1}{\bar{r}^2} + \frac{6w'w''}{\bar{r}} + \frac{3(w')^2}{\bar{r}^2}\right) = -\frac{1}{\bar{r}^2} + \mathcal{O}\left(\frac{e^{-2\bar{r}}}{\bar{r}}\right). \end{aligned} \quad (3.111)$$

Therefore, $R(\bar{r}) \in L^1([r_1, \infty))$ by the limit comparison test for integrals. The dichotomy condition is satisfied. Hence, we apply Levinson's theorem to (3.104), then

$$\mathbf{u}(\bar{r}) = c_1 \left\{ \begin{pmatrix} 1 \\ 0 \end{pmatrix} + o(1) \right\} \exp\left(\int_{r_1}^{\bar{r}} \lambda_1(s) ds\right) + c_2 \left\{ \begin{pmatrix} 0 \\ 1 \end{pmatrix} + o(1) \right\} \exp\left(\int_{r_1}^{\bar{r}} \lambda_2(s) ds\right), \quad (3.112)$$

where

$$\exp\left(\int_{r_1}^{\bar{r}} \lambda_1(s) ds\right) = c_3 \frac{1}{\sqrt{\sqrt{1 + 4\bar{r}^2} + 1}} \exp\left(\frac{1}{2}\sqrt{1 + 4\bar{r}^2}\right) (1 + o(1)), \quad (3.113)$$

$$\exp\left(\int_{r_1}^{\bar{r}} \lambda_2(s) ds\right) = c_4 \frac{1}{\sqrt{\sqrt{1 + 4\bar{r}^2} - 1}} \exp\left(-\frac{1}{2}\sqrt{1 + 4\bar{r}^2}\right) (1 + o(1)) \quad (3.114)$$

for some constant c_3 and $c_4 > 0$.

Transforming back to $\mathbf{w}(\bar{r})$,

$$\begin{aligned} \mathbf{w}(\bar{r}) = \begin{pmatrix} \dot{w} \\ \dot{w}' \end{pmatrix} = & d_1 \begin{pmatrix} 1 + o(1) \\ \lambda_1(\bar{r}) + o(1) \end{pmatrix} \frac{1}{\sqrt{\sqrt{1+4\bar{r}^2} + 1}} \exp\left(\frac{1}{2}\sqrt{1+4\bar{r}^2}\right) \\ & + d_2 \begin{pmatrix} 1 + o(1) \\ \lambda_2(\bar{r}) + o(1) \end{pmatrix} \frac{1}{\sqrt{\sqrt{1+4\bar{r}^2} - 1}} \exp\left(-\frac{1}{2}\sqrt{1+4\bar{r}^2}\right). \end{aligned} \quad (3.115)$$

Since $0 < \dot{w} < 1$ for $\bar{r} \geq r_1$, it implies $d_1 = 0$. Therefore,

$$\dot{w} \sim d \frac{e^{-\bar{r}}}{\sqrt{\bar{r}}} \quad (3.116)$$

as $\bar{r} \rightarrow \infty$, where $d = \frac{d_2}{\sqrt{2}}$. Moreover, since $w \sim c_1 \frac{e^{-\bar{r}}}{\sqrt{\bar{r}}}$, then we have

$$\dot{w} \sim kw \quad (3.117)$$

for some constant k .

3.5.3 Limiting Behavior of $\dot{\bar{r}}(\psi; \phi_0)$ and $\dot{\bar{u}}(\psi; \phi_0)$ as $\psi \rightarrow 0$

From Sec. 3.4, we denote $\dot{\bar{r}} = \frac{\partial}{\partial \sigma} \bar{r}(\psi; \sigma)$ and $\dot{\bar{u}} = \frac{\partial}{\partial \sigma} \bar{u}(\psi; \sigma)$, and have $\sigma(\phi_0)$ is C^1 . In this section, we are interested in the behavior of $\frac{\partial}{\partial \phi_0} \bar{r}(\psi; \phi_0)$ and $\frac{\partial}{\partial \phi_0} \bar{u}(\psi; \phi_0)$. For simplicity, we denote

$$\dot{\bar{r}} = \frac{\partial}{\partial \phi_0} \bar{r}(\psi; \phi_0) \quad \text{and} \quad \dot{\bar{u}} = \frac{\partial}{\partial \phi_0} \bar{u}(\psi; \phi_0). \quad (3.118)$$

These notations in (3.118) are used for the rest of the chapter. It is similar to (3.32) and (3.33), $\dot{\bar{r}}$ and $\dot{\bar{u}}$ satisfy the following DEs,

$$\frac{d\dot{\bar{r}}}{d\psi} = -\frac{\cos \psi (\bar{r}^2 \dot{\bar{u}} + \dot{\bar{r}} \sin \psi)}{(\bar{r} \bar{u} - \sin \psi)^2}, \quad (3.119)$$

$$\frac{d\dot{\bar{u}}}{d\psi} = -\frac{\sin \psi (\bar{r}^2 \dot{\bar{u}} + \dot{\bar{r}} \sin \psi)}{(\bar{r} \bar{u} - \sin \psi)^2}. \quad (3.120)$$

Suppose $\psi < 0$, let $t = -\frac{1}{\psi}$ (similarly, let $t = \frac{1}{\psi}$ if $\psi > 0$), and $\mathbf{x}(t) = (\dot{\bar{r}}(t; \phi_0), \dot{\bar{u}}(t; \phi_0))^T$, where $t \in [t_0, \infty]$ for some $t_0 > 0$. (3.119) and (3.120) become

$$\mathbf{x}'(t) = N(t)\mathbf{x}(t), \quad (3.121)$$

where

$$N(t) = -\frac{1}{t^2(\bar{r}(t)\bar{u}(t) + \sin(t^{-1}))^2} \begin{pmatrix} -\sin(t^{-1})\cos(t^{-1}) & \bar{r}^2(t)\cos(t^{-1}) \\ \sin^2(t^{-1}) & -\bar{r}^2(t)\sin(t^{-1}) \end{pmatrix} \quad (3.122)$$

and $\bar{r}(t) = \bar{r}(t; \phi_0)$ and $\bar{u}(t) = \bar{u}(t; \phi_0)$.

Consider the transformation $\mathbf{x} = T(t)\mathbf{z}$, where

$$T(t) = \begin{pmatrix} 1 & -1/2 \\ 0 & 1/t \end{pmatrix}. \quad (3.123)$$

The idea of the transformation $T(t)$ can be seen in Appendix B.1. Then, (3.121) turns into

$$\mathbf{z}' = \{L(t) + S(t)\}\mathbf{z}, \quad (3.124)$$

where

$$L(t) = \text{diag}(0, l_{22}), \quad (3.125)$$

$$S(t) = \begin{pmatrix} s_{11} & s_{12} \\ s_{21} & s_{22} \end{pmatrix}, \quad (3.126)$$

where

$$l_{22} = \frac{\bar{r}^2(t) \sin(t^{-1})}{t^2(\bar{r}(t)\bar{u}(t) + \sin(t^{-1}))^2} + \frac{1}{t}, \quad (3.127)$$

$$s_{11} = \frac{1}{t^2(\bar{r}(t)\bar{u}(t) + \sin(t^{-1}))^2} \left(\sin(t^{-1}) \cos(t^{-1}) - \frac{1}{2}t \sin^2(t^{-1}) \right), \quad (3.128)$$

$$s_{12} = \frac{-1}{t^2(\bar{r}(t)\bar{u}(t) + \sin(t^{-1}))^2} \left(\frac{1}{2} \sin(t^{-1}) \cos(t^{-1}) - \frac{1}{4}t \sin^2(t^{-1}) + \frac{1}{t} \bar{r}^2(t) \cos(t^{-1}) - \frac{1}{2} \bar{r}^2(t) \sin(t^{-1}) \right) + \frac{1}{2t}, \quad (3.129)$$

$$s_{21} = \frac{-1}{t^2(\bar{r}(t)\bar{u}(t) + \sin(t^{-1}))^2} \sin^2(t^{-1}), \quad (3.130)$$

$$s_{22} = \frac{\sin^2(t^{-1})}{2t^2(\bar{r}(t)\bar{u}(t) + \sin(t^{-1}))^2}. \quad (3.131)$$

From (3.92) and (3.93) in Sec. 3.5.1, with $t = -\frac{1}{\psi}$, we have the asymptotic expansions of $\bar{r}(t)$ and $\bar{u}(t)$ as $t \rightarrow \infty$,

$$\bar{r}(t) = \ln(t) - \frac{1}{2} \ln(\ln(t)) + \ln\left(\sqrt{\frac{\pi}{2}}A\right) + o(1), \quad (3.132)$$

$$\bar{u}(t) = \frac{1}{t} - \frac{1}{2t \ln(t)} + \mathcal{O}\left(\frac{1}{t \ln^2(t)}\right). \quad (3.133)$$

Asymptotically, as $t \rightarrow \infty$,

$$s_{11} \sim \frac{1}{2t \ln^2(t)} \quad \text{and} \quad s_{12} \sim -\frac{1}{4t \ln^2(t)}, \quad (3.134)$$

$$s_{21} \sim -\frac{1}{t \ln^2(t)} \quad \text{and} \quad s_{22} \sim \frac{1}{2t^2 \ln^2(t)}, \quad (3.135)$$

and

$$l_{22} = \frac{2}{t} - \frac{1}{t \ln(t)} + \mathcal{O}\left(\frac{1}{t \ln^2(t)}\right). \quad (3.136)$$

Thus, $S(t)$ is in $L^1([t_0, \infty))$ by the limit comparison test. The dichotomy condition is satisfied as well. According to Theorem 16 (Levinson's Theorem [12]), we obtain,

$$\mathbf{z}(t) = c_1 \left\{ \begin{pmatrix} 1 \\ 0 \end{pmatrix} + o(1) \right\} + c_2 \left\{ \begin{pmatrix} 0 \\ 1 \end{pmatrix} + o(1) \right\} \exp \left(\int_{t_0}^t l_{22}(s) ds \right). \quad (3.137)$$

for some constants c_1 and c_2 . Moreover,

$$\exp \left(\int_{t_0}^t l_{22}(s) ds \right) = c_3 \frac{t^2}{\ln(t)} (1 + o(1)) \quad (3.138)$$

for some constant c_3 .

Transforming back to $\mathbf{x}(t)$, as $t \rightarrow \infty$,

$$\begin{pmatrix} \dot{\bar{r}} \\ \dot{\bar{u}} \end{pmatrix} = \mathbf{x}(t) = \bar{c}_1 \begin{pmatrix} 1 + o(1) \\ o(1/t) \end{pmatrix} + \bar{c}_2 \begin{pmatrix} -\frac{t^2}{2 \ln(t)} + o\left(\frac{t^2}{\ln(t)}\right) \\ \frac{t}{\ln(t)} + o\left(\frac{t}{\ln(t)}\right) \end{pmatrix} \quad (3.139)$$

for some constants \bar{c}_1 and \bar{c}_2 .

3.5.4 Relation between \dot{w} , $\dot{\bar{r}}$ and $\dot{\bar{u}}$

From (3.139) in previous section, we obtain the limiting behavior of $\dot{\bar{r}}$ and $\dot{\bar{u}}$ as $t \rightarrow \infty$ (or $\psi \rightarrow 0$). When $\psi \rightarrow 0$, the solution of the fluid interface must be a graph. So, in this section, we investigate the relation between \dot{w} , $\dot{\bar{r}}$ and $\dot{\bar{u}}$ to achieve the improved limiting behavior of $\dot{\bar{r}}$ and $\dot{\bar{u}}$.

If the fluid interface becomes a graph for large \bar{r} , the following shows a connection between w which is the solution of the graph case and $\bar{u}(t; \phi_0)$ which is the solution of the non-graph case,

$$\bar{u}(t; \phi_0) = w(\bar{r}(t; \phi_0); \bar{r}_1, \bar{u}_1), \quad (3.140)$$

where $\bar{r}_1 = \bar{r}(t_1; \phi_0)$ and $\bar{u}_1 = \bar{u}(t_1; \phi_0)$ for some $t_1 > 0$ with the inclination angle ψ_1 at (\bar{r}_1, \bar{u}_1) , $-\frac{\pi}{2} < \psi_1 < 0$ (suppose the $\psi < 0$ case is considered, the $\psi > 0$ case is similar),

and $t \geq t_1$.

Differentiating both sides of (3.140) with respect to ϕ_0 ,

$$\begin{aligned}\dot{\bar{u}}(t; \phi_0) &= w'(\bar{r}(t; \phi_0); \bar{r}_1, \bar{u}_1) \dot{\bar{r}}(t; \phi_0) + \frac{\partial w}{\partial r_w}(\bar{r}(t; \phi_0); \bar{r}_1, \bar{u}_1) \dot{\bar{r}}(t_1; \phi_0) + \dot{w}(\bar{r}(t; \phi_0); \bar{r}_1, \bar{u}_1) \dot{\bar{u}}(t_1; \phi_0) \\ &= -\tan(t^{-1}) \dot{\bar{r}}(t; \phi_0) - \dot{w}(\bar{r}(t; \phi_0); \bar{r}_1, \bar{u}_1) (\tan(\psi_1) \dot{\bar{r}}(t_1; \phi_0) - \dot{\bar{u}}(t_1; \phi_0)),\end{aligned}\quad (3.141)$$

where $-\tan(t^{-1}) = \tan(\psi)$ and $\frac{\partial w}{\partial r_w}(\bar{r}; \bar{r}_1, \bar{u}_1) = -\dot{w}(\bar{r}; \bar{r}_1, \bar{u}_1) \tan(\psi_1)$ from (3.76).

As $t \rightarrow \infty$,

$$\dot{w}(\bar{r}(t; \phi_0); \bar{r}_1, \bar{u}_1) (\tan(\psi_1) \dot{\bar{r}}(t_1; \phi_0) - \dot{\bar{u}}(t_1; \phi_0)) \rightarrow 0, \quad (3.142)$$

since $\dot{w} \sim kw$ as $\bar{r} \rightarrow \infty$ from (3.117) or equivalently, $\dot{w} \sim \frac{k}{t}$ as $t \rightarrow \infty$ from (3.93). Therefore,

$$\dot{\bar{u}}(t; \phi_0) \sim -\tan(t^{-1}) \dot{\bar{r}}(t; \phi_0). \quad (3.143)$$

(3.143) implies $\bar{c}_2 = 0$ in (3.139). If not, suppose $\bar{c}_2 \neq 0$, as $t \rightarrow \infty$,

$$\dot{\bar{u}}(t; \phi_0) \sim \bar{c}_2 \frac{t}{\ln(t)}, \quad (3.144)$$

$$-\tan(t^{-1}) \dot{\bar{r}}(t; \phi_0) \sim \bar{c}_2 \frac{t}{2 \ln(t)} \quad (3.145)$$

contradicting with the relation in (3.143).

Therefore, as $t \rightarrow \infty$,

$$\begin{pmatrix} \dot{\bar{r}} \\ \dot{\bar{u}} \end{pmatrix} = \bar{c}_1 \begin{pmatrix} 1 + o(1) \\ o(1/t) \end{pmatrix}. \quad (3.146)$$

Transforming back to $\psi \rightarrow 0$ ($\psi < 0$),

$$\begin{pmatrix} \dot{r}(\psi; \phi_0) \\ \dot{u}(\psi; \phi_0) \end{pmatrix} = \bar{c}_1 \begin{pmatrix} 1 + o(1) \\ o(\psi) \end{pmatrix}. \quad (3.147)$$

3.5.5 Improved Error Bounds for $\dot{r}(t; \phi_0)$ and $\dot{u}(t; \phi_0)$ as $t \rightarrow \infty$

The error bounds of $\dot{r}(t; \phi_0)$ and $\dot{u}(t; \phi_0)$ in (3.146) as $t \rightarrow \infty$ can be improved. We solve (3.124) for $\mathbf{z}(t)$ with $\lim_{t \rightarrow \infty} \mathbf{z}(t) = \begin{pmatrix} 1 \\ 0 \end{pmatrix}$ from (3.137), where $\mathbf{z}(t) = (z_1(t), z_2(t))^T$ (since we showed $\bar{c}_2 = 0$ in (3.139), it is equivalent that $c_2 = 0$ in (3.137)). The integral equation of $\mathbf{z}(t)$ is obtained,

$$z_1(t) = 1 - \int_t^\infty s_{11}(\tau)z_1(\tau) + s_{12}(\tau)z_2(\tau) d\tau, \quad (3.148)$$

$$z_2(t) = -e^{\mu(t)} \int_t^\infty e^{-\mu(\tau)} (s_{21}(\tau)z_1(\tau) + s_{22}(\tau)z_2(\tau)) d\tau, \quad (3.149)$$

where $e^{\mu(t)}$ is an integrating factor with $\mu(t) = \int_{t_0}^t l_{22}(\tau) d\tau$.

Since $\mathbf{z}(t)$ is bounded, combined with (3.134) and (3.135), then

$$s_{11}(t)z_1(t) + s_{12}(t)z_2(t) = \mathcal{O}\left(\frac{1}{t \ln^2(t)}\right), \quad (3.150)$$

$$s_{21}(t)z_1(t) + s_{22}(t)z_2(t) = \mathcal{O}\left(\frac{1}{t \ln^2(t)}\right), \quad (3.151)$$

as $t \rightarrow \infty$.

Hence, $z_1(t) = 1 + \mathcal{O}\left(\frac{1}{\ln(t)}\right)$. To find the error bound of $z_2(t)$, we consider

$$\lim_{t \rightarrow \infty} \frac{\int_t^\infty e^{-\mu(\tau)} (s_{21}(\tau)z_1(\tau) + s_{22}(\tau)z_2(\tau)) d\tau}{e^{-\mu(t)} (\ln^2(t))^{-1}}. \quad (3.152)$$

Applying L'Hopital's rule, (3.152) gives $\frac{1}{2}$, thus,

$$z_2(t) = \mathcal{O}\left(\frac{1}{\ln^2(t)}\right). \quad (3.153)$$

Therefore, we obtain the improved error bounds for $\dot{\tilde{r}}$ and $\dot{\tilde{u}}$,

$$\begin{pmatrix} \dot{\tilde{r}} \\ \dot{\tilde{u}} \end{pmatrix} = \bar{c}_1 \begin{pmatrix} 1 + \mathcal{O}\left(\frac{1}{\ln(t)}\right) \\ \mathcal{O}\left(\frac{1}{t \ln^2(t)}\right) \end{pmatrix}. \quad (3.154)$$

as $t \rightarrow \infty$.

Transforming back to $\psi \rightarrow 0$ ($\psi < 0$),

$$\begin{pmatrix} \dot{\tilde{r}}(\psi; \phi_0) \\ \dot{\tilde{u}}(\psi; \phi_0) \end{pmatrix} = \bar{c}_1 \begin{pmatrix} 1 + \mathcal{O}\left(-\frac{1}{\ln(-\psi)}\right) \\ \mathcal{O}\left(-\frac{\psi}{\ln^2(-\psi)}\right) \end{pmatrix}. \quad (3.155)$$

Remark 13. Based on Picard's iterative method, the higher order expansions of $z_1(t)$ and $z_2(t)$ can be obtained (as well as $\dot{\tilde{r}}$ and $\dot{\tilde{u}}$) if the modified expansions of $z_1(t)$ and $z_2(t)$ are applied to (3.148) and (3.149).

3.6 Total Energy, Total Force and Their Relation

Our main purpose is to study the number of equilibrium points and their stability for the floating ball system. In this section, both energy and force analysis are presented. Our approach is similar to that for the floating cylinder problem¹, see [3] and [4]. Following the method of Gauss [18], four types of the potential energies are classified. Due to the unboundedness of the reservoir, the relative energy is considered in order to avoid the confusion of infinite energy, see Sec. 3.6.1. In force analysis, only forces in vertical direction are considered by symmetry. The total force F_T is also classified in Sec. 3.6.2. Both the

¹In the floating cylinder problem, we consider a circular cylinder horizontally floating on an unbounded reservoir.

total energy E_T and the total force F_T can be represented by an attachment angle ϕ_0 . In Sec. 3.6.3, an important relation between E_T and F_T is derived. Based on the relation, the stability criterion is established, see Sec. 3.6.4.

3.6.1 Decomposition of Total Energy E_T

The total energy E_T can be decomposed as follows:

- (i) The gravitational energy, $E_G = mgh$, where $h = a \cos(\phi_0) + u_0$ is the height of the center, u_0 is the height of the fluid interface at the contact point, see Fig. 3.6a. Moreover, if we consider the ball is homogeneous, $m = \rho_m V_B$, where ρ_m is the density difference between the solid and the air, and $V_B = \frac{4}{3}\pi a^3$ is the volume of the ball. Thus, E_G can also be expressed as

$$E_G = \rho_m g \frac{4}{3} \pi a^3 h(\phi_0).$$

- (ii) The wetting energy, $E_w = -\beta\sigma|\Sigma|$, where $\beta = \cos\gamma$ is the adhesion coefficient. $|\Sigma| = 2a^2\pi(1 - \cos\phi_0)$ is the wetting area of the ball (the formula comes from the area of the spherical cap). Thus E_w also has the form

$$E_w = -2a^2\pi\sigma \cos\gamma(1 - \cos\phi_0).$$

- (iii) The surface tension energy, which is the relative energy compared with the energy of the undisturbed level. It has the form

$$\begin{aligned} E_\sigma &= \sigma \int_0^{2\pi} d\theta \int_{r_0}^{\infty} r \left(\sqrt{1 + u_r^2} - 1 \right) dr - \sigma\pi r_0^2 \\ &= 2\pi\sigma \int_{r_0}^{\infty} r \left(\sqrt{1 + u_r^2} - 1 \right) dr - \sigma\pi r_0^2, \end{aligned}$$

where $r_0 = a \sin(\phi_0)$ and σ is known as the surface tension.

- (iv) The fluid potential energy, E_F is divided into two parts, E_{F_1} and E_{F_2} .

$$E_{F_1} = \rho g \int_0^{2\pi} d\theta \int_{r_0}^{\infty} \frac{u^2}{2} r dr = \rho g \pi \int_{r_0}^{\infty} u^2 r dr.$$

$$E_{F_2} = \rho g \int_0^{2\pi} d\theta \int_0^{r_0} \frac{y^2}{2} r dr = \rho g \pi \int_0^{r_0} y^2 r dr,$$

where ρ is the density difference between the liquid and the air, and $y = h - a \cos \phi$ is the vertical height of the bottom of the ball, see Fig. 3.6b. Since $r = a \sin \phi \in [0, r_0]$, E_{F_2} also has the form

$$E_{F_2} = \rho g \pi \int_0^{\phi_0} (h - a \cos \phi)^2 a \sin \phi a \cos \phi d\phi.$$

After some calculation, we have

$$E_{F_2} = \rho g \pi \left[\frac{a^2 h^2(\phi_0)}{2} \sin^2(\phi_0) - \frac{2}{3} a^3 h(\phi_0) (1 - \cos^3(\phi_0)) + \frac{a^4}{4} (1 - \cos^4(\phi_0)) \right]. \quad (3.156)$$

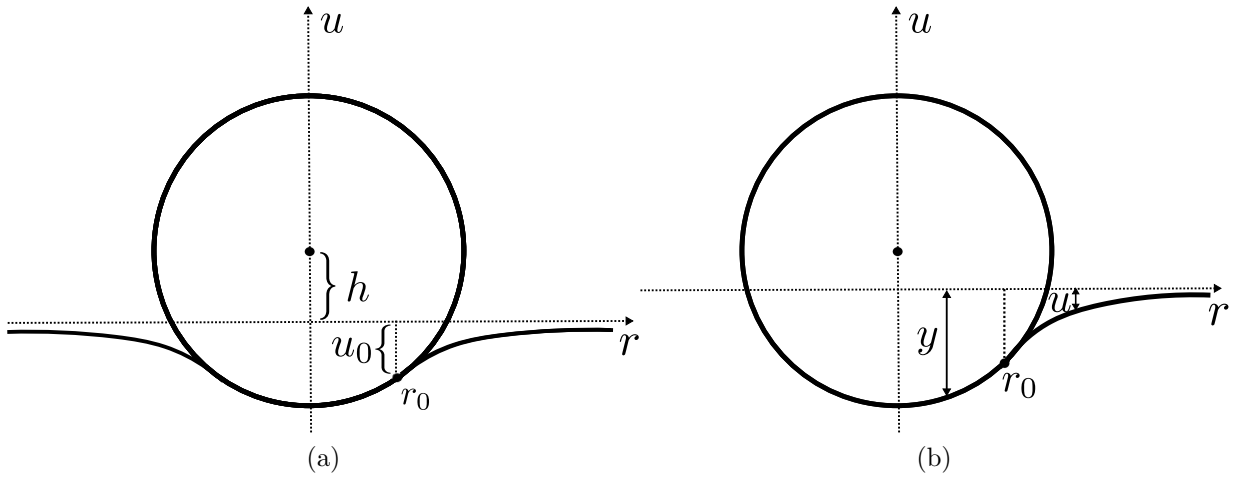


Figure 3.6: (a) The contact point (r_0, u_0) and the height of the center h ; (b) Computation of the fluid potential energy F_F .

With $\kappa = \frac{\rho g}{\sigma}$, finally, we can write down E_T :

$$\begin{aligned}
E_T(\phi_0) = & \pi \rho g \left(\frac{4}{3} \frac{\rho_m}{\rho} a^3 h(\phi_0) \right) + \pi \rho g \left(-\frac{2a^2 \cos \gamma}{\kappa} (1 - \cos \phi_0) \right) \\
& + \pi \rho g \left[\frac{2}{\kappa} \int_{r_0}^{\infty} r \left(\sqrt{1 + u_r^2} - 1 \right) dr - \frac{1}{\kappa} r_0^2 \right] + \pi \rho g \int_{r_0}^{\infty} u^2 r dr \\
& + \rho g \pi \left[\frac{a^2 h^2(\phi_0)}{2} \sin^2(\phi_0) - \frac{2}{3} a^3 h(\phi_0) (1 - \cos^3(\phi_0)) + \frac{a^4}{4} (1 - \cos^4(\phi_0)) \right].
\end{aligned}$$

For convenience, the total energy can be nondimensionalized, we denote $E_c = \pi \rho g a^4$ as the characteristic energy, which shares the same dimension with E_T and denote $l_c = a$ as the characteristic length. Hence, we introduce the following dimensionless variables:

- (i) The dimensionless total energy $\hat{E}_T = \frac{E_T}{E_c}$.
- (ii) The dimensionless height of the center $\hat{h} = \frac{h}{l_c}$.
- (iii) The dimensionless fluid interface $\hat{u} = \frac{u}{l_c}$ and $\hat{r} = \frac{r}{l_c}$.

After some calculation, we have the expression of the dimensionless total energy \hat{E}_T :

$$\begin{aligned}
\hat{E}_T(\phi_0) = & \frac{4\rho_m}{3\rho} \hat{h}(\phi_0) - \frac{2 \cos \gamma}{B} (1 - \cos \phi_0) + \frac{1}{B} \left[2 \int_{\hat{r}_0}^{\infty} \hat{r} \left(\sqrt{1 + \hat{u}_{\hat{r}}^2} - 1 \right) d\hat{r} - (\hat{r}_0)^2 \right] \\
& + \int_{\hat{r}_0}^{\infty} \hat{u}^2 \hat{r} d\hat{r} + \left[\frac{\hat{h}^2(\phi_0)}{2} \sin^2(\phi_0) - \frac{2}{3} \hat{h}(\phi_0) (1 - \cos^3(\phi_0)) + \frac{1}{4} (1 - \cos^4(\phi_0)) \right],
\end{aligned} \tag{3.157}$$

where $\hat{r}_0 = \frac{r_0}{a}$.

3.6.2 Decomposition of Total Force F_T

As for the total force, denoted as F_T , we first observe that the forces in horizontal direction are canceled by symmetry. Only the forces in vertical direction are considered. Moreover, we define the upward as the positive direction. The total force F_T can be decomposed into

(i) The gravitational force, $F_G = -mg$, in detail,

$$F_G = -\frac{4}{3}\pi a^3 \rho_m g.$$

(ii) The surface tension force, $F_\sigma = \sigma \left(2\pi(a \sin \phi_0) \right)$, where we assume F_σ acts only along the fluid interface². Hence, the vertical component of the surface tension force is

$$F_\sigma^{\text{vertical}} = -2\pi\sigma a \sin(\phi_0 + \gamma) \sin(\phi_0).$$

(iii) The buoyant force,

$$F_B = \int_0^{2\pi} d\theta \int_0^{\phi_0} \rho g(-y) \cos \phi (a^2 \sin \phi) d\phi,$$

where $y = h - a \cos \phi$. Explicitly,

$$F_B = -\pi\rho g a^2 h(\phi_0) \sin^2 \phi_0 + \frac{2}{3}\pi\rho g a^3 (1 - \cos^3 \phi_0).$$

The gravitational, surface tension and buoyant forces can be seen in Fig. 3.7 . Thus, F_T has the form

$$F_T(\phi_0) = \pi\rho g \left[-\frac{4}{3} \frac{\rho_m}{\rho} a^3 - \frac{2}{\kappa} a \sin(\phi_0 + \gamma) \sin \phi_0 - a^2 h(\phi_0) \sin^2 \phi_0 + \frac{2}{3} a^3 (1 - \cos^3 \phi_0) \right]. \quad (3.158)$$

By setting the characteristic force $F_c = \pi\rho g a^3$, the dimensionless total force \hat{F}_T is shown as follows,

$$\hat{F}_T(\phi_0) = -\frac{4}{3}\alpha - \frac{2}{B} \sin(\phi_0 + \gamma) \sin \phi_0 - \hat{h}(\phi_0) \sin^2 \phi_0 + \frac{2}{3}(1 - \cos^3 \phi_0), \quad (3.159)$$

where $\alpha = \frac{\rho_m}{\rho}$, which is known as the density ratio and $\hat{h}(\phi_0) = \cos \phi_0 + \hat{u}_0$.

²There is much literature supporting the assumption instead of using Young's diagram, see Gifford and Scriven [27], Finn [20], Bhatnagar and Finn [3], Vella, Lee and Kim [62] and Chen and Siegel [4].

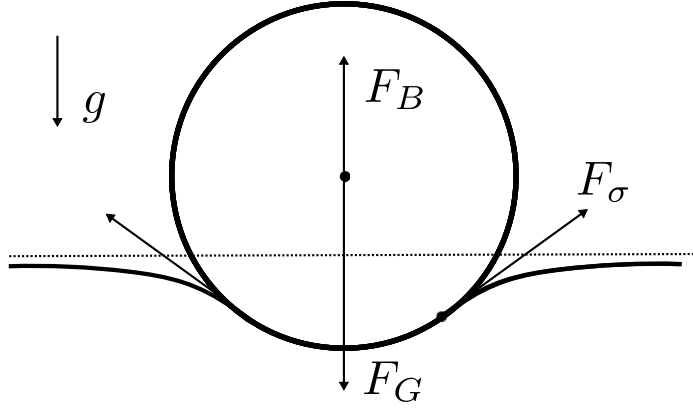


Figure 3.7: The gravitational, surface tension and buoyant forces.

Remark 14. For later usage, we will focus on the dimensionless functions and variables such as the total energy $\hat{E}_T(\phi_0)$, the total force $\hat{F}_T(\phi_0)$, the height of the center $\hat{h}(\phi_0)$, the solutions of the fluid interface (\hat{r}, \hat{u}) and the contact point (\hat{r}_0, \hat{u}_0) .

3.6.3 Relation Between Total Energy \hat{E}_T and Total Force \hat{F}_T

In this section, we present the derivation of the important relation between the total energy \hat{E}_T and the total force \hat{F}_T , which is

$$\frac{d\hat{E}_T}{d\phi_0} = -\hat{F}_T \hat{h}'(\phi_0). \quad (3.160)$$

The relation implies the critical points of the \hat{E}_T can be either a forced balanced point ($\hat{F}_T(\phi_0) = 0$) or a critical point of \hat{h} . To investigate the relation in (3.160), both the graph and the non-graph cases of the fluid interface will be discussed.

The Graph Case

We first consider the fluid interface is a graph with a restriction $|\psi_0| < \frac{\pi}{2}$, and use the convention $\hat{u} = \hat{u}(\hat{r}; \hat{r}_0, \hat{u}_0)$, where $\hat{r}_0 = \sin(\phi_0)$ and $\hat{u}_0 = \hat{u}(\hat{r}_0; \hat{r}_0, \hat{u}_0)$ are the contact point, see Sec. 3.4. To show $\frac{d\hat{E}_T}{d\phi_0}(\phi_0) = -\hat{F}_T(\phi_0)\hat{h}'(\phi_0)$, we note that $\frac{d\hat{E}_G}{d\phi_0}$, $\frac{d\hat{E}_w}{d\phi_0}$ and $\frac{d\hat{E}_F}{d\phi_0}$ can be easily calculated:

$$\frac{d\hat{E}_G}{d\phi_0} = \frac{4\rho_m}{3\rho}\hat{h}'(\phi_0), \quad \frac{d\hat{E}_w}{d\phi_0} = -\frac{2\cos\gamma}{B}\sin\phi_0,$$

and

$$\begin{aligned} \frac{d\hat{E}_{F_1}}{d\phi_0} &= \frac{\partial}{\partial\phi_0} \int_{\hat{r}_0}^{\infty} \hat{u}^2 \hat{r} d\hat{r} = -\sin\phi_0 \cos\phi_0 \hat{u}_0^2 + \int_{\hat{r}_0}^{\infty} 2\hat{u} \left(\frac{\partial}{\partial\phi_0} \hat{u} \right) \hat{r} d\hat{r}, \\ \frac{d\hat{E}_{F_2}}{d\phi_0} &= \hat{u}_0^2 \sin\phi_0 \cos\phi_0 + \sin^2(\phi_0) \hat{h}(\phi_0) \hat{h}'(\phi_0) - \frac{2}{3}(1 - \cos^3\phi_0) \hat{h}'(\phi_0). \end{aligned}$$

Hence,

$$\frac{d\hat{E}_F}{d\phi_0} = \sin^2(\phi_0) \hat{h}(\phi_0) \hat{h}'(\phi_0) - \frac{2}{3}(1 - \cos^3\phi_0) \hat{h}'(\phi_0) + \int_{\hat{r}_0}^{\infty} 2\hat{u} \left(\frac{\partial}{\partial\phi_0} \hat{u} \right) \hat{r} d\hat{r}.$$

Next, we calculate $\frac{d\hat{E}_\sigma}{d\phi_0}$,

$$\begin{aligned} \frac{d\hat{E}_\sigma}{d\phi_0} &= \frac{2}{B} \left\{ \frac{d}{d\phi_0} \left(\int_{\hat{r}_0}^{\infty} \hat{r} \left(\sqrt{1 + \hat{u}_{\hat{r}}^2} - 1 \right) d\hat{r} - \frac{1}{2} \hat{r}_0^2 \right) \right\} \\ &= \frac{2}{B} \left\{ -\cos\phi_0 \sin\phi_0 \left(\sqrt{1 + \tan^2\psi_0} - 1 \right) - \hat{r}_0 \hat{r}'_0 + \int_{\hat{r}_0}^{\infty} \left(\frac{\hat{r} \hat{u}_{\hat{r}}}{\sqrt{1 + \hat{u}_{\hat{r}}^2}} \right) \left(\frac{\partial}{\partial\phi_0} \hat{u}_{\hat{r}} \right) d\hat{r} \right\} \\ &= \frac{2}{B} \left\{ -\frac{\sin\phi_0 \cos\phi_0}{\cos\psi_0} + \left[\left(\frac{\hat{r} \hat{u}_{\hat{r}}}{\sqrt{1 + \hat{u}_{\hat{r}}^2}} \right) \left(\frac{\partial}{\partial\phi_0} \hat{u} \right) \Big|_{\hat{r}_0}^{\infty} \right] - \int_{\hat{r}_0}^{\infty} \left(\frac{d}{d\hat{r}} \frac{\hat{r} \hat{u}_{\hat{r}}}{\sqrt{1 + \hat{u}_{\hat{r}}^2}} \right) \left(\frac{\partial}{\partial\phi_0} \hat{u} \right) d\hat{r} \right\} \\ &= \frac{2}{B} \left\{ -\frac{\sin\phi_0 \cos\phi_0}{\cos\psi_0} + \lim_{\hat{r} \rightarrow \infty} (\hat{r} \sin\psi) \left(\frac{\partial}{\partial\phi_0} \hat{u} \right) - \hat{r}_0 \sin\psi_0 \left(\frac{\partial}{\partial\phi_0} \hat{u} \right) \Big|_{\hat{r}=\hat{r}_0} \right. \\ &\quad \left. - \int_{\hat{r}_0}^{\infty} \left(\frac{d}{d\hat{r}} \frac{\hat{r} \hat{u}_{\hat{r}}}{\sqrt{1 + \hat{u}_{\hat{r}}^2}} \right) \left(\frac{\partial}{\partial\phi_0} \hat{u} \right) d\hat{r} \right\}. \end{aligned} \tag{3.161}$$

The following Lemma 20 determines two terms in (3.161).

Lemma 20. When $|\psi_0| < \frac{\pi}{2}$,

$$\lim_{\hat{r} \rightarrow \infty} (\hat{r} \sin \psi) \left(\frac{\partial}{\partial \phi_0} \hat{u} \right) = 0, \quad (3.162)$$

$$\left(\frac{\partial}{\partial \phi_0} \hat{u} \right) \Big|_{\hat{r}=\hat{r}_0} = -\tan \psi_0 \cos \phi_0 + \frac{d\hat{u}_0}{d\phi_0}. \quad (3.163)$$

Proof. We first calculate

$$\frac{\partial}{\partial \phi_0} \hat{u}(\hat{r}; \hat{r}_0, \hat{u}_0) = \hat{u}_{r_w}(\hat{r}; \hat{r}_0, \hat{u}_0) \frac{d\hat{r}_0}{d\phi_0} + \dot{\hat{u}}(\hat{r}; \hat{r}_0, \hat{u}_0) \frac{d\hat{u}_0}{d\phi_0}, \quad (3.164)$$

where

$$\hat{u}_{r_w}(\hat{r}; \hat{r}_0, \hat{u}_0) = -\dot{\hat{u}}(\hat{r}; \hat{r}_0, \hat{u}_0) p(\hat{r}_0, \hat{u}_0),$$

based on (3.76) in Sec. 3.4. With $p(\hat{r}_0, \hat{u}_0) = \tan \psi_0$, (3.164) implies

$$\frac{\partial}{\partial \phi_0} \hat{u}(\hat{r}; \hat{r}_0, \hat{u}_0) = -\dot{\hat{u}}(\hat{r}; \hat{r}_0, \hat{u}_0) \left(\tan(\psi_0) \cos(\phi_0) - \frac{d\hat{u}_0}{d\phi_0} \right). \quad (3.165)$$

At $\hat{r} = \hat{r}_0$, we obtain (3.163), since $\dot{\hat{u}}(\hat{r}_0; \hat{r}_0, \hat{u}_0) = 1$.

With $\dot{\hat{u}}(\hat{r}; \hat{r}_0, \hat{u}_0) \sim d \frac{e^{-\hat{r}}}{\sqrt{\hat{r}}}$ for some constant $d > 0$ as $\hat{r} \rightarrow \infty$, see Sec. 3.5.2 and $|\psi_0| < \frac{\pi}{2}$, we have $\frac{\partial}{\partial \phi_0} \hat{u}(\hat{r}; \hat{r}_0, \hat{u}_0) \rightarrow 0$ exponentially as $\hat{r} \rightarrow \infty$. In addition, $\hat{r} \sin(\psi) \rightarrow 0$ exponentially as well. Therefore, we obtain (3.162). □

Applying Lemma 20 and

$$\hat{h}'(\phi_0) = -\sin \phi_0 + \frac{d\hat{u}_0}{d\phi_0}, \quad (3.166)$$

we obtain

$$\frac{d\hat{E}_\sigma}{d\phi_0} = \frac{2}{B} \left\{ -\frac{\sin \phi_0 \cos \phi_0}{\cos \psi_0} - \hat{r}_0 \sin \psi_0 \left(\hat{h}'(\phi_0) + \sin \phi_0 - \tan \psi_0 \cos \phi_0 \right) - \int_{\hat{r}_0}^{\infty} \left(\frac{d}{d\hat{r}} \frac{\hat{r}\hat{u}_{\hat{r}}}{\sqrt{1+\hat{u}_{\hat{r}}^2}} \right) \left(\frac{\partial}{\partial \phi_0} \hat{u} \right) d\hat{r} \right\}.$$

We group the integral terms in $\frac{d\hat{E}_\sigma}{d\phi_0}$ and $\frac{d\hat{E}_F}{d\phi_0}$.

$$\begin{aligned} & -\frac{2}{B} \int_{\hat{r}_0}^{\infty} \left(\frac{d}{d\hat{r}} \frac{\hat{r}\hat{u}_{\hat{r}}}{\sqrt{1+\hat{u}_{\hat{r}}^2}} \right) \left(\frac{\partial}{\partial \phi_0} \hat{u} \right) d\hat{r} + \int_{\hat{r}_0}^{\infty} 2\hat{u} \left(\frac{\partial}{\partial \phi_0} \hat{u} \right) \hat{r} d\hat{r} \\ & = -\frac{2}{B} \int_{\hat{r}_0}^{\infty} \left[\frac{d}{d\hat{r}} \frac{\hat{r}\hat{u}_{\hat{r}}}{\sqrt{1+\hat{u}_{\hat{r}}^2}} - B\hat{r}\hat{u} \right] \left(\frac{\partial}{\partial \phi_0} \hat{u} \right) d\hat{r} \\ & = 0. \end{aligned} \tag{3.167}$$

Thus,

$$\begin{aligned} \frac{d\hat{E}_T}{d\phi_0} & = \frac{4\rho_m}{3\rho} \hat{h}'(\phi_0) - \frac{2\cos\gamma}{B} \sin \phi_0 \\ & + \frac{2}{B} \left\{ -\frac{\sin \phi_0 \cos \phi_0}{\cos \psi_0} - \hat{r}_0 \sin \psi_0 \left(\hat{h}'(\phi_0) + \sin \phi_0 - \tan \psi_0 \cos \phi_0 \right) \right\} \\ & + \sin^2(\phi_0) \hat{h}(\phi_0) \hat{h}'(\phi_0) - \frac{2}{3} (1 - \cos^3(\phi_0)) \hat{h}'(\phi_0) \end{aligned} \tag{3.168}$$

After some simplification,

$$\frac{d\hat{E}_T}{d\phi_0} = \left[\frac{4\rho_m}{3\rho} - \frac{2}{B} \sin \phi_0 \sin \psi_0 + \sin^2(\phi_0) \hat{h}(\phi_0) - \frac{2}{3} (1 - \cos^3(\phi_0)) \right] \hat{h}'(\phi_0).$$

Finally,

$$\frac{d\hat{E}_T}{d\phi_0} = -\hat{F}_T \hat{h}'(\phi_0).$$

The Non-graph Case

In this section, we extend the relation between the total energy and the total force to the non-graph case. In the derivation, the parametric form of the fluid interface is applied. Suppose $\hat{r} = \hat{r}(\psi; \phi_0)$ and $\hat{u} = \hat{u}(\psi; \phi_0)$, and denote $\hat{r}_0 = \hat{r}(\psi_0; \phi_0)$, $\hat{u}_0 = \hat{u}(\psi_0; \phi_0)$, $\dot{\hat{r}} = \frac{\partial}{\partial \phi_0} \hat{r}(\psi; \phi_0)$ and $\dot{\hat{u}} = \frac{\partial}{\partial \phi_0} \hat{u}(\psi; \phi_0)$ (In Sec. 3.5.3, we study the limiting behavior of $\dot{\hat{r}}(\psi; \phi_0)$ and $\dot{\hat{u}}(\psi; \phi_0)$ as $\psi \rightarrow 0$. The behavior of $\dot{\hat{r}}$ and $\dot{\hat{u}}$ can be obtained by $\dot{\hat{r}} = \frac{1}{\sqrt{B}} \dot{\hat{r}}$ and $\dot{\hat{u}} = \frac{1}{\sqrt{B}} \dot{\hat{u}}$). We focus on the $\psi < 0$ and $\psi_0 \leq -\frac{\pi}{2}$ case, and the $\psi > 0$ case will be similar.

We note that the terms $\frac{d\hat{E}_G}{d\phi_0}$, $\frac{d\hat{E}_w}{d\phi_0}$ and $\frac{d\hat{E}_{F_2}}{d\phi_0}$ are unchanged in the non-graph case. While the calculation of $\frac{d\hat{E}_{F_1}}{d\phi_0}$ and $\frac{d\hat{E}_\sigma}{d\phi_0}$ needs more work due to the parametric representation of integrals. We define

$$\hat{E}_\sigma^\delta(\phi_0) = \frac{2}{B} \int_{\psi_0}^{\delta} \hat{r} \left(\sqrt{\left(\frac{d\hat{u}}{d\psi}\right)^2 + \left(\frac{d\hat{r}}{d\psi}\right)^2} - \frac{d\hat{r}}{d\psi} \right) d\psi - \frac{\hat{r}_0^2}{B}, \quad (3.169)$$

$$\hat{E}_{F_1}^\delta(\phi_0) = \int_{\psi_0}^{\delta} \hat{u}^2 \hat{r} \left(\frac{d\hat{r}}{d\psi} \right) d\psi, \quad (3.170)$$

where $\delta < 0$ and is close to 0. ψ_0 and ϕ_0 are linked by the geometric constraint $\psi_0 = \phi_0 + \gamma - \pi$. Hence, $\hat{E}_\sigma(\phi_0) = \lim_{\delta \rightarrow 0} \hat{E}_\sigma^\delta(\phi_0)$ and $\hat{E}_{F_1}(\phi_0) = \lim_{\delta \rightarrow 0} \hat{E}_{F_1}^\delta(\phi_0)$.

For $\frac{d\hat{E}_{F_1}^\delta}{d\phi_0}$, by Leibniz's rule, we have

$$\begin{aligned}
\frac{d\hat{E}_{F_1}^\delta}{d\phi_0} &= -\hat{u}^2\hat{r}\left(\frac{d\hat{r}}{d\psi}\right)\Big|_{\psi_0} + \int_{\psi_0}^{\delta} \frac{d}{d\phi_0} \left(\hat{u}^2\hat{r}\left(\frac{d\hat{r}}{d\psi}\right) \right) d\psi \\
&= \hat{u}_0^2\hat{r}_0 \left(\dot{\hat{r}}(\psi_0; \phi_0) - \cos\phi_0 \right) + \int_{\psi_0}^{\delta} 2\hat{u}\dot{\hat{u}} \left(\hat{r}\frac{d\hat{r}}{d\psi} \right) d\psi + \int_{\psi_0}^{\delta} \hat{u}^2 \left(\dot{\hat{r}}\frac{d\hat{r}}{d\psi} \right) d\psi \\
&\quad + \int_{\psi_0}^{\delta} \hat{u}^2 \left(\hat{r}\frac{d\dot{\hat{r}}}{d\psi} \right) d\psi, \tag{3.171}
\end{aligned}$$

where $\left(\frac{d\hat{r}}{d\psi}\right)\Big|_{\psi_0} = \cos\phi_0 - \dot{\hat{r}}(\psi_0; \phi_0)$, which is obtained from differentiating $\hat{r}_0 = \hat{r}(\psi_0; \phi_0)$ with respect to ϕ_0 .

To have a nicer form of $\frac{d\hat{E}_{F_1}^\delta}{d\phi_0}$, we apply integration by parts (IBP),

$$\begin{aligned}
\int_{\psi_0}^{\delta} \hat{u}^2 \left(\hat{r}\frac{d\dot{\hat{r}}}{d\psi} \right) d\psi &= \hat{u}^2\hat{r}\dot{\hat{r}}\Big|_{\psi_0}^{\delta} - \int_{\psi_0}^{\delta} \frac{d}{d\psi} (\hat{u}^2\hat{r}) \dot{\hat{r}} d\psi \\
&= q_1(\delta) - \hat{u}_0^2\hat{r}_0\dot{\hat{r}}(\psi_0; \phi_0) - \int_{\psi_0}^{\delta} 2\hat{u}\frac{d\hat{u}}{d\psi}\hat{r}\dot{\hat{r}} + \hat{u}^2\frac{d\hat{r}}{d\psi}\dot{\hat{r}} d\psi, \tag{3.172}
\end{aligned}$$

where

$$q_1(\delta) = \hat{u}^2(\delta; \phi_0)\hat{r}(\delta; \phi_0)\dot{\hat{r}}(\delta; \phi_0). \tag{3.173}$$

Therefore, $\frac{d\hat{E}_{F_1}^\delta}{d\phi_0}$ can be simplified to

$$\frac{d\hat{E}_{F_1}^\delta}{d\phi_0} = q_1(\delta) - \hat{u}_0^2\hat{r}_0 \cos\phi_0 + 2 \int_{\psi_0}^{\delta} \hat{u}\dot{\hat{u}}\hat{r}\frac{d\hat{r}}{d\psi} d\psi - 2 \int_{\psi_0}^{\delta} \hat{u}\frac{d\hat{u}}{d\psi}\hat{r}\dot{\hat{r}} d\psi. \tag{3.174}$$

Moreover, we arrange equations in (3.15) to obtain

$$\hat{r}\hat{u}\frac{d\hat{r}}{d\psi} = \frac{1}{B} \left(\hat{r} \cos \psi + \sin \psi \frac{d\hat{r}}{d\psi} \right), \quad (3.175)$$

$$\hat{r}\hat{u}\frac{d\hat{u}}{d\psi} = \frac{1}{B} \left(\hat{r} \sin \psi + \sin \psi \frac{d\hat{u}}{d\psi} \right), \quad (3.176)$$

and substitute them into (3.174), then

$$\begin{aligned} \frac{d\hat{E}_{F_1}^\delta}{d\phi_0} &= q_1(\delta) - \hat{u}_0^2 \hat{r}_0 \cos \phi_0 + \frac{2}{B} \int_{\psi_0}^{\delta} \hat{r} \cos \psi \dot{\hat{u}} d\psi + \frac{2}{B} \int_{\psi_0}^{\delta} \sin \psi \frac{d\hat{r}}{d\psi} \dot{\hat{u}} d\psi \\ &\quad - \frac{2}{B} \int_{\psi_0}^{\delta} \sin \psi \hat{r} \dot{\hat{r}} d\psi - \frac{2}{B} \int_{\psi_0}^{\delta} \sin \psi \frac{d\hat{u}}{d\psi} \dot{\hat{r}} d\psi. \end{aligned} \quad (3.177)$$

Furthermore, we apply IBP to one of the integral terms of (3.177),

$$\begin{aligned} \frac{2}{B} \int_{\psi_0}^{\delta} \hat{r} \cos \psi \dot{\hat{u}} d\psi &= \frac{2}{B} \left[\left(\sin \psi \hat{r} \dot{\hat{u}} \right) \Big|_{\psi_0}^{\delta} - \int_{\psi_0}^{\delta} \sin \psi \frac{d}{d\psi} \left(\hat{r} \dot{\hat{u}} \right) d\psi \right] \\ &= \frac{2}{B} \left[q_2(\delta) - \sin \psi_0 \hat{r}_0 \dot{\hat{u}}(\psi_0; \phi_0) - \int_{\psi_0}^{\delta} \sin \psi \frac{d\hat{r}}{d\psi} \dot{\hat{u}} d\psi - \int_{\psi_0}^{\delta} \sin \psi \hat{r} \frac{d\dot{\hat{u}}}{d\psi} d\psi \right], \end{aligned} \quad (3.178)$$

where

$$q_2(\delta) = \sin(\delta) \hat{r}(\delta; \phi_0) \dot{\hat{u}}(\delta; \phi_0). \quad (3.179)$$

Hence, we obtain the desired form of $\frac{d\hat{E}_{F_1}^\delta}{d\phi_0}$,

$$\begin{aligned} \frac{d\hat{E}_{F_1}^\delta}{d\phi_0} &= q_1(\delta) + \frac{2}{B} q_2(\delta) - \hat{u}_0^2 \hat{r}_0 \cos \phi_0 - \frac{2}{B} \sin \psi_0 \hat{r}_0 \dot{\hat{u}}(\psi_0; \phi_0) - \frac{2}{B} \int_{\psi_0}^{\delta} \sin \psi \hat{r} \frac{d\dot{\hat{u}}}{d\psi} d\psi \\ &\quad - \frac{2}{B} \int_{\psi_0}^{\delta} \sin \psi \hat{r} \dot{\hat{r}} d\psi - \frac{2}{B} \int_{\psi_0}^{\delta} \sin \psi \frac{d\hat{u}}{d\psi} \dot{\hat{r}} d\psi. \end{aligned} \quad (3.180)$$

Next, we find $\frac{d\hat{E}_\sigma^\delta}{d\phi_0}$. We first simplify (3.169), then

$$\begin{aligned}
\hat{E}_\sigma^\delta(\phi_0) &= \frac{2}{B} \int_{\psi_0}^{\delta} \frac{\hat{r}^2(1 - \cos \psi)}{B\hat{r}\hat{u} - \sin \psi} d\psi - \frac{\hat{r}_0^2}{B} \\
&= \frac{2}{B} \int_{\psi_0}^{\delta} \left(\frac{1 - \cos \psi}{\cos \psi} \right) \hat{r} \frac{d\hat{r}}{d\psi} d\psi - \frac{\hat{r}_0^2}{B} \\
&= \frac{2}{B} \int_{\psi_0}^{\delta} \left(\frac{\sin^2 \psi}{\cos \psi} \right) \hat{r} \frac{d\hat{r}}{d\psi} + (\cos \psi - 1) \hat{r} \frac{d\hat{r}}{d\psi} d\psi - \frac{\hat{r}_0^2}{B}, \tag{3.181}
\end{aligned}$$

where the identity $\frac{1 - \cos \psi}{\cos \psi} = \frac{\sin^2 \psi}{\cos \psi} + \cos \psi - 1$ is applied.

We differentiate $\hat{E}_\sigma^\delta(\phi_0)$ with respect to ϕ_0 ,

$$\begin{aligned}
\frac{d\hat{E}_\sigma^\delta}{d\phi_0} &= -\frac{2}{B} \left(\frac{1 - \cos \psi_0}{\cos \psi_0} \right) \hat{r}(\psi_0; \phi_0) \frac{d\hat{r}}{d\psi}(\psi_0; \phi_0) - 2 \frac{\sin \phi_0 \cos \phi_0}{B} \\
&\quad + \frac{1}{B} \int_{\psi_0}^{\delta} \left(\frac{\sin^2 \psi}{\cos \psi} \right) \frac{d}{d\phi_0} \left(2\hat{r} \frac{d\hat{r}}{d\psi} \right) d\psi + \frac{1}{B} \int_{\psi_0}^{\delta} (\cos \psi - 1) \frac{d}{d\psi} \left(\frac{d}{d\phi_0} \hat{r}^2 \right) d\psi, \tag{3.182}
\end{aligned}$$

where $\frac{d}{d\phi_0} \hat{r}^2 = 2\hat{r}\dot{\hat{r}}$.

We apply IBP to above (3.182) and rearrange it,

$$\begin{aligned}
\frac{d\hat{E}_\sigma^\delta}{d\phi_0} &= -\frac{2}{B} \left(\frac{1 - \cos \psi_0}{\cos \psi_0} \right) \hat{r}(\psi_0; \phi_0) \frac{d\hat{r}}{d\psi}(\psi_0; \phi_0) - 2 \frac{\sin \phi_0 \cos \phi_0}{B} \\
&\quad + \frac{2}{B} \int_{\psi_0}^{\delta} \left(\frac{\sin^2 \psi}{\cos \psi} \right) \dot{\hat{r}} \frac{d\hat{r}}{d\psi} d\psi + \frac{2}{B} \int_{\psi_0}^{\delta} \left(\frac{\sin^2 \psi}{\cos \psi} \right) \hat{r} \frac{d\dot{\hat{r}}}{d\psi} d\psi \\
&\quad + \frac{2}{B} g_3(\delta) - \frac{2}{B} (\cos \psi_0 - 1) \hat{r}(\psi_0; \phi_0) \dot{\hat{r}}(\psi_0; \phi_0) + \frac{2}{B} \int_{\psi_0}^{\delta} \sin \psi \hat{r} \dot{\hat{r}} d\psi, \tag{3.183}
\end{aligned}$$

where

$$q_3(\delta) = (\cos \delta - 1)\hat{r}(\delta; \phi_0)\dot{\hat{r}}(\delta; \phi_0). \quad (3.184)$$

Moreover, we notice that

$$\begin{aligned} \frac{2}{B} \int_{\psi_0}^{\delta} \left(\frac{\sin^2 \psi}{\cos \psi} \right) \dot{\hat{r}} \frac{d\hat{r}}{d\psi} d\psi &= \frac{2}{B} \int_{\psi_0}^{\delta} \sin \psi \frac{d\hat{u}}{d\psi} \dot{\hat{r}} d\psi \\ \frac{2}{B} \int_{\psi_0}^{\delta} \left(\frac{\sin^2 \psi}{\cos \psi} \right) \hat{r} \frac{d\dot{\hat{r}}}{d\psi} d\psi &= \frac{2}{B} \int_{\psi_0}^{\delta} \sin \psi \hat{r} \frac{d\dot{\hat{u}}}{d\psi} d\psi \end{aligned}$$

$$\text{since } \frac{\sin^2 \psi}{\cos \psi} \frac{d\hat{r}}{d\psi} = \sin \psi \frac{d\hat{u}}{d\psi} \text{ and } \frac{\sin^2 \psi}{\cos \psi} \frac{d\dot{\hat{r}}}{d\psi} = \sin \psi \frac{d\dot{\hat{u}}}{d\psi}.$$

$$\begin{aligned} & - \frac{2}{B} \left(\frac{1 - \cos \psi_0}{\cos \psi_0} \right) \hat{r}(\psi_0; \phi_0) \frac{d\hat{r}}{d\psi}(\psi_0; \phi_0) - \frac{2}{B} (\cos \psi_0 - 1) \hat{r}(\psi_0; \phi_0) \dot{\hat{r}}(\psi_0; \phi_0) \\ &= - \frac{2}{B} (\cos \psi_0 - 1) \hat{r}(\psi_0; \phi_0) \cos \phi_0 - \frac{2}{B} \hat{r}(\psi_0; \phi_0) \frac{d\hat{r}}{d\psi}(\psi_0; \phi_0) \frac{\sin^2 \psi_0}{\cos \psi_0} \\ &= - \frac{2}{B} (\cos \psi_0 - 1) \hat{r}(\psi_0; \phi_0) \cos \phi_0 - \frac{2}{B} \sin \phi_0 \sin \psi_0 \frac{d\hat{u}}{d\psi}(\psi_0; \phi_0) \end{aligned} \quad (3.185)$$

$$\text{since } \dot{\hat{r}}(\psi_0; \phi_0) = \cos \phi_0 - \frac{d\hat{r}}{d\psi}(\psi_0; \phi_0).$$

$$\begin{aligned} & - 2 \frac{\sin \phi_0 \cos \phi_0}{B} - \frac{2}{B} (\cos \psi_0 - 1) \hat{r}(\psi_0; \phi_0) \cos \phi_0 \\ &= - \frac{2}{B} \cos \psi_0 \sin \phi_0 \cos \phi_0 \end{aligned} \quad (3.186)$$

with $\hat{r}(\psi_0; \phi_0) = \sin(\phi_0)$.

Therefore, we obtain the simplified form of $\frac{d\hat{E}_\sigma^\delta}{d\phi_0}$,

$$\begin{aligned} \frac{d\hat{E}_\sigma^\delta}{d\phi_0} &= \frac{2}{B}q_3(\delta) - \frac{2}{B}\cos\psi_0\sin\phi_0\cos\phi_0 - \frac{2}{B}\sin\phi_0\sin\psi_0\frac{d\hat{u}}{d\psi}(\psi_0;\phi_0) \\ &\quad + \frac{2}{B}\int_{\psi_0}^\delta\sin\psi\hat{r}\dot{\hat{r}}d\psi + \frac{2}{B}\int_{\psi_0}^\delta\sin\psi\frac{d\hat{u}}{d\psi}\dot{\hat{r}}d\psi + \frac{2}{B}\int_{\psi_0}^\delta\sin\psi\hat{r}\frac{d\hat{u}}{d\psi}d\psi. \end{aligned} \quad (3.187)$$

Adding $\frac{d\hat{E}_\sigma^\delta}{d\phi_0}$ and $\frac{d\hat{E}_{F_1}^\delta}{d\phi_0}$ together,

$$\begin{aligned} \frac{d\hat{E}_\sigma^\delta}{d\phi_0} + \frac{d\hat{E}_{F_1}^\delta}{d\phi_0} &= q_1(\delta) + \frac{2}{B}q_2(\delta) - \hat{u}_0^2\hat{r}_0\cos\phi_0 - \frac{2}{B}\sin\psi_0\hat{r}_0\dot{\hat{u}}(\psi_0;\phi_0) - \frac{2}{B}\int_{\psi_0}^\delta\sin\psi\hat{r}\frac{d\hat{u}}{d\psi}d\psi \\ &\quad - \frac{2}{B}\int_{\psi_0}^\delta\sin\psi\hat{r}\dot{\hat{r}}d\psi - \frac{2}{B}\int_{\psi_0}^\delta\sin\psi\frac{d\hat{u}}{d\psi}\dot{\hat{r}}d\psi \\ &\quad + \frac{2}{B}q_3(\delta) - \frac{2}{B}\cos\psi_0\sin\phi_0\cos\phi_0 - \frac{2}{B}\sin\phi_0\sin\psi_0\frac{d\hat{u}}{d\psi}(\psi_0;\phi_0) \\ &\quad + \frac{2}{B}\int_{\psi_0}^\delta\sin\psi\hat{r}\dot{\hat{r}}d\psi + \frac{2}{B}\int_{\psi_0}^\delta\sin\psi\frac{d\hat{u}}{d\psi}\dot{\hat{r}}d\psi + \frac{2}{B}\int_{\psi_0}^\delta\sin\psi\hat{r}\frac{d\hat{u}}{d\psi}d\psi. \end{aligned} \quad (3.188)$$

With $\dot{\hat{u}}(\psi_0;\phi_0) = \frac{d\hat{u}_0}{d\phi_0} - \frac{d\hat{u}}{d\psi}(\psi_0;\phi_0)$ and $\hat{h}'(\phi_0) = -\sin\phi_0 + \frac{d\hat{u}_0}{d\phi_0}$, we obtain

$$\begin{aligned} \frac{d\hat{E}_\sigma^\delta}{d\phi_0} + \frac{d\hat{E}_{F_1}^\delta}{d\phi_0} &= q_1(\delta) + \frac{2}{B}q_2(\delta) + \frac{2}{B}q_3(\delta) - \frac{2}{B}\sin\psi_0\sin\phi_0\dot{\hat{u}}(\psi_0;\phi_0) \\ &\quad - \hat{u}_0^2\hat{r}_0\cos\phi_0 - \frac{2}{B}\cos\psi_0\sin\phi_0\cos\phi_0 - \frac{2}{B}\sin\phi_0\sin\psi_0\frac{d\hat{u}}{d\psi}(\psi_0;\phi_0) \\ &= q_1(\delta) + \frac{2}{B}q_2(\delta) + \frac{2}{B}q_3(\delta) - \hat{u}_0^2\hat{r}_0\cos\phi_0 \\ &\quad - \frac{2}{B}\sin\psi_0\sin\phi_0\hat{h}'(\phi_0) - \frac{2}{B}\sin\psi_0\sin^2\phi_0 - \frac{2}{B}\cos\psi_0\sin\phi_0\cos\phi_0 \\ &= q_1(\delta) + \frac{2}{B}q_2(\delta) + \frac{2}{B}q_3(\delta) - \hat{u}_0^2\hat{r}_0\cos\phi_0 \\ &\quad - \frac{2}{B}\sin\psi_0\sin\phi_0\hat{h}'(\phi_0) + \frac{2}{B}\cos\gamma\sin\phi_0. \end{aligned} \quad (3.189)$$

Using the results in Sec. 3.5.1 to evaluate \hat{r} , \hat{u} , $\dot{\hat{r}}$ and $\dot{\hat{u}}$ at $(\delta; \phi_0)$ as $\delta \rightarrow 0$, we have $\hat{r} \sim -\ln(-\delta)$ and $\hat{u} \sim -\delta$, see (3.92) and (3.93), and $\dot{\hat{r}} \sim \hat{c}$ for some constant \hat{c} and $\dot{\hat{u}} = o(\delta)$, see (3.146). Thus, $q_1(\delta)$, $q_2(\delta)$ and $q_3(\delta)$ all go to zero as $\delta \rightarrow 0$.

Therefore, combining each part of $\frac{d\hat{E}_T}{d\phi_0}$, we obtain the same result for the non-graph case,

$$\frac{d\hat{E}_T}{d\phi_0} = -\hat{F}_T \hat{h}'(\phi_0). \quad (3.190)$$

Remark 15. In derivation of (3.190), the graph and non-graph cases are considered. As we know, the parametric solution $\hat{r}(\psi; \phi_0)$ and $\hat{u}(\psi; \phi_0)$ also works in derivation of (3.190) for the graph case. However, $\hat{u} = 0$ is not included in the parametric solutions. Therefore, the derivation based on $\hat{u}(\hat{r}; \hat{r}_0, \hat{u}_0)$ in the graph case is essential (it contains the $\hat{u} = 0$ case). In addition, the derivation in the graph case (use the convention $\hat{u}(\hat{r}; \hat{r}_0, \hat{u}_0)$) is more straightforward compared with the derivation using the parametric solutions.

3.6.4 Stability Criterion

In Sec. 3.6.3, we derived the relation between \hat{E}_T and \hat{F}_T , that is, $\frac{d\hat{E}_T}{d\phi_0} = -\hat{F}_T \hat{h}'$. This relation implies the critical point of \hat{E}_T can be either a force balance point or a critical point of \hat{h} . We are interested in the number of the force balanced points and their stability. Determining the number of the force balanced points requires numerical tests, which is discussed in Sec. 3.8.5. In this section, the stability criterion is developed based on the relation. Equipped with the criterion, we can conclude the stability of a force balanced point (if it exists).

Suppose $\bar{\phi}_0$ is a force balanced point, $\hat{F}_T(\bar{\phi}_0) = 0$. We apply the first derivative test to analyze the stability at $\bar{\phi}_0$. Assume $\hat{F}'_T(\bar{\phi}_0) > 0$ and $\hat{h}'(\bar{\phi}_0) < 0$. There exists an open interval $(\bar{\phi}_0 - \delta, \bar{\phi}_0 + \delta)$ for an arbitrarily small $\delta > 0$ such that $\hat{F}_T(\phi_0) < 0$ on $(\bar{\phi}_0 - \delta, \bar{\phi}_0)$, $\hat{F}_T(\phi_0) > 0$ on $(\bar{\phi}_0, \bar{\phi}_0 + \delta)$ and $\hat{h}'(\phi_0) < 0$ on $(\bar{\phi}_0 - \delta, \bar{\phi}_0 + \delta)$. Thus,

$$\frac{d\hat{E}_T}{d\phi_0}(\phi_0) < 0 \text{ on } (\bar{\phi}_0 - \delta, \bar{\phi}_0), \quad (3.191)$$

$$\frac{d\hat{E}_T}{d\phi_0}(\phi_0) > 0 \text{ on } (\bar{\phi}_0, \bar{\phi}_0 + \delta). \quad (3.192)$$

We conclude $\bar{\phi}_0$ is a local minimum point of $\hat{E}_T(\phi_0)$, hence it is stable. The same result can be obtained if we assume $\hat{F}'_T(\bar{\phi}_0) < 0$ and $\hat{h}'(\bar{\phi}_0) > 0$. Therefore, we summarize the stability criterion in Theorem 20.

Theorem 20. *(Stability criterion) The force balanced point $\bar{\phi}_0$ is locally stable, if $\hat{F}'_T(\bar{\phi}_0)$ and $\hat{h}'(\bar{\phi}_0)$ have the different signs; if $\hat{F}'_T(\bar{\phi}_0)$ and $\hat{h}'(\bar{\phi}_0)$ share the same sign, then $\bar{\phi}_0$ is locally unstable.*

Remark 16. If we assume $\frac{d^2\hat{u}_0}{d\phi_0^2}$ exists, we can apply the second derivative test.

$$\frac{d^2\hat{E}_T}{d\phi_0^2} = -\hat{F}'_T(\phi_0)\hat{h}'(\phi_0) - \hat{F}_T(\phi_0)\hat{h}''(\phi_0). \quad (3.193)$$

At $\phi_0 = \bar{\phi}_0$,

$$\frac{d^2\hat{E}_T}{d\phi_0^2}(\bar{\phi}_0) = -\hat{F}'_T(\bar{\phi}_0)\hat{h}'(\bar{\phi}_0). \quad (3.194)$$

Therefore,

$$\frac{d^2\hat{E}_T}{d\phi_0^2}(\bar{\phi}_0) > 0 \quad \Rightarrow \quad \bar{\phi}_0 \text{ is locally stable,} \quad (3.195)$$

$$\frac{d^2\hat{E}_T}{d\phi_0^2}(\bar{\phi}_0) < 0 \quad \Rightarrow \quad \bar{\phi}_0 \text{ is locally unstable,} \quad (3.196)$$

The result is consistent with the stability criterion.

3.7 Shooting Method

Unfortunately, the BVP shown in (3.15) and (3.16) has no analytic solution and can only be solved numerically. The shooting method is a candidate. Since B appears in the denominator of (3.15), we can apply scaling, $\bar{r} = \sqrt{B}\hat{r}$ and $\bar{u} = \sqrt{B}\hat{u}$ to eliminate it (instead, B appears in the boundary condition). Therefore,

$$\frac{d\bar{r}}{d\psi} = \frac{\bar{r} \cos \psi}{\bar{r}\bar{u} - \sin \psi}, \quad \frac{d\bar{u}}{d\psi} = \frac{\bar{r} \sin \psi}{\bar{r}\bar{u} - \sin \psi}, \quad (3.197)$$

and the boundary conditions become

$$\bar{r}(\psi_0) = \sqrt{B} \sin \phi_0 \quad \text{and} \quad \lim_{\psi \rightarrow 0} \bar{u}(\psi) = 0. \quad (3.198)$$

Before applying the shooting method, we first investigate the behavior of the fluid interface that is far away from the floating ball. Heartland and Hartley [30] give an approximation to the solution for $\bar{r} \gg \bar{r}_0$, which can be treated as a good initial guess. When $\bar{r} \gg \bar{r}_0$, the fluid interface becomes a graph and $|\bar{u}'| \ll 1$, thus, (3.7) turns into a linearized DE

$$\bar{u}_L'' + \frac{1}{\bar{r}} \bar{u}_L' - \bar{u}_L = 0. \quad (3.199)$$

(3.199) is the modified Bessel's equation and has the solution:

$$\bar{u}_L(\bar{r}) = CK_0(\bar{r}) + \bar{C}I_0(\bar{r}), \quad (3.200)$$

where K_0 and I_0 are the modified Bessel function of the second and the first kind, respectively. With $\lim_{\bar{r} \rightarrow \infty} \bar{u}(\bar{r}) = 0$, \bar{C} has to be eliminated, since $I_0(\bar{r}) \rightarrow \infty$ as $\bar{r} \rightarrow \infty$. Hence, for \bar{r} large, the solution of the BVP can be approximated by

$$\bar{u}(\bar{r}) \approx \bar{u}_L = CK_0(\bar{r}), \quad (3.201)$$

where C is a constant. Since $K_0(\bar{r}_{\text{end}}) \approx 10^{-5}$ for $\bar{r}_{\text{end}} = 10$, thus, $\bar{r} = \bar{r}_{\text{end}}$ is good enough as a boundary instead of at infinity.

Remark 17. The scaled DEs are preferred in numerical computation. Since we would like to compute the numerical solution with small values of B , the appearance of B in the denominator of the dimensionless capillary equation, see (3.15), could challenge the robustness of the shooting method algorithm. However, B appears in the boundary condition of the scaled version, it can overcome the problem.

The shooting method has the following algorithm:

- (i) Fix $\bar{r}_{\text{end}} = 10$, guess a small $C = c_0$, and impose the initial condition $(\bar{r}(\psi_{\text{end}}), \bar{u}(\psi_{\text{end}})) = (\bar{r}_{\text{end}}, c_0 K_0(\bar{r}_{\text{end}}))$, where $\psi_{\text{end}} = -\arctan(c_0 K_1(\bar{r}_{\text{end}}))$ (since $\bar{u}(\bar{r}) \approx CK_0(\bar{r})$, then $\bar{u}'(\bar{r}) \approx -CK_1(\bar{r})$).
- (ii) Define a function $f(C; \psi_{\text{end}}, \bar{r}_{\text{end}}, \bar{u}(\bar{r}_{\text{end}}))$ that returns the difference $\bar{r}_{\text{num}}(\psi_0) - \bar{r}(\psi_0)$, where $\bar{r}_{\text{num}}(\psi_0)$ represents the numerical solution of \bar{r} at $\psi = \psi_0$, which can be obtained by integrating (3.197) backwards from ψ_{end} to ψ_0 .
- (iii) Solve $f(C; \psi_{\text{end}}, \bar{r}_{\text{end}}, \bar{u}(\bar{r}_{\text{end}})) = 0$ for C such that $\bar{u} = CK_0(\bar{r})$ gives the correct height \bar{u}_{true} at $\bar{r} = \bar{r}_{\text{end}}$.
- (iv) Based on the true values $(\bar{r}_{\text{end}}, \bar{u}_{\text{true}})$ and good approximation $\psi_{\text{end}} = -\arctan(CK_1(\bar{r}_{\text{end}}))$, we integrate (3.197) backwards again and obtain the numerical solutions:

$$\{\psi_i\}_{i=0}^N, \quad \{\bar{r}_i\}_{i=0}^N, \quad \text{and} \quad \{\bar{u}_i\}_{i=0}^N. \quad (3.202)$$

Fig. 3.8a shows the shooting method algorithm and Fig. 3.8b shows the numerical results with $\gamma = \frac{\pi}{2}$, $\phi_0 = \frac{\pi}{4}$ and $\bar{r}_{\text{end}} = 10$.

Once the numerical solutions of the BVP in (3.197) and (3.198) are obtained, the dimensionless $\hat{r}(\psi)$ and $\hat{u}(\psi)$ will be obtained by rescaling,

$$\hat{r} = \frac{1}{\sqrt{B}} \bar{r} \quad \text{and} \quad \hat{u} = \frac{1}{\sqrt{B}} \bar{u}. \quad (3.203)$$

It is the same with $r(\psi)$ and $u(\psi)$, shown as follows,

$$r = \frac{a}{\sqrt{B}} \bar{r} \quad \text{and} \quad u = \frac{a}{\sqrt{B}} \bar{u}, \quad (3.204)$$

Remark 18. When the fluid interface is a graph, the iterative method can be applied to determine the fluid interface numerically, see Appendix B.3.

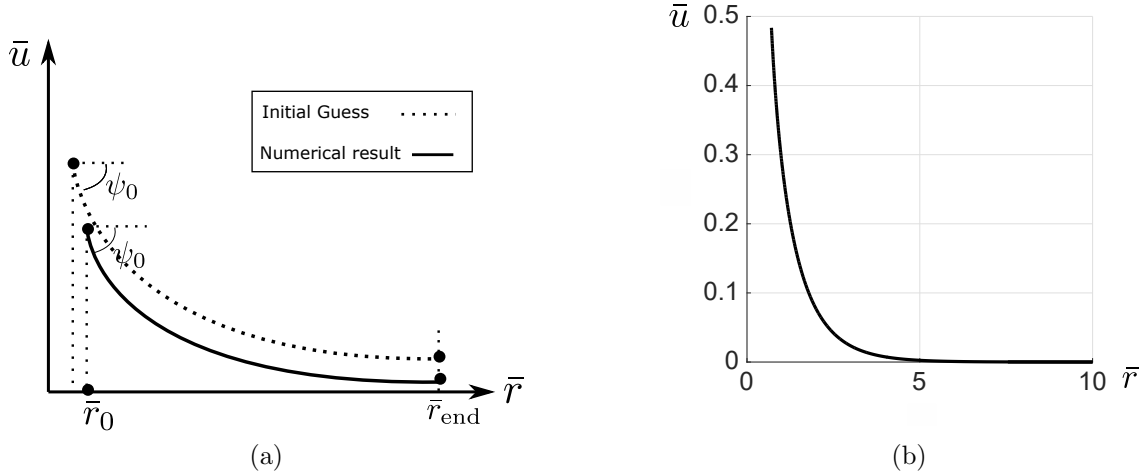


Figure 3.8: (a) The shooting method algorithm; (b) the numerical result for the fluid height $\bar{u}(\bar{r})$.

Recall the height of the center,

$$h(\phi_0) = \cos(\phi_0) + u_0. \quad (3.205)$$

With the numerical solution, we observe an interesting result: the non-monotone relation between $h(\phi_0)$ and ϕ_0 , see Fig. 3.9. Therefore, if we fix the height, there is a possibility to obtain two different configurations. Fig. 3.10a and Fig. 3.10b show that, given $a = 1$, $\gamma = \frac{\pi}{2}$, $\kappa = 1$, the height $h = 1.3$, there are two corresponding configurations with attachment angles $\phi_0 = 0.1028$ and $\phi_0 = 0.6805$.

Remark 19. Due to the non-monotone relation between $h(\phi_0)$ and ϕ_0 , ϕ_0 is preferred as a variable of the total energy E_T , the total force F_T and the fluid height at contact point u_0 rather than h .

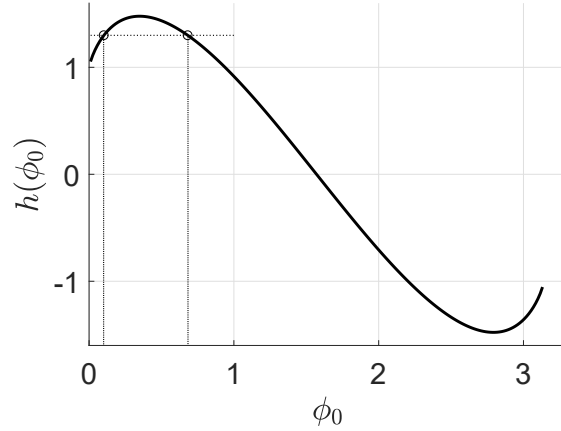


Figure 3.9: The non-monotone relation between ϕ_0 and $h(\phi_0)$. Given $h = 1.3$, there are two corresponding ϕ_0 values: $\phi_0 = 0.1028$ and $\phi_0 = 0.6805$.

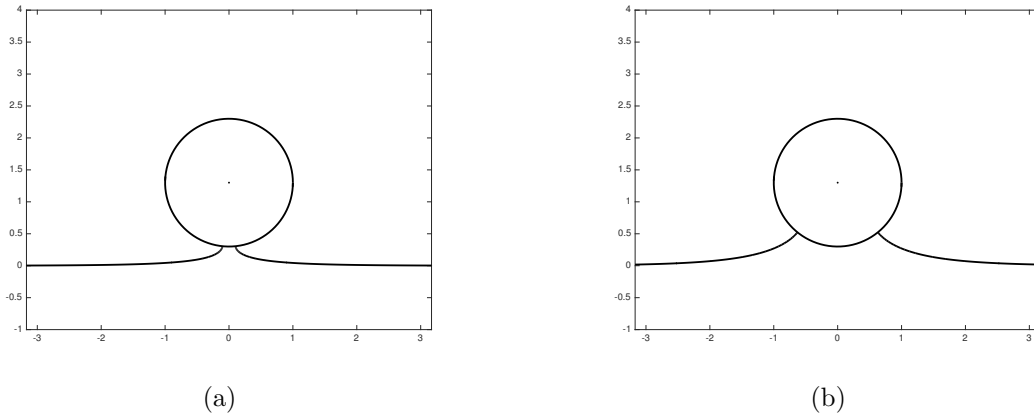


Figure 3.10: (a) The configuration with $\phi_0 = 0.1028$, $h = 1.3$, $a = 1$, $\gamma = \frac{\pi}{2}$, (b) another configuration with the same height $h = 1.3$ and $\phi_0 = 0.6805$.

3.8 Behavior of the Total Force $\hat{F}_T(\phi_0)$ and Height $\hat{h}(\phi_0)$ Curves

To analyze the number of force balanced points and their stability, we need to understand the behavior of the total force $\hat{F}_T(\phi_0)$ and the height $\hat{h}(\phi_0)$. Recall that,

$$\hat{F}_T(\phi_0) = -\frac{4}{3}\alpha - \frac{2}{B} \sin(\phi_0 + \gamma) \sin \phi_0 - \cos(\phi_0) \sin^2(\phi_0) - \sin^2(\phi_0) \hat{u}_0 + \frac{2}{3}(1 - \cos^3 \phi_0), \quad (3.206)$$

$$\hat{h}(\phi_0) = \cos(\phi_0) + \hat{u}_0. \quad (3.207)$$

If we differentiate $\hat{F}_T(\phi_0)$ with respect to ϕ_0 and rearrange the terms, then

$$\hat{F}'_T(\phi_0) = -\frac{2}{B} \sin(2\phi_0 + \gamma) + \sin^3(\phi_0) - 2 \sin(\phi_0) \cos(\phi_0) \hat{u}_0 - \sin^2(\phi_0) \frac{d\hat{u}_0}{d\phi_0}. \quad (3.208)$$

Since \hat{u}_0 appears in both the height $\hat{h}(\phi_0)$ and the total force $\hat{F}_T(\phi_0)$, which has to be calculated numerically, it increases the difficulty of the analysis. Before we carry out the numerical tests in Sec. 3.8.5, we would like to explore the behavior of $\hat{h}(\phi_0)$ and $\hat{F}_T(\phi_0)$ for small and large Bond numbers and the limiting cases $\phi_0 \rightarrow 0, \pi$, see Sec. 3.8.1 - Sec. 3.8.4. In Sec. 3.8.5, we summarize the number of the force balanced points and their stability based on the numerical tests of the behavior of the \hat{F}_T curve with different values of parameters B and γ . A similar approach is applied to analyze the behavior of the \hat{h} curve, as well.

In this section, suppose $B > 0$, $\gamma \in [0, \pi]$ (the $\gamma = 0$ and $\gamma = \pi$ cases will be discussed separately) and $\phi_0 \in (0, \pi)$. Though both $\hat{h}(\phi_0)$ and $\hat{F}_T(\phi_0)$ contains \hat{u}_0 , there still are some interesting properties, shown as follows,

Property 4. With $B > 0$, $\alpha > 0$, $\gamma \in [0, \pi]$ and $\phi_0 \in (0, \pi)$, the height $\hat{h}(\phi_0)$ and the total force $\hat{F}_T(\phi_0)$ curves have the following properties:

- (i) $\hat{F}_T(0) = -\frac{4}{3}\alpha < \hat{F}_T(\pi) = -\frac{4}{3}\alpha + \frac{4}{3}$.
- (ii) $\hat{F}'_T(0) = \hat{F}'_T(\pi) = -\frac{2}{B} \sin(\gamma)$. Moreover, when $\gamma \in (0, \pi)$, $\hat{F}_T(\phi_0) < \hat{F}_T(0)$ on some interval $(0, \mu)$ and $\hat{F}_T(\phi_0) > \hat{F}_T(\pi)$ on some interval $(\pi - \mu, \pi)$ for some small $\mu > 0$.
- (iii) When $\gamma = \frac{\pi}{2}$, both $\hat{u}_0(\phi_0)$ and $\hat{h}(\phi_0)$ are centrally symmetric about $(\frac{\pi}{2}, 0)$ and $\hat{F}_T(\phi_0)$ is centrally symmetric about $(\frac{\pi}{2}, \hat{F}_T(\frac{\pi}{2}))$.

(iv) For $\gamma \in (0, \pi)$, given $\bar{\phi}_0 \in (\pi - \gamma, \pi)$, by varying the value of $\alpha > 0$, $\bar{\phi}_0$ can be a force balanced point such that

$$\hat{F}_T(\bar{\phi}_0) = 0.$$

In this case, $\hat{u}_0(\bar{\phi}_0) < 0$.

(v) For $\gamma \in (0, \pi)$,

$$\hat{F}_T(\pi - \gamma) = -\frac{4}{3}\alpha + \Gamma(\gamma), \quad (3.209)$$

where $\Gamma(\gamma) = \cos(\gamma) \sin^2(\gamma) + \frac{2}{3}(1 + \cos^3(\gamma))$. If $\alpha = \frac{3}{4}\Gamma(\gamma)$, then $\hat{F}_T(\pi - \gamma) = 0$. If $0 < \alpha < \frac{3}{4}\Gamma(\gamma)$, there exists at least one force balanced point $\bar{\phi}_0 \in (0, \pi - \gamma)$. If $\frac{3}{4}\Gamma(\gamma) < \alpha < 1$, there exists at least one force balanced point $\bar{\phi}_0 \in (\pi - \gamma, \pi)$.

Proof. (i) and (ii) will be discussed in Sec. 3.8.3. Let us show (iii). With $\gamma = \frac{\pi}{2}$, $\phi_0 = \frac{\pi}{2}$ implies $\psi_0 = 0$, thus, $\hat{u}_0\left(\frac{\pi}{2}\right) = 0$. Consider $\phi_0 \in \left(0, \frac{\pi}{2}\right)$ and $\check{\phi}_0 = \pi - \phi_0 \in \left(\frac{\pi}{2}, \pi\right)$ such that ϕ_0 and $\check{\phi}_0$ are symmetric about $\phi_0 = \frac{\pi}{2}$. In addition, with the geometric constraint, we have $\psi_0 = -\check{\psi}_0$, where $\psi_0 = \phi_0 - \frac{\pi}{2} < 0$ and $\check{\psi}_0 = \check{\phi}_0 - \frac{\pi}{2} > 0$. Thus, $\hat{r}(\psi_0) = \sin(\phi_0) = \sin(\check{\phi}_0) = \hat{r}(\check{\psi}_0)$. Based on the BVP in (3.15) and (3.16), $\hat{u}(\psi_0) = -\hat{u}(\check{\psi}_0)$. Equivalently, $\hat{u}_0 = -\hat{u}_0(\pi - \phi_0)$, that is, $\hat{u}_0(\phi_0)$ is centrally symmetric about $\left(\frac{\pi}{2}, 0\right)$. So as $\hat{h}(\phi_0)$, since $\hat{h}(\phi_0) = \cos(\phi_0) + \hat{u}_0$. For \hat{F}_T , let $\phi_0 \in \left(0, \frac{\pi}{2}\right)$ again,

$$\begin{aligned} \hat{F}_T(\phi_0) + \hat{F}_T(\pi - \phi_0) &= -\frac{4}{3}\alpha - \frac{2}{B} \cos(\phi_0) \sin(\phi_0) - (\cos(\phi_0) + \hat{u}_0(\phi_0)) \sin^2(\phi_0) \\ &\quad + \frac{2}{3}(1 - \cos^3(\phi_0)) - \frac{4}{3}\alpha - \frac{2}{B} \cos(\pi - \phi_0) \sin(\pi - \phi_0) \\ &\quad - (\cos(\pi - \phi_0) + \hat{u}_0(\pi - \phi_0)) \sin^2(\pi - \phi_0) + \frac{2}{3}(1 - \cos^3(\pi - \phi_0)) \\ &= -\frac{8}{3}\alpha + \frac{4}{3} = 2\hat{F}_T\left(\frac{\pi}{2}\right). \end{aligned}$$

Hence, $\hat{F}_T(\phi_0)$ is centrally symmetric about $\left(\frac{\pi}{2}, \hat{F}_T\left(\frac{\pi}{2}\right)\right)$.

For (iv), We use the identity $\sin^2 \phi_0 + \cos^2 \phi_0 = 1$ and rearrange the total force equation,

$$\hat{F}_T(\phi_0) = -\frac{4}{3}\alpha + f_1(\phi_0) + f_2(\phi_0), \quad (3.210)$$

where

$$f_1(\phi_0) = -\sin \phi_0 \left(\frac{2}{B} \sin(\phi_0 + \gamma) + \hat{u}_0 \sin \phi_0 \right), \quad (3.211)$$

$$f_2(\phi_0) = -\cos \phi_0 + \frac{2}{3} + \frac{1}{3} \cos^3(\phi_0). \quad (3.212)$$

Note that $f_2'(\phi_0) = \sin^3(\phi_0)$, thus it is strictly increasing on $\phi_0 \in (0, \pi)$. Moreover, $f_2(0) = 0$ and $f_2(\pi) = \frac{4}{3}$. Thus, $f_2(\phi_0) > 0$ for $\phi_0 \in (\pi - \gamma, \pi)$.

As for $f_1(\phi_0)$, we observe that $\hat{u}_0 > 0$ if $\psi_0 < 0$ and $\hat{u}_0 < 0$ if $\psi_0 > 0$. With the geometric constraint, we conclude

$$\hat{u}_0 > 0 \Leftrightarrow 0 < \phi_0 + \gamma < \pi, \quad (3.213)$$

$$\hat{u}_0 < 0 \Leftrightarrow \pi < \phi_0 + \gamma < 2\pi. \quad (3.214)$$

(3.213) and (3.214) imply $\frac{2}{B} \sin(\phi_0 + \gamma)$ and $\hat{u}_0 \sin \phi_0$ share the same sign. Therefore, when $\pi - \gamma < \phi_0 < \pi$, we have $f_1(\phi_0) > 0$.

With both $f_1(\phi_0) > 0$ and $f_2(\phi_0) > 0$ for $\pi - \gamma < \phi_0 < \pi$, given $\bar{\phi}_0 \in (\pi - \gamma, \pi)$, we have $f_1(\bar{\phi}_0) + f_2(\bar{\phi}_0) > 0$. By varying the value of α , it is always possible to have $\hat{F}_T(\bar{\phi}_0) = 0$ and in this case, $\hat{u}_0(\bar{\phi}_0) < 0$.

For (v), at $\phi_0 = \pi - \gamma$ ($\psi_0 = 0$), we have $\hat{u}_0 = 0$. Thus, (3.209) is obtained. $\Gamma(\gamma) = \cos(\gamma) \sin^2(\gamma) + \frac{2}{3}(1 + \cos^3(\gamma))$ is a decreasing function in γ and $0 < \Gamma(\gamma) < \frac{4}{3}$. From

(3.209), if $\alpha = \frac{3}{4}\Gamma(\gamma)$, then $\hat{F}_T(\pi - \gamma) = 0$. With (i), if $0 < \alpha < \frac{3}{4}\Gamma(\gamma)$, then $\hat{F}_T(0) < 0$ and $\hat{F}_T(\pi - \gamma) > 0$. So, there exists at least one force balanced point $\bar{\phi}_0 \in (0, \pi - \gamma)$. If $\frac{3}{4}\Gamma(\gamma) < \alpha < 1$, then $\hat{F}_T(\pi - \gamma) < 0$ and $\hat{F}_T(\pi) > 0$. So, there exists at least one force balanced point $\bar{\phi}_0 \in (\pi - \gamma, \pi)$.

□

3.8.1 Asymptotic Expansion of the fluid interface as $B \rightarrow 0$

There is a wide discussion of the asymptotic expansion of the fluid interface (which is a graph) near a vertical circular cylinder with small Bond number, known as the needle problem, see [41], [47] and [57]. In the floating ball problem, the asymptotic expansion of the fluid interface near the contact point as $B \rightarrow 0$ is analogous to that in the needle problem. However, the fluid interface can also be a non-graph. We will explain how to extend the asymptotic expansion of the graph case to the non-graph case.

The Graph Case

When the fluid interface is a graph, the floating ball problem can be fitted into the needle problem by choosing the characteristic length l_c as r_0 . Let $\tilde{u} = \frac{u}{l_c}$ and $\tilde{r} = \frac{r}{l_c}$, BVP in (3.7) and (3.8) turns into

$$\frac{\tilde{u}''}{(1 + \tilde{u}'^2)^{3/2}} + \frac{\tilde{u}'}{\tilde{r}\sqrt{1 + \tilde{u}'^2}} = \tilde{\kappa}\tilde{u}, \quad (3.215)$$

with boundary conditions

$$\psi(1) = \psi_0 \quad \text{and} \quad \lim_{\tilde{r} \rightarrow \infty} \tilde{u}(\tilde{r}) = 0, \quad (3.216)$$

where $\tilde{\kappa} = B \sin^2(\phi_0)$.

Recall from Chapter 2, we have the two-term asymptotic expansion of the fluid interface near the contact point, as $\tilde{\kappa} \rightarrow 0$,

$$\tilde{u}(\tilde{r}) = \frac{\tilde{c}}{2} \ln(\tilde{\kappa}) + \tilde{c} \ln\left(\tilde{r} + \sqrt{\tilde{r}^2 - \tilde{c}^2}\right) + \tilde{c}(\gamma_e - 2 \ln 2) + \mathcal{O}\left(\tilde{\kappa}^{2/3}(-\ln \tilde{\kappa})^{5/3}\right), \quad (3.217)$$

where $\tilde{c} = \sin(\psi_0) = -\sin(\phi_0 + \gamma)$ and γ_e is known as Euler's constant.

Remark 20. In (3.217), the error bound we obtained in Chapter 2 is applied.

We notice $\tilde{\kappa} \rightarrow 0$ as $B \rightarrow 0$. Transforming $\tilde{u}(\tilde{r})$ back to $\hat{u}(\hat{r})$ ($\hat{u} = \tilde{u} \sin(\phi_0)$), as $B \rightarrow 0$,

$$\hat{u}(\hat{r}) = \frac{\hat{c}}{2} \ln(B) + \hat{c} \ln\left(\hat{r} + \sqrt{\hat{r}^2 - \hat{c}^2}\right) + \hat{c}(\gamma_e - 2 \ln 2) + \mathcal{O}(\Delta_1), \quad (3.218)$$

where $\hat{c} = -\sin(\phi_0 + \gamma) \sin(\phi_0)$ and $\Delta_1 = (B \sin^2 \phi_0)^{2/3} (-\ln(B \sin^2 \phi_0))^{5/3}$. The error bound $\mathcal{O}(\Delta_1)$ depends on both B and ϕ_0 .

The Non-graph Case

The fluid interface can be a non-graph. We consider the parametric form with $\psi \in [-\pi + \mu, -\mu]$, where $0 < \mu < \frac{\pi}{2}$, hence $\tilde{u} > 0$ (the $\mu \leq \psi \leq \pi - \mu$ case will be similar). To investigate the asymptotic expansions of $\tilde{u}(\psi)$ and $\tilde{r}(\psi)$, we consider the parametric form

$$\frac{d\tilde{r}}{d\psi} = \frac{\cos \psi}{\tilde{\kappa}\tilde{u} - \frac{\sin \psi}{\tilde{r}}}, \quad \frac{d\tilde{u}}{d\psi} = \frac{\sin \psi}{\tilde{\kappa}\tilde{u} - \frac{\sin \psi}{\tilde{r}}}, \quad (3.219)$$

with boundary conditions

$$\tilde{r}(\psi_0) = 1 \quad \text{and} \quad \lim_{\psi \rightarrow 0} \tilde{u}(\psi) = 0. \quad (3.220)$$

Firstly, we seek for the upper bound of $\tilde{u}(\psi)$, from (3.219),

$$\tilde{u} \frac{d\tilde{u}}{d\psi} \geq \frac{\sin \psi}{\tilde{\kappa}}. \quad (3.221)$$

Integrating from ψ_0 to 0,

$$\int_{\psi_0}^0 \tilde{u} \frac{d\tilde{u}}{d\psi} d\psi \geq \int_{\psi_0}^0 \frac{\sin \psi}{\tilde{\kappa}} d\psi,$$

it implies

$$\tilde{u}(\psi_0) \leq \sqrt{\frac{2}{\tilde{\kappa}}} \sqrt{1 - \cos(\psi_0)} \leq \frac{2}{\sqrt{\tilde{\kappa}}}, \quad (3.222)$$

which gives the upper bound of \tilde{u} .

Therefore, from (3.222),

$$\tilde{\kappa} \tilde{u}(\psi) \leq \tilde{\kappa} \tilde{u}(\psi_0) \leq 2\sqrt{\tilde{\kappa}} \rightarrow 0 \quad \text{as } \tilde{\kappa} \rightarrow 0.$$

Since $\tilde{\kappa} \tilde{u} \rightarrow 0$ as $\tilde{\kappa} \rightarrow 0$, we define $\tilde{r}_1(\psi)$ and $\tilde{u}_1(\psi)$ such that

$$\frac{d\tilde{r}_1}{d\psi} = -\tilde{r}_1 \cot \psi \quad \text{and} \quad \frac{d\tilde{u}_1}{d\psi} = -\tilde{r}_1, \quad (3.223)$$

with $\tilde{r}_1(\psi_0) = 1$. Thus,

$$\tilde{r}_1(\psi) = \frac{\tilde{c}}{\sin \psi}, \quad (3.224)$$

$$\tilde{u}_1(\psi) = \tilde{c} \ln \left| \frac{\cos \psi + 1}{\sin \psi} \right| + \tilde{d}, \quad (3.225)$$

where \tilde{c} is the same as that in (3.217) and \tilde{d} is to be determined.

Lemma 21. Fix $0 < \mu < \frac{\pi}{2}$. For $\psi_0, \psi \in [-\pi + \mu, -\mu]$, then

$$\tilde{r}_1(\psi) \leq \frac{1}{\sin \mu} \quad \text{and} \quad \tilde{r}(\psi) \leq \frac{1}{\sin \mu}. \quad (3.226)$$

Proof. Fix $0 < \mu < \frac{\pi}{2}$. For $\psi_0, \psi \in [-\pi + \mu, -\mu]$, it is easy to see that $\tilde{r}_1(\psi) \leq \frac{1}{\sin \mu}$. For \tilde{r} , the following cases are considered:

(i) When $-\frac{\pi}{2} \leq \psi_0 \leq \psi$, from $\frac{d\tilde{r}}{d\psi} = \frac{\tilde{r} \cos \psi}{\tilde{\kappa} \tilde{r} \tilde{u} - \sin \psi}$, it gives

$$\frac{1}{\tilde{r}} \frac{d\tilde{r}}{d\psi} \leq -\cot \psi. \quad (3.227)$$

Integrating from ψ_0 to ψ , we obtain

$$\int_{\psi_0}^{\psi} \frac{1}{\tilde{r}} \frac{d\tilde{r}}{d\psi} d\psi \leq \int_{\psi_0}^{\psi} -\cot \psi d\psi \leq \int_{-\pi/2}^{-\mu} -\cot \psi d\psi = -\ln(\sin \mu). \quad (3.228)$$

So, $\tilde{r}(\psi) \leq \frac{1}{\sin \mu}$.

(ii) When $\psi_0 \leq \psi \leq -\frac{\pi}{2}$, then $\frac{d\tilde{r}}{d\psi} \leq 0$. Thus, $\tilde{r}(\psi) \leq \tilde{r}(\psi_0) = 1$. So, $\tilde{r}(\psi) \leq \frac{1}{\sin \mu}$.

(iii) When $\psi_0 \leq -\frac{\pi}{2} \leq \psi$, consider

$$\begin{aligned} \int_{\psi_0}^{\psi} \frac{1}{\tilde{r}} \frac{d\tilde{r}}{d\psi} d\psi &= \int_{\psi_0}^{\psi} \frac{\cos \psi}{\tilde{\kappa} \tilde{r} \tilde{u} - \sin \psi} d\psi \\ &= \int_{\psi_0}^{-\pi/2} \frac{\cos \psi}{\tilde{\kappa} \tilde{r} \tilde{u} - \sin \psi} d\psi + \int_{-\pi/2}^{\psi} \frac{\cos \psi}{\tilde{\kappa} \tilde{r} \tilde{u} - \sin \psi} d\psi \\ &\leq \int_{-\pi/2}^{\psi} \frac{\cos \psi}{\tilde{\kappa} \tilde{r} \tilde{u} - \sin \psi} d\psi \leq \int_{-\pi/2}^{\psi} -\cot(\psi) d\psi \\ &\leq \int_{-\pi/2}^{-\mu} -\cot(\psi) d\psi. \end{aligned} \quad (3.229)$$

It implies $\tilde{r} \leq \frac{1}{\sin \mu}$.

(iv) When $-\frac{\pi}{2} \leq \psi \leq \psi_0$, then $\frac{d\tilde{r}}{d\psi} \geq 0$. Thus, $\tilde{r}(\psi) \leq \tilde{r}(\psi_0) = 1$. So, $\tilde{r}(\psi) \leq \frac{1}{\sin \mu}$.

(v) When $\psi \leq \psi_0 \leq -\frac{\pi}{2}$, it is similar to (i). We have

$$\int_{\psi}^{\psi_0} \frac{1}{\tilde{r}} \frac{d\tilde{r}}{d\psi} d\psi \geq \int_{\psi}^{\psi_0} -\cot \psi d\psi \geq \int_{-\pi+\mu}^{-\pi/2} -\cot \psi d\psi = \ln(\sin \mu). \quad (3.230)$$

Hence, $\tilde{r} \leq \frac{1}{\sin \mu}$.

(vi) When $\psi \leq -\frac{\pi}{2} \leq \psi_0$, it is similar to (iii). We have

$$\begin{aligned} \int_{\psi}^{\psi_0} \frac{1}{\tilde{r}} \frac{d\tilde{r}}{d\psi} d\psi &= \int_{\psi}^{\psi_0} \frac{\cos \psi}{\tilde{\kappa} \tilde{r} \tilde{u} - \sin \psi} d\psi \\ &= \int_{\psi}^{-\pi/2} \frac{\cos \psi}{\tilde{\kappa} \tilde{r} \tilde{u} - \sin \psi} d\psi + \int_{-\pi/2}^{\psi_0} \frac{\cos \psi}{\tilde{\kappa} \tilde{r} \tilde{u} - \sin \psi} d\psi \\ &\geq \int_{\psi}^{-\pi/2} \frac{\cos \psi}{\tilde{\kappa} \tilde{r} \tilde{u} - \sin \psi} d\psi \geq \int_{\psi}^{-\pi/2} -\cot(\psi) d\psi \\ &\geq \int_{-\pi+\pi}^{\psi} -\cot(\psi) d\psi. \end{aligned} \quad (3.231)$$

It gives $\tilde{r} \leq \frac{1}{\sin \mu}$.

In summarize, $\tilde{r} \leq \frac{1}{\sin \mu}$ works for all cases. \square

Theorem 21. Fix $0 < \mu < \frac{\pi}{2}$. For $\psi_0, \psi \in [-\pi + \mu, -\mu]$, as $\tilde{\kappa} \rightarrow 0$,

$$|\tilde{e}_1(\psi)| = \mathcal{O}(-\tilde{\kappa} \ln(\tilde{\kappa})), \quad (3.232)$$

$$|\tilde{e}_2(\psi)| = \mathcal{O}(\tilde{\kappa}^{2/3}(-\ln \tilde{\kappa})^{5/3}). \quad (3.233)$$

Therefore,

$$\tilde{r}(\psi) = \frac{\tilde{c}}{\sin \psi} + \mathcal{O}(-\tilde{\kappa} \ln(\tilde{\kappa})), \quad (3.234)$$

$$\tilde{u}(\psi) = \frac{\tilde{c}}{2} \ln(\tilde{\kappa}) + \tilde{c} \ln \left| \tilde{c} \frac{\cos \psi + 1}{\sin \psi} \right| + \tilde{c}(\gamma_e - 2 \ln 2) + \mathcal{O}(\tilde{\kappa}^{2/3}(-\ln \tilde{\kappa})^{5/3}), \quad (3.235)$$

where $\tilde{c} = \sin(\psi_0) = -\sin(\phi_0 + \gamma)$. Moreover, when (3.234) is applied to (3.235), we obtain the asymptotic expansion of $\tilde{u}(\tilde{r})$, which has the same form as which in the graph case, see (3.217).

Proof. Suppose $\psi_0, \psi \in [-\pi + \mu, -\mu]$ for some $0 < \mu < \frac{\pi}{2}$. Previous Lemma gives

$$\tilde{r}\tilde{r}_1 \leq \frac{1}{\sin^2 \mu}. \quad (3.236)$$

Consider

$$\begin{aligned} \frac{d\tilde{r}}{d\psi} - \frac{d\tilde{r}_1}{d\psi} &= \frac{\cos \psi}{\tilde{\kappa}\tilde{u} - \frac{\sin \psi}{\tilde{r}}} - (-\tilde{r}_1 \cot \psi) \\ &= \cos(\psi) \frac{-\sin(\psi) \left(\frac{1}{\tilde{r}_1} - \frac{1}{\tilde{r}} \right) - \tilde{\kappa}\tilde{u}}{\left(\tilde{\kappa}\tilde{u} - \frac{\sin \psi}{\tilde{r}} \right) \left(-\frac{\sin \psi}{\tilde{r}_1} \right)}. \end{aligned} \quad (3.237)$$

Integrating from ψ_0 to ψ ,

$$\tilde{r}(\psi) - \tilde{r}_1(\psi) = \int_{\psi_0}^{\psi} \cos(s) \frac{-\sin(s) \left(\frac{1}{\tilde{r}_1} - \frac{1}{\tilde{r}} \right) - \tilde{\kappa}\tilde{u}}{\left(\tilde{\kappa}\tilde{u} - \frac{\sin(s)}{\tilde{r}} \right) \left(-\frac{\sin(s)}{\tilde{r}_1} \right)} ds. \quad (3.238)$$

With (3.222) and (3.226), (3.238) gives

$$\begin{aligned} |\tilde{e}_1(\psi)| &\leq \left| \int_{\psi_0}^{\psi} \frac{\sin(s) \left(\frac{1}{\tilde{r}_1} - \frac{1}{\tilde{r}} \right) + 2\sqrt{\tilde{\kappa}}}{\left(-\frac{\sin(s)}{\tilde{r}} \right) \left(-\frac{\sin(s)}{\tilde{r}_1} \right)} ds \right| \\ &\leq \left| \int_{\psi_0}^{\psi} \left| \frac{\tilde{e}_1(s)}{\sin(s)} \right| + 2\sqrt{\tilde{\kappa}} \frac{\tilde{r}\tilde{r}_1}{\sin^2(s)} ds \right| \\ &\leq \frac{2\pi}{\sin^4(\mu)} \sqrt{\tilde{\kappa}} + \frac{1}{\sin(\mu)} \left| \int_{\psi_0}^{\psi} |\tilde{e}_1(s)| ds \right|, \end{aligned} \quad (3.239)$$

where $\tilde{r}\tilde{r}_1 \leq \frac{1}{\sin^2(\mu)}$. Applying Gronwall's inequality,

$$|\tilde{e}_1(\psi)| \leq \frac{2\pi}{\sin^4(\mu)} \sqrt{\tilde{\kappa}} \exp\left(\frac{|\psi - \psi_0|}{\sin(\mu)}\right). \quad (3.240)$$

Hence, there exists some constant $C_1 > 0$ such that

$$|\tilde{e}_1(\psi)| \leq C_1 \sqrt{\tilde{\kappa}} \Leftrightarrow \tilde{e}_1(\psi) = \mathcal{O}\left(\sqrt{\tilde{\kappa}}\right). \quad (3.241)$$

Thus,

$$\tilde{r}(\psi) = \tilde{r}_1(\psi) + \mathcal{O}\left(\sqrt{\tilde{\kappa}}\right). \quad (3.242)$$

For $|\tilde{e}_2|$, consider

$$\begin{aligned} \frac{d\tilde{u}}{d\psi} - \frac{d\tilde{u}_1}{d\psi} &= \frac{\sin \psi}{\tilde{\kappa}\tilde{u} - \frac{\sin \psi}{\tilde{r}}} - (-\tilde{r}_1) \\ &= \sin(\psi) \frac{-\sin(\psi) \left(\frac{1}{\tilde{r}_1} - \frac{1}{\tilde{r}}\right) - \tilde{\kappa}\tilde{u}}{\left(\tilde{\kappa}\tilde{u} - \frac{\sin \psi}{\tilde{r}}\right) \left(-\frac{\sin \psi}{\tilde{r}_1}\right)}. \end{aligned} \quad (3.243)$$

Integrating ψ to $-\frac{\pi}{2}$,

$$\left(\tilde{u}\left(-\frac{\pi}{2}\right) - \tilde{u}_1\left(-\frac{\pi}{2}\right)\right) - (\tilde{u}(\psi) - \tilde{u}_1(\psi)) = \int_{\psi}^{-\frac{\pi}{2}} \sin(s) \frac{-\sin(s) \left(\frac{1}{\tilde{r}_1} - \frac{1}{\tilde{r}}\right) - \tilde{\kappa}\tilde{u}}{\left(\tilde{\kappa}\tilde{u} - \frac{\sin(s)}{\tilde{r}}\right) \left(-\frac{\sin(s)}{\tilde{r}_1}\right)} ds. \quad (3.244)$$

$\tilde{u}_1\left(-\frac{\pi}{2}\right)$ is chosen such that it is equal to the asymptotic expansion of $\tilde{u}(\psi)$ at $\psi = -\frac{\pi}{2}$ as $\tilde{\kappa} \rightarrow 0$, where $\tilde{u}\left(-\frac{\pi}{2}\right)$ can be understood using its asymptotic form in the graph case with

appropriate initial data. Recall from (3.242), $\tilde{r}\left(-\frac{\pi}{2}\right) = -\tilde{c} + \mathcal{O}(\sqrt{\tilde{\kappa}})$, where $\tilde{c} = \sin(\psi_0)$. Consider $l_c = \tilde{r}\left(-\frac{\pi}{2}\right)$. Let $\tilde{u} = \tilde{u}/l_c$ and $\tilde{r} = \tilde{r}/l_c$, it is analogue to (3.217), the asymptotic expansion of $\tilde{u}(\tilde{r})$ at $\tilde{r} = 1$ with the inclination angle $-\frac{\pi}{2}$,

$$\tilde{u}(1) = \frac{\tilde{c}}{2} \ln(\tilde{\kappa}) + \tilde{c} \ln\left(\tilde{r} + \sqrt{\tilde{r}^2 - \tilde{c}^2}\right) + \tilde{c}(\gamma_e - 2 \ln 2) + \mathcal{O}\left(\tilde{\kappa}^{2/3}(-\ln \tilde{\kappa})^{5/3}\right), \quad (3.245)$$

where $\tilde{c} = \sin\left(-\frac{\pi}{2}\right) = -1$ and $\tilde{\kappa} = \tilde{\kappa}l_c^2$.

Hence,

$$\begin{aligned} \tilde{u}\left(-\frac{\pi}{2}\right) &= l_c \tilde{u}(1) \\ &= \frac{\tilde{c}}{2} \ln(\tilde{\kappa}) + \tilde{c} \ln|\tilde{c}| + \tilde{c}(\gamma_e - 2 \ln 2) + \mathcal{O}\left(\tilde{c}^2 \tilde{\kappa}^{2/3}(-\ln \tilde{\kappa})^{5/3}\right). \end{aligned} \quad (3.246)$$

With $\tilde{u}_1(\psi) = \tilde{c} \ln\left|\frac{\cos \psi + 1}{\sin \psi}\right| + \tilde{d}$, we have

$$\tilde{d} = \frac{\tilde{c}}{2} \ln(\tilde{\kappa}) + \tilde{c} \ln|\tilde{c}| + \tilde{c}(\gamma_e - 2 \ln 2) + \mathcal{O}\left(\tilde{c}^2 \tilde{\kappa}^{2/3}(-\ln \tilde{\kappa})^{5/3}\right). \quad (3.247)$$

With bounds of \tilde{r} and \tilde{u} , (3.244) implies

$$\begin{aligned} |\tilde{e}_2(\psi)| &\leq \left| \int_{\psi}^{-\frac{\pi}{2}} |\tilde{e}_1(s)| ds \right| + \left| \int_{\psi}^{-\frac{\pi}{2}} 2\sqrt{\tilde{\kappa}} \frac{\tilde{r}\tilde{r}_1}{|\sin(s)|} ds \right| \\ &\leq \frac{\pi\sqrt{\tilde{\kappa}}}{\sin^3 \mu} + \left| \int_{\psi}^{-\frac{\pi}{2}} |\tilde{e}_1(s)| ds \right|. \end{aligned} \quad (3.248)$$

Hence, there exists some constant $C_2 > 0$ such that

$$|\tilde{e}_2(\psi)| \leq C_2 \sqrt{\tilde{\kappa}} \Leftrightarrow \tilde{e}_2(\psi) = \mathcal{O}\left(\sqrt{\tilde{\kappa}}\right). \quad (3.249)$$

Thus,

$$\tilde{u}(\psi) = \tilde{u}_1(\psi) + \mathcal{O}\left(\sqrt{\tilde{\kappa}}\right), \quad (3.250)$$

where

$$\tilde{u}_1(\psi) = \frac{\tilde{c}}{2} \ln(\tilde{\kappa}) + \tilde{c} \ln \left| \tilde{c} \frac{\cos \psi + 1}{\sin \psi} \right| + \tilde{c}(\gamma_e - 2 \ln 2) + \mathcal{O}\left(\tilde{c}^2 \tilde{\kappa}^{2/3} (-\ln \tilde{\kappa})^{5/3}\right), \quad (3.251)$$

where we obtain a more careful bound containing \tilde{c} , which can be loosened to $\mathcal{O}\left(\tilde{\kappa}^{2/3} (-\ln \tilde{\kappa})^{5/3}\right)$. Therefore, \tilde{e}_2 can be modified to $\mathcal{O}\left(\tilde{\kappa}^{2/3} (-\ln \tilde{\kappa})^{5/3}\right)$.

Hence, $\tilde{u}(\psi) = \mathcal{O}(-\ln(\tilde{\kappa}))$. Therefore, replacing $\tilde{\kappa}\tilde{u} \leq 2\sqrt{\tilde{\kappa}}$ by $\tilde{\kappa}\tilde{u} \leq -C_3\tilde{\kappa} \ln(\tilde{\kappa})$ for some $C_3 > 0$, $\tilde{e}_1(\psi)$ can be modified to $\mathcal{O}(-\tilde{\kappa} \ln(\tilde{\kappa}))$.

Therefore,

$$\begin{aligned} \tilde{r}(\psi) &= \frac{\tilde{c}}{\sin \psi} + \mathcal{O}(-\tilde{\kappa} \ln(\tilde{\kappa})), \\ \tilde{u}(\psi) &= \frac{\tilde{c}}{2} \ln(\tilde{\kappa}) + \tilde{c} \ln \left| \tilde{c} \frac{\cos \psi + 1}{\sin \psi} \right| + \tilde{c}(\gamma_e - 2 \ln 2) + \mathcal{O}\left(\tilde{\kappa}^{2/3} (-\ln \tilde{\kappa})^{5/3}\right). \end{aligned}$$

From the expansion of $\tilde{r}(\psi)$, we have $\frac{\tilde{c}}{\sin \psi} = \tilde{r}(\psi) + \mathcal{O}(-\tilde{\kappa} \ln(\tilde{\kappa}))$. Hence, $\ln \left| \tilde{c} \frac{\cos \psi + 1}{\sin \psi} \right| = \ln(\tilde{r} + \sqrt{\tilde{r}^2 - \tilde{c}^2}) + \mathcal{O}(-\tilde{\kappa} \ln(\tilde{\kappa}))$. Then, $\tilde{u}(\psi)$ can be converted back into $\tilde{u}(\tilde{r})$,

$$\tilde{u}(\tilde{r}) = \frac{\tilde{c}}{2} \ln(\tilde{\kappa}) + \tilde{c} \ln \left(\tilde{r} + \sqrt{\tilde{r}^2 - \tilde{c}^2} \right) + \tilde{c}(\gamma_e - 2 \ln 2) + \mathcal{O}\left(\tilde{\kappa}^{2/3} (-\ln \tilde{\kappa})^{5/3}\right),$$

which has the same form as which in the graph case, see (3.217). □

Remark 21. In Theorem 21, we exclude two extreme cases: 1) $\gamma = 0$ and $\phi_0 \rightarrow 0$ and 2) $\gamma = \pi$ and $\phi_0 \rightarrow \pi$, since both extreme cases imply $\psi_0 \rightarrow -\pi$ or π , which invalidates the bound estimates. However, the asymptotic expansion of $\tilde{u}(\psi)$ performs well in those extreme cases, see Fig. 3.14a and Fig. 3.14b in Sec. 3.8.3.

We rescale \tilde{r} and \tilde{u} to \hat{r} and \hat{u} , as $B \rightarrow 0$,

$$\hat{r}(\psi) = \frac{\hat{c}}{\sin \psi} + \mathcal{O}(\Delta_2), \quad (3.252)$$

$$\hat{u}(\psi) = \frac{\hat{c}}{2} \ln(B) + \hat{c} \ln \left| \hat{c} \frac{\cos \psi + 1}{\sin \psi} \right| + \hat{c}(\gamma_e - 2 \ln 2) + \mathcal{O}(\Delta_1), \quad (3.253)$$

$$\Delta_1 = (B \sin^2 \phi_0)^{2/3} (-\ln(B \sin^2 \phi_0))^{5/3}, \quad (3.254)$$

$$\Delta_2 = B \sin^2(\phi_0) (-\ln(B \sin^2(\phi_0))) \quad (3.255)$$

for ψ being away from 0 and $\hat{c} = -\sin(\phi_0 + \gamma) \sin(\phi_0)$.

Remark 22. More precisely, the error bound of the asymptotic expansion of \hat{u} has the form $\mathcal{O}(\hat{c}\Delta_1)$ in both graph and non-graph cases.

When $\psi < 0$, if $-\frac{\pi}{2} \leq \psi_0 \leq 0$, then (3.218) implies

$$\hat{u}_0 = \hat{u}(\hat{r}_0) = \frac{\hat{c}}{2} \ln(B) + \hat{c} \ln \left(\hat{r}_0 + \sqrt{\hat{r}_0^2 - \hat{c}^2} \right) + \hat{c}(\gamma_e - 2 \ln 2) + \mathcal{O}(\Delta_1). \quad (3.256)$$

Moreover, if $\psi_0 = 0$, then $\mathcal{O}(\Delta_1) = 0$ exactly.

If $-\pi + \mu \leq \psi_0 \leq -\frac{\pi}{2}$ for some $0 < \mu < \frac{\pi}{2}$, then (3.253) gives

$$\hat{u}_0 = \hat{u}(\psi_0) = \frac{\hat{c}}{2} \ln(B) + \hat{c}(\gamma_e - 2 \ln 2) + \hat{c} \ln [\sin \phi_0 (1 - \cos(\phi_0 + \gamma))] + \mathcal{O}(\Delta_1). \quad (3.257)$$

It can be verified that (3.256) and (3.257) have the same asymptotic expansion with error bound $\mathcal{O}(\Delta_1)$. Therefore, we obtain the asymptotic expansion of \hat{u}_0 as $B \rightarrow 0$,

$$\hat{u}_0 = \frac{\hat{c}}{2} \ln(B) + \hat{c}(\gamma_e - 2 \ln 2) + \hat{c} \ln [\sin \phi_0 (1 - \cos(\phi_0 + \gamma))] + \mathcal{O}(\Delta_1). \quad (3.258)$$

The following Fig. 3.11 gives an example of the comparison between the numerical result and the asymptotic expansion with a small Bond number when the fluid interface is not a graph. We can see that the asymptotic expansions in (3.252) and (3.253) perform well in the case $\gamma = \frac{\pi}{8}$, $\phi_0 = \frac{\pi}{8}$ and $B = 0.01$.

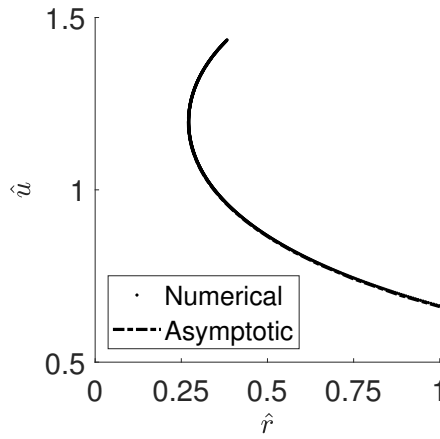


Figure 3.11: A comparison between the numerical result and the asymptotic expansion with data $\gamma = \frac{\pi}{8}$, $\phi_0 = \frac{\pi}{8}$ and $B = 0.01$.

3.8.2 Behavior of $\hat{h}(\phi_0)$ and $\hat{F}_T(\phi_0)$ As $B \rightarrow 0$

Recall the center of the height equation and rewrite the total force equation as follows,

$$\hat{F}_T(\phi_0) = \hat{F}_1(\phi_0) - \frac{2}{B} \sin(\phi_0 + \gamma) \sin \phi_0 - \sin^2(\phi_0) \hat{u}_0, \quad (3.259)$$

$$\hat{h}(\phi_0) = \cos(\phi_0) + \hat{u}_0, \quad (3.260)$$

where

$$\hat{F}_1(\phi_0) = -\frac{4}{3}\alpha - \cos \phi_0 + \frac{2}{3} + \frac{1}{3} \cos^3(\phi_0),$$

which is known as Archimedes' total force, see McCuan and Treinen [43]. Recall from (3.258),

$$\hat{u}_0 = \frac{\hat{c}}{2} \ln(B) + \hat{c}(\gamma_e - 2 \ln 2) + \hat{c} \ln [\sin \phi_0 (1 - \cos(\phi_0 + \gamma))] + \mathcal{O}(\Delta_1), \quad (3.261)$$

where $\hat{c} = -\sin \phi_0 \sin(\phi_0 + \gamma)$ and Δ_1 is defined in (3.254), as $B \rightarrow 0$.

Suppose $\gamma \in (0, \pi)$ and $\phi_0 \in (0, \pi)$. Hence, as $B \rightarrow 0$, with (3.261), we have,

$$\begin{aligned} \hat{h}(\phi_0) &= \frac{\hat{c}}{2} \ln(B) + \cos(\phi_0) + \hat{c}(\gamma_e - 2 \ln 2) + \hat{c} \ln [\sin \phi_0 (1 - \cos(\phi_0 + \gamma))] \\ &\quad + \mathcal{O}(\Delta_1), \end{aligned} \quad (3.262)$$

$$\begin{aligned} \hat{F}_T(\phi_0) &= -\frac{2}{B} \sin(\phi_0 + \gamma) \sin(\phi_0) - \sin^2(\phi_0) \frac{\hat{c}}{2} \ln(B) + \hat{F}_1(\phi_0) \\ &\quad - \sin^2(\phi_0) [\hat{c}(\gamma_e - 2 \ln 2) + \hat{c} \ln [\sin \phi_0 (1 - \cos(\phi_0 + \gamma))]] + \mathcal{O}(\Delta_1), \end{aligned} \quad (3.263)$$

where Δ_1 is defined in (3.254).

The following Fig. 3.12a and Fig. 3.12b compare the numerical results and the asymptotic expansions of $\hat{h}(\phi_0)$ and $\hat{F}_T(\phi_0)$ in (3.262) and (3.263), respectively. We can see that they are indistinguishable with $B = 0.01$ and $\gamma = \frac{\pi}{3}$, thus, the asymptotic expansions perform

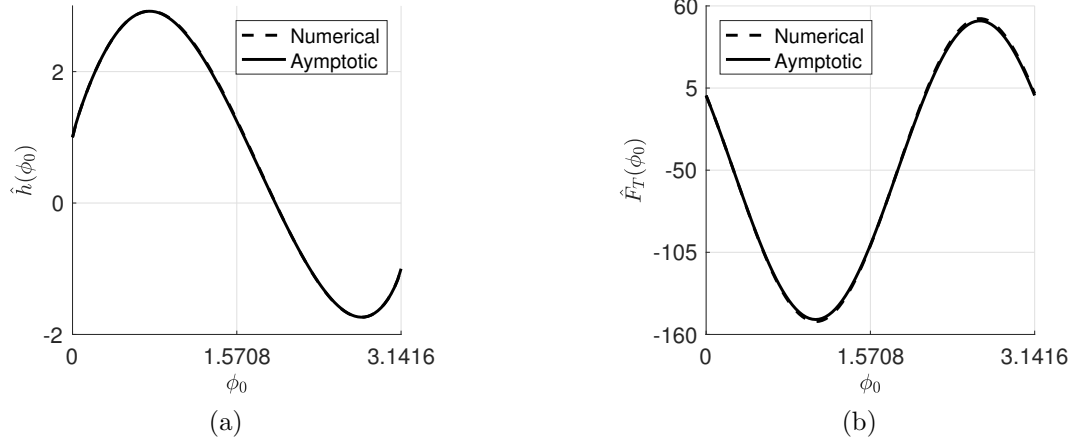


Figure 3.12: (a) The comparison between the numerical solution and the asymptotic expansion of $\hat{h}(\phi_0)$ with $B = 0.01$, $\gamma = \frac{\pi}{3}$; (b) the comparison between the numerical solution and the asymptotic expansion of $\hat{F}_T(\phi_0)$ with the same data and $\alpha = 0$.

well. The comparison in the $\gamma = 0$ and $\gamma = \pi$ cases can be seen in Fig. 3.26a, Fig. 3.26b, Fig. 3.27a and Fig. 3.27b in Sec. 3.8.5.

From (3.263),

$$\begin{aligned} \hat{F}_T(\phi_0) = & -\sin(\phi_0)\sin(\phi_0 + \gamma) \left(\frac{2}{B} - \frac{\sin^2(\phi_0)}{2} \ln B - \sin^2(\phi_0)(\gamma_e - 2 \ln 2) \right. \\ & \left. - \sin^2(\phi_0) \ln[\sin(\phi_0)(1 - \cos(\phi_0 + \gamma))] \right) + \hat{F}_1(\phi_0) + \mathcal{O}(\Delta_1), \end{aligned} \quad (3.264)$$

where $\hat{F}_1 = \mathcal{O}(1)$ for $0 < \alpha \leq \alpha_0$ with $\alpha_0 > 0$. We consider $\hat{F}_T(\phi_0) = 0$ and write it in terms of ψ_0 . So,

$$-\sin(\psi_0)\sin(\psi_0 - \gamma) = \mathcal{O}(B). \quad (3.265)$$

Let $G(\psi_0) = -\sin(\psi_0)\sin(\psi_0 - \gamma)$. We have $G(0) = 0$ and $G'(0) = \sin(\gamma) > 0$. Therefore,

$$\bar{\psi}_0 = G^{-1}(\mathcal{O}(B)) = 0 + \mathcal{O}(B). \quad (3.266)$$

Hence, we obtain a force balanced point

$$\bar{\phi}_0 = \pi - \gamma + \mathcal{O}(B). \quad (3.267)$$

To investigate the behavior of $\hat{h}'(\phi_0)$ and $\hat{F}'(\phi_0)$, we have to understand the behavior of $\frac{d\hat{u}_0}{d\phi_0}$. Assume we can differentiate the asymptotic expansion of \hat{u}_0 , then

$$\begin{aligned} \frac{d\hat{u}_0}{d\phi_0} \approx & -\frac{\sin(2\phi_0 + \gamma)}{2} \ln(B) - \sin(2\phi_0 + \gamma) \ln[\sin(\phi_0)(1 - \cos(\phi_0 + \gamma))] \\ & - \sin(2\phi_0 + \gamma)(\gamma_e - 2 \ln 2) - \frac{\sin(\phi_0 + \gamma)(\cos \phi_0 - \cos(2\phi_0 + \gamma))}{1 - \cos(\phi_0 + \gamma)}. \end{aligned} \quad (3.268)$$

As we can see, $\frac{d\hat{u}_0}{d\phi_0}$ tends to infinity as $\phi_0 \rightarrow 0, \pi$, see Sec. 3.8.3 for more discussion of the asymptotic behavior of \hat{u}_0 and $\frac{d\hat{u}_0}{d\phi_0}$ as $\phi_0 \rightarrow 0, \pi$. The singularity does not appear in the leading order term of $\frac{d\hat{u}_0}{d\phi_0}$, it comes from the $\mathcal{O}(1)$ term instead. “ \approx ” is used in (3.268) since we do not have enough information to determine the error bound of $\frac{d\hat{u}_0}{d\phi_0}$. Fig. 3.13 illustrates the comparison between the numerical results and the asymptotic expansion of $\frac{d\hat{u}_0}{d\phi_0}$, they are indistinguishable. The details of the numerical differentiation of \hat{u}_0 can be seen in Appendix B.2.

Fortunately, we can determine signs of \hat{F}'_T and \hat{h}' at $\bar{\phi}_0$ (or $\bar{\psi}_0$) without assuming the differentiability of \hat{u}_0 with respect to ϕ_0 . From Siegel [56], the (scaled) attachment height \bar{u}_0 is understood as a function with two variables \bar{r}_0 and ψ_0 , see as follows,

$$\bar{u}_0 = \bar{u}(\bar{r}_0; \bar{r}_0, \psi_0) = \bar{u}(\bar{r}_0, \psi_0), \quad (3.269)$$

where \bar{r}_0 and ψ_0 are considered as the initial radial distance and the corresponding inclination angle. $\bar{u}(\bar{r}_0; \bar{r}_0, \psi_0)$ is an odd function in ψ_0 , that is, $\bar{u}(\bar{r}_0, \psi_0) = -\bar{u}(\bar{r}_0, -\psi_0)$. Recall the slope function from Vogel [63],

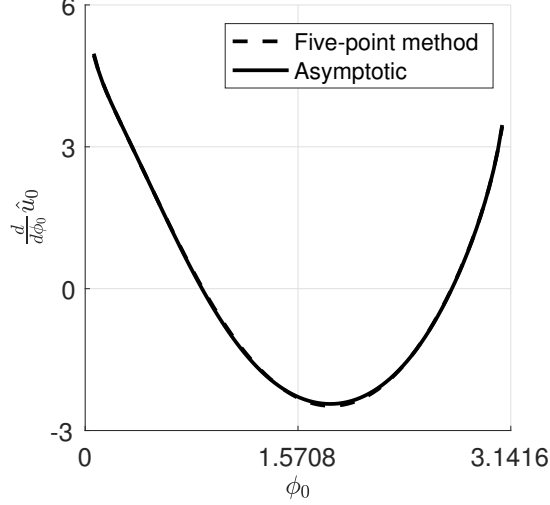


Figure 3.13: The comparison between the numerical solution by the five-point method and the asymptotic expansion of $\frac{d\hat{u}_0}{d\phi_0}$ with $B = 0.01$ and $\gamma = \frac{\pi}{3}$.

$$p(\bar{r}_0; \bar{u}_0) = \tan(\psi_0). \quad (3.270)$$

We differentiate the slope function with respect to ψ_0 , then

$$p_u(\bar{r}_0; \bar{u}_0) \frac{\partial \bar{u}_0}{\partial \psi_0} = \sec^2(\psi_0), \quad (3.271)$$

From (3.62), $p_u \geq -\omega$, where ω satisfies the condition in Lemma 15. Recall that,

$$\omega^2 - \left(\frac{1}{r_w} + \frac{d_2}{d_1} \right) \omega - \frac{1}{d_1} > 0, \quad (3.272)$$

where $d_1, d_2 > 0$ satisfy the inequalities in Lemma 14 and $r_w = \bar{r}_0$ in this case.

To find the asymptotics of ω at the force balanced point $\bar{\phi}_0$, we first obtain bounds on $w(\bar{r}; \bar{r}_0, \bar{u}_0)$, $w'(\bar{r}; \bar{r}_0, \bar{u}_0)$ and $w''(\bar{r}; \bar{r}_0, \bar{u}_0)$. Suppose $\bar{\psi}_0 \in [-\mu_0, \mu_0]$ with $\mu_0 = cB$ for some $c > 0$. Consider $\psi_0 < 0$ (the $\psi_0 \geq 0$ case is similar). By the comparison principle,

$$w \leq \frac{\bar{u}_0}{K_0(\bar{r}_0)} K_0(\bar{r}), \quad (3.273)$$

where the equality holds at $\bar{r} = \bar{r}_0$. So,

$$w'(\bar{r}_0; \bar{r}_0, \bar{u}_0) \leq -\bar{u}_0 \frac{K_1(\bar{r}_0)}{K_0(\bar{r}_0)}. \quad (3.274)$$

The capillary equation gives

$$(\bar{r} \sin \psi)_{\bar{r}} = \bar{r} w \leq \frac{\bar{u}_0}{K_0(\bar{r}_0)} \bar{r} K_0(\bar{r}). \quad (3.275)$$

Integrating from \bar{r} to infinity, we obtain

$$\sin \psi \geq -\frac{\bar{u}_0}{K_0(\bar{r}_0)} K_1(\bar{r}) = b(\bar{r}; \bar{r}_0, \bar{u}_0). \quad (3.276)$$

This implies

$$w' = \tan \psi \geq \frac{b(\bar{r}; \bar{r}_0, \bar{u}_0)}{\sqrt{1 - b^2(\bar{r}; \bar{r}_0, \bar{u}_0)}}. \quad (3.277)$$

At $\bar{r} = \bar{r}_0$,

$$w'(\bar{r}_0; \bar{r}_0, \bar{u}_0) \geq \frac{b(\bar{r}_0)}{\sqrt{1 - b^2(\bar{r}_0)}}. \quad (3.278)$$

From capillary equation of w ,

$$w'' = (1 + w'^2)^{3/2} \left[w - \frac{1}{\bar{r}} \frac{w'}{\sqrt{1 + w'^2}} \right]. \quad (3.279)$$

As $B \rightarrow 0$, at $\phi_0 = \bar{\phi}_0$ (say the corresponding $\psi_0 = \bar{\psi}_0$), from (3.263),

$$\bar{r}_0 = \sqrt{B} \sin \bar{\phi}_0 \quad \text{and} \quad \bar{u}_0 = \mathcal{O}(B^{3/2} \ln B). \quad (3.280)$$

So, $b(\bar{r}_0) = \mathcal{O}(B)$. From (3.278) and (3.279), we have $w'(\bar{r}_0, \bar{r}_0, \bar{u}_0) = \mathcal{O}(B)$ and $w''(\bar{r}_0, \bar{r}_0, \bar{u}_0) = \mathcal{O}(\sqrt{B})$. These gives $q(\bar{r}_0) = 1 - \mathcal{O}(B^2)$, which is defined in (3.66) and $q' = \mathcal{O}(B^{3/2})$. Since $d_1 \leq q$ and $q' \leq d_2$, we take arbitrary $d_1 < 1$ and $d_2 > 0$. Thus, we may take $\omega = \frac{2}{\bar{r}_0}$ satisfying (3.272). Hence, for B sufficiently small,

$$-\frac{2}{\bar{r}_0} < p_u. \quad (3.281)$$

Hence, at $\bar{\psi}_0$,

$$\frac{\partial \bar{u}_0}{\partial \psi_0} = \frac{\sec^2(\bar{\psi}_0)}{p_u(\bar{r}_0, \bar{u}_0)} \leq -\frac{\bar{r}_0 \sec^2(\bar{\psi}_0)}{2}. \quad (3.282)$$

For $\bar{\psi}_0 \in [-\mu_0, \mu_0]$ for some $0 < \mu_0 < \frac{\pi}{2}$, we have

$$\bar{u}(\bar{r}_0, \mu_0) \leq \bar{u}(\bar{r}_0, \bar{\psi}_0) \leq \bar{u}(\bar{r}_0, -\mu_0). \quad (3.283)$$

From Lemma 3.7 in Vogel [63],

$$\left| \frac{\partial \bar{u}_0}{\partial \bar{r}_0} \right| \leq \left| \frac{\bar{u}(\bar{r}_0, \bar{\psi}_0)}{\bar{r}_0} \right| \leq \frac{\bar{u}(\bar{r}_0, -\mu_0)}{\bar{r}_0}. \quad (3.284)$$

Hence, $\frac{\partial \bar{u}_0}{\partial \bar{r}_0} = \mathcal{O}(B \ln B)$. Therefore,

$$\begin{aligned} \frac{d}{d\phi_0} \bar{u}_0(\bar{r}_0, \bar{\psi}_0) &= \frac{\partial \bar{u}_0}{\partial \bar{r}_0} \sqrt{B} \cos \bar{\phi}_0 + \frac{\partial \bar{u}_0}{\partial \psi_0} \\ &\leq -\frac{\bar{r}_0 \sec^2(\bar{\psi}_0)}{2} + \mathcal{O}(B^{3/2} \ln B). \end{aligned} \quad (3.285)$$

Thus, $\frac{d}{d\phi_0} \bar{u}_0(\bar{r}_0, \bar{\psi}_0) < 0$ and

$$\frac{d}{d\phi_0} \hat{u}_0(\bar{r}_0, \bar{\psi}_0) \leq -\frac{1}{2\sqrt{B}} + \mathcal{O}(B \ln B). \quad (3.286)$$

Recall \hat{F}'_T in (3.208) and \hat{h}' ,

$$\begin{aligned}\hat{F}'_T(\phi_0) &= -\frac{2}{B} \sin(2\phi_0 + \gamma) + \sin^3(\phi_0) - 2 \sin(\phi_0) \cos(\phi_0) \hat{u}_0 - \sin^2(\phi_0) \frac{d\hat{u}_0}{d\phi_0}, \\ \hat{h}'(\phi_0) &= -\sin \phi_0 + \frac{d\hat{u}_0}{d\phi_0}.\end{aligned}$$

At $\bar{\phi}_0$, as $B \rightarrow 0$,

$$\hat{F}'_T(\bar{\phi}_0) > 0 \quad \text{and} \quad \hat{h}'(\bar{\phi}_0) < 0. \quad (3.287)$$

Hence, $\bar{\phi}_0$ is stable. In detail, with fixed $0 < \alpha \leq \alpha_0$ with $\alpha_0 > 0$, for $\bar{\psi}_0 \in [-\mu_0, \mu_0]$ with $\mu_0 = cB$ for some large enough $c > 0$ (c is chosen such that $\hat{F}_T(\phi_0) < 0$ on $[\mu_0, \pi - \gamma - \mu_0]$ and $\hat{F}_T(\phi_0) > 0$ on $[\pi - \gamma + \mu_0, \pi - \mu_0]$), then $\hat{F}'_T(\phi_0) > 0$ for $\phi_0 \in (\pi - \gamma - \mu_0, \pi - \gamma + \mu_0)$. For $\alpha > 1$, $\hat{F}_T(\pi) < 0$ and $\hat{F}_T(\pi - \mu_0) > 0$. Thus, there is a second equilibrium $\bar{\phi}_{02} \in (\pi - \mu_0, \pi)$. Moreover, $\bar{\phi}_{02} = \pi + \mathcal{O}(B)$ as $B \rightarrow 0$. We summarize the result in the following Theorem 22.

Theorem 22. *With $\gamma \in (0, \pi)$ and fixed $0 < \alpha \leq \alpha_0$ with $\alpha_0 > 0$, consider $\phi_0 \in [\mu_0, \pi - \mu_0]$ with $\mu_0 = cB$ for some large enough $c > 0$, as $B \rightarrow 0$, there exists a unique force balanced point*

$$\bar{\phi}_0 = \pi - \gamma + \mathcal{O}(B), \quad (3.288)$$

where the fluid interface becomes flat. And it is stable. For $\alpha > 1$, there is a second equilibrium $\bar{\phi}_{02} \in (\pi - \mu_0, \pi)$ for B sufficiently small. Moreover, $\bar{\phi}_{02} = \pi + \mathcal{O}(B)$ as $B \rightarrow 0$.

Remark 23. For $\alpha > 1$, we have two equilibria $\bar{\phi}_0$ and $\bar{\phi}_{02}$, with $\bar{\phi}_0 = \pi - \gamma + \mathcal{O}(B)$ and $\bar{\phi}_{02} = \pi + \mathcal{O}(B)$ as $B \rightarrow 0$. This could be a guide for some experiment to see two stable equilibria.

3.8.3 Behavior of $\hat{h}(\phi_0)$ and $\hat{F}_T(\phi_0)$ as $\phi_0 \rightarrow 0$ or π

In this section, we explore the behavior of $\hat{h}(\phi_0)$ and $\hat{F}_T(\phi_0)$ as $\phi_0 \rightarrow 0$ or π . We note that $\tilde{\kappa} \rightarrow 0$ as $\phi_0 \rightarrow 0$ or π . The problem can be fitted to the asymptotic expansion of $\tilde{u}(\psi)$ as $\tilde{\kappa} \rightarrow 0$, see Sec. 3.8.1. Therefore, as $\phi_0 \rightarrow 0$ or π , the asymptotic expansion of \hat{u} is the same as that in (3.218) (the graph case) or (3.253) (the parametric form). We obtain

$$\hat{u}_0 = \hat{c} \ln(\sin \phi_0) + \frac{\hat{c}}{2} \ln(B) + \hat{c}(\gamma_e - 2 \ln 2) + \hat{c} \ln(1 - \cos(\phi_0 + \gamma)) + \mathcal{O}(\Delta_1), \quad (3.289)$$

where $\hat{c} = -\sin \phi_0 \sin(\phi_0 + \gamma)$ and Δ_1 is defined in (3.254), as $\phi_0 \rightarrow 0, \pi$. However, they have different meaning. In Sec. 3.8.2, we have ϕ_0 fixed and let $B \rightarrow 0$. In this section, we fix the value of B , which is not necessarily small and let $\phi_0 \rightarrow 0, \pi$, instead. In addition, from Remark 21, there are two extreme cases³ invalidating the bound estimate of $\hat{u}(\psi)$. Fortunately, the numerical tests show that the asymptotic expansion of \hat{u}_0 also performs well in those extreme cases, see Fig. 3.14a and Fig. 3.14b.

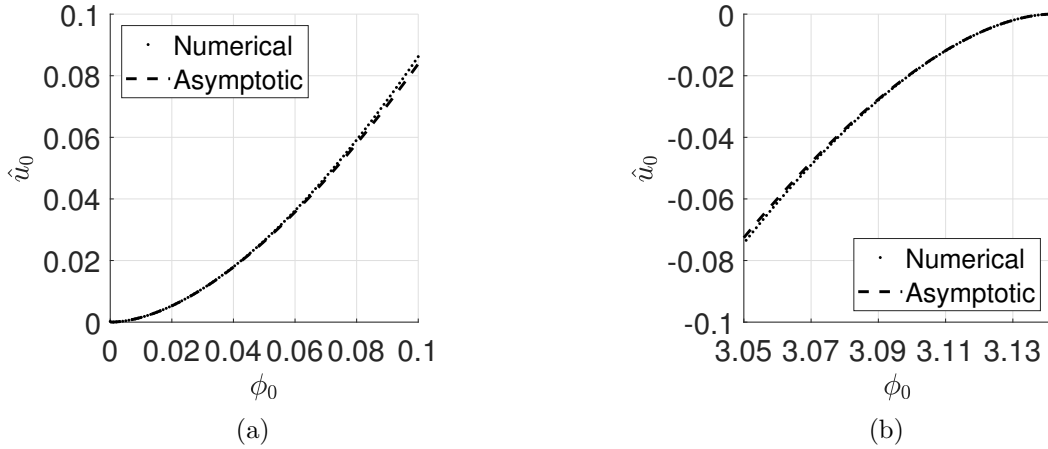


Figure 3.14: (a) The comparison between the asymptotic expansion of \hat{u}_0 and the numerical result near $\phi_0 = 0$ with $\gamma = 0$; (b) the comparison near $\phi_0 = \pi$ with $\gamma = \pi$.

(3.289) helps us extend the continuity of $\hat{F}_T(\phi_0)$ and $\hat{h}(\phi_0)$ to closed interval $[0, \pi]$ for $\gamma \in (0, \pi)$. Let $g(\phi_0) = \sin^2(\phi_0)\hat{u}_0(\phi_0)$, which is a term containing \hat{u}_0 in $\hat{F}_T(\phi_0)$. It suffices to show that $g'(0) = g'(\pi) = 0$. From (3.289),

$$|\hat{u}_0(\phi_0)| \leq C \sin(\phi_0) |\ln(\sin(\phi_0))| \quad (3.290)$$

for some constant C . The RHS $\rightarrow 0$ as $\phi_0 \rightarrow 0, \pi$. So, we may define $\hat{u}_0(0) = \hat{u}_0(\pi) = 0$ and \hat{u}_0 will be continuous at 0 and π . Therefore,

³Two extreme cases are the $\gamma = 0$ and $\phi_0 \rightarrow 0$ case and the $\gamma = \pi$ and $\phi_0 \rightarrow \pi$ case.

$$\hat{h}(0) = 1 \quad \text{and} \quad \hat{h}(\pi) = -1. \quad (3.291)$$

We may also take $g(0) = g(\pi) = 0$ and g will be continuous at 0 and π . Now consider

$$\frac{g(\delta) - g(0)}{\delta} = \frac{g(\delta)}{\delta}. \quad (3.292)$$

We have $\frac{|g(\delta)|}{|\delta|} \leq C \frac{\sin^3 \delta}{\delta} |\ln(\sin(\delta))|$. The RHS $\rightarrow 0$ as $\delta \rightarrow 0$, showing that $g'(0) = 0$. Showing $g'(\pi) = 0$ is done the same way. Therefore,

$$\hat{F}_T(0) = -\frac{4}{3}\alpha < \hat{F}_T(\pi) = -\frac{4}{3}\alpha + \frac{4}{3}, \quad (3.293)$$

$$\hat{F}'_T(0) = \hat{F}'_T(\pi) = -\frac{2}{B} \sin(\gamma), \quad (3.294)$$

where given $\alpha \geq 0$. From $\hat{F}'_T(0) = -b$, $b = \frac{2}{B} \sin \gamma$, we may deduce

$$\frac{\hat{F}_T(\delta) - \hat{F}_T(0)}{\delta} \rightarrow -b \quad (3.295)$$

as $\delta \rightarrow 0$ so that $\hat{F}_T(\delta) - \hat{F}_T(0) = (-b + o(1))\delta$. Thus, $\hat{F}_T(\phi_0) < \hat{F}_T(0)$ on some interval $(0, \mu)$, for some small $\mu > 0$. Similarly, $\hat{F}_T(\phi_0) > \hat{F}_T(\pi)$ on some interval $(\pi - \mu, \pi)$. The above argument proves (i) and (ii) in Property 4.

Moreover, the differentiation of the asymptotic expansion of \hat{u}_0 in (3.268) also explains the different behavior of $\frac{d\hat{u}_0}{d\phi_0}$ with different values of γ as $\phi_0 \rightarrow 0, \pi$. Asymptotically, if $\gamma \in (0, \pi)$,

$$\frac{d\hat{u}_0}{d\phi_0} \approx -\sin(2\phi_0 + \gamma) \ln(\sin(\phi_0)) \rightarrow +\infty, \quad (3.296)$$

see Fig. 3.15a and Fig. 3.15b. If $\gamma = 0$ or $\gamma = \pi$,

$$\frac{d\hat{u}_0}{d\phi_0} \approx -\text{sign}(\cos(\gamma)) \sin(2\phi_0) \ln(\sin(\phi_0)) \rightarrow 0, \quad (3.297)$$

see Fig. 3.16a, Fig. 3.16b, Fig. 3.17a and Fig. 3.17b.

In order to capture the limiting behavior of the numerical results of $\frac{d\hat{u}_0}{d\phi_0}$ near end points, the numerical differentiation with different uniform step sizes are considered, where $\Delta\phi_0 = \frac{\pi}{N}$, $N = 500, 1000$. The following figures, Fig. 3.15a and Fig. 3.15b, show the comparison between the asymptotic expansion of $\frac{d\hat{u}_0}{d\phi_0}$ in (3.268) and the numerical results near $\phi_0 = 0$ and $\phi_0 = \pi$ with $B = 1$ and $\gamma = \frac{\pi}{3}$.

Fig. 3.16a and Fig. 3.16b show the comparison of the extreme case $\gamma = 0$. And Fig. 3.17a and Fig. 3.17b show the comparison of the extreme case $\gamma = \pi$. The performance of the asymptotic expansion in both extreme cases is pretty well.

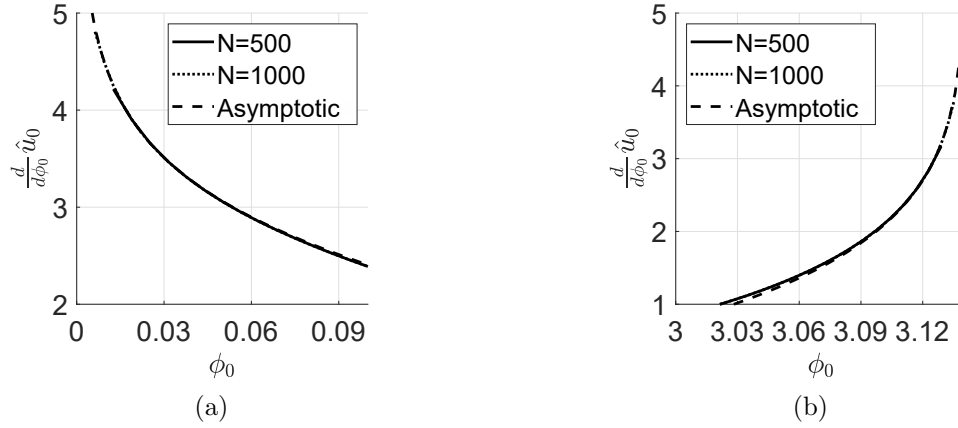


Figure 3.15: (a) The comparison between the asymptotic expansion of $\frac{d\hat{u}_0}{d\phi_0}$ and the numerical results by the five-point method near $\phi_0 = 0$ with $B = 1$, $\gamma = \frac{\pi}{3}$, and uniform step size $\Delta\phi_0 = \frac{\pi}{N}$, $N = 500, 1000$; (b) the comparison near $\phi_0 = \pi$ with the same data.

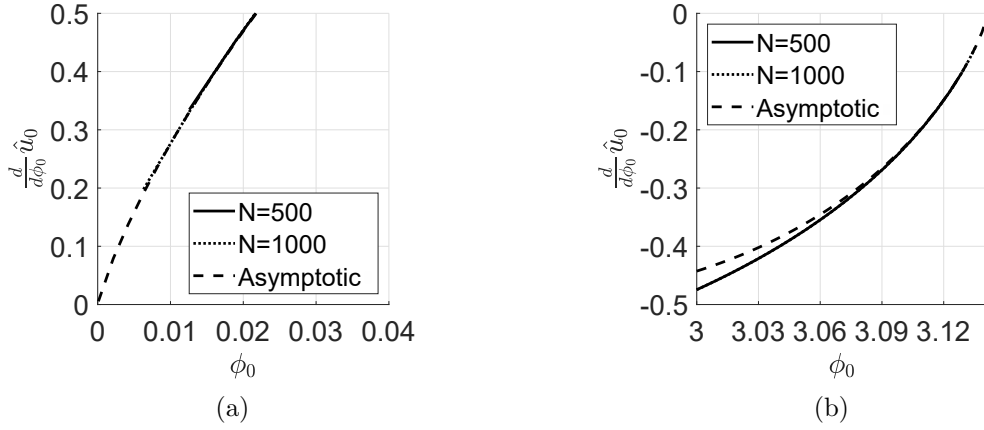


Figure 3.16: (a) The comparison between the asymptotic expansion of $\frac{d\hat{u}_0}{d\phi_0}$ and the numerical results by the five-point method near $\phi_0 = 0$ with $B = 1$, $\gamma = 0$, and uniform step size $\Delta\phi_0 = \frac{\pi}{N}$, $N = 500, 1000$; (b) the comparison near $\phi_0 = \pi$ with the same data.

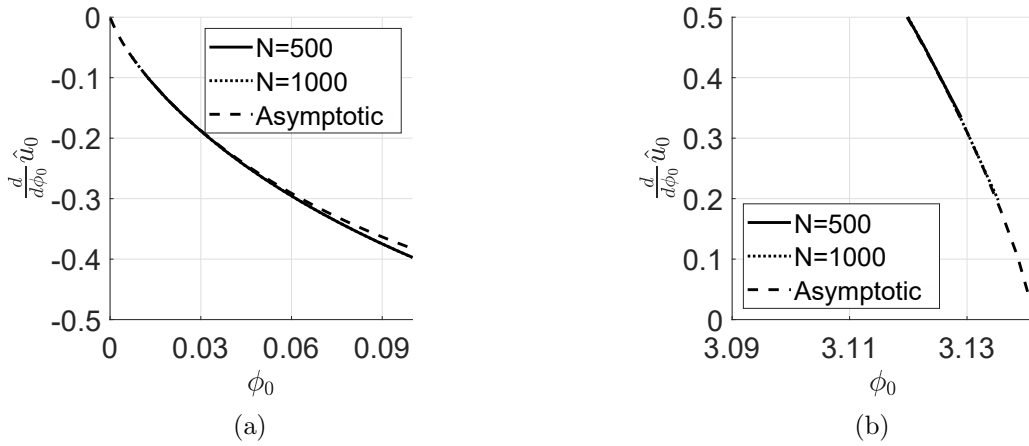


Figure 3.17: (a) The comparison between the asymptotic expansion of $\frac{d\hat{u}_0}{d\phi_0}$ and the numerical results by the five-point method near $\phi_0 = 0$ with $B = 1$, $\gamma = \pi$, and uniform step size $\Delta\phi_0 = \frac{\pi}{N}$, $N = 500, 1000$; (b) the comparison near $\phi_0 = \pi$ with the same data.

Besides differentiation of asymptotic expansion of $\hat{u}_0(\phi_0)$, the behavior of $\frac{d\hat{u}_0}{d\phi_0}$ at $\phi_0 = 0, \pi$ is analyzed analytically in Lemma 22.

Lemma 22. *When $\gamma \in (0, \pi)$, then $\frac{d\hat{u}_0}{d\phi_0}(0) = +\infty$ and $\frac{d\hat{u}_0}{d\phi_0}(\pi) = +\infty$. If $\gamma = 0$ or $\gamma = \pi$, then $\frac{d\hat{u}_0}{d\phi_0}(0) = \frac{d\hat{u}_0}{d\phi_0}(\pi) = 0$.*

Proof. When $\gamma \in (0, \pi)$, we evaluate $\frac{d\hat{u}_0}{d\phi_0}(0)$ (the $\frac{d\hat{u}_0}{d\phi_0}(\pi)$ case is similar).

$$\frac{d\hat{u}_0}{d\phi_0}(0) = \lim_{\phi_0 \rightarrow 0} \frac{\hat{u}_0(\phi_0) - \hat{u}_0(0)}{\phi_0} = +\infty \quad (3.298)$$

since $\hat{u}_0(0) = 0$ and $\hat{u}_0(\phi_0) \sim -\sin(\phi_0) \sin(\phi_0 + \gamma) \ln(\sin \phi_0)$ as $\phi_0 \rightarrow 0$.

Next, we consider the case $\gamma = \pi$ and $\phi_0 \rightarrow 0$ (the $\gamma = 0$ and $\phi_0 \rightarrow \pi$ case is similar). This is a graph case ($\psi_0 \rightarrow 0$). So, from (3.289), with $\gamma = \pi$, as $\phi_0 \rightarrow 0$,

$$\hat{u}_0 = \sin^2(\phi_0) \left[\ln(B) + \ln(\sin \phi_0) + \ln(1 + \cos \phi_0) + (\gamma_e - 2 \ln 2) \right] + \mathcal{O}(\Delta_1), \quad (3.299)$$

where $\Delta_1 = (B \sin^2 \phi_0)^{2/3} (-\ln(B \sin^2 \phi_0))^{5/3}$. Therefore,

$$\begin{aligned} \frac{d\hat{u}_0}{d\phi_0}(0) &= \lim_{\phi_0 \rightarrow 0} \frac{\hat{u}_0(\phi_0) - \hat{u}_0(0)}{\phi_0} \\ &= \lim_{\phi_0 \rightarrow 0} \frac{\sin \phi_0}{\phi_0} \sin(\phi_0) \left[\ln(B) + \ln(\sin \phi_0) + \ln(1 + \cos \phi_0) + (\gamma_e - 2 \ln 2) \right] + \frac{\mathcal{O}(\Delta_1)}{\phi_0} \\ &= 0. \end{aligned} \quad (3.300)$$

Finally, we show the case $\gamma = 0$ and $\phi_0 \rightarrow 0$ (the $\gamma = \pi$ and $\phi_0 \rightarrow \pi$ case is similar). In this case, $\psi_0 \rightarrow -\pi$. From Vogel [63], $T(\sigma) \sim -\sigma \ln(\sigma)$ as $\sigma \rightarrow 0$. With $\hat{T} = \frac{T}{\sqrt{B}}$ and $\hat{\sigma} = \frac{\sigma}{\sqrt{B}}$, $\hat{T} \sim -\hat{\sigma} \ln(\hat{\sigma})$ as $\hat{\sigma} \rightarrow 0$. Moreover,

$$\hat{u}_0(\phi_0) \leq 2\hat{T}(\hat{\sigma}_0) < 2\hat{T}(\hat{r}_0), \quad (3.301)$$

where $\hat{r}(\psi_0; \hat{\sigma}_0) = \hat{r}_0$. So,

$$\hat{T}(\hat{r}_0) \sim -2 \sin(\phi_0) \ln(\sin \phi_0). \quad (3.302)$$

Let $b = 2B\hat{T}(\hat{r}_0)$. So, $b \rightarrow 0$ as $\phi_0 \rightarrow 0$. Consider $N\hat{v} = b$ and the inclination angle $\psi_{\hat{v}}$ of \hat{v} satisfies $\psi_{\hat{v}} = \psi_0$ at the attachment point $\hat{r} = \hat{r}_0$. Thus,

$$N\hat{u} = B\hat{u} \leq b = N\hat{v}. \quad (3.303)$$

We consider $\psi = \psi(\hat{r})$, $\psi_{\hat{v}} = \psi_{\hat{v}}(\hat{r})$ and restrict $\psi, \psi_{\hat{v}} \in [\psi_0, -\pi/2]$. (3.303) implies

$$(\hat{r} \sin \psi)_{\hat{r}} \leq (\hat{r} \sin \psi_{\hat{v}})_{\hat{r}}. \quad (3.304)$$

Integrating from \hat{r} to \hat{r}_0 , it gives $\sin \psi \geq \sin \psi_{\hat{v}}$ or $\psi \leq \psi_{\hat{v}}$. Let $\psi_{\hat{v}}(\hat{\sigma}_{\hat{v}}) = -\pi/2$. Therefore, $\psi(\hat{\sigma}_{\hat{v}}) \leq -\pi/2$ and $\hat{\sigma}_0 \leq \hat{\sigma}_{\hat{v}}$. Solving for $\psi_{\hat{v}}(\hat{r})$ based on $N\hat{v} = b$, we obtain

$$\sin(\psi_{\hat{v}}) = \frac{\hat{r}_0 \sin \psi_0}{\hat{r}} - \frac{b(\hat{r}_0^2 - \hat{r}^2)}{2\hat{r}}. \quad (3.305)$$

At $\psi_{\hat{v}} = -\pi/2$,

$$\hat{\sigma}_{\hat{v}} = \frac{-2\hat{r}_0 \sin(\psi_0) + b\hat{r}_0^2}{1 + \sqrt{1 - 2b(\hat{r}_0 \sin(\psi_0) - b/2\hat{r}_0^2)}}. \quad (3.306)$$

When $\gamma = 0$, then $\hat{\sigma}_{\hat{v}} \sim \sin^2(\phi_0)$. Thus,

$$\hat{u}_0 \leq 2\hat{T}(\hat{\sigma}_0) \leq 2\hat{T}(\hat{\sigma}_{\hat{v}}). \quad (3.307)$$

As $\phi_0 \rightarrow 0$,

$$\left| \frac{\hat{u}_0}{\phi_0} \right| \leq \frac{2\hat{T}(\hat{\sigma}_{\hat{v}})}{\phi_0} \leq -C \frac{\sin^2 \phi_0}{\phi_0} \ln(\sin^2 \phi_0) \rightarrow 0 \quad (3.308)$$

for some $C > 2$. Therefore, $\frac{d\hat{u}_0}{d\phi_0}(0) = \lim_{\phi_0 \rightarrow 0} \frac{\hat{u}_0(\phi_0) - \hat{u}_0(0)}{\phi_0} = 0$. \square

Therefore, with (3.291) and Lemma 22, we obtain Property 5.

Property 5. At $\phi_0 = 0, \pi$, $\hat{h}(\phi_0)$ has the following properties:

(i) $\hat{h}(0) = 1$ and $\hat{h}(\pi) = -1$.

(ii) $\hat{h}'(\phi_0)$ behaves differently with different values of γ , at $\phi_0 = 0, \pi$,

$$\hat{h}'(0) = +\infty \quad \text{and} \quad \hat{h}'(\pi) = +\infty \quad \text{if } \gamma \in (0, \pi), \quad (3.309)$$

$$\hat{h}'(0) = \hat{h}'(\pi) = 0 \quad \text{if } \gamma = 0, \pi. \quad (3.310)$$

3.8.4 Behavior of $\hat{h}(\phi_0)$ and $\hat{F}_T(\phi_0)$ As $B \rightarrow \infty$

In this section, the behavior of $\hat{F}_T(\phi_0)$ as well as $\hat{h}(\phi_0)$ as $B \rightarrow \infty$ is studied. Recall that

$$\frac{d\hat{r}}{d\psi} = \frac{\cos \psi}{B\hat{u} - \frac{\sin \psi}{\hat{r}}}, \quad \frac{d\hat{u}}{d\psi} = \frac{\sin \psi}{B\hat{u} - \frac{\sin \psi}{\hat{r}}}. \quad (3.311)$$

We first obtain a lower bound on \hat{r} . If $\psi_0 < \psi < -\frac{\pi}{2}$, then

$$\frac{d\hat{r}}{d\psi} \geq -\hat{r} \frac{\cos \psi}{\sin \psi}. \quad (3.312)$$

Integrating gives $\hat{r} \geq \hat{r}_0 \frac{|\sin(\psi_0)|}{|\sin(\psi)|}$. If $\psi_0 \geq -\frac{\pi}{2}$, then $\frac{d\hat{r}}{d\psi} \geq 0$. Hence, $\hat{r} \geq \hat{r}_0$. Thus,

$$\hat{r} \geq b_0, \quad (3.313)$$

where

$$b_0 = \begin{cases} \hat{r}_0 |\sin(\psi_0)| & \text{if } \psi_0 < -\frac{\pi}{2}, \\ \hat{r}_0 & \text{if } \psi_0 \geq -\frac{\pi}{2}. \end{cases} \quad (3.314)$$

We next estimate \hat{u} ,

$$\frac{d\hat{u}}{d\psi} \geq \frac{\sin \psi}{B\hat{u}} \quad (3.315)$$

and $\hat{u} \rightarrow 0$ as $\psi \rightarrow 0$. Integrating from ψ to 0, (3.315) gives

$$\hat{u} \leq \hat{u}_1, \quad (3.316)$$

where

$$\hat{u}_1 = -\frac{2}{\sqrt{B}} \sin\left(\frac{\psi}{2}\right). \quad (3.317)$$

Moreover,

$$\frac{d\hat{u}}{d\psi} \leq \frac{\sin \psi}{B\hat{u} + b_1}, \quad (3.318)$$

where $b_1 = \frac{1}{b_0}$. Integrating gives

$$\frac{B}{2}\hat{u}^2 + b_1\hat{u} \geq 1 - \cos(\psi) = 2 \sin^2\left(\frac{\psi}{2}\right). \quad (3.319)$$

Solving this gives

$$\begin{aligned} \hat{u} &\geq \frac{1}{B} \left[-b_1 + \sqrt{b_1^2 + 4B \sin^2\left(\frac{\psi}{2}\right)} \right] \\ &= \frac{4 \sin^2(\psi/2)}{b_1 + \sqrt{b_1^2 + 4B \sin^2\left(\frac{\psi}{2}\right)}} \\ &= \frac{\hat{u}_1}{-\frac{b_1}{2\sqrt{B} \sin(\psi/2)} + \sqrt{1 + \frac{b_1^2}{4B \sin^2(\psi/2)}}}. \end{aligned} \quad (3.320)$$

Combine (3.316) and (3.320), as $B \rightarrow \infty$,

$$\hat{u}_1 \left(1 + \mathcal{O}\left(\frac{1}{\sqrt{B}}\right) \right) \leq \hat{u} \leq \hat{u}_1. \quad (3.321)$$

In above inequalities, there is no restriction on the upper bound \hat{u}_1 . So, $\hat{u}_0 = \mathcal{O}\left(\frac{1}{\sqrt{B}}\right)$ uniformly for $\phi_0 \in [0, \pi]$. However, the lower bound is valid for $\phi_0 \in (\delta, \pi - \delta)$ for an arbitrary $0 < \delta < \pi/2$ and $\psi \leq \psi_0 < -\mu < 0$ for an arbitrary $0 < \mu < \pi/2$ (ψ_0 stays away from 0). Therefore, $\hat{u} \sim \hat{u}_1 = -\frac{2}{\sqrt{B}} \sin\left(\frac{\psi}{2}\right)$ as $B \rightarrow \infty$. \hat{u} converges uniformly to \hat{u}_1 on $[\psi_0, -\mu]$, for any $\psi \leq \psi_0 < -\mu < 0$. In addition, \hat{r} converges uniformly to

$$\hat{r}_1 = \hat{r}_0 + \int_{\psi_0}^{\psi} \frac{\cos(s)}{B\hat{u}_1(s)} ds \quad (3.322)$$

on $[\psi_0, -\mu]$. (3.322) can be evaluated analytically, see Vogel [63] and Chen and Siegel [4].

Remark 24. (\hat{r}_1, \hat{u}_1) is the solution of one-dimensional capillary equation with the same boundary conditions. A similar uniform convergence result is established by Vogel [63].

We can summarize above results in the following Theorem 23.

Theorem 23. As $B \rightarrow \infty$,

$$\hat{u}_0 = \mathcal{O}\left(\frac{1}{\sqrt{B}}\right) \quad (3.323)$$

uniformly for $\phi_0 \in [0, \pi]$. When $\phi_0 \in (\delta, \pi - \delta)$ for an arbitrary $0 < \delta < \pi/2$, as $B \rightarrow \infty$, if $\psi \leq \psi_0 < -\mu < 0$ for an arbitrary $0 < \mu < \pi/2$,

$$\hat{u}_1 \left(1 + \mathcal{O}\left(\frac{1}{\sqrt{B}}\right)\right) \leq \hat{u} \leq \hat{u}_1, \quad (3.324)$$

where \hat{u}_1 is defined in (3.317). Hence, $\hat{u} - \hat{u}_1 = \mathcal{O}\left(\frac{1}{B}\right)$ in this case. Moreover,

$$\hat{u} \sim -\frac{2}{\sqrt{B}} \sin\left(\frac{\psi}{2}\right) \quad (3.325)$$

and solution (\hat{r}, \hat{u}) converges uniformly to (\hat{r}_1, \hat{u}_1) , the solution of one-dimensional capillary equation in (3.317) and (3.322), on $[\psi_0, -\mu]$.

In Fig. 3.18a, it shows the comparison between the numerical \hat{u}_0 and the approximate form in (3.325) with $B = 1000$ and $\gamma = \frac{\pi}{3}$. We can see that the approximate form performs well.

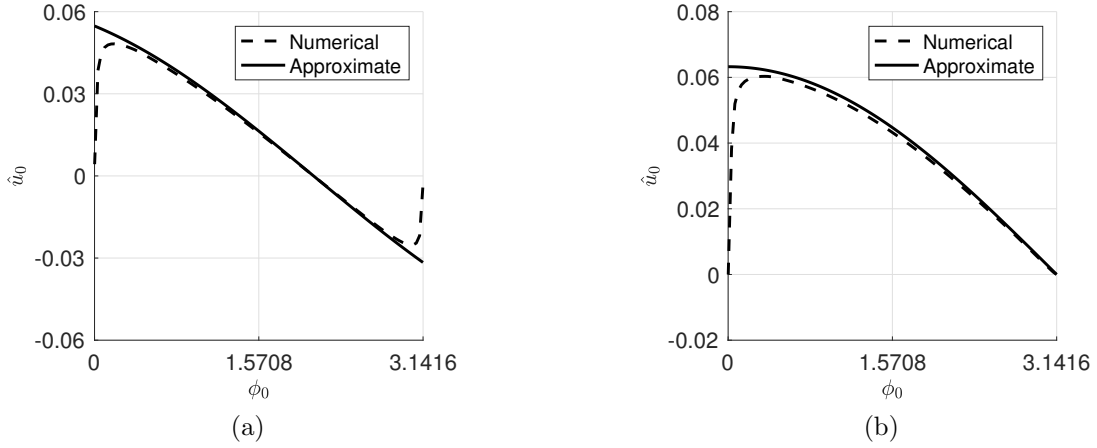


Figure 3.18: (a) The comparison between the numerical solution and the approximate form with $B = 1000$ and $\gamma = \frac{\pi}{3}$; (b) the comparison between the numerical solution and the approximate form with $B = 1000$ and $\gamma = 0$.

When applying Theorem 23 to \hat{h} and \hat{F}_T , for $\phi_0 \in (0, \pi)$, as $B \rightarrow \infty$, we have

$$\hat{h}(\phi_0) = \cos(\phi_0) + \mathcal{O}\left(\frac{1}{\sqrt{B}}\right), \quad (3.326)$$

$$\hat{F}_T(\phi_0) = \hat{F}_1(\phi_0) + \mathcal{O}\left(\frac{1}{\sqrt{B}}\right), \quad (3.327)$$

where

$$\hat{F}_1(\phi_0) = -\frac{4}{3}\alpha - \cos \phi_0 + \frac{2}{3} + \frac{1}{3} \cos^3(\phi_0), \quad (3.328)$$

where $\hat{F}_1(\phi_0)$ is known as Archimedes' total force, see McCuan and Treinen [43]. $\hat{F}_1(\phi_0)$ is a strictly increasing function with $\hat{F}_1(0) = -\frac{4}{3}\alpha$ and $\hat{F}_1(\pi) = -\frac{4}{3}\alpha + \frac{4}{3}$. There is exact

one root $\bar{\phi}_0^*$ for $\hat{F}_1(\phi_0)$ when $\alpha \in (0, 1)$. When $\alpha > 1$, there is no force balance point for $\hat{F}_1(\phi_0)$. Moreover, the effect of γ is negligible in \hat{F}_1 .

To find asymptotics of $\hat{F}'_T(\phi_0)$ and $\hat{h}'(\phi_0)$, we need the estimate of $\frac{d\hat{u}_0}{d\phi_0}$ for $B \rightarrow \infty$ in the following Lemma 23.

Lemma 23. *For $\phi_0 \in (\delta, \pi - \delta)$ for an arbitrary $0 < \delta < \pi/2$, with $\gamma \in [0, \pi]$, as $B \rightarrow \infty$, then*

$$\frac{d\hat{u}_0}{d\phi_0} = \mathcal{O}\left(\frac{1}{\sqrt{B}}\right). \quad (3.329)$$

Proof. Suppose $\phi_0 \in (\delta, \pi - \delta)$ for an arbitrary $0 < \delta < \pi/2$ and $\gamma \in [0, \pi]$. We first consider $\psi_0 < -\mu < 0$ for an arbitrary $0 < \mu < \pi/2$ (the $\psi_0 > 0$ case is similar). So, both the $\psi_0 \in \left(-\pi, -\frac{\pi}{2}\right]$ and $\psi_0 \in \left[-\frac{\pi}{2}, 0\right)$ cases will be discussed, with the $\psi_0 \in [-\mu, \mu]$ case considered separately. Recall the scaled capillary equation,

$$\frac{d\bar{r}}{d\psi} = \frac{\bar{r} \cos \psi}{\bar{r}\bar{u} - \sin \psi}, \quad \frac{d\bar{u}}{d\psi} = \frac{\bar{r} \sin \psi}{\bar{r}\bar{u} - \sin \psi}. \quad (3.330)$$

with boundary conditions

$$\bar{r}(\psi_0) = \sqrt{B} \sin(\phi_0) \quad \text{and} \quad \lim_{\psi \rightarrow 0} \bar{u} = 0. \quad (3.331)$$

We use the solution of the form

$$\bar{r} = \bar{r}(\psi; \sigma) \quad \text{and} \quad \bar{u} = \bar{u}(\psi; \sigma). \quad (3.332)$$

We first consider the case $\psi_0 \in \left[-\frac{\pi}{2}, 0\right)$ and find the lower bound of σ .

$$\frac{d\bar{r}}{d\psi} \leq -\frac{\bar{r} \cos \psi}{\sin \psi}. \quad (3.333)$$

Integrating from $-\frac{\pi}{2}$ to ψ_0 ,

$$\int_{-\pi/2}^{\psi_0} \frac{1}{\bar{r}} \frac{d\bar{r}}{d\psi} \psi \leq \int_{-\pi/2}^{\psi_0} -\cot(\psi) d\psi. \quad (3.334)$$

We obtain

$$\bar{r}(\psi_0)(-\sin \psi_0) \leq \sigma, \quad (3.335)$$

where $\bar{r}(\psi_0) = \sqrt{B} \sin \phi_0$ and $\sigma = \bar{r} \left(-\frac{\pi}{2}; \sigma \right)$.

Differentiating $\bar{u}_0(\phi_0) = \bar{u}(\psi_0; \sigma(\phi_0))$,

$$\frac{d\bar{u}_0}{d\phi_0} = \left. \frac{d\bar{u}}{d\psi} \right|_{\psi_0} \frac{d\psi_0}{d\phi_0} + \dot{\bar{u}}(\psi_0; \sigma) \frac{d\sigma}{d\phi_0}. \quad (3.336)$$

For $\frac{d\bar{u}}{d\psi}$,

$$\frac{d\bar{u}}{d\psi} = \frac{\sin \psi}{\bar{u} - \frac{\sin \psi}{\bar{r}}} \sim \frac{\sin \psi}{\bar{u}} \sim -\cos \left(\frac{\psi}{2} \right). \quad (3.337)$$

For $\dot{\bar{u}}(\psi_0; \sigma)$,

$$\begin{aligned} \frac{d\dot{\bar{u}}}{d\psi} &= - \frac{\sin \psi \left(\dot{\bar{u}} + \dot{\bar{r}} \frac{\sin \psi}{\bar{r}^2} \right)}{\left(\bar{u} - \frac{\sin \psi}{\bar{r}} \right)^2} \\ &\leq - \frac{\sin \psi \dot{\bar{u}}}{\bar{u}^2}, \end{aligned} \quad (3.338)$$

since $\dot{\bar{r}} > 0$ and $\dot{\bar{u}} > 0$. Integrating from $-\frac{\pi}{2}$ to ψ_0 ,

$$\int_{-\pi/2}^{\psi_0} \frac{1}{\dot{\bar{u}}} \frac{d\dot{\bar{u}}}{d\psi} \psi \leq \int_{-\pi/2}^{\psi_0} -\frac{\sin \psi}{\bar{u}^2} d\psi \leq C_1 \quad (3.339)$$

for some constant $C_1 > 0$.

$$\dot{\bar{u}}(\psi_0; \sigma) \leq C_1 \dot{\bar{u}}\left(-\frac{\pi}{2}; \sigma\right), \quad (3.340)$$

where $\bar{u}\left(-\frac{\pi}{2}; \sigma\right) = T(\sigma)$ and $T'(\sigma) \leq \frac{\sqrt{2}}{\sigma}$, see Vogel [63]. So, combined with (3.335), we obtain

$$\dot{\bar{u}}(\psi_0; \sigma) \leq \frac{C_1}{\sqrt{B} \sin \phi_0 (-\sin \psi_0)}. \quad (3.341)$$

We differentiate

$$\bar{r}(\psi_0; \sigma) = \sqrt{B} \sin(\phi_0), \quad (3.342)$$

then

$$\left. \frac{d\bar{r}}{d\psi} \right|_{\psi_0} \frac{d\psi_0}{d\phi_0} + \dot{\bar{r}}(\psi_0; \sigma) \frac{d\sigma}{d\phi_0} = \sqrt{B} \cos(\phi_0). \quad (3.343)$$

This implies

$$\frac{d\sigma}{d\phi_0} = \frac{\sqrt{B} \cos(\phi_0) - \left. \frac{d\bar{r}}{d\psi} \right|_{\psi_0}}{\dot{\bar{r}}(\psi_0; \sigma)}, \quad (3.344)$$

where

$$\frac{d\bar{r}}{d\psi} = \frac{\cos \psi}{\bar{u} - \frac{\sin \psi}{\bar{r}}} \sim \frac{\cos \psi}{\bar{u}} \sim -\frac{\cos \psi}{2 \sin(\psi/2)}. \quad (3.345)$$

For $\dot{\bar{r}}$,

$$\begin{aligned}\frac{d\dot{r}}{d\psi} &= -\frac{\cos\psi\left(\dot{u} + \frac{\dot{r}\sin\psi}{\bar{r}^2}\right)}{\left(\bar{u} - \frac{\sin\psi}{\bar{r}}\right)^2} \\ &\geq -\frac{\cos\psi\dot{u}}{\bar{u}^2} \geq -\frac{C_2}{\sqrt{B}}\end{aligned}\tag{3.346}$$

from (3.341) and for some $C_2 > 0$. Integrating from $-\frac{\pi}{2}$ to ψ_0 ,

$$\dot{r}(\psi_0; \sigma) \geq 1 - \frac{\bar{C}_2}{\sqrt{B}}.\tag{3.347}$$

So, there exists some $\epsilon > 0$,

$$\frac{1}{\dot{r}(\psi_0; \sigma)} \leq 1 + \epsilon.\tag{3.348}$$

(3.344) gives

$$\frac{d\sigma}{d\phi_0} = \mathcal{O}(\sqrt{B})\tag{3.349}$$

uniformly on $[-\pi/2, -\mu]$, $0 < \mu < \frac{\pi}{2}$. Combined with (3.337), (3.340) and (3.349), (3.336) gives

$$\frac{d\bar{u}_0}{d\phi_0} = \mathcal{O}(1).\tag{3.350}$$

Therefore,

$$\frac{d\hat{u}_0}{d\phi_0} = \frac{1}{\sqrt{B}} \frac{d\bar{u}_0}{d\phi_0} = \mathcal{O}\left(\frac{1}{\sqrt{B}}\right).\tag{3.351}$$

When $\psi_0 \in \left(-\pi, -\frac{\pi}{2}\right]$, suppose $B \geq 1$, Equations of $\frac{d\dot{u}}{d\psi}$ and $\frac{d\dot{r}}{d\psi}$ give

$$\frac{d\dot{u}}{d\psi} \geq -b_1\dot{u} - \frac{b_2}{B}\dot{r}, \quad (3.352)$$

$$\frac{d\dot{r}}{d\psi} \geq -b_1\dot{u} - \frac{b_2}{B}\dot{r} \quad (3.353)$$

with some $b_1, b_2 > 0$ and from $\bar{r}_0 = \mathcal{O}(\sqrt{B})$. Consider a Lyapunov function $V(\psi) = \sqrt{B}\dot{u} + \dot{r}$. We have

$$V' \geq -bV, \quad (3.354)$$

where $b = \max\{b_1, b_2\} > 0$. Integrating from ψ_0 to $-\frac{\pi}{2}$, we obtain

$$V(\psi_0) \leq e^{b(-\pi/2-\psi_0)}V(-\pi/2) \quad (3.355)$$

where

$$\begin{aligned} V(-\pi/2) &\leq \sqrt{B}\dot{u}\left(-\frac{\pi}{2}; \sigma\right) + \dot{r}\left(-\frac{\pi}{2}; \sigma\right) \\ &\leq \sqrt{B}\frac{\sqrt{2}}{\sqrt{B}} + 1. \end{aligned} \quad (3.356)$$

Hence,

$$0 < \sqrt{B}\dot{u}(\psi_0; \sigma) + \dot{r}(\psi_0; \sigma) \leq K \quad (3.357)$$

for some constant $K > 0$. Therefore, $\dot{u}(\psi_0; \sigma) = \mathcal{O}\left(\frac{1}{\sqrt{B}}\right)$ and $\dot{r}(\psi_0; \sigma) = \mathcal{O}(1)$ on $[-\pi, -\mu]$, $0 < \mu < \frac{\pi}{2}$. Hence, (3.350) is concluded in the $\psi_0 \in \left(-\pi, -\frac{\pi}{2}\right]$ case.

Finally, we show $\frac{d\bar{u}_0}{d\phi_0} = \mathcal{O}(1)$ for $\psi_0 \in [-\mu, \mu]$, $0 < \mu < \frac{\pi}{2}$. Hence, $\frac{d\hat{u}_0}{d\phi_0} = \mathcal{O}\left(\frac{1}{\sqrt{B}}\right)$ on $[\pi - \gamma - \mu, \pi - \gamma + \mu]$. Consider $\psi_0 \in [-\mu, 0]$ (the $\psi_0 \in [0, \mu]$ case is similar). Again, we consider the graph description, see as follows,

$$\bar{u}_0 = \bar{u}(\bar{r}_0; \bar{r}_0, \psi_0) = \bar{u}(\bar{r}_0, \psi_0), \quad (3.358)$$

where \bar{r}_0 and ψ_0 are considered as the initial radial distance and the corresponding inclination angle. Recall the slope function from Vogel [63],

$$p(\bar{r}_0; \bar{u}_0) = \tan(\psi_0). \quad (3.359)$$

We differentiate the slope function with respect to ψ_0 , then

$$p_u(\bar{r}_0; \bar{u}_0) \frac{\partial \bar{u}_0}{\partial \psi_0} = \sec^2(\psi_0), \quad (3.360)$$

where $p_u \leq -C$ for some positive constant C from Lemma 15 and (3.62). So, $\frac{\partial \bar{u}_0}{\partial \psi_0} = \frac{\sec^2(\psi_0)}{p_u(\bar{r}_0; \bar{u}_0)} = \mathcal{O}(1)$. Moreover, when the initial data for the floating ball problem is used, $\bar{r}_0 = \sqrt{B} \sin(\phi_0)$ and $\psi_0 = \phi_0 + \gamma - \pi$,

$$\begin{aligned} \frac{d}{d\phi_0} \bar{u}_0(\bar{r}_0, \psi_0) &= \frac{\partial \bar{u}_0}{\partial \bar{r}_0} \sqrt{B} \cos \phi_0 + \frac{\partial \bar{u}_0}{\partial \psi_0} \\ &\leq \frac{\sqrt{2}}{\sqrt{B} \sin(\phi_0)} \sqrt{B} \cos \phi_0 + \frac{\sec^2(\psi_0)}{p_u(\bar{r}_0; \bar{u}_0)} \\ &= \mathcal{O}(1), \end{aligned} \quad (3.361)$$

where $\frac{\partial \bar{u}_0}{\partial \bar{r}_0} \leq \frac{\sqrt{2}}{\bar{r}_0}$ from Lemma 3.7 in Vogel [63]. Therefore,

$$\frac{d\hat{u}_0}{d\phi_0} = \mathcal{O}\left(\frac{1}{\sqrt{B}}\right). \quad (3.362)$$

□

Therefore, Lemma 23 gives

$$\hat{F}'_T(\phi_0) = \sin^3(\phi_0) + \mathcal{O}\left(\frac{1}{\sqrt{B}}\right), \quad (3.363)$$

$$\hat{h}'(\phi_0) = -\sin(\phi_0) + \mathcal{O}\left(\frac{1}{\sqrt{B}}\right). \quad (3.364)$$

With the asymptotics of \hat{F}_T , \hat{h} , \hat{F}'_T and \hat{h}' , we can tell the number of equilibrium points and their stability for large Bond number. Recall the total force defined in (3.327),

$$\hat{F}_T(\phi_0) = \hat{F}_1(\phi) + \mathcal{O}\left(\frac{1}{\sqrt{B}}\right),$$

where

$$\hat{F}_1(\phi_0) = -\frac{4}{3}\alpha - \cos\phi_0 + \frac{2}{3} + \frac{1}{3}\cos^3(\phi_0).$$

For $\alpha \in (0, 1)$, choose $0 < \delta_1 < \pi/2$ such that $\bar{\phi}_0^* \in (\delta_1, \pi - \delta_1)$, where $\bar{\phi}_0^*$ is the root of \hat{F}_1 . Choose $B \geq B_1 > 0$ such that $\hat{F}_T < 0$ on $[0, \delta_1]$ and $\hat{F}_T > 0$ on $[\pi - \delta_1, \pi]$ and $\hat{F}'_T > 0$ and $\hat{h}' < 0$ on $[\delta_1, \pi - \delta_1]$. Therefore, there is a unique stable force balanced point $\bar{\phi}_0 \in [\delta_1, \pi - \delta_1]$, see as follows,

$$\hat{F}_T(\bar{\phi}_0) = \hat{F}_1(\bar{\phi}_0) + \mathcal{O}\left(\frac{1}{\sqrt{B}}\right) = 0. \quad (3.365)$$

Thus,

$$\hat{F}_1(\bar{\phi}_0) = \mathcal{O}\left(\frac{1}{\sqrt{B}}\right). \quad (3.366)$$

With $\hat{F}'_1(\bar{\phi}_0^*) > 0$, then

$$\bar{\phi}_0 = \hat{F}_1^{-1}\left(\mathcal{O}\left(\frac{1}{\sqrt{B}}\right)\right) = \bar{\phi}_0^* + \mathcal{O}\left(\frac{1}{\sqrt{B}}\right). \quad (3.367)$$

Moreover, we can show $\hat{F}_T(\phi_0)$ has no force balanced point when $\alpha > 1$. Let $\alpha = 1 + \epsilon$, for some $\epsilon > 0$.

$$\hat{F}_T(\phi_0) \leq \hat{F}_1(\pi) + \frac{C}{\sqrt{B}} \leq -\frac{4}{3}\epsilon + \frac{C}{\sqrt{B}} < 0 \quad (3.368)$$

for some $C > 0$, if $B \rightarrow \infty$. We summarize the above results for $B \rightarrow \infty$ in the following theorem:

Theorem 24. *For $\alpha \in (0, 1)$, choose $0 < \delta_1 < \pi/2$ such that $\bar{\phi}_0^* \in (\delta_1, \pi - \delta_1)$, where $\bar{\phi}_0^*$ is the root of \hat{F}_1 . Choose $B \geq B_1 > 0$ such that $\hat{F}_T < 0$ on $[0, \delta_1]$ and $\hat{F}_T > 0$ on $[\pi - \delta_1, \pi]$ and $\hat{F}'_T > 0$ and $\hat{h}' < 0$ on $[\delta_1, \pi - \delta_1]$. Therefore, there is a unique stable force balanced point $\bar{\phi}_0 \in [\delta_1, \pi - \delta_1]$ such that*

$$\bar{\phi}_0 = \bar{\phi}_0^* + \mathcal{O}\left(\frac{1}{\sqrt{B}}\right). \quad (3.369)$$

If $\alpha > 1$, there is no force balanced point if Bond number is large enough.

We consider two large Bond number cases $B = 1000$ and $B = 5000$ with $\gamma = \frac{\pi}{3}$ and $\alpha = 0$. The results are also consistent with our analysis. However, the numerical results converge slowly to the limiting forms in (3.326) and (3.327), see Fig. 3.19a, Fig. 3.19b, Fig. 3.20a and Fig. 3.20b.

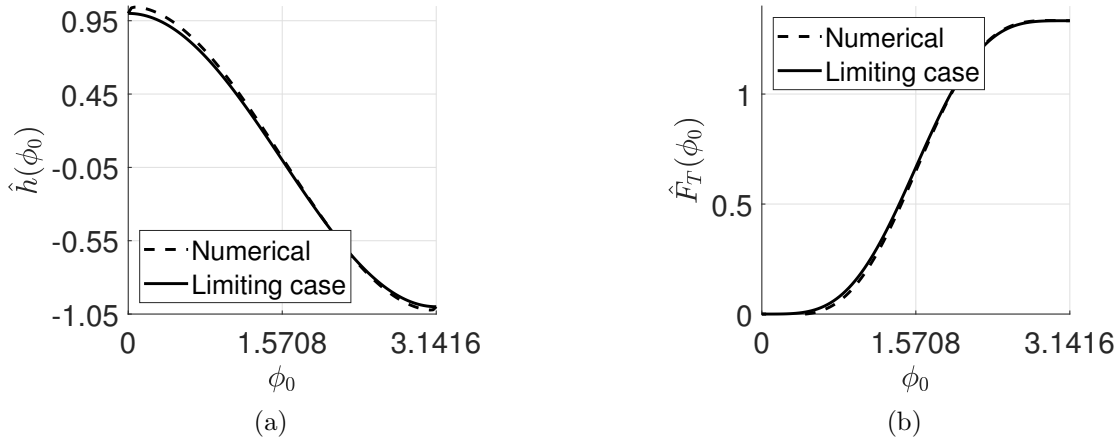


Figure 3.19: (a) The comparison between the numerical solution and the limiting case of the height curve with $B = 1000$, $\gamma = \frac{\pi}{3}$; (b) the comparison between the numerical solution and the limiting case of the total force curve with the same data and $\alpha = 0$.

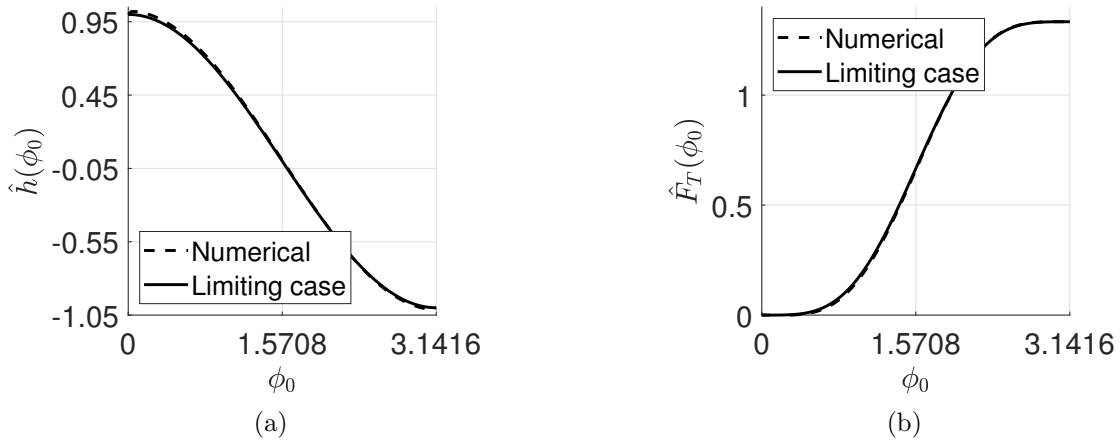


Figure 3.20: (a) The comparison between the numerical solution and the limiting case of the height curve with $B = 5000$, $\gamma = \frac{\pi}{3}$; (b) the comparison between the numerical solution and the limiting case of the total force curve with the same data and $\alpha = 0$.

3.8.5 Numerical Observation of the Total Force $\hat{F}_T(\phi_0)$ and Height $\hat{h}(\phi_0)$ Curves

In this section, we state the numerical observation of the behavior of the \hat{F}_T and the \hat{h} curves based on different values of parameters. Since $-\frac{4}{3}\alpha$ is the constant term of \hat{F}_T , as the value of $\alpha > 0$ increasing, the \hat{F}_T curve shifts downward without changing the shape of the curve. Thus, for convenience, $\alpha = 0$ is considered for the \hat{F}_T curve.

Consider 50 evenly spaced points of $\gamma \in [0.01, 3.14]$, 150 evenly spaced points of $B \in [0.01, 15]$ and 100 evenly spaced point of $\phi_0 \in [\epsilon, \pi - \epsilon]$, $\epsilon = 0.001$, thus, there are, in total, 7500 pairs of values of (γ, B) . We test the behavior of both curves with above values of B and γ , and state the following Observation 1.

Observation 1. For $\phi_0 \in [\epsilon, \pi - \epsilon]$, $\epsilon = 0.001$, with $\gamma \in [0, 3.14]$ and $B \in [0.01, 15]$, we have

- (i) There are exact two critical points of $\hat{h}(\phi_0)$, the smaller one is the local maximum point, which is less than $\frac{\pi}{2}$, the larger one is the local minimum point, which is greater than $\frac{\pi}{2}$. Thus, the $\hat{h}(\phi_0)$ curve increases to the local maximum point, then decreases to the local minimum point and then increases.
- (ii) There are exact two critical points of $\hat{F}_T(\phi_0)$, the smaller one is the local minimum, which is less than $\frac{\pi}{2}$, the larger one is the local maximum, which is greater than $\frac{\pi}{2}$. Thus, the $\hat{F}_T(\phi_0)$ curve decreases to the local minimum point, then increases to the local maximum point and then decreases.
- (iii) Suppose $\phi_0^{**} > \frac{\pi}{2}$ and $\phi_0^* > \frac{\pi}{2}$ are the critical points of $\hat{h}(\phi_0)$ and $\hat{F}_T(\phi_0)$, respectively, then $\phi_0^{**} > \phi_0^*$.

Remark 25. Instead of $B = 0$, $B = 0.01$ is considered as the minimum value. Similarly, $\gamma = 0.01$ and $\gamma = 3.14$ are considered as the minimum and the maximum values of γ . $\phi_0 = \epsilon$ and $\phi_0 = \pi - \epsilon$ are considered as the minimum and the maximum values of ϕ_0 .

The above numerical observation is consistent with the properties of \hat{h} and \hat{F}_T , i.e. $\hat{F}_T(0) = -\frac{4}{3}\alpha$, $\hat{F}_T(\pi) = -\frac{4}{3}\alpha + \frac{4}{3}$, $\hat{F}'_T(0) = \hat{F}'_T(\phi_0) = -\frac{2}{B}\sin(\gamma)$, see Property 4. Fig. 3.21a and

Fig. 3.21b show an example of the behavior of \hat{F}_T and \hat{h} with $B = 5$, $\gamma = \frac{\pi}{2}$ and $\alpha = 0$. In this case, \hat{h} and \hat{F}_T have the behavior described above.

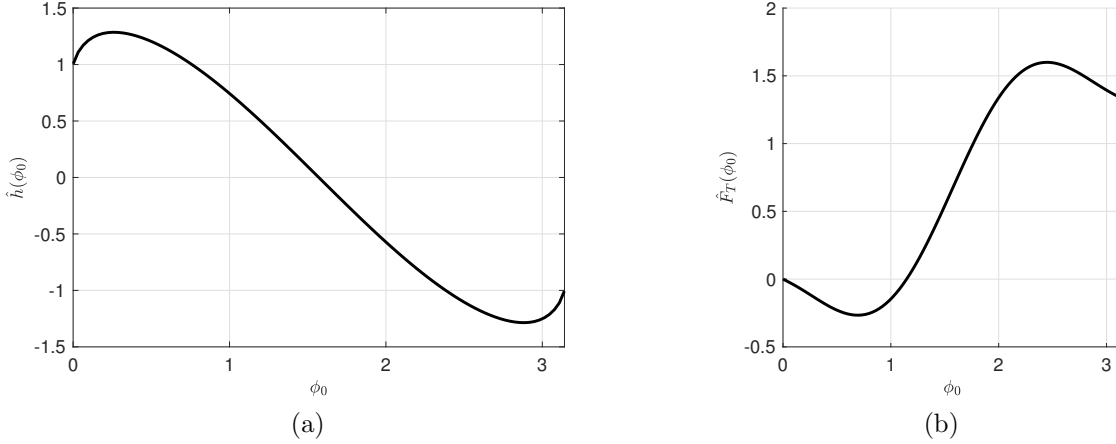


Figure 3.21: (a) The height curve with $B = 5$, $\gamma = \frac{\pi}{2}$; (b) the total force curve with the same data and $\alpha = 0$.

In above numerical tests, we only consider $B = 0.01$ and $B = 15$ as the minimum and the maximum values, respectively. When $0 < B < 0.01$ and $B > 15$, only a few cases are tested, see Fig. 3.22a, Fig. 3.22b, Fig. 3.23a and Fig. 3.23b. The behavior of $\hat{F}_T(\phi_0)$ and $\hat{h}(\phi_0)$ is still consistent with Observation 1. When $0 < B < 0.01$, the asymptotic forms of $\hat{F}_T(\phi_0)$ and $\hat{h}(\phi_0)$ as $B \rightarrow 0$ in Sec. 3.8.2 can be applied. Recall that, Fig. 3.12a and Fig. 3.12b compare the asymptotic forms and the numerical results of $\hat{F}_T(\phi_0)$ and $\hat{h}(\phi_0)$ with $B = 0.01$. They are indistinguishable. And the behavior is consistent with Observation 1. Based on Sec. 3.8.4, we have $\hat{h}(\phi_0)$ and $\hat{F}_T(\phi_0)$ converging slowly to the asymptotic forms as $B \rightarrow \infty$, see Fig. 3.19a, Fig. 3.19b, Fig. 3.20a and Fig. 3.20b. So, for a large Bond number, the behavior of $\hat{F}_T(\phi_0)$ and $\hat{h}(\phi_0)$ is also consistent with Observation 1 except the limiting case.

Hence, based on Observation 1 and the stability criterion in Sec. 3.6.4, we have the following Conjecture 1,

Conjecture 1. For $\phi_0 \in (0, \pi)$, with $\alpha > 0$, $\gamma \in (0, \pi)$ and $B > 0$. Suppose $\phi_0^{*} > \frac{\pi}{2}$ and

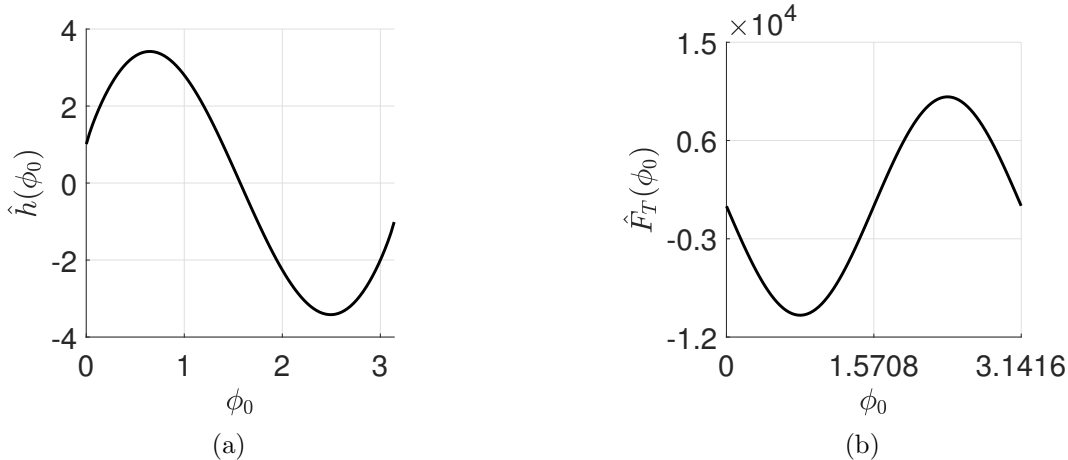


Figure 3.22: (a) The height curve with $B = 0.0001$, $\gamma = \frac{\pi}{2}$; (b) the total force curve with the same data and $\alpha = 0$.

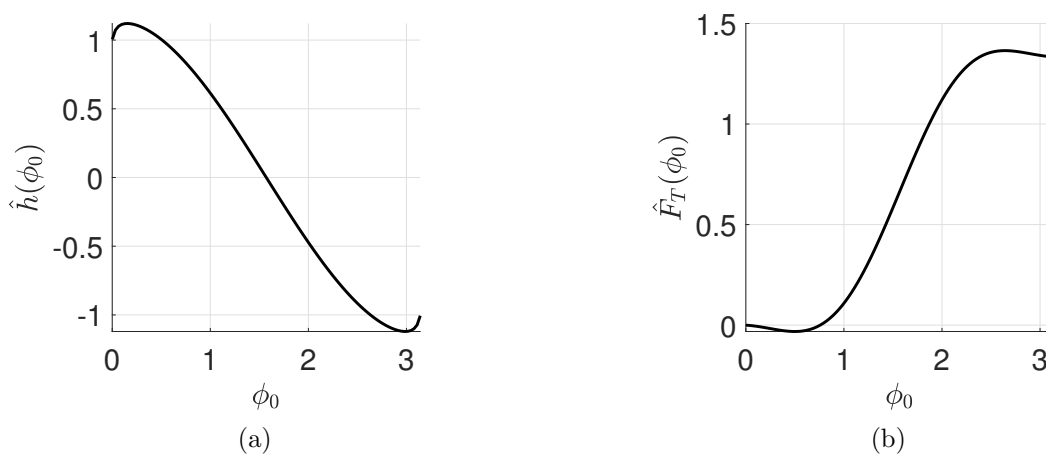


Figure 3.23: (a) The height curve with $B = 50$, $\gamma = \frac{\pi}{2}$; (b) the total force curve with the same data and $\alpha = 0$.

$\phi_0^* > \frac{\pi}{2}$ are the critical points of $\hat{h}(\phi_0)$ and $\hat{F}_T(\phi_0)$, respectively. By varying the value of $\alpha > 0$, \hat{F}_T admits at most two forced balanced points.

(i) If there is only one forced balanced point, denoted as $\bar{\phi}_0$, then $\bar{\phi}_0 \leq \phi_0^*$, and $\bar{\phi}_0$ must

be a stable equilibrium point.

- (ii) If there are two forced balanced points, denoted as $\bar{\phi}_{01}$ and $\bar{\phi}_{02}$, then, $\bar{\phi}_{01} < \phi_0^* < \bar{\phi}_{02}$, the smaller one must be stable, the larger one can be either stable or unstable.

In above numerical tests, we avoid the $\gamma = 0$ and the $\gamma = \pi$ cases since $\hat{h}(\phi_0)$ and \hat{F}_T behave differently in those cases as $\phi_0 \rightarrow 0, \pi$. Based on the discussion in Sec. 3.8.3, with $\gamma = 0, \pi$, $\hat{h}'(\phi_0) \rightarrow 0$ as $\phi_0 \rightarrow 0, \pi$, see Fig. 3.24a and Fig. 3.25a. From (3.294), $\hat{F}'_T(0) = \hat{F}'_T(\pi) = 0$ with $\gamma = 0$ or $\gamma = \pi$, see Fig. 3.24b and Fig. 3.25b. Therefore, we summarize the behavior of \hat{h} and \hat{F}_T for the $\gamma = 0$ and the $\gamma = \pi$ cases in Observation 2.

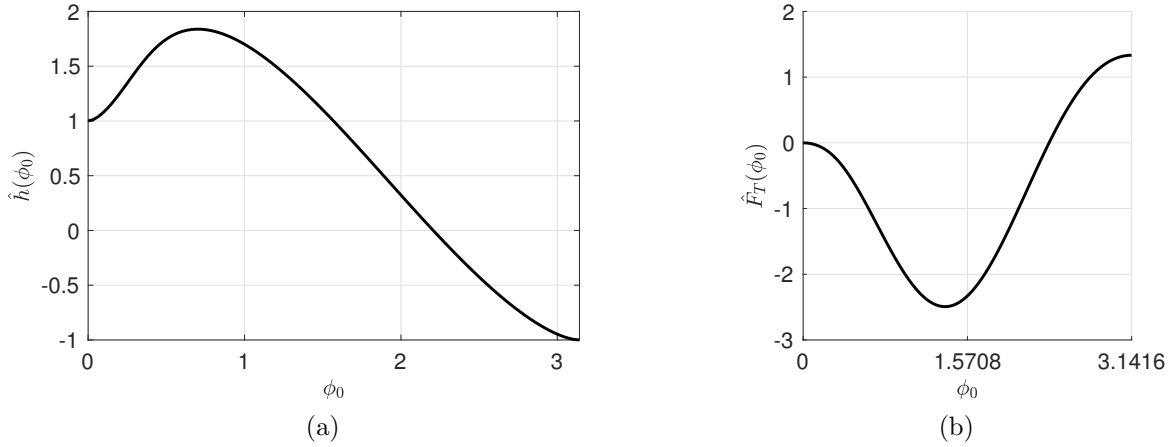


Figure 3.24: (a) The height curve with $B = 1$, $\gamma = 0$; (b) the total force curve with the same data and $\alpha = 0$.

Observation 2. For $\phi_0 \in [\epsilon, \pi - \epsilon]$, $\epsilon = 0.001$, with $B > 0$, we have

- (i) If $\gamma = 0$, $\hat{h}(\phi_0)$ has only one local maximum point, which is less than $\frac{\pi}{2}$ and has no local minimum point. The $\hat{F}_T(\phi_0)$ has only one local minimum point, which is less than $\frac{\pi}{2}$ and has no local maximum point. As $\phi_0 \rightarrow 0, \pi$, $\hat{h}'(\phi_0) \rightarrow 0$ and $\hat{F}'_T(\phi_0) \rightarrow 0$. Thus, the $\hat{h}(\phi_0)$ curve increases to the local maximum point, then decreases. And the $\hat{F}_T(\phi_0)$ curve decreases to the local minimum point, then increases.
- (ii) If $\gamma = \pi$, $\hat{h}(\phi_0)$ has only one local minimum point, which is greater than $\frac{\pi}{2}$ and

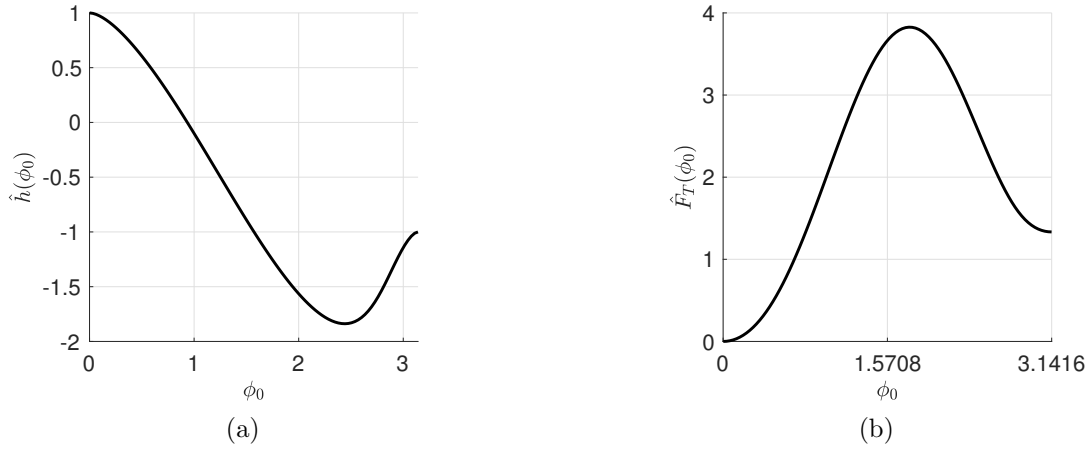


Figure 3.25: (a) The height curve with $B = 1$, $\gamma = \pi$; (b) the total force curve with the same data and $\alpha = 0$.

has no local maximum point. The $\hat{F}_T(\phi_0)$ has only one local maximum point, which is greater than $\frac{\pi}{2}$ and has no local minimum point. As $\phi_0 \rightarrow 0, \pi$, $\hat{h}'(\phi_0) \rightarrow 0$ and $\hat{F}_T'(\phi_0) \rightarrow 0$. Thus, the $\hat{h}(\phi_0)$ curve decreases to the local minimum point, then increases. And the $\hat{F}_T(\phi_0)$ curve increases to the local maximum point, then decreases.

- (iii) In the $\gamma = \pi$ case, suppose $\phi_0^{**} > \frac{\pi}{2}$ and $\phi_0^* > \frac{\pi}{2}$ are the critical points of $\hat{h}(\phi_0)$ and $\hat{F}_T(\phi_0)$, respectively, then $\phi_0^{**} > \phi_0^*$.

If B is given sufficiently small, with $\gamma = 0$ or $\gamma = \pi$, $\hat{h}(\phi_0)$ and $\hat{F}_T(\phi_0)$ behave almost the same as Observation 2 except that the local maximum/minimum point of $\hat{F}_T(\phi_0)$ is close to $\phi_0 = \frac{\pi}{2}$. see Fig. 3.26a, Fig. 3.26b, Fig. 3.27a and Fig. 3.27b.

Hence, based on Observation 2 and the stability criterion in Sec. 3.6.4, we have the following Conjecture 2,

Conjecture 2. For $\phi_0 \in (0, \pi)$, with $\alpha > 0$, and $B > 0$. Suppose ϕ_0^{**} and ϕ_0^* are the critical points of $\hat{h}(\phi_0)$ and $\hat{F}_T(\phi_0)$ in $(0, \pi)$, respectively. By varying the value of $\alpha > 0$,

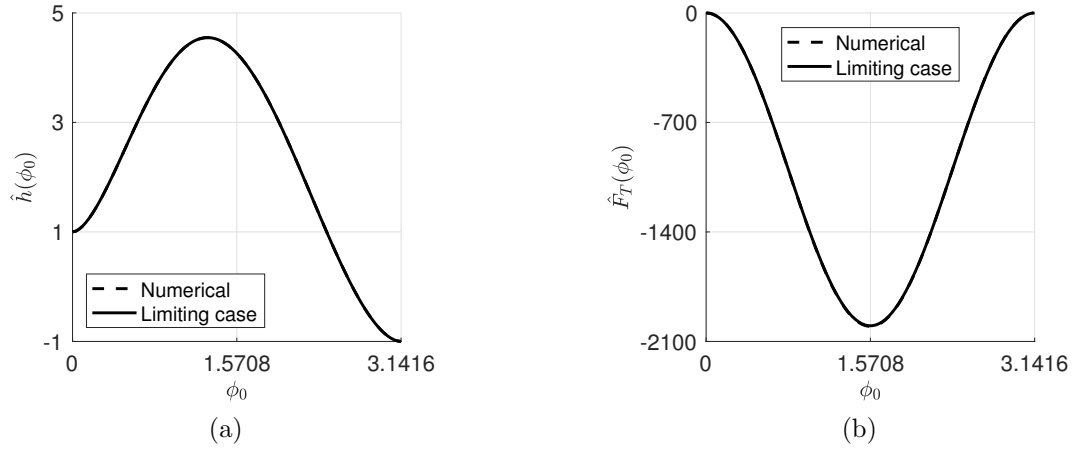


Figure 3.26: (a) The comparison between the numerical solution and the limiting case of the height curve with $B = 0.001$, $\gamma = 0$; (b) the comparison between the numerical solution and the limiting case of the total force curve with the same data and $\alpha = 0$.

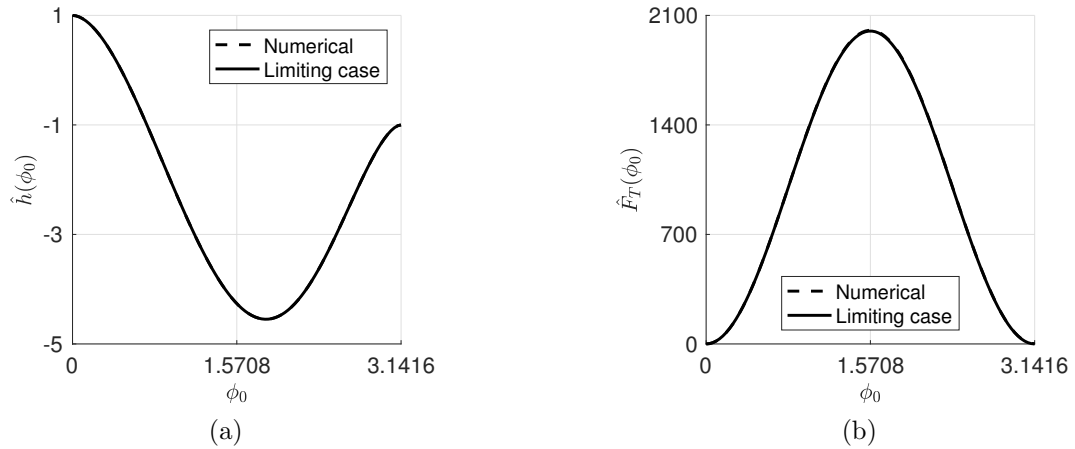


Figure 3.27: (a) The comparison between the numerical solution and the limiting case of the height curve with $B = 0.001$, $\gamma = \pi$; (b) the comparison between the numerical solution and the limiting case of the total force curve with the same data and $\alpha = 0$.

(i) when $\gamma = 0$, \hat{F}_T admits at most one forced balanced point. If there is only one forced balanced point, denoted as $\bar{\phi}_0$, then $\bar{\phi}_0$ must be a stable equilibrium point.

(ii) When $\gamma = \pi$, \hat{F}_T admits at most two forced balanced points.

(a) If there is only one forced balanced point, denoted as $\bar{\phi}_0$, then $\bar{\phi}_0 \leq \phi_0^*$, and $\bar{\phi}_0$ must be a stable equilibrium point.

(b) If there are two forced balanced points, denoted as $\bar{\phi}_{01}$ and $\bar{\phi}_{02}$, then, $\bar{\phi}_{01} < \phi_0^* < \bar{\phi}_{02}$, the smaller one must be stable, the larger one can be either stable or unstable.

As discussed in Sec. 3.8.4, as $B \rightarrow \infty$, the limiting total force \hat{F}_1 behaves quite different from the other cases. When $\alpha \in (0, 1)$, there is a stable force balanced point. When $\alpha > 1$, there is no force balanced point.

Therefore, we can summarize above observations and conjectures in Conjecture 3.

Conjecture 3. *With $B > 0$, $\alpha > 0$ and $\gamma \in [0, \pi]$, there are at most two force balance points for the floating ball system. If there is only one forced balanced point, it must be a stable equilibrium point. If there are two forced balanced points, the smaller one must be stable, the larger one can be either stable or unstable.*

3.9 Illustrating the Number of Equilibria and their Stability

We discuss the number of equilibria and their stability in Sec. 3.8.5 based on the numerical observation. The values of parameters B , α and γ play important roles in determining the number of equilibrium points and their stability. In this section, we would like to illustrate those information in B versus α region with a given $\gamma \in [0, \pi]$, where $B > 0$ and $\alpha > 0$. Examples with typical contact angles, $\gamma = 0, \frac{\pi}{10}, \frac{\pi}{4}, \frac{\pi}{2}, \frac{3\pi}{4}, \frac{5\pi}{6}$ and π will be given. The boundary curves, denoted as \mathcal{C}_i , are used to distinguish the regions with different number of equilibria and their stability. The boundary curves \mathcal{C}_i can be expressed as follows,

$$(i) \mathcal{C}_1: \hat{F}_T(\pi) = 0 \quad \Leftrightarrow \quad \alpha = 1.$$

$$(ii) \mathcal{C}_2: \hat{F}_T(\phi_0^{**}) = 0, \text{ where } \phi_0^{**} > \frac{\pi}{2} \text{ satisfying } \hat{h}'(\phi_0^{**}) = 0.$$

$$(iii) \mathcal{C}_3: \hat{F}_T(\phi_0^*) = 0, \text{ where } \phi_0^* > \frac{\pi}{2} \text{ satisfying } \frac{d\hat{F}_T}{d\phi_0}(\phi_0^*) = 0.$$

From the property of \hat{F}_T (Property 4), $\hat{F}_T(\pi) = 0$ with $\alpha = 1$ and any $B > 0$ and $\gamma \in [0, \pi]$. If $\gamma = 0$, \hat{h} and \hat{F}_T have no critical point in $(\frac{\pi}{2}, \pi)$, see Conjecture 2 in Sec. 3.8.5. Hence, the boundary curves \mathcal{C}_2 and \mathcal{C}_3 do not exist. Thus, \mathcal{C}_1 , $\alpha = 1$, is the boundary curve between the region with one equilibrium point, denoted as \mathcal{R}_1 and the region with no equilibrium point, denoted as \mathcal{R}_0 . Moreover, the equilibrium point lying in \mathcal{R}_1 is always stable from the result in Sec. 3.8.5. Therefore, when $\gamma = 0$, only \mathcal{C}_1 curve appears in B vs α region, see Fig. 3.28.

When $\gamma \in (0, \pi]$ and any given $B > 0$, the boundary curve \mathcal{C}_1 is $\alpha = 1$, which is the same that in the $\gamma = 0$ case. However, in the $\gamma > 0$ case, \mathcal{C}_1 is the boundary curve between the region with one stable equilibrium point, which is \mathcal{R}_1 and the region with two stable equilibrium points, denoted as $\mathcal{R}_{2,2}$. According to the discussion in Sec. 3.8.5, it guarantees the existence of the boundary curves \mathcal{C}_2 and \mathcal{C}_3 , but they have to be found numerically. With $\gamma \in (0, \pi]$ being fixed, to obtain the point, (α, B) , of the boundary curve \mathcal{C}_2 , given the value of B , we solve $\hat{h}'(\phi_0^{**}) = 0$ for $\phi_0^{**} > \frac{\pi}{2}$ numerically, and plug ϕ_0^{**} into \hat{F}_T such that $\hat{F}_T(\phi_0^{**}) = 0$ to achieve the corresponding value of α . The similar procedure can be applied to obtain the boundary curve \mathcal{C}_3 . The boundary curve \mathcal{C}_2 distinguishes between the region $\mathcal{R}_{2,1}$ and the region $\mathcal{R}_{2,2}$, where $\mathcal{R}_{2,1}$ means the region has two equilibrium points and the smaller one is stable and the larger one is unstable. The boundary curve \mathcal{C}_3 distinguishes between the region $\mathcal{R}_{2,1}$ and the region \mathcal{R}_0 . Fig. 3.29, Fig. 3.30, Fig. 3.31, Fig. 3.32, Fig. 3.33a and Fig. 3.34 illustrate the $\gamma = \frac{\pi}{10}$ case, the $\gamma = \frac{\pi}{4}$ case, the $\gamma = \frac{\pi}{2}$ case, the $\gamma = \frac{3\pi}{4}$ case, the $\gamma = \frac{5\pi}{6}$ and the $\gamma = \pi$ case respectively. As we can see, the boundary curves $\mathcal{C}_1 - \mathcal{C}_3$ behave similarly in the $\gamma > 0$ cases. As γ getting large, the $\mathcal{R}_{2,1}$ region is getting large, as well.

One special case with $\gamma = \frac{5\pi}{6}$ is considered. Suppose a ping-pong ball floating on a basin of water (at a temperature of 25°C), based on the data from Gabriel [25] and Wentz [64], the ping-pong ball has a radius $a = 2$ cm and the contact angle $\gamma \approx \frac{5\pi}{6}$, the value of κ for a basin of water is around 13.5 (cm) $^{-2}$. Thus, $B = \kappa a^2 \approx 54$. The B versus α region is zoomed in to fit the data, see Fig. 3.33b. As we can see, it is possible to observe two stable equilibrium points if the density ratio of the ping-pong ball to water is adjusted between 1 and 1.01. The comparison between the experiments with these data and our theoretical results can be interesting. Unfortunately, we are unable to do the experiments.

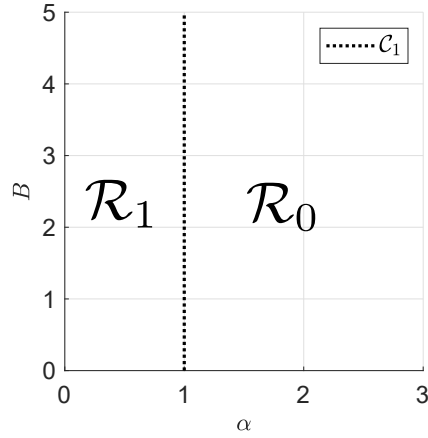


Figure 3.28: B versus α : the $\gamma = 0$ case. \mathcal{R}_1 region represents there is only one equilibrium point, which is stable. \mathcal{R}_0 is the region with no equilibrium point.

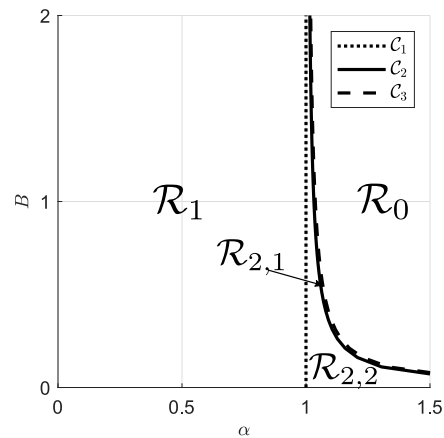


Figure 3.29: B versus α : the $\gamma = \frac{\pi}{10}$ case.

According to Vella's survey paper [61], the load-bearing capacity problem has been widely discussed in many papers. In the floating ball system, the \mathcal{C}_3 curve, the boundary curve between the region $\mathcal{R}_{2,1}$ and the region \mathcal{R}_0 , gives the maximum load-bearing condition. Unfortunately, the \mathcal{C}_3 curve has to be obtained numerically. A good approximate \mathcal{C}_3 curve suffices for experimental purpose. From above figures, \mathcal{C}_3 behaves like the hyperbolic decline curve with the vertical asymptote $\alpha = 1$. Suppose an approximate \mathcal{C}_3 curve has the form

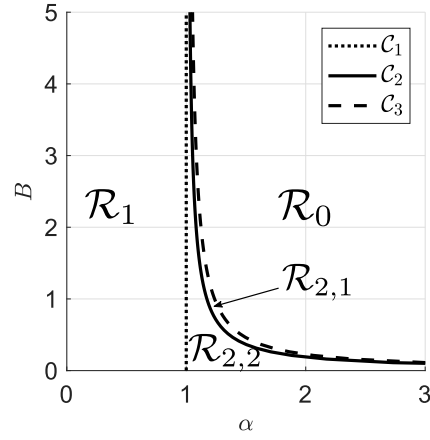


Figure 3.30: B versus α : the $\gamma = \frac{\pi}{4}$ case.

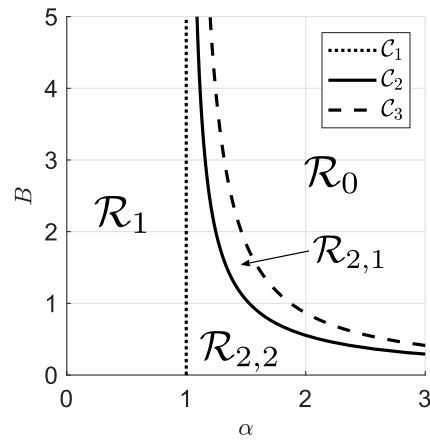


Figure 3.31: B versus α : the $\gamma = \frac{\pi}{2}$ case.

$$\hat{B} = \frac{\beta_1}{(\alpha - 1)^{\beta_2}}, \quad (3.370)$$

where $\beta_1 > 0$ and $\beta_2 > 0$ are to be determined. Rearranging (3.370), we have

$$\ln(\hat{B}) = \ln(\beta_1) - \beta_2 \ln(\alpha - 1). \quad (3.371)$$

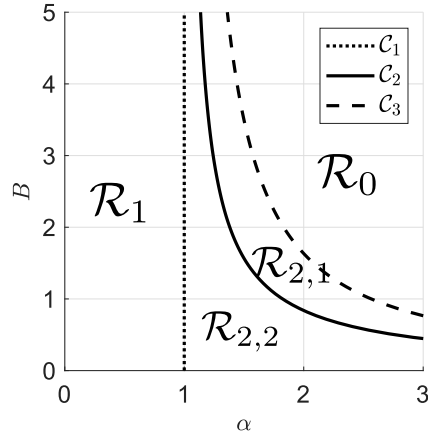


Figure 3.32: B versus α : the $\gamma = \frac{3\pi}{4}$ case.

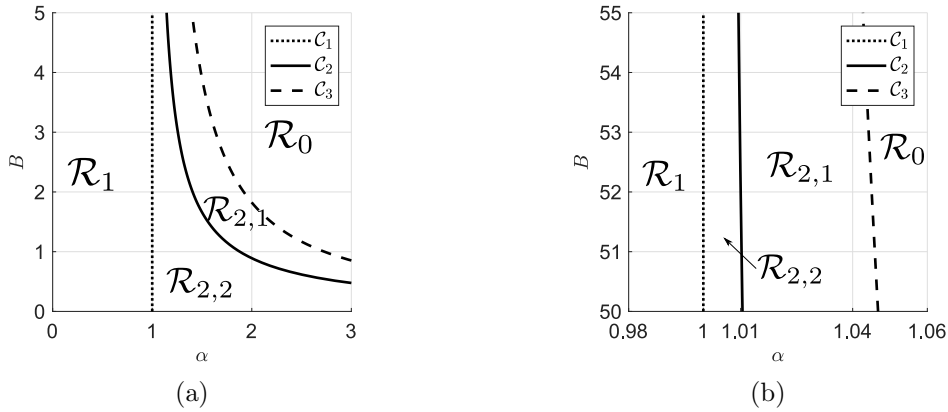


Figure 3.33: (a) B versus α : the $\gamma = \pi$ case; (b) the zoomed in region.

(3.371) becomes the linear equation of $\ln(B)$ and $\ln(\alpha - 1)$. The least squares method can be applied to determine β_1 and β_2 given the data set of (α, B) . Recall that the coefficient of determination R^2 is defined as follows,

$$R^2 = 1 - \frac{\sum_{i=1}^n (B_i - \hat{B}_i)^2}{\sum_{i=1}^n (B_i - \bar{B})^2}, \quad (3.372)$$

where \hat{B}_i is the calculated value from (3.370) and \bar{B} denotes the mean of B_i . R^2 is used to

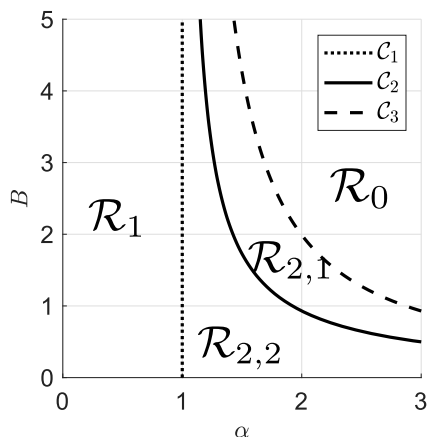


Figure 3.34: B versus α : the $\gamma = \pi$ case.

measure the performance of the fitted curve (the more R^2 close to 1, the better the overall performance of the fitted curve is).

In Fig. 3.35, it shows the comparison between the numerical \mathcal{C}_3 curve and the approximate \mathcal{C}_3 curve, see (3.373) for the $\gamma = \frac{3\pi}{4}$ case. They are indistinguishable, which is consistent with $R^2 = 0.9999$.

$$\hat{B} = \frac{0.8307}{(\alpha - 1)^{0.9053}}. \quad (3.373)$$

Remark 26. The boundary curve between $\mathcal{R}_{2,1}$ and $\mathcal{R}_{2,2}$, \mathcal{C}_2 , has the similar behavior as the \mathcal{C}_3 curve. (3.370) can also be applied to approximate the \mathcal{C}_2 curve.

3.10 Numerical Results

In this section, we present two examples. One admits two stable equilibrium configurations. Another example has no force balanced point where there is an energy minimizer. A modification is considered to explain this case.

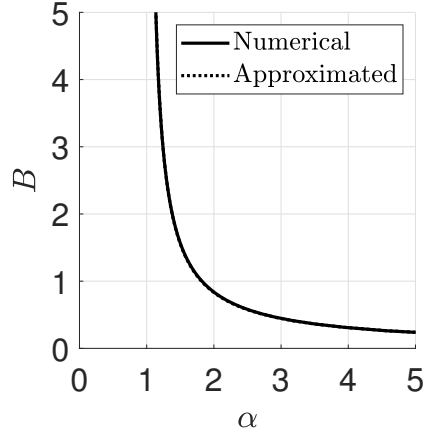


Figure 3.35: The comparison between the numerical \mathcal{C}_3 curve and the approximated \mathcal{C}_3 curve for the $\gamma = \frac{3\pi}{4}$ case

3.10.1 An Example with Two Stable Equilibria

Consider contact angle $\gamma = \frac{\pi}{2}$, capillary constant $\kappa = 1$, the radius of the ball $a = 1$ (hence, $B = 1$) and the density ratio $\alpha = 1.4$ (hence, $\frac{\rho_m}{\rho} = 1.4$). It implies two force balanced points: $\phi_0 = 1.9262$ and $\phi_0 = 2.8791$, see Fig. 3.37b. The corresponding \hat{E}_T can be shown in Fig. 3.36. There are 4 critical points of \hat{E}_T : $\phi_0 = 0.3551$ and $\phi_0 = 2.8765$ (in black squares), and $\phi_0 = 1.9262$ and $\phi_0 = 2.8791$ (in black circles). The critical points (in black squares) are the critical points of $\hat{h}(\phi_0)$, see Fig. 3.37a. The critical points (in black circles) are the force balanced points. Based on Theorem 20 (Stability criterion) in Sec. 3.6.4, both force balanced points are stable and are local minimum of \hat{E}_T , see Fig. 3.36 and Fig. 3.38.

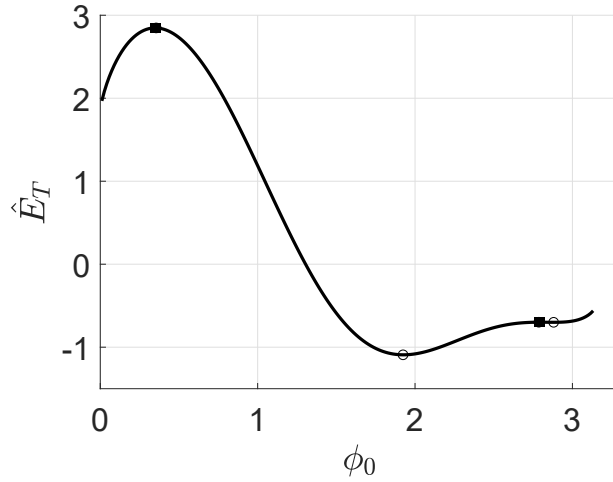


Figure 3.36: Given the density ratio 1.4, there are four critical points for \hat{E}_T : $\phi_0 = 0.3551$ and $\phi_0 = 2.7865$ (in black squares), and $\phi_0 = 1.9262$ and $\phi_0 = 2.8791$ (in black circles).

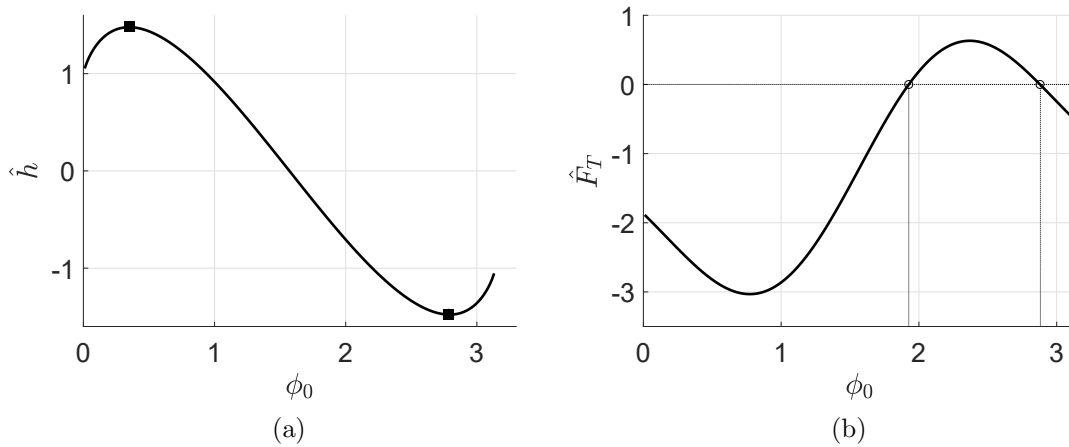


Figure 3.37: (a) There are two critical points of height $\hat{h}(\phi_0)$, the smaller one $\phi_0 = 0.3551$ and the larger one $\phi_0 = 2.7865$. Those two extreme points are shown in the black squares; (b) two force balanced points $\phi_0 = 1.9262$ and $\phi_0 = 2.8791$.

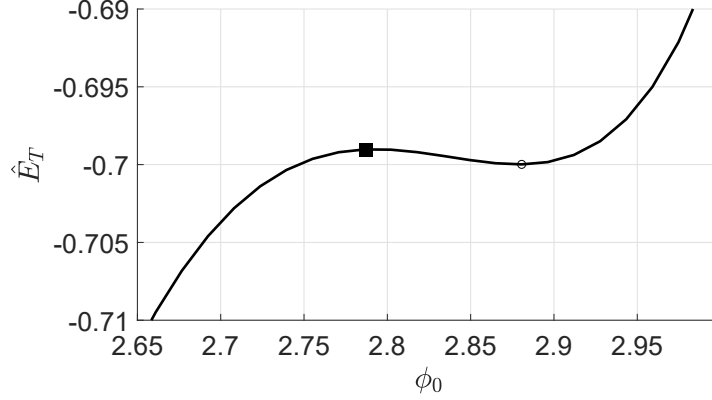


Figure 3.38: The zoomed in figure for \hat{E}_T with the density ratio 1.4, the critical point $\phi_0 = 2.7865$ (in black square) is the critical point of $\hat{h}(\phi_0)$ and the critical point $\phi_0 = 2.8791$ (in black circle) is the force balanced point.

3.10.2 An Example with No Force Balanced Point

According to the observation in Sec. 3.8.5, it is possible to obtain the case that there is no force balanced point but the critical point of the height exists. Consider $\gamma = \frac{\pi}{2}$, $B = 1$ and $\alpha = 2.2$, there is no force balanced point, see in Fig. 3.39a. The corresponding \hat{E}_T can be seen in Fig. 3.39b. There are two critical points of \hat{E}_T , $\phi_0 = 0.3551$ and $\tilde{\phi}_0 = 2.7865$, but they are the critical points of $\hat{h}(\phi_0)$, see Fig. 3.37a. A similar argument in Sec. 3.6.4 will show the critical point of height, $\tilde{\phi}_0$, is a local minimum point of \hat{E}_T . Based on Fig. 3.37a and Fig. 3.39a, $\hat{F}_T(\tilde{\phi}_0) < 0$ and $\hat{h}'(\tilde{\phi}_0) = 0$. There exists an open interval $(\tilde{\phi}_0 - \delta, \tilde{\phi}_0 + \delta)$ for some arbitrarily small $\delta > 0$ such that $\hat{h}'(\tilde{\phi}_0) < 0$ on $(\tilde{\phi}_0 - \delta, \tilde{\phi}_0)$, $\hat{h}'(\tilde{\phi}_0) > 0$ on $(\tilde{\phi}_0, \tilde{\phi}_0 + \delta)$ and $\hat{F}_T(\phi_0) < 0$ on $(\tilde{\phi}_0 - \delta, \tilde{\phi}_0 + \delta)$. Thus,

$$\frac{d\hat{E}_T}{d\phi_0}(\tilde{\phi}_0) < 0 \text{ on } (\tilde{\phi}_0 - \delta, \tilde{\phi}_0), \quad (3.374)$$

$$\frac{d\hat{E}_T}{d\phi_0}(\tilde{\phi}_0) > 0 \text{ on } (\tilde{\phi}_0, \tilde{\phi}_0 + \delta). \quad (3.375)$$

Therefore, $\tilde{\phi}_0$ is a local minimum point of $\hat{E}_T(\phi_0)$. Moreover, Fig. 3.39b shows that $\tilde{\phi}_0 = 2.7865$ is a global energy minimizer.

However, the total force $\hat{F}_T < 0$, the ball cannot float. McCuan and Treinen [44] explained that the force balanced condition is necessary. In the derivation of the equilibrium configuration of a floating particle with only vertical movement, Miersemann [48] argued that the vertical force balance should be satisfied. We consider a modification. We plot \hat{E}_T vs \hat{h} in Fig. 3.41a. \hat{E}_T is not a graph with respect to \hat{h} . Near \hat{h}_{\max} and \hat{h}_{\min} , the system tends to have the configuration with smaller energy. We keep the monotonic portion between \hat{h}_{\max} and \hat{h}_{\min} , and consider the different topological structures for $\hat{h} \leq \hat{h}_{\min}$ and $\hat{h} \geq \hat{h}_{\max}$, see (3.376) and (3.377). When $\hat{h} \geq \hat{h}_{\max}$, the ball has no attachment with and is above the undisturbed liquid surface, there is only the gravitational energy. When $\hat{h} \leq \hat{h}_{\min}$, the ball is fully immersed in the liquid, the system contains only the gravitational energy and the fluid potential energy, see Fig. 3.40a and Fig. 3.40b.

$$\hat{E}_T(\hat{h}) = \frac{4}{3}\alpha\hat{h} \quad \text{for } \hat{h} \geq \hat{h}_{\max}, \quad (3.376)$$

$$\hat{E}_T(\hat{h}) = \frac{4}{3}(\alpha - 1)\hat{h} \quad \text{for } \hat{h} \leq \hat{h}_{\min}. \quad (3.377)$$

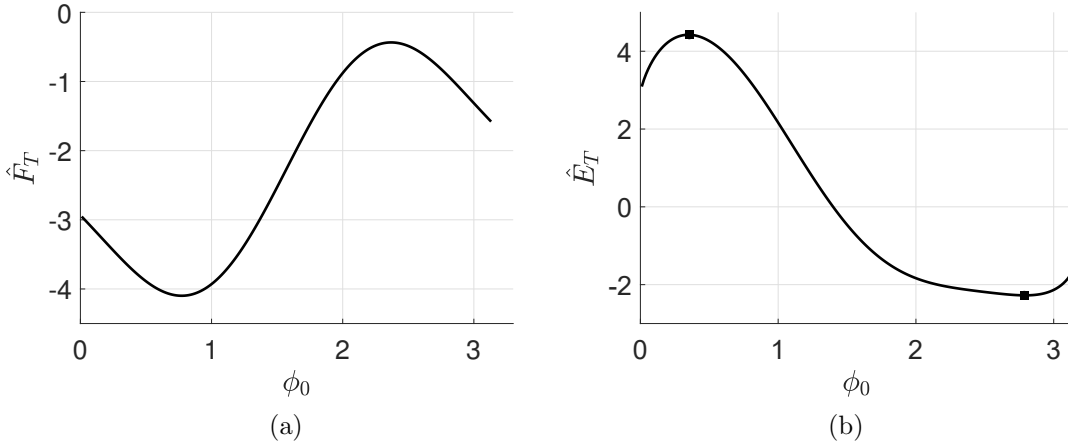


Figure 3.39: (a) Given the density ratio 2.2, there is no force balanced point, (b) the corresponding \hat{E}_T has two critical points: $\phi_0 = 0.3551$ and $\phi_0 = 2.7865$ (in black squares), which are related with the critical points of $\hat{h}(\phi_0)$.

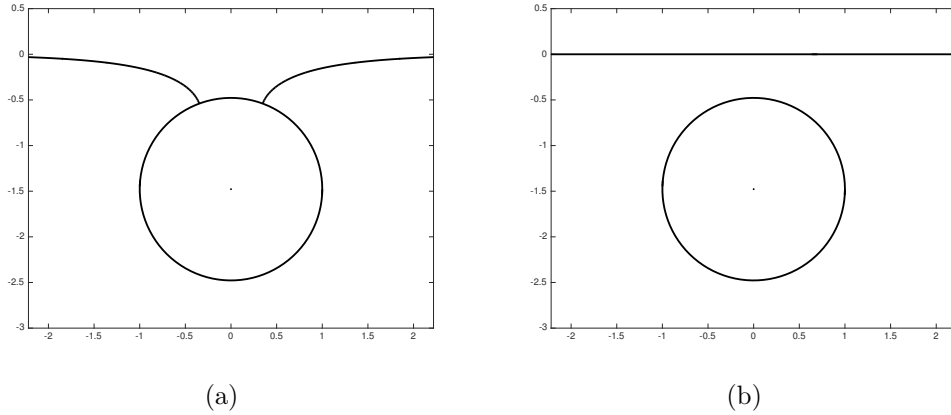


Figure 3.40: (a) The configuration for $\hat{h} = \hat{h}_{\min}$, (b) a different topological structure for $\hat{h} = \hat{h}_{\min}$.

The Fig. 3.41b shows the modified \hat{E}_T vs \hat{h} figure. We can see that there is no locally minimum pointed with respect to \hat{h} . There are energy discontinuities at $\hat{h} = \hat{h}_{\min}$ and $\hat{h} = \hat{h}_{\max}$. The jump difference $\Delta\hat{E}_T \approx 0.089$. Such jump discontinuities are also found in Finn and Vogel [23].

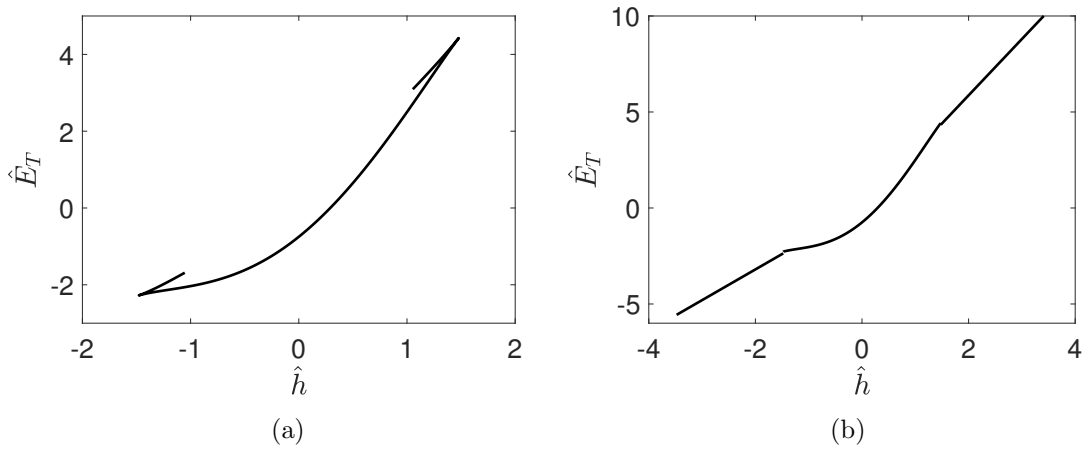


Figure 3.41: (a) \hat{E}_T vs \hat{h} with data: $\gamma = \frac{\pi}{2}$, $B = 1$ and $\alpha = 2.2$, (b) the modified \hat{E}_T vs \hat{h} with the same data.

3.11 Conclusion

In this chapter, we studied the number of equilibria and their stability of a ball floating on an unbounded bath. First of all, the behavior of the fluid height is investigated. When the uniqueness argument [13] and the geometric constraint are applied, the fluid interface can be uniquely determined by an attachment angle ϕ_0 . The fluid interface can be either a graph or a non-graph. Both graph and parametric descriptions of solutions are considered. In the non-graph case, we write the parametric solutions as $\bar{r}(\psi; \phi_0)$ and $\bar{u}(\psi; \phi_0)$. The zero solution $\bar{u} = 0$ is not contained in the parametric form so the graph description of the form $\bar{u}(\bar{r}; \bar{r}_0, \bar{u}_0)$ is considered as in Vogel [63]. We develop C^1 smoothness of u_0 with respect to ϕ_0 . This requires an extension of Vogel's description of solutions and monotonicity results. As a by-product, Vogel's conjecture on the smoothness of the envelope of exterior solutions is shown. The limiting behavior of solutions is investigated. By applying Theorem 2 (Olver [49]) and Theorem 16 (Levinson's theorem [12]), we develop the asymptotic behavior of $\bar{r}(\psi; \phi_0)$ and $\bar{u}(\psi; \phi_0)$, $\dot{w}(\bar{r}, r_w, \xi)$, $\dot{\bar{r}}(\psi; \phi_0)$ and $\dot{\bar{u}}(\psi; \phi_0)$.

In the study of the number of equilibrium points and their stability, two approaches are considered, the energy and the force analysis. With the limiting behavior of solutions, we establish a relation between the total energy \hat{E}_T and the total force \hat{F}_T , that is, $\frac{d\hat{E}_T}{d\phi_0} = -\hat{F}_T \hat{h}'(\phi_0)$. Therefore, a critical point of \hat{E}_T can be either a force balanced point or a critical point of the height. A stability criterion is developed based on the relation. The fluid height at the contact point \hat{u}_0 appears in both $\hat{F}_T(\phi_0)$ and $\hat{h}(\phi_0)$, which is found by the shooting method numerically. This makes it difficult to analyze the problem. We investigate the behavior of \hat{u}_0 in the limiting cases $B \rightarrow 0$, $\phi_0 \rightarrow 0, \pi$ and $B \rightarrow \infty$. These help us understand the limiting behavior of the total force \hat{F}_T and the height \hat{h} . In numerical observation, we perform a series of numerical tests to study the behavior of $\hat{F}_T(\phi_0)$ and $\hat{h}(\phi_0)$ curves with different values of γ and B . We conjecture that the floating ball system admits at most two force balanced points. If there is only one forced balanced point, it must be stable. If there are two forced balanced points, the one with smaller attachment angle must be stable, the one with larger attachment angle can be either stable or unstable.

Moreover, we illustrate the information on the number of equilibria and their stability in B versus α figures with typical contact angles. The B versus α region can be divided into at most 4 sub-regions, the region with one equilibrium point \mathcal{R}_1 , the region with no equilibrium point \mathcal{R}_1 , the region with one stable and one unstable equilibrium points $\mathcal{R}_{2,1}$ and the region with two stable equilibrium points $\mathcal{R}_{2,2}$. The regions are separated by the boundary

curves. There are two boundary curves of our interest. The \mathcal{C}_2 curve is the boundary curve between the $\mathcal{R}_{2,2}$ region and the $\mathcal{R}_{2,1}$ region. The \mathcal{C}_3 curve is the boundary curve between the $\mathcal{R}_{2,1}$ region and the \mathcal{R}_0 region. The \mathcal{C}_3 curve gives the maximum load-bearing for a floating ball. We apply the curve fitting and obtain the approximate \mathcal{C}_3 curve with high accuracy, which can be used for experimental purpose.

Finally, we present two examples. One example admits two stable equilibrium configurations. Another example shows the case with no force balanced point where there is an energy minimizer. It is not physically realizable. We cannot simply write the total energy as a function of \hat{h} due to the non-uniqueness of the floating configurations with the same height. A modification of changing topological structure for the floating configurations is considered to explain this issue.

The conjecture of the number of equilibria and their stability is based on the numerical observation. An analytical approach is anticipated, which requires understanding on the behavior of \hat{u}_0 as well as $\hat{F}_T(\phi_0)$ and $\hat{h}(\phi_0)$. In limiting cases, the asymptotic expansion of \hat{u}_0 is assumed to be differentiable. The behavior of $\frac{d\hat{u}_0}{d\phi_0}$ plays an important rule on the study of stability. We studied the signs of $\hat{F}'_T(\bar{\phi}_0)$ and $\hat{h}'(\bar{\phi}_0)$, where $\bar{\phi}_0 = \pi - \gamma + \mathcal{O}(B)$, for small Bond number, the limits of $\frac{d\hat{u}_0}{d\phi_0}$ at $\phi_0 = 0, \pi$ and the asymptotics of $\frac{d\hat{u}_0}{d\phi_0}$ for large Bond number. The full analysis of $\frac{d\hat{u}_0}{d\phi_0}$ can be a potential future work. For a given contact angle, the number of equilibria and their stability can be illustrated in B versus α figure. We have not compared the theoretical results with experiments due to constraints. An experiment is expected to validate the result of two stable configurations in future study. In Appendix B.3, we discuss an iterative method to find the fluid interface numerically when it is a graph. Practically, it works well and converges fast. However, we cannot prove the convergence by error analysis. It can be another potential topic.

Chapter 4

The Capillary Surface in a Tilted Wedge

4.1 Introduction

The behavior of the capillary surface in a vertical wedge has been studied in recent decades. Suppose there is a wedge domain Ω in xy -plane with a vertex located at the origin $O = (0, 0)$. Near the origin, the x -axis bisects the wedge with the opening angle 2α , $0 < \alpha < \frac{\pi}{2}$. The wall (the boundary of the wedge) is denoted as Σ . Assume that the capillary surface $u = u(x, y)$ over the wedge Ω is a graph and meets the wall Σ with the prescribed contact angle γ , $0 \leq \gamma < \frac{\pi}{2}$. The capillary surface can be determined by the BVP in (1.3) and (1.4). Recall that,

$$Nu = \kappa u \quad \text{in } \Omega, \quad (4.1)$$

$$\nu \cdot Tu = \cos \gamma \quad \text{on } \Sigma, \quad (4.2)$$

where ν is the outward normal of Σ .

When $0 < \alpha + \gamma < \frac{\pi}{2}$, Concus and Finn [6] and Finn [18] introduced an approximate solution $v_1(r, \theta)$ near the corner,

$$v_1(r, \theta) = \frac{h_1(\theta)}{r}, \quad (4.3)$$

where $h_1(\theta) = \frac{\cos \theta - \sqrt{k^2 - \sin^2 \theta}}{k\kappa}$ and $k = \frac{\sin \alpha}{\cos \gamma}$. Near the corner, the error bound $u = v_1 + \mathcal{O}(1)$ is established. Miersemann [45, 46] studied the $0 < \alpha + \gamma < \frac{\pi}{2}$ case. He improved the error bound of $|u - v_1|$ to $\mathcal{O}(r^\lambda)$ for some $\lambda > 0$. In [46], Miersemann showed that there exists an asymptotic expansion of u near the corner and its leading order term is v_1 . The error bound is improved to $\mathcal{O}(r^3)$. The $\alpha + \gamma \geq \frac{\pi}{2}$ case has been studied, as well. Concus and Finn [6] showed that u is bounded if and only if $\alpha + \gamma \geq \frac{\pi}{2}$. More related topics can be seen in Siegel and Lancaster [39] and Aoki and Siegel [2].

In this chapter, the $0 < \alpha + \gamma < \frac{\pi}{2}$ case is considered. We are interested in whether the capillary surface is still unbounded if the wedge is tilted by a small angle from the vertical axis. A rotation of a coordinate system can be described by Euler's angles, see Sec. 4.1.2. Using the invariance of mean curvature under rotation, a tilted capillary equation is obtained, which is an equation of mean curvature type, see Korevaar and Simon [36].

The main tool to study the problem is the comparison principle. Following Miersemann's idea [45] [46], the particular forms of a sub-solution, $w_-(r, \theta)$, and a super-solution, $w_+(r, \theta)$, are considered. Under the construction, an approximate solution $v(r, \theta)$ is employed, which has the same form as v_1 in (4.3) but with a different capillary constant. The discussion of the approximate solution $v(r, \theta)$ can be seen in Sec. 4.2. In Sec. 4.3, we consider the sub-solution and super-solution of the forms $w_\pm(r, \theta) = v(r, \theta) \pm Ar^\lambda$ for $0 < r \leq r_0 < 1$ with small $r_0 > 0$. We show that $|u - v| \leq Ar^\lambda$ in Ω_{r_0} , see conditions in Theorem 26. In Sec. 4.4, a more general form of $w_\pm(r, \theta)$ is considered. The error bound can be improved to $\mathcal{O}(r)$. The conclusion is addressed in Sec. 4.5.

4.1.1 A Wedge Domain in Cylindrical Coordinates

To work with a bounded domain, consider a disk B_{r_0} centered at the origin with a radius $r_0 > 0$. Define $\Omega_{r_0} = (\Omega \cap B_{r_0}) \setminus \{O\}$, $\Sigma_{r_0} = (\Sigma \cap B_{r_0}) \setminus \{O\}$ and $\Gamma_{r_0} = \Omega \cap \partial B_{r_0}$, see Fig. 4.1a. For convenience, we use the cylindrical coordinates (r, θ, z) . The bounded wedge can be decomposed into

- (i) the interior region $\Omega_{r_0} = \{(r, \theta), 0 < r < r_0, -\alpha < \theta < \alpha\}$;
- (ii) the wall $\Sigma_{r_0} = \{(r, \theta), 0 < r < r_0, \theta = \pm\alpha\}$;

(iii) the arc $\Gamma_{r_0} = \{(r, \theta), r = r_0, -\alpha < \theta < \alpha\}$.

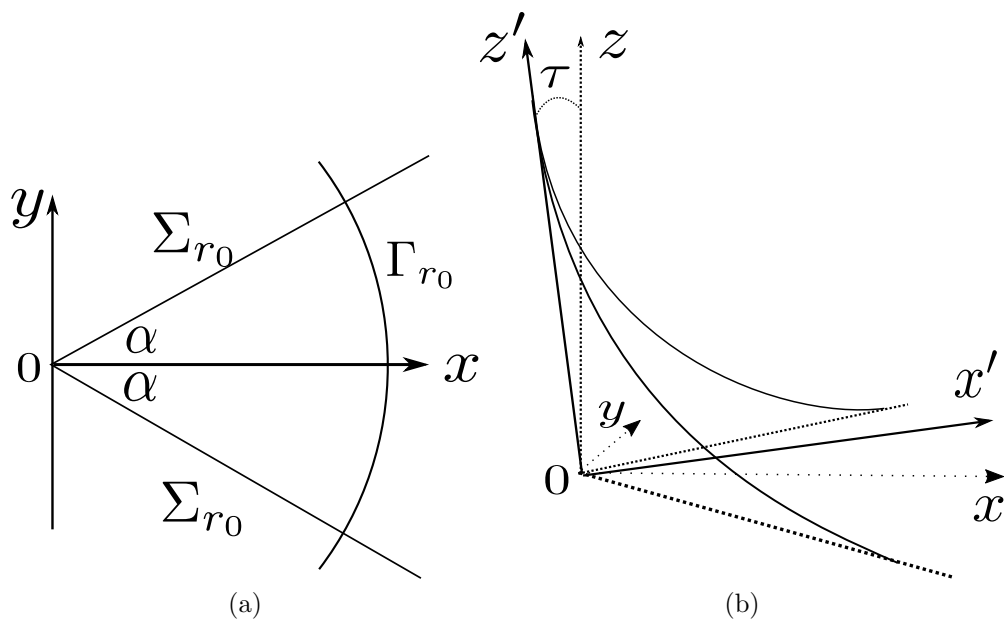


Figure 4.1: (a) A bounded wedge domain; (b) a tilted wedge along the negative x axis with an angle $\tau \in \left(0, \frac{\pi}{2}\right)$.

In (4.1), $Nu = \text{div}Tu$, where Tu represents the inward-pointing unit normal of the surface u , in cylindrical coordinates. Tu has the form

$$Tu = \frac{\nabla u}{\sqrt{1 + |\nabla u|^2}} = Tu_1 \hat{\mathbf{r}} + Tu_2 \hat{\theta}. \quad (4.4)$$

where

$$Tu_1 = \frac{\frac{\partial u}{\partial r}}{\sqrt{1 + \left(\frac{\partial u}{\partial r}\right)^2 + \left(\frac{1}{r} \frac{\partial u}{\partial \theta}\right)^2}},$$

$$Tu_2 = \frac{\frac{1}{r} \frac{\partial u}{\partial \theta}}{\sqrt{1 + \left(\frac{\partial u}{\partial r}\right)^2 + \left(\frac{1}{r} \frac{\partial u}{\partial \theta}\right)^2}}.$$

Therefore, in cylindrical coordinates, twice the mean curvature Nu has the form

$$Nu = \operatorname{div}Tu = \frac{1}{r} \frac{\partial}{\partial r}(rTu_1) + \frac{1}{r} \frac{\partial}{\partial \theta}Tu_2. \quad (4.5)$$

4.1.2 Tilted Capillary Equation

A rotation of a coordinate system can be described by three angles ϕ , τ and ψ , known as Euler's angles. The detailed description of Euler's angles can be seen in Appendix C.1. When tilting the wedge from $x - y - z$ coordinates to $x' - y' - z'$ coordinates with Euler's angles, we restrict $\phi \in (0, 2\pi]$, $\tau \in \left(0, \frac{\pi}{2}\right)$ and $\psi \in (0, 2\pi]$ to ensure the tilted z' axis pointing upward. Two coordinate systems are linked by a rotation matrix $R(\phi, \tau, \psi)$. Therefore,

$$\begin{pmatrix} x' \\ y' \\ z' \end{pmatrix} = R(\phi, \tau, \psi) \begin{pmatrix} x \\ y \\ z \end{pmatrix}, \quad (4.6)$$

where the rotation matrix $R(\phi, \tau, \psi)$ is defined in (C.4) in Appendix C.1.

Both coordinates (x, y, z) and (x', y', z') can be converted to cylindrical coordinates as well, saying (r, θ, z) and (r', θ', z') , respectively. The original z component of the cylindrical coordinates can be expressed by the tilted cylindrical coordinates, that is,

$$z = r_{31}x' + r_{32}y' + r_{33}z', \quad (4.7)$$

where r_{31} , r_{32} , r_{33} are elements in the third row of $R^T(\phi, \tau, \psi)$. In detail,

$$r_{31} = -\sin \tau \cos \phi, \quad r_{32} = \sin \tau \sin \phi \quad \text{and} \quad r_{33} = \cos \tau. \quad (4.8)$$

In the tilted coordinates, due to the invariance of the mean curvature of the surface, we have

$$N_{(r', \theta')} u' = N_{(r, \theta)} u = \kappa u, \quad (4.9)$$

where $u' = u'(r', \theta')$ represents the tilted capillary surface.

Thus, the tilted capillary equation becomes

$$N_{(r', \theta')} u' = \kappa \cos \tau u' + \kappa \sin \tau (\sin \phi \sin \theta' - \cos \phi \cos \theta') r'. \quad (4.10)$$

In addition, the contact angle between the tilted capillary surface and the wall is unchanged (the contact angle is invariant under the coordinate systems), then,

$$\nu' \cdot T_{(r', \theta')} u' = \cos \gamma, \quad (4.11)$$

where ν' denotes the outward normal of the tilted wall Σ' .

In the later discussion, we focus on the tilted coordinates. As a convenience, we replace (r', θ', z') by (r, θ, z) . The BVP of the tilted capillary equation is obtained, shown as follows,

$$Nu = \bar{\kappa} u + f(\theta; \kappa, \phi, \tau) r \quad \text{in } \Omega_{r_0}, \quad (4.12)$$

$$\nu \cdot Tu = \cos \gamma \quad \text{on } \Sigma_{r_0}, \quad (4.13)$$

where $\bar{\kappa} = \kappa \cos \tau > 0$ and

$$f(\theta; \kappa, \phi, \tau) = -\kappa \sin \tau \cos(\theta + \phi). \quad (4.14)$$

Moreover, $|f(\theta; \kappa, \phi, \tau)| \leq \kappa$. (4.12) is an equation of mean curvature type, see Korevaar and Simon [36] and it shows twice the mean curvature of the tilted capillary surface is

linear in u . Existence of a solution to (4.12) and (4.13) will be assumed. The work of Korevaar and Simon provides the key boundary gradient estimate needed for an existence proof.

For a special case, we tilt the corner of the wedge (z axis) along the negative x axis with an angle $\tau \in \left(0, \frac{\pi}{2}\right)$, shown in Fig. 4.1b. To use Euler's angles, in this case, we have $\phi = \pi, \tau = \tau$ and $\psi = \pi$. The coordinates transformation can be expressed as

$$\begin{pmatrix} x \\ y \\ z \end{pmatrix} = \underbrace{\begin{pmatrix} \cos \tau & 0 & -\sin \tau \\ 0 & 1 & 0 \\ \sin \tau & 0 & \cos \tau \end{pmatrix}}_{R^T(\pi, \tau, \pi)} \begin{pmatrix} x' \\ y' \\ z' \end{pmatrix}. \quad (4.15)$$

And in this case, $f(\theta; \kappa, \phi, \tau) = \kappa \sin \tau \cos \theta$.

4.2 Approximate Solution $v(r, \theta)$

Near the corner of the wedge, the gradient of the tilted solution to (4.12) is sufficiently large (i.e. $|\nabla u| \gg 1$). Thus, $Tu \approx \frac{\nabla u}{|\nabla u|}$. Let $v(r, \theta)$ be the solution of the ‘‘approximate’’ equation, see as follows,

$$\operatorname{div} \hat{T}v = \bar{\kappa}v \quad \text{in } \Omega_{r_0}, \quad (4.16)$$

$$\nu \cdot \hat{T}v = \cos \gamma \quad \text{on } \Sigma_{r_0}, \quad (4.17)$$

where $\hat{T}v = \frac{\nabla v}{|\nabla v|}$. Geometrically, $\hat{T}v$ represents the inward-pointing unit normal of the level curve $v = C$, for some $C > 0$. Therefore, (4.16) shows the curvature of $v = C$ is equal to $\bar{\kappa}v$ and (4.17) shows the level curve meets the boundary Σ_{r_0} with the angle γ , see Ron [28]. Fortunately, the above BVP of this fully non-linear PDE has an explicit solution, see King and Ockendon [35]. We reproduce the details for a reference. In polar coordinates, the level curve $v(r, \theta) = C$ has the form:

$$(r \cos \theta - x_0)^2 + (r \sin \theta - y_0)^2 = \left(\frac{1}{\bar{\kappa}v}\right)^2, \quad (4.18)$$

where $x_0 = \frac{1}{k\bar{k}v}$, $y_0 = 0$, see Fig. 4.2, and $k = \frac{\sin \alpha}{\cos \gamma}$ from (4.17). In addition, $0 < k = \frac{\sin \alpha}{\cos \gamma} < \frac{\sin \alpha}{\cos(\frac{\pi}{2} - \alpha)} = 1$ with $0 < \alpha + \gamma < \frac{\pi}{2}$.

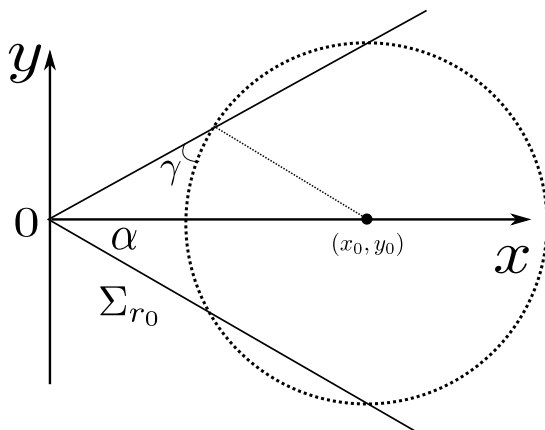


Figure 4.2: The level curve of $v(r, \theta) = C$.

(4.18) gives a quadratic equation of x_0 ,

$$(1 - k^2)x_0^2 - 2(r \cos \theta)x_0 + r^2 = 0. \quad (4.19)$$

By solving (4.19),

$$x_0 = \frac{r \cos \theta \pm r \sqrt{k^2 - \sin^2 \theta}}{1 - k^2}, \quad (4.20)$$

where + is valid ($x_0 > r$) and $k^2 - \sin^2 \theta > 0$ with $0 < \alpha + \gamma < \frac{\pi}{2}$, since $k^2 - \sin^2 \theta \geq \left(\frac{\sin \alpha}{\cos \gamma}\right)^2 - \sin^2 \alpha > 0$.

Therefore, we obtain

$$v(r, \theta) = \frac{h(\theta)}{r}, \quad (4.21)$$

where $h(\theta) = \frac{\cos \theta - \sqrt{k^2 - \sin^2 \theta}}{k\bar{k}}$ and $k = \frac{\sin \alpha}{\cos \gamma}$.

The following Lemma 24 show the properties of $v(r, \theta)$, which is useful later on.

Lemma 24. *We restate the following properties based on Finn [18], with $\gamma \geq 0$,*

$$Nv - \bar{k}v = \mathcal{O}(r^3) \quad \text{in } \Omega_{r_0}, \quad (4.22)$$

$$\nu \cdot Tv - \cos \gamma = \mathcal{O}(r^4) \quad \text{on } \Sigma_{r_0}. \quad (4.23)$$

(4.22) stands for $|Nv - \bar{k}v| \leq c_v r^3$ for some constant $c_v > 0$, and (4.23) represents $|\nu \cdot Tv - \cos \gamma| \leq \hat{c}_v r^4$ for some constant $\hat{c}_v > 0$, $\forall 0 < r < r_0$. More precisely, it can be shown $\nu \cdot Tv = \cos \gamma - \zeta(r)$, for some $\zeta(r) > 0$ and $\zeta(r) = \mathcal{O}(r^4)$. In addition, when $\gamma = 0$, as $\theta \rightarrow \pm\alpha$, estimate in (4.22) is still valid and $\nu \cdot Tv = 1$ exactly.

Miersemann discussed the properties of $h(\theta)$ in [46]. We summarize the properties of $h(\theta)$ in the following Property 6,

Property 6. With $0 < \alpha + \gamma < \frac{\pi}{2}$ and $h(\theta)$ defined in (4.21), $-\alpha \leq \theta \leq \alpha$, the following properties are satisfied:

(i) $0 < h(\theta) \leq \frac{1}{k\bar{k}}$ for $\gamma \geq 0$ and $\theta \in [-\alpha, \alpha]$.

(ii) When $\gamma \geq 0$ and $\theta \in [-\alpha, \alpha]$, $c_h \bar{k} \leq \frac{1}{h(\theta)} \leq \frac{2k}{1-k^2} \bar{k}$ for some constant $c_h > 0$.

(iii) $h'(\theta) = \frac{\sin \theta}{\sqrt{k^2 - \sin^2 \theta}} h(\theta)$ for $\gamma > 0$ and $\theta \in [-\alpha, \alpha]$, or $\gamma = 0$ and $\theta \in (-\alpha, \alpha)$.

Moreover, when $\gamma = 0$, $h'(\theta)$ becomes singular as $\theta \rightarrow \pm\alpha$,

$$h'(\theta) \sim \frac{b_1 \text{sign}(\theta)}{\sqrt{\sin^2 \alpha - \sin^2 \theta}}, \quad (4.24)$$

where $b_1 = \frac{\cos \alpha}{\bar{k}}$.

(iv) $h''(\theta) = \left(\frac{k^2 \cos \theta}{(k^2 - \sin^2 \theta)^{3/2}} + \frac{\sin^2 \theta}{k^2 - \sin^2 \theta} \right) h(\theta)$ for $\gamma > 0$ and $\theta \in [-\alpha, \alpha]$, or $\gamma = 0$ and $\theta \in (-\alpha, \alpha)$. Moreover, when $\gamma = 0$, $h''(\theta)$ becomes singular as $\theta \rightarrow \pm\alpha$,

$$h''(\theta) \sim \frac{b_2}{(\sin^2 \alpha - \sin^2 \theta)^{3/2}}, \quad (4.25)$$

$$\text{where } b_2 = \frac{\sin \alpha \cos^2 \alpha}{\bar{\kappa}}.$$

(v) $h'(\theta)$ and $h''(\theta)$ are both bounded if $\gamma > 0$ and $\theta \in [-\alpha, \alpha]$, or $\gamma = 0$ and $\theta \in (-\alpha, \alpha)$.

Proof. Since $0 < \alpha + \gamma < \frac{\pi}{2}$ and with $\gamma \geq 0$ and $\theta \in [-\alpha, \alpha]$, thus, $0 < k < 1$ and $k^2 - \sin^2 \theta \geq 0$, where $k = \frac{\sin \alpha}{\cos \gamma}$. For (ii),

$$\begin{aligned} \frac{1}{h(\theta)} &= \frac{k\bar{\kappa}}{\cos \theta - \sqrt{k^2 - \sin^2 \theta}} \\ &= \frac{k\bar{\kappa}}{\cos \theta - \sqrt{k^2 - \sin^2 \theta}} \cdot \frac{\cos \theta + \sqrt{k^2 - \sin^2 \theta}}{\cos \theta + \sqrt{k^2 - \sin^2 \theta}} \\ &= \frac{k \left(\cos \theta + \sqrt{k^2 - \sin^2 \theta} \right)}{1 - k^2} \bar{\kappa}. \end{aligned} \quad (4.26)$$

From (4.26), there exists some constant $c_h > 0$ such that

$$c_h \bar{\kappa} \leq \frac{1}{h(\theta)} \leq \frac{2k}{1 - k^2} \bar{\kappa}.$$

(ii) implies $h(\theta) > 0$, and $0 < \cos \theta - \sqrt{k^2 - \sin^2 \theta} \leq 1$ gives $h(\theta) \leq \frac{1}{k\bar{\kappa}}$.

For $\gamma > 0$ and $\theta \in [-\alpha, \alpha]$, or $\gamma = 0$ and $\theta \in (-\alpha, \alpha)$, the first half parts of (iii) and (iv) can be easily calculated. When $\gamma = 0$, $h'(\theta)$ and $h''(\theta)$ become singular as $\theta \rightarrow \pm\alpha$, with $h(\pm\alpha) = \frac{\cos \alpha}{k\bar{\kappa}}$, $k = \sin \alpha$, we obtain

$$h'(\theta) \sim \frac{b_1 \text{sign}(\theta)}{\sqrt{\sin^2 \alpha - \sin^2 \theta}},$$

$$h''(\theta) \sim \frac{b_2}{(\sin^2 \alpha - \sin^2 \theta)^{3/2}},$$

where $b_1 = \frac{\cos \alpha}{\bar{\kappa}}$ and $b_2 = \frac{\sin \alpha \cos^2 \alpha}{\bar{\kappa}}$. Finally, (i),(iii) and (iv) imply (iv). \square

4.3 Error Bounds on the Tilted Capillary Surface

In this section, the comparison principle (see Theorem 1) will be applied to construct an upper bound and a lower bound of the tilted capillary surface. We state the version of the comparison principle appropriate to the problem in a wedge domain, see Miersemann [45, 46].

Theorem 25. (*Comparison Principle in a Wedge Domain*) Suppose $\bar{\kappa} > 0$, and consider u and w defined in $\Omega_{r_0} \cup \Sigma_{r_0} \cup \Gamma_{r_0}$, where the interior domain Ω_{r_0} , the boundary Σ_{r_0} , and the arc Γ_{r_0} are defined in Section 4.1.1 with $r_0 > 0$. If

$$(i) \quad Nu - Nw \geq \bar{\kappa}(u - w) \text{ in } \Omega_{r_0},$$

$$(ii) \quad u \leq w \text{ on } \Gamma_{r_0},$$

$$(iii) \quad \nu \cdot Tu \leq \nu \cdot Tw \text{ on } \Sigma_{r_0} \text{ and } \nu \text{ is the outward unit normal of } \Sigma_{r_0},$$

then $u \leq w$ in Ω_{r_0} .

Consider Miersemann's choices [46],

$$w_{\pm}(r, \theta) = v(r, \theta) \pm Aq(\theta)r^{\lambda}, \quad (4.27)$$

where $v(r, \theta)$ is defined in (4.21). Conditions for A and λ and choices of $q(\theta)$ will be discussed. We will show that w_{\pm} can also be applied to construct a sub-solution and a super-solution in Ω_{r_0} , see Sec. 4.3.1. Conditions on boundary Σ_{r_0} and arc Γ_{r_0} will be discussed in Sec. 4.3.2 and Sec. 4.3.3, respectively. The results are summarized in Sec. 4.3.4.

We first consider the $q(\theta) = 1$ case, $w_{\pm}(r, \theta) = v(r, \theta) \pm Ar^{\lambda}$ for $0 < r \leq r_0 < 1$ with small $r_0 > 0$ and assume $0 < A\lambda \leq K_0$, $A > 0$ and $0 < \lambda < 1$ for some constant $K_0 > 0$.

4.3.1 Sub-solution and Super-solution in Ω_{r_0}

In this section, we discuss the conditions on A , λ and r_0 such that w_- and w_+ satisfy sub-solution and super-solution conditions in Ω_{r_0} , respectively. With $\gamma \geq 0$, we first try

$$w_-(r, \theta) = v(r, \theta) - Ar^{\lambda}. \quad (4.28)$$

By using the calculation in Appendix C.2, we expand Nw_- in Ω_{r_0} ,

$$Nw_- = Nv - P_1(\theta)r^{\lambda} + \eta_{1-} + \eta_{2-}, \quad (4.29)$$

where

$$P_1(\theta) = A\lambda(\lambda + 2)(h')^2 (h^2 + h'^2)^{-3/2} + A\lambda \left[h(\theta)h'(\theta) (h^2 + h'^2)^{-3/2} \right]_{\theta}, \quad (4.30)$$

$$|\eta_{1-}| \leq d'_{1-}A\lambda r^{\lambda+4} \quad \text{and} \quad |\eta_{2-}| \leq d'_{2-}A^2\lambda^2 r^{2\lambda+1} \quad (4.31)$$

for some constants $d'_{1-}, d'_{2-} > 0$.

From Property 6, if $\gamma \geq 0$, and h', h'' are away from their singularities, there exists some constant $c_{P_1} > 0$,

$$|P_1(\theta)r^{\lambda}| \leq c_{P_1}A\lambda r^{\lambda}. \quad (4.32)$$

While $\gamma = 0$, as $\theta \rightarrow \pm\alpha$, $P_1(\theta) \rightarrow 0$, (4.32) is also valid.

Remark 27. The expansion in (4.29) first appeared in Miersemann's work [45, 46]. But it has relatively few explanations. We follow Miersemann's idea and reproduce the expansion in details, see Appendix C.2.

The following Lemma 25 gives the conditions such that the sub-solution condition of w_- holds in Ω_{r_0} .

Lemma 25. *With $\gamma \geq 0$, and the assumption $0 < A\lambda \leq K_0$, $A > 0$ and $0 < \lambda < 1$, and under the conditions on A , λ and r_0 such that*

$$-c_{P_1}\lambda + \bar{\kappa} > 0 \quad (4.33)$$

and

$$A[-c_{P_1}\lambda + \bar{\kappa}]r^\lambda - \kappa r - d'_{2-}A^2\lambda^2r^{2\lambda+1} - d'_{1-}A\lambda r^{\lambda+4} - c_v r^3 \geq 0 \quad (4.34)$$

for $0 < r < r_0 < 1$. $c_v > 0$ is defined in Lemma 24, $d'_{1-} > 0$ and $d'_{2-} > 0$ are defined in (4.31) and $c_{P_1} > 0$ is defined in (4.32). Then w_- satisfies

$$Nw_- - Nu \geq \bar{\kappa}(w_- - u) \quad \text{in } \Omega_{r_0}.$$

Proof.

$$\begin{aligned} Nw_- - \bar{\kappa}w_- - f(\theta; \kappa, \phi, \tau)r &= Nv - \bar{\kappa}(v - Ar^\lambda) - P_1(\theta)r^\lambda + \eta_{1-} + \eta_{2-} - fr \\ &\geq (Nv - \bar{\kappa}v) + A[-c_{P_1}\lambda + \bar{\kappa}]r^\lambda - \kappa r - d'_{1-}A\lambda r^{\lambda+4} - d'_{2-}A^2\lambda^2r^{2\lambda+1} \\ &\geq A[-c_{P_1}\lambda + \bar{\kappa}]r^\lambda - \kappa r - d'_{2-}A^2\lambda^2r^{2\lambda+1} - d'_{1-}A\lambda r^{\lambda+4} - c_v r^3 \\ &\geq 0, \end{aligned}$$

based on conditions on (4.33), (4.34), $|f| \leq \kappa$ and $|Nv - \bar{\kappa}v| \leq c_v r^3$ for some constant $c_v > 0$ from Lemma 24. □

Similarly, we calculate Nw_+ :

$$Nw_+ = Nv + P_1(\theta)r^\lambda + \eta_{1+} + \eta_{2+}, \quad (4.35)$$

where

$$|\eta_{1+}| \leq d'_{1+}A\lambda r^{\lambda+4} \quad \text{and} \quad |\eta_{2+}| \leq d'_{2+}A^2\lambda^2r^{2\lambda+1} \quad (4.36)$$

for some constants $d'_{1+}, d'_{2+} > 0$.

Remark 28. In Lemma 25 - Lemma 28 and Lemma 30, we simply state the conditions. Those conditions will be checked together in Theorem 26.

The following Lemma 26 gives the conditions such that the super-solution condition of w_+ holds in Ω_{r_0} .

Lemma 26. *With $\gamma \geq 0$, and the assumption $0 < A\lambda \leq K_0$, $A > 0$ and $0 < \lambda < 1$, and under the conditions on A , λ and r_0 such that*

$$-c_{P_1}\lambda + \bar{\kappa} > 0 \quad (\text{the same as (4.33)}) \quad (4.37)$$

and

$$-A[\bar{\kappa} - c_{P_1}\lambda]r^\lambda + \kappa r + d'_{2+}A^2\lambda^2r^{2\lambda+1} + d'_{1+}A\lambda r^{\lambda+4} + c_v r^3 \leq 0 \quad (4.38)$$

for $0 < r < r_0 < 1$. $c_v > 0$ is defined in Lemma 24, $d'_{1+} > 0$ and $d'_{2+} > 0$ are defined in (4.36) and $c_{P_1} > 0$ is defined in (4.32). Then w_+ satisfies

$$Nw_+ - Nu \leq \bar{\kappa}(w_+ - u) \quad \text{in } \Omega_{r_0}.$$

Proof.

$$\begin{aligned} Nw_+ - \bar{\kappa}w_+ - f(\theta; \kappa, \phi, \tau)r &= Nv - \bar{\kappa}(v + Ar^\lambda) + P_1(\theta)r^\lambda + \eta_{1+} + \eta_{2+} - f(\theta; \kappa, \phi, \tau)r \\ &\leq (Nv - \bar{\kappa}v) - A[\bar{\kappa} - c_{P_1}\lambda]r^\lambda + \kappa r + d'_{1+}A\lambda r^{\lambda+4} + d'_{2+}A^2\lambda^2r^{2\lambda+1} \\ &\leq -A[\bar{\kappa} - c_{P_1}\lambda]r^\lambda + \kappa r + d'_{2+}A^2\lambda^2r^{2\lambda+1} + d'_{1+}A\lambda r^{\lambda+4} + c_v r^3 \\ &\leq 0, \end{aligned}$$

based on conditions on (4.37), (4.38), $|f| \leq \kappa$ and $|Nv - \bar{\kappa}v| \leq c_v r^3$ for some constant $c_v > 0$ from Lemma 24. □

4.3.2 Conditions on Boundary Σ_{r_0}

In this section, we discuss the conditions on A , λ and r_0 such that w_- and w_+ satisfy desired conditions on Σ_{r_0} , respectively. We consider the $\theta = \alpha$ case (similar for the $\theta = -\alpha$ case with only a sign difference), and have

$$\nu \cdot Tw_{\pm} = \frac{\frac{1}{r}w_{\pm\theta}}{\sqrt{1 + |\nabla w_{\pm}|^2}}, \quad \text{at } \theta = \alpha,$$

where ν is the outward normal of Σ_{r_0} with $\theta = \alpha$.

For $w_-(r, \theta)$, based on Appendix C.3, we have

$$\nu \cdot Tw_- = \frac{\frac{1}{r}w_{-\theta}}{\sqrt{1 + |\nabla w_-|^2}} = \nu \cdot Tv - G_1(\theta)r^{\lambda+1} + \hat{\eta}_{1-} + \hat{\eta}_{2-}, \quad (4.39)$$

where

$$G_1(\theta) = A\lambda h(\theta)h'(\theta) (h^2 + h'^2)^{-3/2} \quad (4.40)$$

and

$$|\hat{\eta}_{1-}| \leq \hat{d}'_{1-}A\lambda r^{\lambda+5} \quad \text{and} \quad |\hat{\eta}_{2-}| \leq \hat{d}'_{2-}A^2\lambda^2 r^{2\lambda+2} \quad (4.41)$$

for some constant $\hat{d}'_{1-}, \hat{d}'_{2-} > 0$.

From Property 6, if $\gamma > 0$, there exists some constant c_{G_1} , at $\theta = \alpha$,

$$c_{G_1}A\lambda r^{\lambda+1} \leq G_1(\theta)r^{\lambda+1}. \quad (4.42)$$

The following Lemma 27 gives the conditions such that the desired condition of w_- , $\nu \cdot Tw_- \leq \nu \cdot Tu$ holds on Σ_{r_0} .

Lemma 27. *With $\gamma > 0$, and the assumption $0 < A\lambda \leq K_0$, $A > 0$ and $0 < \lambda < 1$, and under the conditions on A , λ and r_0 such that*

$$-c_{G_1}A\lambda r^{\lambda+1} + \hat{d}'_{2-}A^2\lambda^2 r^{2\lambda+2} + \hat{c}_v r^4 + \hat{d}'_{1-}A\lambda r^{\lambda+5} \leq 0, \quad (4.43)$$

for $0 < r < r_0 < 1$. $\hat{c}_v > 0$ is defined in Lemma 24, $\hat{d}'_{1-} > 0$ and $\hat{d}'_{2-} > 0$ are defined in (4.41) and $c_{G_1} > 0$ is defined in (4.42). Then w_- satisfies

$$\nu \cdot Tw_- \leq \nu \cdot Tu \quad \text{on } \Sigma_{r_0}. \quad (4.44)$$

Moreover, when $\gamma = 0$, the inequality in (4.44) is an equality.

Proof.

$$\begin{aligned} \nu \cdot Tw_- - \nu \cdot Tu &\leq (\nu \cdot Tv - \nu \cdot Tu) - G_1(\theta)r^{\lambda+1} + \hat{\eta}_{1-} + \hat{\eta}_{2-} \\ &\leq -c_{G_1}A\lambda r^{\lambda+1} + \hat{d}'_{2-}A^2\lambda^2r^{2\lambda+2} + \hat{c}_v r^4 + \hat{d}'_{1-}A\lambda r^{\lambda+5} \\ &\leq 0, \end{aligned}$$

based on the condition on (4.43), and $|\nu \cdot Tv - \cos \gamma| \leq \hat{c}_v r^4$ for some constant $\hat{c}_v > 0$ from Lemma 24. In addition, when $\gamma = 0$, $\nu \cdot Tw_-$ meets the contact angle condition exactly. \square

Similarly, we calculate $\nu \cdot Tw_+$:

$$\nu \cdot Tw_+ = \nu \cdot Tv + G_1(\theta)r^{\lambda+1} + \hat{\eta}_{1+} + \hat{\eta}_{2+}, \quad (4.45)$$

where

$$|\hat{\eta}_{1+}| \leq \hat{d}'_{1+}A\lambda r^{\lambda+5} \quad \text{and} \quad |\hat{\eta}_{2+}| \leq \hat{d}'_{2+}A^2\lambda^2r^{2\lambda+2} \quad (4.46)$$

for some constant $\hat{d}'_{1+}, \hat{d}'_{2+} > 0$.

The following Lemma 28 gives the conditions such that the desired condition of w_+ , $\nu \cdot Tw_+ \geq \nu \cdot Tu$ holds on Σ_{r_0} .

Lemma 28. *With $\gamma > 0$, and the assumption $0 < A\lambda \leq K_0$, $A > 0$ and $0 < \lambda < 1$, and under the conditions on A , λ and r_0 such that*

$$c_{G_1}A\lambda r^{\lambda+1} - \hat{d}'_{2+}A^2\lambda^2r^{2\lambda+2} - \hat{c}_v r^4 - \hat{d}'_{1+}A\lambda r^{\lambda+5} \geq 0, \quad (4.47)$$

for $0 < r < r_0 < 1$. $\hat{c}_v > 0$ is defined in Lemma 24, $\hat{d}'_{1+} > 0$ and $\hat{d}'_{2+} > 0$ are defined in (4.46) and $c_{G_1} > 0$ is defined in (4.42). Then w_+ satisfies

$$\nu \cdot Tw_+ \geq \nu \cdot Tu \quad \text{on } \Sigma_{r_0}. \quad (4.48)$$

Moreover, when $\gamma = 0$, the inequality in (4.48) is an equality.

Proof.

$$\begin{aligned} \nu \cdot Tw_+ - \nu \cdot Tu &\geq (\nu \cdot Tv - \nu \cdot Tu) + G_1(\theta)r^{\lambda+1} + \hat{\eta}_{1+} + \hat{\eta}_{2+} \\ &\geq c_{G_1}A\lambda r^{\lambda+1} - \hat{d}'_{2+}A^2\lambda^2r^{2\lambda+2} - \hat{c}_v r^4 - \hat{d}'_{1+}A\lambda r^{\lambda+5} \\ &\geq 0, \end{aligned}$$

based on the condition on (4.47), and $|\nu \cdot Tv - \cos \gamma| \leq \hat{c}_v r^4$ for some constant $\hat{c}_v > 0$ from Lemma 24. In addition, when $\gamma = 0$, $\nu \cdot Tw_+$ meets the contact angle condition exactly. \square

4.3.3 Conditions on Boundary Γ_{r_0}

In this section, we discuss the conditions on A , λ and r_0 such that w_- and w_+ give a lower and an upper bound of u on Γ_{r_0} . Recall that the capillary equation $Nu_c = \kappa u_c$ with $\kappa > 0$. Let B_δ be a disk with radius $\delta > 0$ and $B_\delta \subset \Omega$. From Concus and Finn [7] and Finn [18], u_c is bounded in B_δ ,

$$|u_c| \leq \frac{2}{\kappa\delta} + \delta \quad \text{in } B_\delta.$$

The result can be modified and extended to the tilted capillary equation in (4.12), shown in the following Lemma 29.

Lemma 29. *Let u be the solution of the tilted capillary equation in (4.12). Consider a fixed disk centred at $(x_B, 0)$ with radius $\delta_0 > 0$ is tangent to the wedges Σ_{r_0} and covers the arc Γ_{r_0} (see Fig. 4.3). The disk is denoted as $B_{\delta_0} = B_{\delta_0}(x_B, 0)$, where $\delta_0 = r_0 \tan \alpha$ and $x_B = \frac{\delta_0}{\sin \alpha}$. Then*

$$|u| \leq \frac{2}{\bar{\kappa}\delta_0} + \left[1 + \frac{1}{\cos \tau} \left(1 + \frac{1}{\sin \alpha} \right) \right] \delta_0 \quad \text{in } B_{\delta_0}, \quad (4.49)$$

where $\bar{\kappa} = \kappa \cos \tau$.

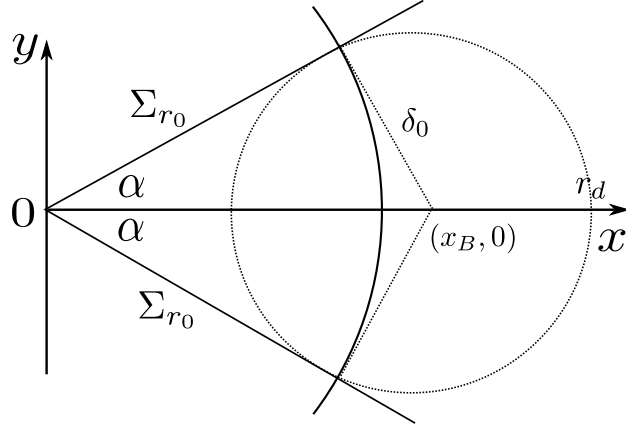


Figure 4.3: The bound of u in B_{δ_0} .

Proof. Let v_h be the lower hemisphere with radius δ_0 in B_{δ_0} . The lowest point of v_h is chosen as $\frac{2}{\bar{\kappa}\delta_0} + \frac{r_d}{\cos \tau}$. Note that $\frac{\kappa}{\bar{\kappa}} = \frac{1}{\cos \tau}$ and $r_d = \frac{\delta_0}{\sin \alpha} + \delta_0$ (see Fig. 4.3).

$$\begin{aligned}
Nv_h &= \frac{2}{\delta_0} = \bar{\kappa} \frac{2}{\bar{\kappa}\delta_0} \leq \bar{\kappa} \left(v_h - \frac{\kappa}{\bar{\kappa}} r_d \right) \\
&= \bar{\kappa} v_h - \kappa r_d \leq \bar{\kappa} v_h + f(\theta; \kappa, \phi, \tau) r \\
&\leq \bar{\kappa} v_h + Nu - \bar{\kappa} u.
\end{aligned}$$

It implies

$$Nv_h - Nu \leq \bar{\kappa}(v_h - u) \quad \text{in } B_{\delta_0},$$

and on ∂B_{δ_0} ,

$$\nu \cdot Tv_h = 1 \geq \nu \cdot Tu$$

for $\gamma \geq 0$ and ν is the outward normal of ∂B_{δ_0} . According to the comparison principle (Theorem 1), we have $u \leq v_h \leq \frac{2}{\bar{\kappa}\delta_0} + \frac{r_d}{\cos \tau} + \delta_0 = \frac{2}{\bar{\kappa}\delta_0} + \left[1 + \frac{1}{\cos \tau} \left(1 + \frac{1}{\sin \alpha} \right) \right] \delta_0$.

Similarly, for the lower bound, we define \bar{v}_h be the upper hemisphere with the highest point $-\frac{2}{\bar{\kappa}\delta_0} - \frac{r_d}{\cos \tau}$. Hence $\bar{v}_h \leq -\frac{2}{\bar{\kappa}\delta_0} - \frac{r_d}{\cos \tau}$.

$$\begin{aligned}
N\bar{v}_h - Nu &= -\frac{2}{\delta_0} - \bar{\kappa}u - f(\theta; \kappa, \phi, \tau)r \\
&\geq \bar{\kappa}(\bar{v}_h - u) + \kappa r_d - f(\theta; \kappa, \phi, \tau)r \geq \bar{\kappa}(\bar{v}_h - u) \quad \text{in } B_{\delta_0},
\end{aligned}$$

and on ∂B_{δ_0} ,

$$\nu \cdot T\bar{v}_h = -1 \leq \nu \cdot Tu = \cos \gamma.$$

By the comparison principle (Theorem 1), we have $-\frac{2}{\bar{\kappa}\delta_0} - \frac{r_d}{\cos \tau} - \delta_0 \leq \bar{v}_h \leq u$. Therefore,

$$|u| \leq \frac{2}{\bar{\kappa}\delta_0} + \left[1 + \frac{1}{\cos \tau} \left(1 + \frac{1}{\sin \alpha}\right)\right] \delta_0 \quad \text{in } B_{\delta_0}.$$

□

Since $\Gamma_{r_0} \subset B_\delta$, it is possible to make $w_-(r, \theta) \leq u \leq w_+(r, \theta)$ on Γ_{r_0} based on the following Lemma 30,

Lemma 30. *With the assumption $0 < A\lambda \leq K_0$, $A > 0$ and $0 < \lambda < 1$, $0 < r_0 < 1$, under the condition on A , λ and r_0 such that*

$$A = \frac{a_1}{r_0^{1+\lambda}} + a_2 r_0^{1-\lambda}, \quad (4.50)$$

where a_1 and a_2 are constants such that

$$a_1 \geq \left(\frac{1}{k} + \frac{2}{\tan \alpha}\right) \frac{1}{\bar{\kappa}}, \quad (4.51)$$

$$a_2 \geq \left[1 + \frac{1}{\cos \tau} \left(1 + \frac{1}{\sin \alpha}\right)\right] \tan \alpha, \quad (4.52)$$

then

$$w_-(r, \theta) \leq u \leq w_+(r, \theta) \quad \text{on } \Gamma_{r_0} \quad (4.53)$$

is satisfied.

Proof. We start with $w_-(r_0, \theta)$, since $|h(\theta)| \leq \frac{1}{k\bar{k}}$ from Property 6 and using the choice of A in (4.50),

$$\begin{aligned} w_-(r_0, \theta) &= \frac{h(\theta)}{r_0} - Ar_0^\lambda \\ &\leq \frac{1}{k\bar{k}r_0} - Ar_0^\lambda \\ &= \frac{1}{k\bar{k}r_0} - \frac{a_1}{r_0} - a_2r_0. \end{aligned}$$

With $a_1 \geq \left(\frac{1}{k} + \frac{2}{\tan \alpha}\right) \frac{1}{\bar{k}}$ and $a_2 \geq \left[1 + \frac{1}{\cos \tau} \left(1 + \frac{1}{\sin \alpha}\right)\right] \tan \alpha$, $\delta_0 = r_0 \tan \alpha$ and Lemma 29,

$$\begin{aligned} w_-(r_0, \theta) &\leq -\frac{2}{\bar{k}r_0 \tan \alpha} - \left[1 + \frac{1}{\cos \tau} \left(1 + \frac{1}{\sin \alpha}\right)\right] r_0 \tan \alpha \\ &= -\frac{2}{\bar{k}\delta_0} - \left[1 + \frac{1}{\cos \tau} \left(1 + \frac{1}{\sin \alpha}\right)\right] \delta_0 \\ &\leq u. \end{aligned}$$

Similarly,

$$\begin{aligned} w_+(r_0, \theta) &= \frac{h(\theta)}{r_0} + Ar_0^\lambda \\ &\geq -\frac{1}{k\bar{k}r_0} + Ar_0^\lambda \\ &= -\frac{1}{k\bar{k}r_0} + \frac{a_1}{r_0} + a_2r_0. \end{aligned}$$

$$w_+(r_0, \theta) \geq \frac{2}{\bar{k}r_0 \tan \alpha} + \left[1 + \frac{1}{\cos \tau} \left(1 + \frac{1}{\sin \alpha}\right)\right] r_0 \tan \alpha \geq u.$$

□

4.3.4 Results

Combining the conditions obtained from Lemma 25 - Lemma 30, we lead to the following Theorem 26:

Theorem 26. *There exist A, λ such that the assumption $0 < A\lambda \leq K_0$, $A > 0$ and $0 < \lambda < 1$ holds for some constant $K_0 > 0$. for $0 < r < r_0 < 1$. Then conditions in Lemma 25 - Lemma 30 (conditions in (4.33), (4.34), (4.38), (4.43), (4.47) and (4.50), these conditions are listed as follows for the sake of convenience) are satisfied.*

$$-c_{P_1}\lambda + \bar{\kappa} > 0 \quad (4.54)$$

$$A[-c_{P_1}\lambda + \bar{\kappa}]r^\lambda - \kappa r - d'_{2-}A^2\lambda^2r^{2\lambda+1} - d'_{1-}A\lambda r^{\lambda+4} - c_v r^3 \geq 0 \quad (4.55)$$

$$-A[\bar{\kappa} - c_{P_1}\lambda]r^\lambda + \kappa r + d'_{2+}A^2\lambda^2r^{2\lambda+1} + d'_{1+}A\lambda r^{\lambda+4} + c_v r^3 \leq 0 \quad (4.56)$$

$$-c_{G_1}A\lambda r^{\lambda+1} + \hat{d}'_{2-}A^2\lambda^2r^{2\lambda+2} + \hat{c}_v r^4 + \hat{d}'_{1-}A\lambda r^{\lambda+5} \leq 0, \quad (4.57)$$

$$c_{G_1}A\lambda r^{\lambda+1} - \hat{d}'_{2+}A^2\lambda^2r^{2\lambda+2} - \hat{c}_v r^4 - \hat{d}'_{1+}A\lambda r^{\lambda+5} \geq 0, \quad (4.58)$$

$$A = \frac{a_1}{r_0^{1+\lambda}} + a_2 r_0^{1-\lambda}, \quad (4.59)$$

where a_1 and a_2 are constants such that

$$a_1 \geq \left(\frac{1}{k} + \frac{2}{\tan \alpha} \right) \frac{1}{\bar{\kappa}}, \quad (4.60)$$

$$a_2 \geq \left[1 + \frac{1}{\cos \tau} \left(1 + \frac{1}{\sin \alpha} \right) \right] \tan \alpha. \quad (4.61)$$

Proof. Let $A\lambda = K_0$, A is defined in (4.59), thus,

$$\left(\frac{a_1}{r_0^\lambda} + a_2 r_0^{2-\lambda} \right) \lambda = K_0 r_0, \quad (4.62)$$

where we denote LHS of (4.62) as $g(r_0)$. Moreover, we notice that for $r_0 > 0$, $g(r_0)$ is a strictly convex function with

$$g'(r_0) = \lambda r_0^{-(\lambda+1)} (-\lambda a_1 + (2 - \lambda) a_2 r_0^2)$$

and

$$g''(r_0) = \lambda^2(\lambda + 1) a_1 r_0^{-(\lambda+2)} + \lambda(2 - \lambda)(1 - \lambda) a_2 r_0^{-\lambda} > 0.$$

When solving $g'(r_0^*) = 0$, $r_0^* = \sqrt{\frac{\lambda a_1}{(2 - \lambda) a_2}}$ is obtained (note: $r_0^* \rightarrow 0$ as $\lambda \rightarrow 0$). (4.62) shows $g(r_0)$ intersects with a straight line $y(r_0) = K_0 r_0$ at two distinct points. One is less than r_0^* and the other is greater than r_0^* . With small λ and $r_0 < 1$, the smaller intersection point is desired to obtain. Rearranging (4.62),

$$(a_1 + a_2 r_0^2) \lambda = K_0 r_0^{1+\lambda}. \quad (4.63)$$

Some inequalities imply

$$\left(\frac{K_0}{a_1 + a_2} \right) r_0^{1+\lambda} \leq \lambda \leq \left(\frac{K_0}{a_1} \right) r_0^{1+\lambda} \quad (4.64)$$

After some arrangement,

$$\frac{\ln(\lambda) - \ln\left(\frac{K_0}{a_1}\right)}{1 + \lambda} \leq \ln(r_0) \leq \frac{\ln(\lambda) - \ln\left(\frac{K_0}{a_1 + a_2}\right)}{1 + \lambda}. \quad (4.65)$$

Hence, we have $r_0 \rightarrow 0$ as $\lambda \rightarrow 0$. Asymptotically, $\ln(r_0) \sim \frac{\ln(\lambda)}{1 + \lambda}$. Therefore, $r_0 \sim \lambda$ as $\lambda \rightarrow 0$.

Thus, by choosing λ sufficiently small, we have the condition in (4.54) satisfied and r_0 becomes sufficiently small, as well. For $0 < r < r_0$, the first terms in (4.55), (4.56), (4.57), (4.58) become the leading order terms, therefore the inequalities hold.

□

From Theorem 26, we set up the following conditions:

$$\begin{aligned} Nw_- - Nu &\geq \bar{\kappa}(w_- - u) \quad \text{in } \Omega_{r_0}, \\ \nu \cdot Tw_- &\leq \nu \cdot Tu \quad \text{on } \Sigma_{r_0}, \\ w_- &\leq u \quad \text{on } \Gamma_{r_0}, \end{aligned}$$

and

$$\begin{aligned} Nw_+ - Nu &\leq \bar{\kappa}(w_+ - u) \quad \text{in } \Omega_{r_0}, \\ \nu \cdot Tw_+ &\geq \nu \cdot Tu \quad \text{on } \Sigma_{r_0}, \\ u &\leq w_+(r, \theta) \quad \text{on } \Gamma_{r_0}. \end{aligned}$$

The comparison principle (Theorem 25) gives

$$w_-(r, \theta) \leq u \leq w_+(r, \theta) \quad \text{in } \Omega_{r_0}.$$

Therefore, we obtain the error bound for u ,

$$|u - v| \leq Ar^\lambda \quad \text{in } \Omega_{r_0}, \tag{4.66}$$

where A does not depend on r and u .

4.4 Improved Error Bounds on u

In this section, we improve the error bounds on u by following the recipe of Miersemann [46]. Suppose $w_\pm(r, \theta)$ are defined in Ω_{r_0} , $0 < r \leq r_0 < 1$ for small $r_0 > 0$ and have more general forms

$$w_\pm(r, \theta) = v(r, \theta) \pm Aq(\theta)r^\lambda, \tag{4.67}$$

where $A > 0$ and $q(\theta)$ is chosen as

$$q(\theta) = \frac{1}{\bar{\kappa}h(\theta)} + \epsilon_0 \tag{4.68}$$

for some small $\epsilon_0 > 0$ (there should be some other possible choices of $q(\theta)$). Different from λ discussed in Section 4.3, in this section, we set $\lambda = 1$ with another assumption $Ar^{\lambda+1} \ll 1$.

4.4.1 Sub-solution and Super-solution in Ω_{r_0}

Consider $w_-(r, \theta) = v(r, \theta) - Aq(\theta)r$. We expand Nw_- again based on the calculation in Appendix C.2,

$$Nw_- = Nv - P_1(\theta)r + \eta_{1-} + \eta_{2-}, \quad (4.69)$$

where

$$\begin{aligned} P_1(\theta) = & 3A(h')^2 (h^2 + h'^2)^{-3/2} q(\theta) + 3Ah'(\theta)h(\theta) (h^2 + h'^2)^{-3/2} q'(\theta) \\ & + A \left[h(\theta)h'(\theta) (h^2 + h'^2)^{-3/2} q(\theta) \right]_{\theta} + A \left[h^2 (h^2 + h'^2)^{-3/2} q'(\theta) \right]_{\theta} \end{aligned} \quad (4.70)$$

and

$$|\eta_{1-}| \leq d_{\eta_{1-}} Ar^5 \quad \text{and} \quad |\eta_{2-}| \leq d_{\eta_{2-}} A^2 r^3 \quad (4.71)$$

for some λ dependent $d_{\eta_{1-}}, d_{\eta_{2-}} > 0$.

Thus,

$$\begin{aligned} Nw_- - \bar{\kappa}w_- - f(\theta; \kappa, \phi, \tau)r = & Nv - P_1(\theta)r + \eta_{1-} + \eta_{2-} - \bar{\kappa}(v - Aq(\theta)r) - f(\theta; \kappa, \phi, \tau)r \\ = & (Nv - \bar{\kappa}v) + L(\theta)r - f(\theta; \kappa, \phi, \tau)r + \eta_{1-} + \eta_{2-}, \end{aligned}$$

where

$$L(\theta) = A\bar{\kappa}q(\theta) - P_1(\theta). \quad (4.72)$$

Similarly, from Appendix C.2, we have

$$Nw_+ = Nv + P_1(\theta)r + \eta_{1+} + \eta_{2+}, \quad (4.73)$$

where

$$|\eta_{1+}| \leq d_{\eta_{1+}}Ar^5 \quad \text{and} \quad |\eta_{2+}| \leq d_{\eta_{2+}}A^2r^3. \quad (4.74)$$

Thus,

$$\begin{aligned} Nw_+ - \bar{\kappa}w_+ - f(\theta; \kappa, \phi, \tau)r &= Nv - \bar{\kappa}(v + Aq(\theta)r) + P_1(\theta)r + \eta_{1+} + \eta_{2+} - f(\theta; \kappa, \phi, \tau)r \\ &= (Nv - \bar{\kappa}v) - L(\theta)r - f(\theta; \kappa, \phi, \tau)r + \eta_{1+} + \eta_{2+}. \end{aligned}$$

Recall from Sec. 4.3, when $0 < r \leq \bar{r}_0 < 1$, there exist $A_0 > 0$, $0 < \mu < 1$ and $0 < A_0\mu \leq K_0$ such that

$$v - A_0r^\mu \leq u \leq v + A_0r^\mu \quad \text{in } \Omega_{\bar{r}_0}. \quad (4.75)$$

Remark 29. To avoid confusion, we use positive constants A_0 , μ and \bar{r}_0 instead, where all of them satisfy the conditions discussed in Section 4.3 (see Theorem 26). Moreover, r_0 in this section is chosen such that $r_0 \ll \bar{r}_0$.

Lemma 31 is useful to construct a sub-solution and a super-solution.

Lemma 31. *With $\gamma \geq 0$ and the choice of $q(\theta)$ defined in (4.68), there exists some constant $C_3 > 0$ such that*

$$|P_1(\theta)| \leq C_3 \frac{A\epsilon_0}{h(\theta)}. \quad (4.76)$$

Moreover, let

$$0 < \epsilon_0 < \frac{1}{C_3}, \quad (4.77)$$

$$A = \frac{A_0}{c_h r_0^{1-\mu}}, \quad (4.78)$$

where c_h is defined in Property 6, $r_0 \ll \bar{r}_0$ and μ , A_0 and \bar{r}_0 are described in Remark 29 (or Theorem 26) with $0 < A_0\mu \leq K_0 = c_h$. When μ is chosen sufficiently small, then the assumption $Ar^2 \ll 1$ is satisfied for $0 < r \leq r_0 \ll \bar{r}_0 < 1$ and

$$A > \frac{1}{\cos \tau [c_h(1 - C_3\epsilon_0) + \epsilon_0]}. \quad (4.79)$$

And $L(\theta)$ defined in (4.72) satisfies

$$L(\theta) > \kappa. \quad (4.80)$$

Proof. Since $q(\theta) = \frac{1}{\bar{\kappa}h(\theta)} + \epsilon_0$, then $q'(\theta) = -\frac{h'(\theta)}{\bar{\kappa}h^2(\theta)}$. We first simplify $P_1(\theta)$:

$$\begin{aligned} P_1(\theta) &= 3A(h')^2 (h^2 + h'^2)^{-3/2} \left(\frac{1}{\bar{\kappa}h(\theta)} + \epsilon_0 \right) - 3Ah'(\theta)h(\theta) (h^2 + h'^2)^{-3/2} \frac{h'(\theta)}{\bar{\kappa}h^2(\theta)} \\ &\quad + A \left[h(\theta)h'(\theta) (h^2 + h'^2)^{-3/2} \left(\frac{1}{\bar{\kappa}h(\theta)} + \epsilon_0 \right) \right]_{\theta} - A \left[h^2 (h^2 + h'^2)^{-3/2} \frac{h'(\theta)}{\bar{\kappa}h^2(\theta)} \right]_{\theta} \\ &= 3A(h')^2 (h^2 + h'^2)^{-3/2} \epsilon_0 + A \left[h(\theta)h'(\theta) (h^2 + h'^2)^{-3/2} \right]_{\theta} \epsilon_0 \\ &= \frac{A\epsilon_0}{h(\theta)} \left\{ \frac{1}{|k|^3} \left(\cos \theta (k^2 - \sin^2 \theta) - 2 \sin^2 \theta \left(\cos \theta - \sqrt{k^2 - \sin^2 \theta} \right) \right) \right\} \end{aligned}$$

It is easy to see that $|P_1(\theta)| \leq C_3 \frac{A\epsilon_0}{h(\theta)}$ for some constant $C_3 > 0$ for $\gamma \geq 0$. And from

Property 6, $c_h \bar{\kappa} \leq \frac{1}{h(\theta)} \leq \frac{2k}{1 - k^2} \bar{\kappa}$ for some constant $c_h > 0$. Let $0 < \epsilon_0 < \frac{1}{C_3}$. So,

$\frac{1}{\cos \tau [c_h(1 - C_3\epsilon_0) + \epsilon_0]}$ is a positive constant. Choose $K_0 = c_h$ and $A = \frac{A_0}{c_h r_0^{1-\mu}}$, where $0 < r_0 \ll \bar{r}_0 < 1$. μ , A_0 and \bar{r}_0 satisfy the restriction $0 < A_0\mu \leq K_0$ and conditions on Theorem 26, see Sec. 4.3. Moreover, in the proof of Theorem 26, we choose $A_0\mu = K_0$ and $\bar{r}_0 \sim \mu$ as $\mu \rightarrow 0$. Therefore, when $0 < r \leq r_0$,

$$Ar^2 \leq Ar_0^2 = \frac{1}{c_h} A_0 r_0^{1+\mu} \ll \frac{A_0}{c_h} \bar{r}_0 \bar{r}_0^\mu = \frac{\bar{r}_0}{\mu} \bar{r}_0^\mu \sim 1, \quad (4.81)$$

and

$$\begin{aligned}
A &= \frac{A_0}{c_h r_0^{1-\mu}} \gg \frac{A_0}{c_h} \left(\frac{1}{\bar{r}_0} \right) \bar{r}_0^\mu \\
&= \left(\frac{1}{\mu \bar{r}_0} \right) \bar{r}_0^\mu > \frac{1}{\cos \tau [c_h(1 - C_3 \epsilon_0) + \epsilon_0]}.
\end{aligned} \tag{4.82}$$

In addition,

$$\begin{aligned}
L(\theta) - \kappa &= A\bar{\kappa}q(\theta) - P_1(\theta) - \kappa \\
&\geq \frac{A}{h}(1 - C_3 \epsilon_0) + A\bar{\kappa}\epsilon_0 - \kappa \\
&\geq A\bar{\kappa} [c_h(1 - C_3 \epsilon_0) + \epsilon_0] - \kappa > 0,
\end{aligned} \tag{4.83}$$

from (4.82).

□

Therefore, we can state the following Lemma 32,

Lemma 32. *With $\gamma \geq 0$ and the choices in Lemma 31, if the following inequalities are satisfied,*

$$\{A\bar{\kappa} [c_h(1 - C_3 \epsilon_0) + \epsilon_0] - \kappa\} r - d_{\eta_1-} A r^5 - d_{\eta_2-} A^2 r^3 - c_v r^3 > 0, \tag{4.84}$$

$$- \{A\bar{\kappa} [c_h(1 - C_3 \epsilon_0) + \epsilon_0] - \kappa\} r + d_{\eta_1+} A r^5 + d_{\eta_2+} A^2 r^3 + c_v r^3 < 0, \tag{4.85}$$

then

(i) w_- satisfies the sub-solution condition, that is,

$$Nw_- - Nu \geq \bar{\kappa}(w_- - u) \quad \text{in } \Omega_{r_0}. \tag{4.86}$$

(ii) w_+ satisfies the super-solution condition, that is,

$$Nw_+ - Nu \leq \bar{\kappa}(w_+ - u) \quad \text{in } \Omega_{r_0}. \tag{4.87}$$

Proof. With such choice of ϵ_0 and the inequality of $L(\theta)$ in Lemma 31, and $|f| \leq \kappa$,

$$\begin{aligned}
Nw_- - \bar{\kappa}w_- - f(\theta; \kappa, \phi, \tau)r &= (Nv - \bar{\kappa}v) + L(\theta)r - f(\theta; \kappa, \phi, \tau)r + \eta_{1-} + \eta_{2-} \\
&\geq L(\theta)r - \kappa r - c_v r^3 - d_{\eta_{1-}} Ar^5 - d_{\eta_{2-}} A^2 r^3 \\
&= \{A\bar{\kappa} [c_h(1 - C_3\epsilon_0) + \epsilon_0] - \kappa\} r - d_{\eta_{1-}} Ar^5 - d_{\eta_{2-}} A^2 r^3 - c_v r^3 > 0,
\end{aligned} \tag{4.88}$$

where $Ar^2 \ll 1$ and $|Nv - \bar{\kappa}v| \leq c_v r^3$ for some constant $c_v > 0$ from Lemma 24.

Thus,

$$Nw_- - Nu \geq \bar{\kappa}(w_- - u) \quad \text{in } \Omega_{r_0}. \tag{4.89}$$

Similarly,

$$\begin{aligned}
Nw_+ - \bar{\kappa}w_+ - f(\theta; \kappa, \phi, \tau)r &= (Nv - \bar{\kappa}v) - L(\theta)r - f(\theta; \kappa, \phi, \tau)r + \eta_{1+} + \eta_{2+} \\
&\leq -L(\theta)r + \kappa r + c_v r^3 + d_{\eta_{1+}} Ar^5 + d_{\eta_{2+}} A^2 r^3 \\
&= -\{A\bar{\kappa} [c_h(1 - C_3\epsilon_0) + \epsilon_0] - \kappa\} r + d_{\eta_{1+}} Ar^5 + d_{\eta_{2+}} A^2 r^3 + c_v r^3 < 0.
\end{aligned} \tag{4.90}$$

Therefore,

$$Nw_+ - Nu \leq \bar{\kappa}(w_+ - u) \quad \text{in } \Omega_{r_0}. \tag{4.91}$$

□

4.4.2 Conditions on Boundary Σ_{r_0}

The argument of conditions on wedges is similar to that we have in Section 4.3.2 except the usage of different forms of $w_{\pm}(r, \theta)$. Recall that, on Σ_{r_0} , we have

$$\nu \cdot Tw_{\pm} = \frac{\frac{1}{r}w_{\pm\theta}}{\sqrt{1 + |\nabla w_{\pm}|^2}}, \quad \text{at } \theta = \alpha,$$

where ν is the outer-normal of Σ_{r_0} with $\theta = \alpha$ (similar for the $\theta = -\alpha$ case with only a sign difference).

For $w_-(r, \theta)$, we expand $\nu \cdot Tw_-$ based on Appendix C.3, with $\gamma > 0$, we have

$$\nu \cdot Tw_- = \frac{\frac{1}{r}w_{-\theta}}{(1 + |\nabla w_-|^2)^{1/2}} = \nu \cdot Tv - G_1(\theta)r^2 + \hat{\eta}_{1-} + \hat{\eta}_{2-}, \quad (4.92)$$

where

$$G_1(\theta) = Ah(\theta)h'(\theta) (h^2 + h'^2)^{-3/2} q(\theta) + Ah^2 (h^2 + h'^2)^{-3/2} q'(\theta), \quad (4.93)$$

and

$$|\hat{\eta}_{1-}| \leq d_{\hat{\eta}_{1-}} Ar^6 \quad \text{and} \quad |\hat{\eta}_{2-}| \leq d_{\hat{\eta}_{2-}} A^2 r^4 \quad (4.94)$$

for some λ dependent $d_{\hat{\eta}_{1-}}, d_{\hat{\eta}_{2-}} > 0$. In addition, when $\gamma = 0$, at $\theta = \alpha$, $G_1(\theta) \rightarrow 0$, and $\hat{\eta}_{1-}, \hat{\eta}_{2-} \rightarrow 0$. $\nu \cdot Tw_- = \nu \cdot Tv = 1$, the contact angle condition is met exactly.

With the choice of $q(\theta) = \frac{1}{\bar{\kappa}h(\theta)} + \epsilon_0$,

$$G_1(\theta) = Ahh' (h^2 + h'^2)^{-3/2} \epsilon_0,$$

where $h'(\theta) > 0$ at $\theta = \alpha$ based on Property 6. Moreover, with $\gamma > 0$, there exists some constant $c_{G_1} > 0$, at $\theta = \alpha$, such that

$$c_{G_1} Ar^2 \leq G_1(\theta)r^2. \quad (4.95)$$

Therefore, we have the following Lemma 33,

Lemma 33. *Suppose $A > 0$, $0 < r < r_0$ are such that $Ar^2 \ll 1$. In addition, suppose that A and r satisfy*

$$A(c_{G_1} - d_{\hat{\eta}_{1-}}r^4 - d_{\hat{\eta}_{2-}}Ar^2) - \hat{c}_v r^2 > 0 \quad (4.96)$$

for all $0 < r < r_0$ and that $\gamma > 0$. Then we have

$$\nu \cdot Tw_- \leq \nu \cdot Tu \quad \text{on } \Sigma_{r_0}. \quad (4.97)$$

In addition, when $\gamma = 0$, $\nu \cdot Tw_-$ meets the contact angle condition exactly.

Proof. The $\gamma = 0$ case has been discussed. For $\gamma > 0$,

$$\begin{aligned} \nu \cdot Tw_- - \nu \cdot Tu &= \nu \cdot Tv - \cos \gamma - G_1(\theta)r^2 + d_{\hat{\eta}_{1-}}Ar^6 + d_{\hat{\eta}_{2-}}A^2r^4 \\ &\leq -c_{G_1}Ar^2 + \hat{c}_v r^4 + d_{\hat{\eta}_{1-}}Ar^6 + d_{\hat{\eta}_{2-}}A^2r^4 \\ &= -r^2 [A(c_{G_1} - d_{\hat{\eta}_{1-}}r^4 - d_{\hat{\eta}_{2-}}Ar^2) - \hat{c}_v r^2] < 0, \end{aligned} \quad (4.98)$$

where the contact angle is unchanged $\nu \cdot Tu = \cos \gamma$, and $|\nu \cdot Tv - \cos \gamma| \leq \hat{c}_v r^4$ for some constant $\hat{c}_v > 0$ from Lemma 24. □

Similarly, we expand $\nu \cdot Tw_+$:

$$\nu \cdot Tw_+ = \nu \cdot Tv + G_1(\theta)r^2 + \hat{\eta}_{1+} + \hat{\eta}_{2+},$$

where

$$|\hat{\eta}_{1+}| \leq d_{\hat{\eta}_{1+}}Ar^6 \quad \text{and} \quad |\hat{\eta}_{2+}| \leq d_{\hat{\eta}_{2+}}A^2r^4 \quad (4.99)$$

for some λ dependent $d_{\hat{\eta}_{1+}}, d_{\hat{\eta}_{2+}} > 0$. In addition, when $\gamma = 0$, at $\theta = \alpha$, $G_1(\theta) \rightarrow 0$, and $\hat{\eta}_{1+}, \hat{\eta}_{2+} \rightarrow 0$. $\nu \cdot Tw_+ = \nu \cdot Tv = 1$, the contact angle condition is met exactly.

Therefore, we have the following Lemma 34,

Lemma 34. *Suppose $A > 0$, $0 < r < r_0$ are such that $Ar^2 \ll 1$. In addition, suppose that A and r satisfy*

$$A(c_{G_1} - d_{\hat{\eta}_{1+}}r^4 - d_{\hat{\eta}_{2+}}Ar^2) - \hat{c}_v r^2 > 0 \quad (4.100)$$

for all $0 < r < r_0$ and that $\gamma > 0$. Then we have

$$\nu \cdot Tw_+ \geq \nu \cdot Tu \quad \text{on } \Sigma_{r_0}. \quad (4.101)$$

In addition, when $\gamma = 0$, $\nu \cdot Tw_+$ meets the contact angle condition exactly.

Proof. The $\gamma = 0$ case has been discussed. For $\gamma > 0$,

$$\begin{aligned} \nu \cdot Tw_+ - \nu \cdot Tu &= \nu \cdot Tv - \cos \gamma + G_1(\theta)r^2 + d_{\hat{\eta}_{1+}}Ar^6 + d_{\hat{\eta}_{2+}}A^2r^4 \\ &\geq c_{G_1}Ar^2 - \hat{c}_v r^4 - d_{\hat{\eta}_{1+}}Ar^6 - d_{\hat{\eta}_{2+}}A^2r^4 \\ &= r^2 [A(c_{G_1} - d_{\hat{\eta}_{1+}}r^4 - d_{\hat{\eta}_{2+}}Ar^2) - \hat{c}_v r^2] > 0, \end{aligned} \quad (4.102)$$

where the contact angle is unchanged $\nu \cdot Tu = \cos \gamma$, and $|\nu \cdot Tv - \cos \gamma| \leq \hat{c}_v r^4$ for some constant $\hat{c}_v > 0$ from Lemma 24. □

4.4.3 Conditions on Boundary Γ_{r_0}

The desired conditions of the modified $w_{\pm}(r, \theta)$ on boundary Γ_{r_0} are based on the results we obtained in Section 4.3. In the following Lemma 35, we construct the bounds of modified $w_{\pm}(r, \theta)$ on Γ_{r_0} based on the choice of A in Lemma 31.

Lemma 35. *With the choice of A in Lemma 31, then*

$$w_-(r, \theta) \leq u \leq w_+(r, \theta) \quad \text{on } \Gamma_{r_0}.$$

Proof. From Section 4.3, for $0 < r \leq r_0 \ll \bar{r}_0 < 1$, we show that

$$v - A_0 r_0^\mu \leq u \leq v + A_0 r_0^\mu \quad \text{in } \Omega_{\bar{r}_0}. \quad (4.103)$$

Since $\Gamma_{r_0} \subset \Omega_{\bar{r}_0}$, the above inequalities hold on Γ_{r_0} as well. With $A = \frac{A_0}{c_h r_0^{1-\mu}}$,

$$\begin{aligned} Aq(\theta)r_0 &\geq \frac{A_0}{c_h r_0^{1-\mu}} \left(\frac{1}{\bar{\kappa}h(\theta)} + \epsilon_0 \right) r_0 \\ &> A_0 r_0^\mu \left(\frac{1}{c_h \bar{\kappa}h(\theta)} \right) \geq A_0 r_0^\mu, \end{aligned}$$

where $\frac{1}{h(\theta)} \geq c_h \bar{\kappa}$ from Property 6. Hence $A_0 r_0^\mu \leq Aq(\theta)r_0$. Therefore,

$$|u - v| \leq A_0 r_0^\mu \leq Aq(\theta)r_0 \quad \text{on } \Gamma_{r_0}.$$

Hence, the result is proved. \square

4.4.4 Results

Combining the conditions obtained from Lemma 31 - Lemma 35, we lead to the following Theorem 27:

Theorem 27. *With $\gamma \geq 0$, and the choices in Lemma 31, the assumption $Ar^2 \ll 1$ holds for $0 < r \leq r_0 < 1$, then conditions in Lemma 32 - Lemma 34 (conditions in (4.84), (4.85), (4.96), and (4.100) these conditions are listed as follows for the sake of convenience) are satisfied.*

$$\{A\bar{\kappa} [c_h(1 - C_3\epsilon_0) + \epsilon_0] - \kappa\} r - d_{\eta_{1-}} Ar^5 - d_{\eta_{2-}} A^2 r^3 - c_v r^3 > 0, \quad (4.104)$$

$$- \{A\bar{\kappa} [c_h(1 - C_3\epsilon_0) + \epsilon_0] - \kappa\} r + d_{\eta_{1+}} Ar^5 + d_{\eta_{2+}} A^2 r^3 + c_v r^3 < 0, \quad (4.105)$$

$$A(c_{G_1} - d_{\hat{\eta}_{1-}} r^4 - d_{\hat{\eta}_{2-}} Ar^2) - \hat{c}_v r^2 > 0, \quad (4.106)$$

$$A(c_{G_1} - d_{\hat{\eta}_{1+}} r^4 - d_{\hat{\eta}_{2+}} Ar^2) - \hat{c}_v r^2 > 0. \quad (4.107)$$

Proof. With such choices of A and ϵ_0 , for all $0 < r \leq r_0 < 1$, the first terms in (4.104), (4.105), (4.106) and (4.107) are dominating and great than 0, the desired inequalities hold. \square

From Lemma 35 and Theorem 27, we set up the following conditions:

$$\begin{aligned} Nw_- - Nu &\geq \bar{\kappa}(w_- - u) \quad \text{in } \Omega_{r_0}, \\ \nu \cdot Tw_- &\leq \nu \cdot Tu \quad \text{on } \Sigma_{r_0}, \\ w_- &\leq u \quad \text{on } \Gamma_{r_0}, \end{aligned} \quad (4.108)$$

and

$$\begin{aligned}
Nw_+ - Nu &\leq \bar{\kappa}(w_+ - u) && \text{in } \Omega_{r_0}, \\
\nu \cdot Tw_+ &\geq \nu \cdot Tu && \text{on } \Sigma_{r_0}, \\
u &\leq w_+ && \text{on } \Gamma_{r_0}.
\end{aligned} \tag{4.109}$$

The comparison principle (Theorem 25) gives

$$w_-(r, \theta) \leq u \leq w_+(r, \theta) \quad \text{in } \Omega_{r_0}.$$

Thus,

$$|u - v| \leq Aq(\theta)r \quad \text{in } \Omega_{r_0}. \tag{4.110}$$

Therefore, we obtain the modified error bound on u ,

$$|u - v| \leq Cr \quad \text{in } \Omega_{r_0}, \tag{4.111}$$

where $C = A \left(\frac{2k}{1 - k^2} + \epsilon_0 \right)$, which is independent on r and u .

4.5 Conclusion

In this chapter, we study the behavior of the capillary surface in a tilted wedge domain near the corner. Without tilting, the capillary surface is unbounded at the corner under the condition $0 < \alpha + \gamma < \frac{\pi}{2}$, see Finn [18]. When the coordinate system is rotated by the rotation matrix $R(\phi, \tau, \psi)$, a tilted capillary equation is obtained

$$Nu = \bar{\kappa}u + f(\theta; \kappa, \phi, \tau)r \tag{4.112}$$

in Ω_{r_0} , which is understood as an equation of mean curvature type, see Korevaar and Simon [36].

Miersemann's choices of a sub-solution and a super-solution are applied to analyze the error bound of a tilted capillary surface near the corner. We first show that

$$u(r, \theta) = v(r, \theta) + \mathcal{O}(r^\lambda) \tag{4.113}$$

in Ω_{r_0} for small r_0 and $\lambda > 0$ under the conditions in Theorem 26. The error bound is improved to $\mathcal{O}(r)$, when the modified super-solution and sub-solution are considered, see Theorem 27. In Miersemann's work [46], he improved the error bound for a vertical wedge problem by showing there exists an asymptotic expansion of $u(r)$. A similar approach is suggested to improve the error bound for the tilted wedge problem in the future.

Chapter 5

Conclusion

In this thesis, a floating ball and two asymptotic problems in capillarity are studied. We summarize our work and mention open questions and suggestions for future research.

In Chapter 2, we study an asymptotic problem for the capillary surface around a vertical needle cylindrical tube when Bond number is small. This needle problem has been widely discussed for decades. Lo [41] obtained a five-term asymptotic expansion of $u(r)$ as $\epsilon \rightarrow 0$. Her result is accepted as a correct expansion but has not been rigorously proven. Miersemann's work [47] confirmed a two-term asymptotic expansion of $u(r)$ and obtained the error bound $\mathcal{O}(\epsilon^{2/5} \ln^2(\epsilon))$, which is inferior to Lo's, $\mathcal{O}(\epsilon^2 \ln^2 \epsilon)$. Our goal is to improve Miersemann's error bound. We construct two C^1 , piecewise C^2 approximate solutions of $u(r)$. Each approximate solution consists of an inner solution and an outer solution. The first approximate solution $u_1(r)$ gives an upper bound of u and the second approximate solution $u_2(r)$ gives a lower bound of u . Near the boundary, $u_1(r)$ has zero mean curvature and $u_2(r)$ has constant mean curvature. As $\epsilon \rightarrow 0$, we show $u_1(r)$ and $u_2(r)$ have the same two-term asymptotic expansion which is the two-term asymptotic expansion of $u(r)$. The error bound $\mathcal{O}(\epsilon(-\ln \epsilon)^{3/2})$ is obtained by optimizing the choice of a transition radius q , where Theorem 2 (Olver [49]) is applied. Our error bound is an improvement of Miersemann's. When we apply another modified outer solution, the improved error bound $\mathcal{O}(\epsilon^{4/3}(-\ln \epsilon)^{5/3})$ is achieved but it is inferior to Lo's. Lo's higher order expansion is based on a more complicated form of inner solution. However, in our study, zero mean curvature and constant mean curvature inner solutions are used. So, another modified inner solution is suggested for future work. Moreover, Miersemann [47] conjectured a full asymptotic expansion. A proof of his conjecture is anticipated.

In Chapter 3, a floating ball on an unbounded bath is studied. Our discussion consists two parts: 1) the behavior of solutions 2) the number of equilibrium configurations and their stability. The floating configuration is assumed to be radially symmetric. By a result of Elcrat, Neel and Siegel [13], the fluid interface is determined uniquely by r_0 and ψ_0 . Both of these are given in terms of ϕ_0 . However, the zero solution $\hat{u} = 0$ is not included in the parametric description. The graph description of fluid height is considered as well. We develop C^1 smoothness of u_0 with respect to ϕ_0 . This requires an extension of Vogel's description of solutions and monotonicity results [63]. As a by-product, Vogel's conjecture on the smoothness of the envelope of exterior solutions is shown. Theorem 2 (Olver [49]) and Theorem 16 (Levinson's Theorem [12]) are used in analysis of the limiting behavior of solutions at infinity. McCuan and Treinen [43] found an example of two equilibrium configurations for a ball floating on an unbounded bath. We give a more comprehensive study of the number of equilibria and their stability. Both force and energy analysis are applied. We establish a relation between the total energy \hat{E}_T and the total force \hat{F}_T , that is,

$$\frac{d\hat{E}_T}{d\phi_0} = -\hat{F}_T \hat{h}'(\phi_0). \quad (5.1)$$

A stability criterion is derived based on this relation. However, \hat{u}_0 is contained in both \hat{F}_T and $\hat{h}(\phi_0)$ equations, which has to be found numerically. The limiting behavior of \hat{u}_0 as well as \hat{F}_T and \hat{h} is studied. For small Bond number, the asymptotic expansion obtained in Chapter 2 can be fitted into the floating ball problem. We extend the expansion to parametric form. To address the stability result in the $B \rightarrow 0$ case, signs of $\hat{F}'_T(\bar{\phi}_0)$ and $\hat{h}'(\bar{\phi}_0)$ with $\bar{\phi}_0 = \pi - \gamma + \mathcal{O}(B)$ are studied without the assumption that the asymptotic expansion of \hat{u}_0 can be differentiated. The $\phi_0 \rightarrow 0, \pi$ and the $B \rightarrow \infty$ cases are analyzed, as well. In numerical observation, we perform thousands of numerical tests with different values of Bond numbers and contact angles. The following conjecture is proposed:

Conjecture. *In the floating ball system, there are at most two force balanced points. If there is only one force balanced point, it is stable. If there are two force balanced points, the one with smaller attachment angle must be stable and the one with larger attachment angle can be either stable or unstable.*

For a given contact angle, the information on the number of equilibria and their stability can be illustrated in a Bond number versus density ratio figure. Several figures with typical contact angles are presented. Finally, we give two examples. One shows a case with two

stable equilibrium configurations. Another example shows a case with no force balanced point but there is an energy minimizer. This prompts discussion of the necessary condition of the floating configuration and a modification of changing topological structure for the floating configurations in this example. For future study, a proof of the conjecture of the number of equilibria and their stability is anticipated. Our theoretical stability results have not been confirmed by experiments. An experiment is expected to validate the result of two stable configurations for a floating ball. In Appendix B.3, we discuss an iterative method to find the fluid interface numerically when it is a graph. Practically, it works well and converges fast. However, we cannot prove the convergence by error analysis. It can be another potential topic.

In Chapter 4, we study an asymptotic problem for a capillary surface in a tilted wedge domain. The asymptotic problem of a capillary surface in a vertical wedge has been studied. Under the condition $0 < \alpha + \gamma < \frac{\pi}{2}$, Concus and Finn [6] showed the capillary surface is unbounded near the corner. They applied an approximate solution $v_1(r)$ and concluded $u = v_1 + \mathcal{O}(1)$ near the corner. Miersemann [45, 46] improved the error bound to $\mathcal{O}(r^3)$. We are interested in whether the capillary surface is still unbounded if the wedge is tilted from the vertical axis. Euler's angles are used to describe the tilting. A tilted capillary equation is obtained using the invariance of mean curvature under rotation. The unboundedness of the tilted capillary surface is shown by the comparison principle. We construct sub-solutions and super-solutions based on Concus and Finn's approximate solution and Miersemann's two different choices. An error bound is obtained and improved to $\mathcal{O}(r)$. In Miersemann's work [46], he improved the error bound for a vertical wedge problem by showing there exists an asymptotic expansion of $u(r)$. A similar approach is suggested to improve the error bound for the tilted wedge problem in the future.

References

- [1] Milton Abramowitz, Irene A Stegun, and Robert H Romer. Handbook of mathematical functions with formulas, graphs, and mathematical tables, 1988.
- [2] Yasunori Aoki and David Siegel. Bounded and unbounded capillary surfaces in a cusp domain. *Pac. J. Math.*, 257(1):143–165, 2012.
- [3] Rajat Bhatnagar and Robert Finn. Equilibrium configurations of an infinite cylinder in an unbounded fluid. *Phys. Fluids*, 18(4):047103, 2006.
- [4] Hanzhe Chen and David Siegel. A floating cylinder on an unbounded bath. *J. Math. Fluid Mech.*, 20(4):1373–1404, 2018.
- [5] Paul Concus. Static menisci in a vertical right circular cylinder. *J. Fluid Mech.*, 34(3):481–495, 1968.
- [6] Paul Concus and Robert Finn. On a class of capillary surfaces. *Journal d’Analyse Mathématique*, 23(1):65–70, 1970.
- [7] Paul Concus and Robert Finn. On capillary free surfaces in a gravitational field. *Acta Math.*, 132:207–223, 1974.
- [8] Paul Concus and Robert Finn. The shape of a pendant liquid drop. *Philosophical Transactions of the Royal Society of London. Series A, Mathematical and Physical Sciences*, 292(1391):307–340, 1979.
- [9] Pierre-Gilles De Gennes, Françoise Brochard-Wyart, and David Quéré. *Capillarity and wetting phenomena: drops, bubbles, pearls, waves*. Springer Science & Business Media, 2013.
- [10] Pierre-Simon de Laplace. *Traité de Mécanique celeste: supplement 2*. Number 900-945, au Livre X. Crapelet, 1805/1806.
- [11] Boris Derjaguin. Theory of the distortion of a plane surface of a liquid by small objects and its application to the measurement of the contact angles of thin filaments and fibres. *Dokl. Akad. Nauk. SSSR*, 51:519–522, 1946.

- [12] M.S.P. Eastham. *The Asymptotic Solution of Linear Differential Systems: Applications of the Levinson Theorem*. London Mathematical Society monographs. Clarendon Press, 1989.
- [13] Alan Elcrat, Robert Neel, and David Siegel. Equilibrium configurations for a floating drop. *J. Math. Fluid Mech.*, 6(4):405–429, Dec 2004.
- [14] Alan Elcrat and Ray Treinen. Numerical results for floating drops. In *Conference Publications*, volume 2005, page 241. American Institute of Mathematical Sciences, 2005.
- [15] Paul Erdős, Gérard Schibler, and Roy C Herndon. Floating equilibrium of symmetrical objects and the breaking of symmetry. part 1: Prisms. *American journal of physics*, 60(4):335–345, 1992.
- [16] Paul Erdős, Gérard Schibler, and Roy C Herndon. Floating equilibrium of symmetrical objects and the breaking of symmetry. part 2: The cube, the octahedron, and the tetrahedron. *American journal of physics*, 60(4):345–356, 1992.
- [17] Robert Finn. The sessile liquid drop. i. symmetric case. *Pac. J. Math.*, 88(2):541–587, 1980.
- [18] Robert Finn. *Equilibrium capillary surfaces*. Springer-Verlag, New York, 1986.
- [19] Robert Finn. Floating and partly immersed balls in a weightless environment. *Funct. Differ. Equ.*, 12(1-2):167–173, 2005.
- [20] Robert Finn. On Young’s paradox, and the attractions of immersed parallel plates. *Phys. Fluids*, 22(1):017103, 2010.
- [21] Robert Finn. Criteria for floating I. *J. Math. Fluid Mech.*, 13(1):103–115, Mar 2011.
- [22] Robert Finn and Jenn-Fang Hwang. On the comparison principle for capillary surfaces. *Journal of the Faculty of Science, the University of Tokyo. Sect. 1 A, Math.*, 36(1):131–134, 1989.
- [23] Robert Finn and Thomas I Vogel. Floating criteria in three dimensions. *Analysis*, 29(2):125–140, 2009.
- [24] L.E. Fraenkel. On the method of matched asymptotic expansions, i-iii. In *Mathematical Proceedings of the Cambridge Philosophical Society*, volume 65, pages 209–284. Cambridge University Press, 1969.
- [25] Elaina L. Gabriel. Superhydrophobic particle ejections from liquid surfaces in microgravity environments. *University Honors Theses*, page 800, 2019.

- [26] Carl Friedrich Gauss. *Principia generalia theoriae figurae fluidorum in statu aequilibrii*. Springer Berlin Heidelberg, Berlin, Heidelberg, 1877.
- [27] WA Gifford and LE Scriven. On the attraction of floating particles. *Chemical Engineering Science*, 26(3):287–297, 1971.
- [28] Ron Goldman. Curvature formulas for implicit curves and surfaces. *Computer Aided Geometric Design*, 22(7):632–658, 2005.
- [29] James Gordon and David Siegel. Approximating annular capillary surfaces with equal contact angles. *Pac. J. Math.*, 247:371–387, 2010.
- [30] Stanley Hartland and Richard W. Hartley. *Axisymmetric fluid-liquid interfaces*. Amsterdam ; New York : Elsevier Scientific Pub. Co., 1976.
- [31] Chun Huh and Stanley G. Mason. The flotation of axisymmetric particles at horizontal liquid interfaces. *J. Colloid Interface Sci.*, 47(2):271–289, 1974.
- [32] David F James. The meniscus on the outside of a small circular cylinder. *J. Fluid Mech.*, 63(4):657–664, 1974.
- [33] William Ernest Johnson and Lawrence M Perko. Interior and exterior boundary value problems from the theory of the capillary tube. *Archive for Rational Mechanics and Analysis*, 29(2):125–143, 1968.
- [34] Todd M Kemp and David Siegel. Floating bodies in two dimensions without gravity. *Phys. Fluids*, 23(4):043303, 2011.
- [35] JR King, JR Ockendon, and H Ockendon. The Laplace-Young equation near a corner. *Quarterly Journal of Mechanics and Applied Mathematics*, 52(1):73–97, 1999.
- [36] Nicholas J. Korevaar and Leon Simon. Equations of mean curvature type with contact angle boundary conditions. *Geometric analysis and the calculus of variations*, pages 175–201, 1996.
- [37] Steven G Krantz and Harold R. Parks. *A primer of real analytic functions*. Boston : Birkhäuser., 2002.
- [38] Paco Axel Lagerstrom. *Matched asymptotic expansions: ideas and techniques*, volume 76. Springer Science & Business Media, 2013.
- [39] Kirk Lancaster and David Siegel. Existence and behavior of the radial limits of a bounded capillary surface at a corner. *Pac. J. Math.*, 176(1):165–194, 1996.
- [40] Jian-Lin Liu, Xi-Qiao Feng, and Gang-Feng Wang. Buoyant force and sinking conditions of a hydrophobic thin rod floating on water. *Phys. Rev. E*, 76:066103, Dec 2007.

- [41] Lilian L. Lo. The meniscus on a needle – a lesson in matching. *J. Fluid Mech.*, 132:65–78, 1983.
- [42] John McCuan. A variational formula for floating bodies. *Pac. J. Math.*, 231(1):167–191, 2007.
- [43] John McCuan and Ray Treinen. Capillarity and Archimedes’ principle of flotation. *Pac. J. Math.*, 265(1):123–150, 2013.
- [44] John McCuan and Ray Treinen. On floating equilibria in a laterally finite container. *SIAM J. Appl. Math.*, 78(1):551–570, 2018.
- [45] Erich Miersemann. On the behaviour of capillaries at a corner. *Pac. J. Math.*, 140(1):149–153, 1989.
- [46] Erich Miersemann. Asymptotic expansion at a corner for the capillary problem: the singular case. *Pac. J. Math.*, 157(1):95–107, 1993.
- [47] Erich Miersemann. The ascent of a liquid on a circular needle. *Pac. J. Math.*, 224:291–319, 04 2006.
- [48] Erich Miersemann. *Mathematical Theory of Liquid Interfaces: Liquid Layers, Capillary Interfaces, Floating Drops and Particles*. World Scientific, 2020.
- [49] Frank Olver. *Asymptotics and Special Functions*. CRC Press, 1997.
- [50] Murray H Protter and Hans F Weinberger. *Maximum principles in differential equations*. Springer Science & Business Media, 2012.
- [51] A.V Rapacchietta and A.W Neumann. Force and free-energy analyses of small particles at fluid interfaces: ii. spheres. *J. Colloid Interface Sci.*, 59(3):555 – 567, 1977.
- [52] Elie Raphaël, Jean-Marc Di Meglio, Marcel Berger, and Eugenio Calabi. Convex particles at interfaces. *Journal de physique I*, 2(5):571–579, 1992.
- [53] Lord Rayleigh. On the theory of the capillary tube. *Proceedings of the Royal Society of London. Series A, Containing Papers of a Mathematical and Physical Character*, 92(637):184–195, 1916.
- [54] J.J. Sakurai and Jim J Napolitano. *Modern Quantum Mechanics*. Pearson, 2014.
- [55] Thomas C. Sideris. *Ordinary Differential Equations and Dynamical Systems*. Atlantis Studies in Differential Equations. Atlantis Press, 2013.
- [56] David Siegel. Height estimates for capillary surfaces. *Pac. J. Math.*, 88(2):471–515, 1980.

- [57] David Siegel. Approximating symmetric capillary surfaces. *Pac. J. Math.*, 224:355–366, 2006.
- [58] Ray Treinen. Examples of non-uniqueness of the equilibrium states for a floating ball. *Adv. Materials Phys. Chem.*, 6(7):177–194, 2016.
- [59] Bruce Turkington. Height estimates for exterior problems of capillarity type. *Pac. J. Math.*, 88(2):517–540, 1980.
- [60] Milton Van Dyke. Perturbation methods in fluid mechanics. *STIA*, 75:46926, 1975.
- [61] Dominic Vella. Floating versus sinking. *Annual Review of Fluid Mechanics*, 47(1):115–135, 2015.
- [62] Dominic Vella, Duck-Gyu Lee, and Ho-Young Kim. The load supported by small floating objects. *Langmuir*, 22(14):5979–5981, 2006.
- [63] Thomas I. Vogel. Symmetric unbounded liquid bridges. *Pac. J. Math.*, 103(1):205–241, 1982.
- [64] Henry C. Wente. Exotic capillary tubes. *J. Math. Fluid Mech.*, 13(3):355–370, Sep 2011.
- [65] Thomas Young. An essay on the cohesion of fluids. *Philos. Trans. R. Soc. London*, 95:65–87, 1805.
- [66] Quan-Shui Zheng, Yang Yu, and Xi-Qiao Feng. The role of adaptive-deformation of water strider leg in its walking on water. *J. Adhes. Sci. Technol.*, 23(3):493–501, 2009.

APPENDICES

Appendix A

A.1 Asymptotic Expansions of Some Functions

In this section, the following asymptotic expansions of functions are listed, which are used in Chapter 2.

$$\frac{1}{\epsilon q K_1(\epsilon q)} = 1 - \frac{1}{2}(\epsilon q)^2 \ln(\epsilon q) + \frac{1}{4}(1 - 2\gamma_e + 2 \ln 2)(\epsilon q)^2 + \mathcal{O}((\epsilon q)^4) \quad \text{as } \epsilon q \rightarrow 0, \quad (\text{A.1})$$

where γ_e is known as Euler's constant.

$$\frac{q}{\sqrt{q^2 - c^2}} = 1 + \frac{c^2}{2q^2} + \frac{3}{8} \frac{c^4}{q^4} + \mathcal{O}\left(\frac{1}{q^6}\right) \quad \text{as } q \rightarrow \infty, \quad (\text{A.2})$$

where $c = -\cos(\gamma)$ is defined in (2.10) in Chapter 2. Since $c \in [-1, 0)$, the error term will be bounded by $\frac{1}{q^6}$, so c is absorbed in the big- \mathcal{O} notation.

$$K_0(\epsilon q) = -\ln(\epsilon q) + (-\gamma_e + \ln 2) - \frac{1}{4}(\epsilon q)^2 \ln(\epsilon q) + \frac{1}{4}(1 - \gamma_e + \ln 2)(\epsilon q)^2 + \mathcal{O}((\epsilon q)^4) \quad \text{as } \epsilon q \rightarrow 0. \quad (\text{A.3})$$

$$\ln\left(q + \sqrt{q^2 - c^2}\right) = \ln(2q) - \frac{c^2}{4q^2} + \mathcal{O}\left(\frac{1}{q^4}\right) \quad \text{as } q \rightarrow \infty. \quad (\text{A.4})$$

$$\begin{aligned}
\frac{K_0(\epsilon q)}{\epsilon q K_1(\epsilon q)} &= -\ln(\epsilon q) + (-\gamma_e + \ln 2) + \frac{1}{2}(\epsilon q)^2 \ln^2(\epsilon q) - \frac{1}{2}(1 - 2\gamma_e + 2\ln 2)(\epsilon q)^2 \ln(\epsilon q) \\
&\quad + \frac{1}{8}(\epsilon q)^4 \ln^2(\epsilon q) + \frac{1}{4}(1 - 2\gamma_e + 2\ln 2 + 2\gamma_e^2 - 4\gamma_e \ln 2 + 2\ln^2 2)(\epsilon q)^2 + \mathcal{O}((\epsilon q)^4)
\end{aligned} \tag{A.5}$$

as $\epsilon q \rightarrow 0$.

A.2 Asymptotic Expansions of p_3 , k_3 , p_4 and k_4

In this section, we present the detailed derivation of the asymptotic expansions of p_3 and k_3 and p_4 and k_4 as $\epsilon \rightarrow 0$, $q \rightarrow \infty$ and $\epsilon q \rightarrow 0$ in Sec. 2.5. Recall that,

$$p_3 = -\frac{\epsilon q K_1(\epsilon q)}{\epsilon^3 q \frac{d\bar{u}_2^{\text{out}}}{dR}(\epsilon q)} \quad \text{and} \quad k_3 = -\frac{\frac{cq}{\sqrt{q^2 - c^2}}}{\epsilon^3 q \frac{d\bar{u}_2^{\text{out}}}{dR}(\epsilon q)}.$$

Asymptotically,

$$\frac{d\bar{u}_2^{\text{out}}}{dR}(\epsilon q) \sim -\frac{1}{2\epsilon^3 q^3} - \frac{\ln(\epsilon q)}{2\epsilon q} + \frac{1}{4\epsilon q}, \tag{A.6}$$

$$\epsilon^3 q \frac{d\bar{u}_2^{\text{out}}}{dR}(\epsilon q) \sim -\frac{1}{2q^2} - \frac{1}{2}\epsilon^2 \ln(\epsilon q) + \frac{1}{4}\epsilon^2. \tag{A.7}$$

Moreover, recall that,

$$\epsilon q K_1(\epsilon q) \sim 1 + \frac{1}{2}(\epsilon q)^2 \ln(\epsilon q) - \frac{1}{4}(\epsilon q)^2(1 + 2a), \tag{A.8}$$

$$\frac{cq}{\sqrt{q^2 - c^2}} \sim c + \frac{c^3}{2q^2} + \frac{3c^5}{8q^4}. \tag{A.9}$$

Thus,

$$p_3 \sim 2q^2 \quad \text{and} \quad k_3 \sim 2cq^2. \quad (\text{A.10})$$

Moreover, let $p_3 = 2q^2 + \bar{p}_3$ and $k_3 = 2cq^2 + \bar{k}_3$. Substitute into p_3 and q_3 , then

$$\bar{p}_3 = -\frac{\epsilon q K_1(\epsilon q) + 2\epsilon^3 q^3 \frac{d\bar{u}_2^{\text{out}}}{dR}(\epsilon q)}{\epsilon^3 q \frac{d\bar{u}_2^{\text{out}}}{dR}(\epsilon q)} \sim (\epsilon q)^2 q^2 \ln(\epsilon q), \quad (\text{A.11})$$

where

$$\epsilon q K_1(\epsilon q) + 2\epsilon^3 q^3 \frac{d\bar{u}_2^{\text{out}}}{dR}(\epsilon q) \sim -\frac{1}{2}(\epsilon q)^2 \ln(\epsilon q). \quad (\text{A.12})$$

Moreover,

$$\bar{k}_3 = -\frac{\frac{cq}{\sqrt{q^2 - c^2}} + 2c\epsilon^3 q^3 \frac{d\bar{u}_2^{\text{out}}}{dR}(\epsilon q)}{\epsilon^3 q \frac{d\bar{u}_2^{\text{out}}}{dR}(\epsilon q)} \sim c^3 + \frac{3c^5}{4q^2} - 2c(\epsilon q)^2 q^2 \ln(\epsilon q), \quad (\text{A.13})$$

where

$$\frac{cq}{\sqrt{q^2 - c^2}} + 2c\epsilon^3 q^3 \frac{d\bar{u}_2^{\text{out}}}{dR}(\epsilon q) \sim \frac{c^3}{2q^2} + \frac{3c^5}{8q^4} - c(\epsilon q)^2 \ln(\epsilon q). \quad (\text{A.14})$$

Therefore,

$$p_3 = 2q^2 + (\epsilon q)^2 q^2 \ln(\epsilon q) + o((\epsilon q)^2 q^2 \ln(\epsilon q)), \quad (\text{A.15})$$

$$k_3 \sim 2cq^2 + c^3 + \frac{3c^5}{4q^2} - 2c(\epsilon q)^2 q^2 \ln(\epsilon q). \quad (\text{A.16})$$

It is similar for p_4 and k_4 . Recall that,

$$p_4 = \frac{\epsilon q K_1(\epsilon q)}{\epsilon^2 \int_{\epsilon q}^{\infty} R \bar{u}_2(R) dR} \quad \text{and} \quad k_4 = \frac{q \sin \psi_4^{\text{in}}(q)}{\epsilon^2 \int_{\epsilon q}^{\infty} R \bar{u}_2(R) dR},$$

where $\sin \psi_4^{\text{in}}(q) = \frac{c}{q} + \bar{D}(\epsilon, q) \frac{q^2 - 1}{2q}$ with $\bar{D}(\epsilon, q) \sim c\epsilon^2 \ln(\epsilon)$, where $\sin \psi_4^{\text{in}}(q)$ is defined in (2.234) in Se. 2.5.3.

Asymptotically,

$$q \sin \psi_4^{\text{in}}(q) \sim c + c(\epsilon q)^2 \ln(\epsilon), \quad (\text{A.17})$$

$$\epsilon^2 \int_{\epsilon q}^{\infty} R \bar{u}_2(R) dR \sim -\frac{1}{4} \epsilon^2 \ln(\epsilon q) - \frac{1}{4} \epsilon^2. \quad (\text{A.18})$$

Therefore,

$$p_4 \sim -\frac{4}{\epsilon^2 \ln(\epsilon q)} \quad \text{and} \quad k_4 \sim -\frac{4c}{\epsilon^2 \ln(\epsilon q)}. \quad (\text{A.19})$$

Moreover, let $p_4 = -\frac{4}{\epsilon^2 \ln(\epsilon q)} + \bar{p}_4$ and $k_4 = -\frac{4c}{\epsilon^2 \ln(\epsilon q)} + \bar{k}_4$. Substitute into p_4 and q_4 , then

$$\bar{p}_4 = \frac{\epsilon q K_1(\epsilon q) + \frac{4}{\ln(\epsilon q)} \int_{\epsilon q}^{\infty} R \bar{u}_2(R) dR}{\epsilon^2 \int_{\epsilon q}^{\infty} R \bar{u}_2(R) dR} \sim \frac{4}{\epsilon^2 \ln^2(\epsilon q)} - 2q^2, \quad (\text{A.20})$$

where

$$\epsilon q K_1(\epsilon q) + \frac{4}{\ln(\epsilon q)} \int_{\epsilon q}^{\infty} R \bar{u}_2(R) dR \sim -\frac{1}{\ln(\epsilon q)} + \frac{1}{2} (\epsilon q)^2 \ln(\epsilon q). \quad (\text{A.21})$$

Moreover,

$$\bar{k}_4 = \frac{q \sin \psi_4^{\text{in}}(q) + \frac{4c}{\ln(\epsilon q)} \int_{\epsilon q}^{\infty} R \bar{u}_2(R) dR}{\epsilon^2 \int_{\epsilon q}^{\infty} R \bar{u}_2(R) dR} \sim \frac{4c}{\epsilon^2 \ln^2(\epsilon q)} - 2c \frac{\ln(\epsilon)(q^2 - 1)}{\ln(\epsilon q)}, \quad (\text{A.22})$$

where

$$q \sin \psi_4^{\text{in}}(q) + \frac{4c}{\ln(\epsilon q)} \int_{\epsilon q}^{\infty} R \bar{u}_2(R) dR \sim -\frac{c}{\ln(\epsilon q)} + \frac{c}{2} \epsilon^2 \ln(\epsilon) (q^2 - 1). \quad (\text{A.23})$$

Therefore,

$$p_4 \sim -\frac{4}{\epsilon^2 \ln(\epsilon q)} + \frac{4}{\epsilon^2 \ln^2(\epsilon q)} - 2q^2, \quad (\text{A.24})$$

$$k_4 \sim -\frac{4c}{\epsilon^2 \ln(\epsilon q)} + \frac{4c}{\epsilon^2 \ln^2(\epsilon q)} - 2c \frac{\ln(\epsilon) (q^2 - 1)}{\ln(\epsilon q)}. \quad (\text{A.25})$$

Appendix B

B.1 Transformation $T(t)$

In this section, we will explain the transformation $T(t)$ in (3.123) in Sec. 3.5.3. Recall that,

$$N(t) = -\frac{1}{t^2(\bar{r}(t)\bar{u}(t) + \sin(t^{-1}))^2} \begin{pmatrix} -\sin(t^{-1})\cos(t^{-1}) & \bar{r}^2(t)\cos(t^{-1}) \\ \sin^2(t^{-1}) & -\bar{r}^2(t)\sin(t^{-1}) \end{pmatrix},$$

and $\bar{r}(t) = \bar{r}(t; \phi_0)$ and $\bar{u}(t) = \bar{u}(t; \phi_0)$.

Asymptotically, as $t \rightarrow \infty$,

$$N(t) \sim \tilde{N}(t), \tag{B.1}$$

where

$$\tilde{N}(t) = \begin{pmatrix} \frac{1}{t \ln^2(t)} & -1 \\ -\frac{1}{t^2 \ln^2(t)} & \frac{1}{t} \end{pmatrix}. \tag{B.2}$$

Hence, we consider

$$\tilde{\mathbf{x}}' = \tilde{N}(t)\tilde{\mathbf{x}}. \tag{B.3}$$

Next, we will transform the system to the form of Levinson's theorem by using two transformation matrices,

$$T_1(t) = \begin{pmatrix} 1 & \tau_1(t) \\ 0 & 1 \end{pmatrix} \quad \text{and} \quad T_2(t) = \text{diag}(1, \tau_2(t)), \quad (\text{B.4})$$

where $\tau_1(t)$ and $\tau_2(t)$ are to be determined.

Let $\tilde{\mathbf{x}}(t) = T_1(t)\tilde{\mathbf{y}}(t)$, then (B.3) turns into

$$\tilde{\mathbf{y}}' = \tilde{N}_1(t)\tilde{\mathbf{y}}, \quad (\text{B.5})$$

where

$$\tilde{N}_1(t) = T_1^{-1}(t)\tilde{N}(t)T_1(t) - T_1^{-1}(t)T_1'(t). \quad (\text{B.6})$$

In details,

$$\tilde{N}_1(t) = \begin{pmatrix} \frac{1}{t \ln^2(t)} + \frac{\tau_1(t)}{t^2 \ln^2(t)} & \tilde{n}_{12}(t) \\ \tilde{n}_{21}(t) & -\frac{\tau_1}{t^2 \ln^2(t)} + \frac{1}{t} \end{pmatrix}, \quad (\text{B.7})$$

where

$$\tilde{n}_{12}(t) = \frac{\tau_1^2(t)}{t^2 \ln^2(t)} + \left(\frac{1}{t \ln^2(t)} - \frac{1}{t} \right) \tau_1(t) - 1 - \tau_1'(t), \quad (\text{B.8})$$

$$\tilde{n}_{21}(t) = -\frac{1}{t^2 \ln^2(t)}. \quad (\text{B.9})$$

$\tilde{n}_{21}(t)$ is in $L^1([\tilde{t}_0, \infty))$ for some large \tilde{t}_0 and we try to make $\tilde{n}_{12}(t)$ in $L^1([\tilde{t}_0, \infty))$ as well. We notice that $\tilde{n}_{12}(t) = 0$ is a Riccati equation. To make it easy, assume $\tau_1(t) \ll t \ln(t)$, we have

$$\tau_1' \sim -\frac{\tau_1}{t} - 1. \quad (\text{B.10})$$

Solving $\tau_1' = -\frac{\tau_1}{t} - 1$, we obtain a special solution $\tau_1(t) = -\frac{t}{2}$, which satisfies our assumption. Thus,

$$\tilde{n}_{12}(t) = -\frac{1}{4\ln^2(t)}. \quad (\text{B.11})$$

Unfortunately, $\tilde{n}_{12}(t) \notin L^1([\tilde{t}_0, \infty))$, so we transform again, let $\tilde{\mathbf{y}} = T_2\tilde{\mathbf{z}}$, which gives

$$\tilde{\mathbf{z}}' = \tilde{N}_2(t)\tilde{\mathbf{z}}, \quad (\text{B.12})$$

where, in details,

$$\tilde{N}_2(t) = \begin{pmatrix} \frac{1}{2t\ln^2(t)} & -\frac{\tau_2(t)}{4\ln^2(t)} \\ -\frac{1}{t^2\ln^2(t)}\frac{1}{\tau_2(t)} & \frac{1}{2t\ln^2(t)} + \frac{1}{t} - \frac{\tau_2'(t)}{\tau_2(t)} \end{pmatrix}. \quad (\text{B.13})$$

With the choice $\tau_2(t) = \frac{1}{t}$,

$$\tilde{N}_2(t) = \tilde{L}(t) + \tilde{S}(t). \quad (\text{B.14})$$

where

$$\tilde{L}(t) = \text{diag}\left(0, \frac{2}{t}\right) \quad \text{and} \quad \tilde{S}(t) = \begin{pmatrix} \frac{1}{2t\ln^2(t)} & -\frac{1}{4t\ln^2(t)} \\ -\frac{1}{t\ln^2(t)} & \frac{1}{2t\ln^2(t)} \end{pmatrix}. \quad (\text{B.15})$$

Hence, $\tilde{S}(t)$ is $L^1([\tilde{t}_0, \infty))$ and the dichotomy condition is satisfied. Thus, by Theorem 16, as $t \rightarrow \infty$,

$$\tilde{\mathbf{z}}(t) = \tilde{c}_1 \left\{ \begin{pmatrix} 1 \\ 0 \end{pmatrix} + o(1) \right\} + \tilde{c}_2 t^2 \left\{ \begin{pmatrix} 0 \\ 1 \end{pmatrix} + o(1) \right\}. \quad (\text{B.16})$$

By defining $T(t) = T_1(t)T_2(t)$, $\tilde{\mathbf{x}}(t) = T(t)\tilde{\mathbf{z}}(t)$, thus,

$$\tilde{\mathbf{x}}(t) = \tilde{c}_1 \begin{pmatrix} 1 + o(1) \\ o(1/t) \end{pmatrix} + \tilde{c}_2 \begin{pmatrix} -\frac{t^2}{2} + o(t^2) \\ t + o(t) \end{pmatrix}, \quad (\text{B.17})$$

as $t \rightarrow \infty$.

B.2 Numerical Differentiation

It is difficult to analyze $\hat{F}'_T(\phi_0)$ analytically, since both \hat{u}_0 and $\frac{d\hat{u}_0}{d\phi_0}$ have to be obtained numerically. We present three numerical differentiation methods for $\frac{d\hat{u}_0}{d\phi_0}$ with enough smoothness of \hat{u}_0 with respect to ϕ_0 is assumed.

- (i) The standard centred approximation of the first-derivative:

$$\frac{d\hat{u}_0}{d\phi_0}(\bar{\phi}_0) \approx \frac{1}{2\Delta\phi_0} [\hat{u}_{0,1} - \hat{u}_{0,-1}], \quad (\text{B.18})$$

where $\Delta\phi_0$ is the uniform step size and $\hat{u}_{0,i} = \hat{u}_0(\phi_{0,i})$, $\phi_{0,i} = \bar{\phi}_0 + i\Delta\phi_0$.

- (ii) The five-point method (see Abramowitz & Stegun [1], Table 25.2.):

$$\frac{d\hat{u}_0}{d\phi_0}(\bar{\phi}_0) \approx \frac{1}{12\Delta\phi_0} [\hat{u}_{0,-2} - 8\hat{u}_{0,-1} + 8\hat{u}_{0,1} - \hat{u}_{0,2}]. \quad (\text{B.19})$$

- (iii) The Lagrange interpolation polynomial. Given three interpolation points $(\phi_{0,-1}, \hat{u}_{0,-1})$, $(\phi_{0,0}, \hat{u}_{0,0})$, $(\phi_{0,1}, \hat{u}_{0,1})$, the Lagrange interpolation polynomial for $\phi_0 \in [\phi_{0,-1}, \phi_{0,1}]$ is

$$L(\phi_0) = \hat{u}_{0,-1}l_{-1}(\phi_0) + \hat{u}_{0,0}l_0(\phi_0) + \hat{u}_{0,1}l_1(\phi_0) \quad (\text{B.20})$$

with

$$l_{-1}(\phi_0) = \frac{(\phi_0 - \phi_{0,0})(\phi_0 - \phi_{0,1})}{2\Delta\phi_0^2}, \quad (\text{B.21})$$

$$l_0(\phi_0) = -\frac{(\phi_0 - \phi_{0,-1})(\phi_0 - \phi_{0,1})}{\Delta\phi_0^2}, \quad (\text{B.22})$$

$$l_1(\phi_0) = \frac{(\phi_0 - \phi_{0,-1})(\phi_0 - \phi_{0,0})}{2\Delta\phi_0^2}. \quad (\text{B.23})$$

Hence,

$$\begin{aligned} \frac{d\hat{u}_0}{d\phi_0}(\phi_0) &\approx L'(\phi_0) \\ &= \hat{u}_{0,-1}l'_{-1}(\phi_0) + \hat{u}_{0,0}l'_0(\phi_0) + \hat{u}_{0,1}l'_1(\phi_0). \end{aligned} \quad (\text{B.24})$$

with

$$l'_{-1}(\phi_0) = \frac{2\phi_0 - \phi_{0,0} - \phi_{0,1}}{2\Delta\phi_0^2}, \quad (\text{B.25})$$

$$l'_0(\phi_0) = -\frac{2\phi_0 - \phi_{0,-1} - \phi_{0,1}}{\Delta\phi_0^2}, \quad (\text{B.26})$$

$$l'_1(\phi_0) = \frac{2\phi_0 - \phi_{0,-1} - \phi_{0,0}}{2\Delta\phi_0^2}. \quad (\text{B.27})$$

Moreover, the centered approximation has the accuracy $\mathcal{O}(\Delta\phi_0^2)$, the five-point method has accuracy $\mathcal{O}(\Delta\phi_0^4)$, and the derivative of the Lagrange interpolation polynomial has accuracy $\mathcal{O}(\Delta\phi_0^2)$. Especially, in (iii), if $\phi_0 = \bar{\phi}_0$, the formula in (B.24) is equivalent to the standard centred approximation.

Example 1. The aim of this example is to compare above (i) and (ii) approaches to obtain $\frac{d\hat{u}_0}{d\phi_0}$. Suppose

$$\begin{aligned} \hat{u}_1 = & -\frac{\sin \phi_0 \sin(\phi_0 + \gamma)}{2} \ln(B) - \sin \phi_0 \sin(\phi_0 + \gamma)(\gamma_e - 2 \ln 2) \\ & - \sin \phi_0 \sin(\phi_0 + \gamma) \ln [\sin \phi_0(1 - \cos(\phi_0 + \gamma))]. \end{aligned}$$

It comes from the asymptotic expansion of \hat{u}_0 for the small Bond number. If we differentiate it,

$$\begin{aligned} \frac{d\hat{u}_1}{d\phi_0} = & -\frac{\sin(2\phi_0 + \gamma)}{2} \ln(B) - \sin(2\phi_0 + \gamma) \ln[\sin(\phi_0)(1 - \cos(\phi_0 + \gamma))] \\ & - \sin(2\phi_0 + \gamma)(\gamma_e - 2 \ln 2) - \frac{\sin(\phi_0 + \gamma)(\cos \phi_0 - \cos(2\phi_0 + \gamma))}{1 - \cos(\phi_0 + \gamma)}. \end{aligned} \quad (\text{B.28})$$

Fig. B.1 shows the case comparing the two different numerical approaches with the analytic form in (B.28) for $\frac{d\hat{u}_1}{d\phi_0}$. The results are indistinguishable. Hence, the centered approximation of the first-derivative is good enough, but we prefer to use the five-point method for later use to obtain the more accurate result.

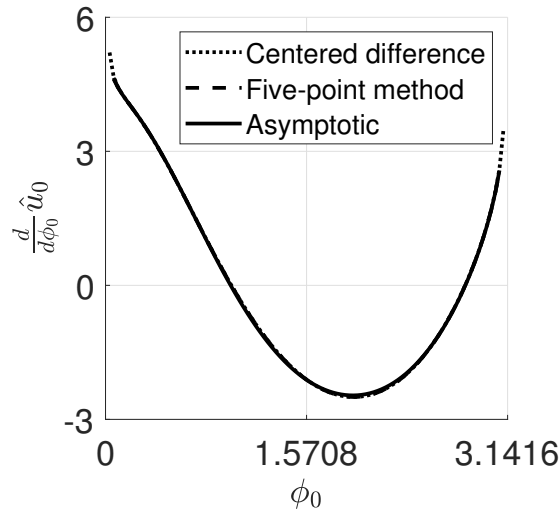


Figure B.1: the case $\phi_0 \in (0, \pi)$, $B = 0.01$, $\gamma = \frac{\pi}{4}$, and uniform step size $\Delta\phi_0 = \frac{\pi}{N}$, $N = 100$.

Fig. B.2 illustrates the numerical result of $\frac{d\hat{u}_0}{d\phi_0}$ based on the five-point method with data $B = 1$, $\gamma = \frac{\pi}{3}$, and the uniform step size $\Delta\phi_0 = \frac{\pi}{N}$, $N = 500, 1000$.

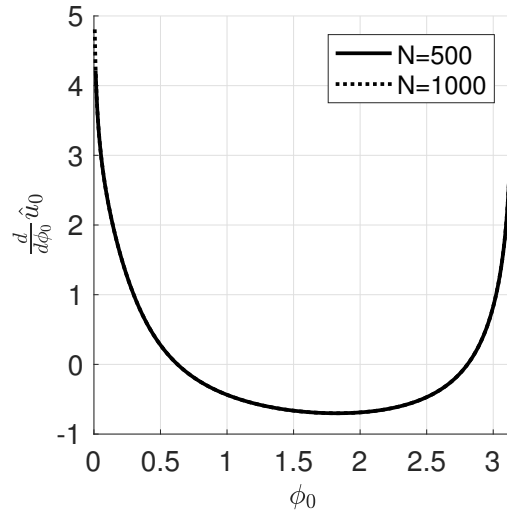


Figure B.2: The five-point method for $\frac{d\hat{u}_0}{d\phi_0}$ with data: $B = 1$, $\gamma = \frac{\pi}{3}$, and uniform step size $\Delta\phi_0 = \frac{\pi}{N}$, $N = 500, 1000$.

Next, we apply the Lagrange interpolation polynomial to find the critical point of the total force $\hat{F}_T(\phi_0)$ and the height $\hat{h}(\phi_0)$. The critical point which is greater than $\frac{\pi}{2}$ is of our interest, see Fig. B.3a, Fig. B.3b and Fig. B.4a, Fig. B.4b.

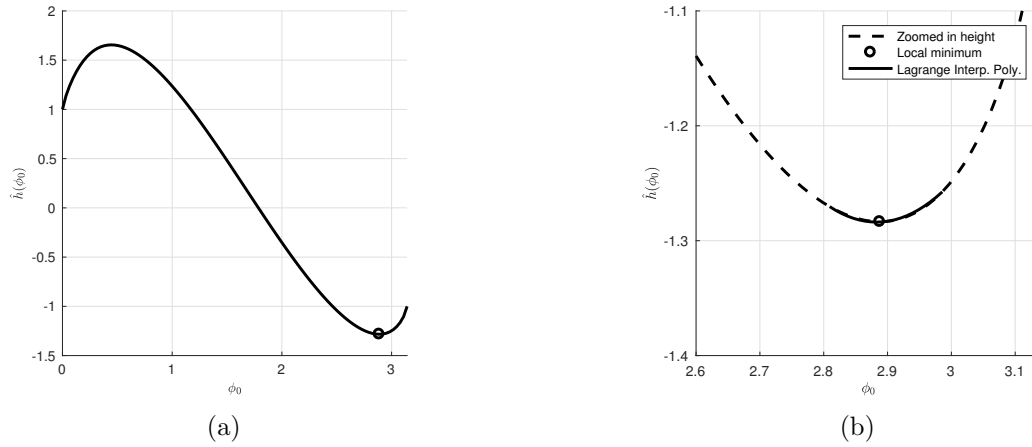


Figure B.3: (a) The height curve with $B = 1$, $\gamma = \frac{\pi}{3}$, the local minimum point is $(2.8879, -1.2835)$; (b) The corresponding zoomed in figure shows the Lagrange interpolation polynomial is used to find the local minimum of the height.

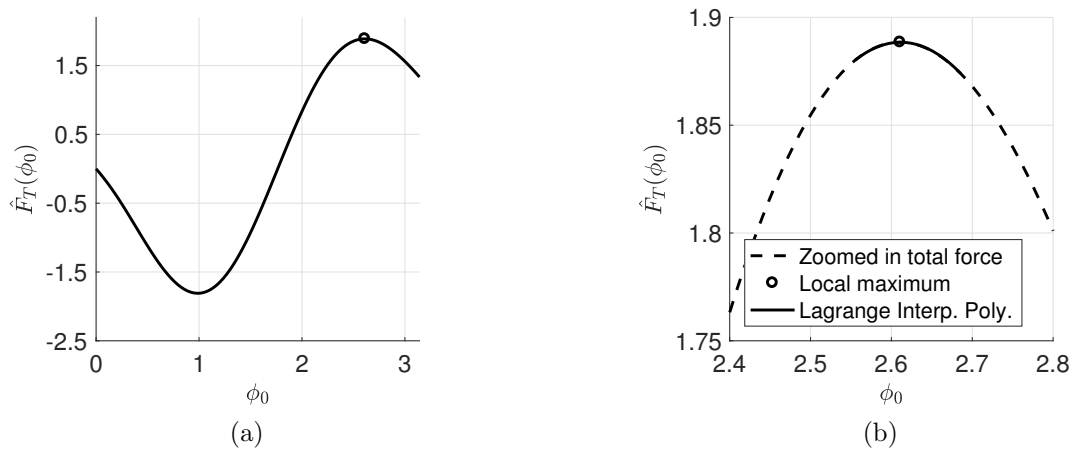


Figure B.4: (a) The total force curve with $B = 1$, $\gamma = \frac{\pi}{3}$, $\alpha = 0$, the local maximum point is $(2.6108, 1.8885)$; (b) The corresponding zoomed in figure shows the Lagrange interpolation polynomial is used to find the local maximum of the total force.

B.3 Iterative Method

In this section, we present another approach to determine the fluid interface when it is a graph, the iterative method. The iterative approach has been applied to the capillary problem. Siegel and Gordan applied the iterative method successfully to the annular problem, see [29]. For the exterior problem, Siegel [57] used the iterative procedure to determine the leading order term of the asymptotic expansion of the fluid height as $B \rightarrow 0$. We cannot simply apply the iterative method to determine the fluid interface for the exterior problem, which will cause the divergence. However, if the volume adjustment is applied after each iterative step, the iterative solution reaches convergence tolerance in a few steps. Unfortunately, we cannot apply error analysis to our iterative method. This could be a potential topic for future research.

Suppose the BVP of the scaled capillary equation is considered. Recall that,

$$(\bar{r} \sin \psi(\bar{r}))_{\bar{r}} = \bar{r} \bar{u} \quad (\text{B.29})$$

with boundary conditions

$$\psi(\bar{r}_0) = \psi_0 \quad \text{and} \quad \lim_{\bar{r} \rightarrow \infty} \bar{u}(\bar{r}) = 0. \quad (\text{B.30})$$

Based on Siegel [57], we consider a particular solution of the linearized capillary equation as the initial guess, denoted as $v_1(\bar{r})$,

$$v_1(\bar{r}) = A_1 K_0(\bar{r}), \quad (\text{B.31})$$

where A_1 is to be determined by the “correct” volume, see later explanation.

To find A_1 , we integrate over the domain on both sides of (B.29).

$$-\bar{r}_0 \sin \psi_0 = \int_{\bar{r}_0}^{\infty} s \bar{u}(s) ds. \quad (\text{B.32})$$

(B.32) stands for the lifted up or pushed down volume outside of \bar{r}_0 , which is consider as the “correct” volume. Therefore, A_1 can be determined by

$$-\bar{r}_0 \sin \psi_0 = \int_{\bar{r}_0}^{\infty} s v_1(s) ds. \quad (\text{B.33})$$

Fortunately, the above integral can be evaluated explicitly. We have

$$A_1 = -\frac{\sin \psi_0}{K_1(\sqrt{B} \sin \phi_0)}, \quad (\text{B.34})$$

where K_1 is known as the modified Bessel function of the second kind.

With the initial guess, $v_1 = A_1 K_0(\bar{r})$, the next step iterative procedure is defined as follows,

$$(\bar{r} \sin \psi_2(\bar{r}))_{\bar{r}} = \bar{r} v_1(\bar{r}), \quad (\text{B.35})$$

where $\psi_2(\bar{r})$ satisfies $\psi_2(\bar{r}_0) = \psi_0$ and $\lim_{\bar{r} \rightarrow \infty} \bar{r} \sin(\psi_2(\bar{r})) = 0$.

After some calculation, we have

$$\sin \psi_2(\bar{r}) = -A_1 K_1(\bar{r}). \quad (\text{B.36})$$

Therefore, after one step iterative procedure, the approximated solution can be defined as

$$v_2(\bar{r}) = -\int_{\bar{r}}^{\infty} \frac{\sin \psi_2(s)}{\sqrt{1 - (\sin \psi_2(s))^2}} ds. \quad (\text{B.37})$$

Unfortunately, (B.37) cannot be evaluated analytically. While, the numerical integration method can be applied (MATLAB built-in integration function is applied).

We cannot simply apply $v_2(\bar{r})$ to obtain $v_3(\bar{r})$, which will cause the divergence. The volume adjustment has to be done after each iterative step. Thus, we define

$$\tilde{v}_2(\bar{r}) = A_2 v_2(\bar{r}), \quad (\text{B.38})$$

where A_2 is to be determined by the ‘‘correct’’ volume. In detail,

$$A_2 = -\frac{\bar{r}_0 \sin \psi_0}{\int_{\bar{r}_0}^{\infty} s v_2(s) ds}, \quad (\text{B.39})$$

where $\int_{\bar{r}_0}^{\infty} s v_2(s) ds$ contains double integrals, it can be simplified using the integration by parts. Thus,

$$A_2 = \frac{2\bar{r}_0 \sin \psi_0}{\bar{r}_0^2 v_2(\bar{r}_0) + \int_{\bar{r}_0}^{\infty} s^2 \frac{\sin \psi_2(s)}{\sqrt{1 - (\sin \psi_2(s))^2}} ds}. \quad (\text{B.40})$$

Therefore, the iterative procedure can be modified as

$$(\bar{r} \sin \psi_{n+1}(\bar{r}))_{\bar{r}} = \bar{r} \tilde{v}_n(\bar{r}), \quad (\text{B.41})$$

for the positive integer $n \geq 2$. $\psi_{n+1}(\bar{r})$ satisfies $\psi_{n+1}(\bar{r}_0) = \psi_0$ and $\lim_{\bar{r} \rightarrow \infty} \bar{r} \sin(\psi_{n+1}(\bar{r})) = 0$.

Solving (B.41) for $\sin \psi_{n+1}$,

$$\sin \psi_{n+1}(\bar{r}) = -\frac{1}{\bar{r}} \int_{\bar{r}}^{\infty} s \tilde{v}_n(s) ds. \quad (\text{B.42})$$

Then,

$$v_{n+1}(\bar{r}) = - \int_{\bar{r}}^{\infty} \frac{\sin \psi_{n+1}(s)}{\sqrt{1 - (\sin \psi_{n+1}(s))^2}} ds. \quad (\text{B.43})$$

Moreover,

$$\tilde{v}_{n+1}(\bar{r}) = A_{n+1} v_{n+1}(\bar{r}), \quad (\text{B.44})$$

where

$$A_{n+1} = -\frac{\bar{r}_0 \sin \psi_0}{\int_{\bar{r}_0}^{\infty} s v_{n+1}(s) ds}. \quad (\text{B.45})$$

In Fig. B.5, two approaches, the shooting method and the iterative method, are applied to determine the fluid interface for the floating ball problem with data $B = 1$, $\gamma = \frac{\pi}{4}$ and $\phi_0 = \frac{\pi}{3}$. Recall the formulas, we have $\bar{r}_0 = \sqrt{B} \sin(\phi_0) = \frac{\sqrt{3}}{2}$ and $\psi_0 = \phi_0 + \gamma - \pi = -\frac{5\pi}{12}$. As we can see, \tilde{v}_2 performs very well. Moreover, the fluid height at the contact point \bar{u}_0 is

of our interest. We define the relative error of the fluid height at the contact point between the result from the shooting method and the iterative solution, as follows,

$$\text{error}_{\text{rel}}(\tilde{v}_n) = \left| \frac{\bar{u}_0 - \tilde{v}_n(\bar{r}_0)}{\bar{u}_0} \right|, \quad (\text{B.46})$$

where \bar{u}_0 is considered as the result obtained from the shooting method.

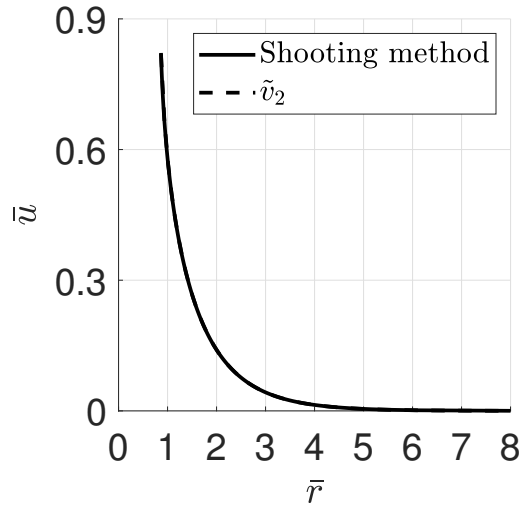


Figure B.5: The comparison between the shooting method result and the iterative solution \tilde{v}_2 with data: $B = 1$, $\gamma = \frac{\pi}{4}$, $\bar{r}_0 = \frac{\sqrt{3}}{2}$ and $\psi_0 = -\frac{5\pi}{12}$.

With the same data, we obtain $\bar{u}_0 = 0.821805$, $\tilde{v}_2(\bar{r}_0) = 0.819883$ and $\tilde{v}_3(\bar{r}_0) = 0.821781$. The relative errors $\text{error}_{\text{rel}}(\tilde{v}_2) = 0.23\%$ and $\text{error}_{\text{rel}}(\tilde{v}_3) = 2.9 \times 10^{-5}$. Therefore, after two iterations and volume adjustment, solution \tilde{v}_3 performs well.

Appendix C

C.1 Tilting Coordinates Using Euler's Angles

According to Euler's rotation theorem, tilting the coordinates from $x - y - z$ (we call them the space-fixed axes) to $x' - y' - z'$ (we call them the body-fixed axes) can be described by Euler angles ϕ , τ and ψ (measured counter-clockwise). Among many different conventions, the "ZYZ" convention is chosen. In details, we first rotate the coordinates about z axis by angle $\phi \in (0, 2\pi]$, then we rotate about y' axis by angle $\tau \in (0, \pi)$, finally, we rotate about z' axis by angle $\psi \in (0, 2\pi]$, shown in Fig. C.1. Therefore, the composite rotation matrix $R(\phi, \tau, \psi)$ (the active transformation) can be decomposed into

$$R(\phi, \tau, \psi) = R_{z'}(\psi)R_{y'}(\tau)R_z(\phi), \quad (\text{C.1})$$

where $R_{z'}$ and $R_{y'}$ are elementary rotation matrices for rotations about the body axes z' and y' , respectively. Hence, the rotation in (C.1) is called the body-fixed rotation (see Sakurai and Napolitano [54]). It is more convenient to express the rotation using the original coordinates (the space-fixed rotation). We obtain the equivalent R :

$$R(\phi, \tau, \psi) = R_z(\phi)R_y(\tau)R_z(\psi), \quad (\text{C.2})$$

where $R_z(\phi)$, $R_y(\tau)$ and $R_z(\psi)$ are elementary rotation matrices about the space-fixed axes. In details,

$$R_z(\phi) = \begin{pmatrix} \cos \phi & \sin \phi & 0 \\ -\sin \phi & \cos \phi & 0 \\ 0 & 0 & 1 \end{pmatrix}, R_y(\tau) = \begin{pmatrix} \cos \tau & 0 & -\sin \tau \\ 0 & 1 & 0 \\ \sin \tau & 0 & \cos \tau \end{pmatrix}, R_z(\psi) = \begin{pmatrix} \cos \psi & \sin \psi & 0 \\ -\sin \psi & \cos \psi & 0 \\ 0 & 0 & 1 \end{pmatrix}. \quad (\text{C.3})$$

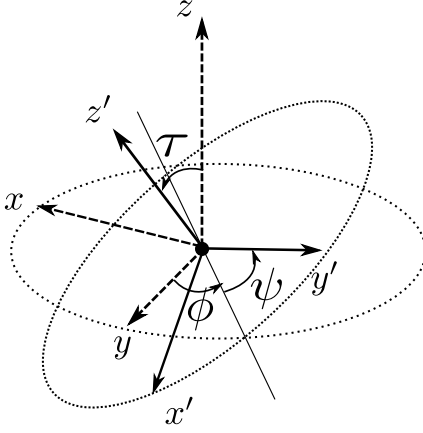


Figure C.1: Euler's angles with "ZYZ" convention.

Thus, the full expression of $R(\phi, \tau, \psi)$ is

$$R(\phi, \tau, \psi) = \begin{pmatrix} \cos \phi \cos \tau \cos \psi - \sin \phi \sin \psi & \cos \psi \sin \phi + \cos \phi \cos \tau \sin \psi & -\cos \phi \sin \tau \\ -\cos \phi \sin \psi + \cos \tau \cos \psi \sin \phi & \cos \phi \cos \psi - \cos \tau \sin \phi \sin \psi & \sin \phi \sin \tau \\ \cos \psi \sin \tau & \sin \tau \sin \psi & \cos \tau \end{pmatrix}. \quad (\text{C.4})$$

Therefore, changing the coordinates can be expressed as

$$\begin{pmatrix} x' \\ y' \\ z' \end{pmatrix} = R(\phi, \tau, \psi) \begin{pmatrix} x \\ y \\ z \end{pmatrix}. \quad (\text{C.5})$$

Moreover, its inverse can be found by $R^{-1} = R^T$.

C.2 Calculation of Nw , where $w(r, \theta) = v(r, \theta) + Aq(\theta)r^\lambda$

In this section, we present the detailed calculation of the expansion of the fully nonlinear term Nw in the interior domain Ω_{r_0} with small $r_0 > 0$ and the contact angle $\gamma \geq 0$, where $w(r, \theta)$ takes the form $w(r, \theta) = v(r, \theta) + Aq(\theta)r^\lambda$, defined in Ω_{r_0} . This work was originally done by Miersemann [45, 46], but has relatively few explanations. We follow Miersemann's idea and reproduce the expansion with detailed calculation.

Two cases will be discussed with different assumptions imposed, respectively.

- (1) When $q(\theta) = \frac{1}{\bar{\kappa}h(\theta)} + \epsilon_0$, for some small $\epsilon_0 > 0$, we assume $Ar^{\lambda+1} \ll 1$, $A > 0$ and $\lambda \geq 1$.
- (2) When $q(\theta) = 1$, we assume $0 < A\lambda \leq K_0$ for some $K_0 > 0$ and require $A > 0$, $0 < \lambda < 1$ (λ is sufficiently small).

Consider the general form: $w(r, \theta) = v(r, \theta) + Aq(\theta)r^\lambda$, in polar coordinates,

$$\begin{aligned}\nabla w &= \frac{\partial w}{\partial r} \hat{\mathbf{r}} + \frac{1}{r} \frac{\partial w}{\partial \theta} \hat{\boldsymbol{\theta}} \\ &= (v_r + Aq(\theta)\lambda r^{\lambda-1}) \hat{\mathbf{r}} + \left(\frac{1}{r} v_\theta + Aq'(\theta)r^{\lambda-1} \right) \hat{\boldsymbol{\theta}}.\end{aligned}$$

Moreover,

$$1 + |\nabla w|^2 = 1 + |\nabla v|^2 + Q(r, \theta),$$

where

$$v(r, \theta) = \frac{h(\theta)}{r}, \quad \nabla v = -\frac{h(\theta)}{r^2} \hat{\mathbf{r}} + \frac{h'(\theta)}{r^2} \hat{\boldsymbol{\theta}} \quad \text{and} \quad |\nabla v| = \frac{1}{r^2} (h^2 + h'^2)^{1/2},$$

$$Q(r, \theta) = -2A\lambda h(\theta)q(\theta)r^{\lambda-3} + 2Aq'(\theta)h'(\theta)r^{\lambda-3} + A^2\lambda^2 q^2 r^{2\lambda-2} + A^2 (q')^2 r^{2\lambda-2}.$$

Remark 30. When $\gamma = 0$, $h'(\theta)$ and $h''(\theta)$ become singular as $\theta \rightarrow \pm\alpha$. Recall from Property 6, as $\theta \rightarrow \pm\alpha$,

$$\begin{aligned}h'(\theta) &\sim \frac{b_1 \text{sign}(\theta)}{\sqrt{\sin^2 \alpha - \sin^2 \theta}}, \\ h''(\theta) &\sim \frac{b_2}{(\sin^2 \alpha - \sin^2 \theta)^{3/2}},\end{aligned}$$

where $b_1 = \frac{\cos \alpha}{\bar{\kappa}}$ and $b_2 = \frac{\sin \alpha \cos^2 \alpha}{\bar{\kappa}}$.

When $\gamma = 0$, as $\theta \rightarrow \pm\alpha$, the asymptotics of the following functions will be used later on:

$$|\nabla v| \sim \frac{1}{r^2} |h'(\theta)|, \quad (\text{C.6})$$

$$|\nabla v|_\theta = \frac{1}{r^2} \frac{h'}{\sqrt{h^2 + h'^2}} (h + h'') \sim \frac{1}{r^2} h''(\theta). \quad (\text{C.7})$$

For the $q(\theta) = \frac{1}{\bar{\kappa}h(\theta)} + \epsilon_0$ case, with $\gamma = 0$, as $\theta \rightarrow \pm\alpha$,

$$Q(r, \theta) \sim A \frac{h'^2}{\bar{\kappa}h^2} r^{\lambda-3} + A^2 \frac{h'^3}{\bar{\kappa}^2 h^4} r^{2\lambda-2}, \quad (\text{C.8})$$

$$Q_\theta \sim A \frac{h'h''}{\bar{\kappa}h^2} r^{\lambda-3} + A^2 \frac{h'h''}{\bar{\kappa}^2 h^4} r^{2\lambda-2}. \quad (\text{C.9})$$

While, for the $q(\theta) = 1$ case, with $\gamma = 0$, as $\theta \rightarrow \pm\alpha$, $Q(r, \theta)$ has no singularity, and Q_θ can be easily calculated.

$$Q(r, \theta) = -2A\lambda h(\theta) r^{\lambda-3} + A^2 \lambda^2 r^{2\lambda-2} \text{ is bounded,} \quad (\text{C.10})$$

$$Q_\theta = -2A\lambda h' r^{\lambda-3}. \quad (\text{C.11})$$

Next, we expand Nw ,

$$\begin{aligned} Nw &= \frac{1}{r} \left\{ \left[\frac{rw_r}{(1 + |\nabla w|^2)^{1/2}} \right]_r + \left[\frac{\frac{1}{r}w_\theta}{(1 + |\nabla w|^2)^{1/2}} \right]_\theta \right\} \\ &= \frac{1}{r} \left\{ \left[\frac{rv_r + A\lambda q(\theta)r^\lambda}{(1 + |\nabla v|^2)^{1/2}} \left(1 + \frac{Q}{1 + |\nabla v|^2} \right)^{-1/2} \right]_r + \left[\frac{\frac{1}{r}v_\theta + Aq'(\theta)r^{\lambda-1}}{(1 + |\nabla v|^2)^{1/2}} \left(1 + \frac{Q}{1 + |\nabla v|^2} \right)^{-1/2} \right]_\theta \right\}. \end{aligned} \quad (\text{C.12})$$

Remark 31. The expression of Nw in (C.12) follows Miersemann's work in [46].

When expanding Nw , we list some useful expansions and their bound estimates in the following Lemma 36 - Lemma 39.

Lemma 36. *In Ω_{r_0} , with $0 < r \leq r_0 \ll 1$ such that $|\nabla v| \gg 1$, and $\gamma \geq 0$, then*

$$\frac{1}{(1 + |\nabla v|^2)^{1/2}} = \frac{1}{|\nabla v|} + \Delta_1(r, \theta), \quad (\text{C.13})$$

where, based on Taylor's theorem (the integral form),

$$\Delta_1(r, \theta) = -\frac{1}{2|\nabla v|} \int_0^1 \frac{1}{|\nabla v|^2} \frac{1}{(1+s)^{3/2}} ds. \quad (\text{C.14})$$

It is more convenient to do differentiation. Moreover,

(i) when $\gamma \geq 0$, and h', h'' are away from their singularities,

$$|\Delta_1(r, \theta)| \leq \frac{1}{2|\nabla v|^3} = \frac{r^6}{2(h^2 + h'^2)^{3/2}} \leq d_{\Delta_1} r^6, \quad (\text{C.15})$$

$$|\Delta_{1r}(r, \theta)| \leq \frac{3}{2} \left| \frac{|\nabla v|_r}{|\nabla v|^4} \right| = \frac{3r^5}{(h^2 + h'^2)^{3/2}} \leq d_{\Delta_{1r}} r^5, \quad (\text{C.16})$$

and

$$|\Delta_{1\theta}(r, \theta)| \leq \frac{3}{2} \left| \frac{|\nabla v|_\theta}{|\nabla v|^4} \right| = \frac{3 \left[(h^2 + h'^2)^{1/2} \right]_\theta r^6}{2(h^2 + h'^2)^2} \leq d_{\Delta_{1\theta}} r^6 \quad (\text{C.17})$$

for some constant $d_{\Delta_1}, d_{\Delta_{1r}}, d_{\Delta_{1\theta}} > 0$.

(ii) when $\gamma = 0$, as $\theta \rightarrow \pm\alpha$,

$$|\Delta_1(r, \theta)| \sim \frac{1}{2|h'|^3} r^6 \rightarrow 0, \quad |\Delta_{1r}(r, \theta)| \sim \frac{3}{|h'|^3} r^5 \rightarrow 0, \quad |\Delta_{1\theta}(r, \theta)| \sim \frac{3h''}{2h'^4} r^6 \rightarrow 0. \quad (\text{C.18})$$

Thus, estimates in (C.15), (C.16) and (C.17) are all valid in this case.

Lemma 37. In Ω_{r_0} , with $0 < r \leq r_0 \ll 1$ such that $|\nabla v| \gg 1$, and $\gamma \geq 0$,

$$\frac{Q}{1 + |\nabla v|^2} = \frac{Q}{|\nabla v|^2} + \Delta_2(r, \theta), \quad (\text{C.19})$$

where, based on Taylor's theorem (the integral form),

$$\Delta_2(r, \theta) = -\frac{Q}{|\nabla v|^2} \int_0^1 \frac{1}{|\nabla v|^2} \frac{1}{(1+s)^2} ds. \quad (\text{C.20})$$

Moreover,

(i) when $q(\theta) = \frac{1}{\bar{\kappa}h(\theta)} + \epsilon_0$, $\gamma \geq 0$, and h' , h'' are away from their singularities,

$$\begin{aligned} |\Delta_2(r, \theta)| &\leq \frac{|Q|}{|\nabla v|^4} \leq \frac{1}{(h^2 + h'^2)^2} [2A\lambda h(\theta)q(\theta)r^{\lambda+5} + 2A|q'||h'|r^{\lambda+5} \\ &\quad + A^2\lambda^2 q^2 r^{2\lambda+6} + A^2(q')^2 r^{2\lambda+6}] \\ &\leq d_{1\Delta_2} A r^{\lambda+5} + d_{2\Delta_2} A^2 r^{2\lambda+6}, \end{aligned} \quad (\text{C.21})$$

$$|\Delta_{2r}(r, \theta)| \leq \frac{|Q_r|}{|\nabla v|^4} + 4 \left| \frac{Q|\nabla v|_r}{|\nabla v|^5} \right| \leq d_{1\Delta_{2r}} A r^{\lambda+4} + d_{2\Delta_{2r}} A^2 r^{2\lambda+5}, \quad (\text{C.22})$$

and

$$|\Delta_{2\theta}(r, \theta)| \leq \frac{|Q_\theta|}{|\nabla v|^4} + 4 \left| \frac{Q|\nabla v|_\theta}{|\nabla v|^5} \right| \leq d_{1\Delta_{2\theta}} A r^{\lambda+5} + d_{2\Delta_{2\theta}} A^2 r^{2\lambda+6} \quad (\text{C.23})$$

for some λ dependent $d_{1\Delta_2}, d_{2\Delta_2}, d_{1\Delta_{2r}}, d_{2\Delta_{2r}}, d_{1\Delta_{2\theta}}, d_{2\Delta_{2\theta}} > 0$.

(ii) When $q(\theta) = \frac{1}{\bar{\kappa}h(\theta)} + \epsilon_0$ and $\gamma = 0$, as $\theta \rightarrow \pm\alpha$,

$$|\Delta_2(r, \theta)| \leq \frac{|Q|}{|\nabla v|^4} \sim 2A \frac{1}{\bar{\kappa}h^2h'^2} r^{\lambda+5} + A^2 \frac{1}{\bar{\kappa}^2h^4h'^2} r^{2\lambda+6} \rightarrow 0, \quad (\text{C.24})$$

$$|\Delta_{2r}(r, \theta)| \leq \frac{|Q_r|}{|\nabla v|^4} + 4 \left| \frac{Q|\nabla v|_r}{|\nabla v|^5} \right| \sim A \frac{b_{1\Delta_{2r}}}{\bar{\kappa}h^2h'^2} r^{\lambda+4} + A^2 \frac{b_{2\Delta_{2r}}}{\bar{\kappa}^2h^4h'^2} r^{2\lambda+5} \rightarrow 0, \quad (\text{C.25})$$

$$|\Delta_{2\theta}(r, \theta)| \leq \frac{|Q_\theta|}{|\nabla v|^4} + 4 \left| \frac{Q|\nabla v|_\theta}{|\nabla v|^5} \right| \sim Ab_{1\Delta_{2\theta}} \frac{h''}{\bar{\kappa}|h'|^3h^2} r^{\lambda+5} + A^2 b_{2\Delta_{2\theta}} \frac{h''}{\bar{\kappa}^2|h'|^3h^4} r^{2\lambda+6} \rightarrow 0 \quad (\text{C.26})$$

for some λ dependent $b_{1\Delta_{2r}}, b_{2\Delta_{2r}}, b_{1\Delta_{2\theta}}, b_{2\Delta_{2\theta}} > 0$. Thus, estimates in (C.21), (C.22) and (C.23) are all valid in this case.

(iii) When $q(\theta) = 1$, $\gamma \geq 0$, and h', h'' are away from their singularities,

$$\begin{aligned} |\Delta_2(r, \theta)| &\leq \frac{|Q|}{|\nabla v|^4} \leq \frac{1}{(h^2 + h'^2)^2} [2A\lambda h(\theta)r^{\lambda+5} + A^2\lambda^2 r^{2\lambda+6}] \\ &\leq d'_{1\Delta_2} A\lambda r^{\lambda+5} + d'_{2\Delta_2} A^2\lambda^2 r^{2\lambda+6}, \end{aligned} \quad (\text{C.27})$$

$$|\Delta_{2r}(r, \theta)| \leq \frac{|Q_r|}{|\nabla v|^4} + 4 \left| \frac{Q|\nabla v|_r}{|\nabla v|^5} \right| \leq d'_{1\Delta_{2r}} A\lambda r^{\lambda+4} + d'_{2\Delta_{2r}} A^2\lambda^2 r^{2\lambda+5}, \quad (\text{C.28})$$

and

$$|\Delta_{2\theta}(r, \theta)| \leq \frac{|Q_\theta|}{|\nabla v|^4} + 4 \left| \frac{Q|\nabla v|_\theta}{|\nabla v|^5} \right| \leq d'_{1\Delta_{2\theta}} A\lambda r^{\lambda+5} + d'_{2\Delta_{2\theta}} A^2\lambda^2 r^{2\lambda+6} \quad (\text{C.29})$$

for some λ dependent $d'_{1\Delta_2}, d'_{2\Delta_2}, d'_{1\Delta_{2r}}, d'_{2\Delta_{2r}}, d'_{1\Delta_{2\theta}}, d'_{2\Delta_{2\theta}} > 0$.

(iv) When $q(\theta) = 1$ and $\gamma = 0$, as $\theta \rightarrow \pm\alpha$,

$$|\Delta_2(r, \theta)| \leq \frac{|Q|}{|\nabla v|^4} \sim 2A\lambda \frac{h}{h'^4} r^{\lambda+5} + A^2 \lambda^2 \frac{1}{h'^4} r^{2\lambda+6} \rightarrow 0, \quad (\text{C.30})$$

$$|\Delta_{2r}(r, \theta)| \leq \frac{|Q_r|}{|\nabla v|^4} + 4 \left| \frac{Q|\nabla v|_r}{|\nabla v|^5} \right| \sim A\lambda b'_{1\Delta_{2r}} \frac{h}{h'^4} r^{\lambda+4} + A^2 \lambda^2 b'_{2\Delta_{2r}} \frac{1}{h'^4} r^{2\lambda+5} \rightarrow 0, \quad (\text{C.31})$$

$$\begin{aligned} |\Delta_{2\theta}(r, \theta)| &\leq \frac{|Q_\theta|}{|\nabla v|^4} + 4 \left| \frac{Q|\nabla v|_\theta}{|\nabla v|^5} \right| \sim A\lambda b'_{1\Delta_{2\theta}} \frac{1}{|h'|^3} r^{\lambda+5} + A\lambda b'_{2\Delta_{2\theta}} \frac{hh''}{|h'|^5} r^{\lambda+5} \\ &\quad + A^2 \lambda^2 b'_{3\Delta_{2\theta}} \frac{h''}{|h'|^5} r^{2\lambda+6} \rightarrow 0, \end{aligned} \quad (\text{C.32})$$

for some λ dependent $b'_{1\Delta_{2r}}, b'_{2\Delta_{2r}}, b'_{1\Delta_{2\theta}}, b'_{2\Delta_{2\theta}}$ and $b'_{3\Delta_{2\theta}} > 0$. Thus, estimates in (C.27), (C.28) and (C.29) are all valid in this case.

From Lemma 37, let $g(r, \theta) = \frac{Q}{1 + |\nabla v|^2}$,

(i) when $q(\theta) = \frac{1}{\bar{\kappa}h(\theta)} + \epsilon_0$, $\gamma \geq 0$, and h', h'' are away from their singularities,

$$|g(r, \theta)| \leq \frac{|Q|}{|\nabla v|^2} + |\Delta_2(r, \theta)| \leq d_{1g} A r^{\lambda+1} + d_{2g} A^2 r^{2\lambda+2}, \quad (\text{C.33})$$

$$|g_r(r, \theta)| \leq \frac{|Q_r|}{|\nabla v|^2} + 2 \left| \frac{Q|\nabla v|_r}{|\nabla v|^3} \right| + |\Delta_{2r}(r, \theta)| \leq d_{1g_r} A r^\lambda + d_{2g_r} A^2 r^{2\lambda+1}, \quad (\text{C.34})$$

and

$$|g_\theta(r, \theta)| \leq \frac{|Q_\theta|}{|\nabla v|^2} + 2 \left| \frac{Q|\nabla v|_\theta}{|\nabla v|^3} \right| + |\Delta_{2\theta}(r, \theta)| \leq d_{1g_\theta} A r^{\lambda+1} + d_{2g_\theta} A^2 r^{2\lambda+2} \quad (\text{C.35})$$

for some λ dependent $d_{1g}, d_{2g}, d_{1g_r}, d_{2g_r}, d_{1g_\theta}, d_{2g_\theta} > 0$.

(ii) When $q(\theta) = \frac{1}{\bar{\kappa}h(\theta)} + \epsilon_0$ and $\gamma = 0$, as $\theta \rightarrow \pm\alpha$,

$$|g(r, \theta)| \sim \frac{|Q|}{|\nabla v|^2} \sim 2A \frac{1}{\bar{\kappa}h^2} r^{\lambda+1} + A^2 \frac{1}{\bar{\kappa}^2 h^4} r^{2\lambda+2} \rightarrow 0, \quad (\text{C.36})$$

$$|g_r(r, \theta)| \sim Ab_{1g_r} \frac{1}{\bar{\kappa}h^2} r^\lambda + A^2 b_{2g_r} \frac{1}{\bar{\kappa}^2 h^4} r^{2\lambda+1}, \quad (\text{C.37})$$

$$|g_\theta(r, \theta)| \sim Ab_{1g_\theta} \frac{h''}{\bar{\kappa}|h'|h^2} r^{\lambda+1} + A^2 b_{2g_\theta} \frac{h''}{\bar{\kappa}^2 |h'|h^4} r^{2\lambda+2}, \quad (\text{C.38})$$

for some λ dependent $b_{1g_r}, b_{2g_r}, b_{1g_\theta}, b_{2g_\theta} > 0$. Thus, estimates in (C.33) and (C.34) are both valid, while, in this case, $|g_\theta(r, \theta)|$ tends to infinity. Fortunately, we do not need to worry about the estimate for $|g_\theta(r, \theta)|$ (see Remark 32).

(iii) When $q(\theta) = 1$, $\gamma \geq 0$, and h', h'' are away from their singularities,

$$|g(r, \theta)| \leq \frac{|Q|}{|\nabla v|^2} + |\Delta_2(r, \theta)| \leq d'_{1g} A \lambda r^{\lambda+1} + d'_{2g} A^2 \lambda^2 r^{2\lambda+2}, \quad (\text{C.39})$$

$$|g_r(r, \theta)| \leq \frac{|Q_r|}{|\nabla v|^2} + 2 \left| \frac{Q|\nabla v|_r}{|\nabla v|^3} \right| + |\Delta_{2r}(r, \theta)| \leq d'_{1g_r} A \lambda r^\lambda + d'_{2g_r} A^2 \lambda^2 r^{2\lambda+1}, \quad (\text{C.40})$$

and

$$|g_\theta(r, \theta)| \leq \frac{|Q_\theta|}{|\nabla v|^2} + 2 \left| \frac{Q|\nabla v|_\theta}{|\nabla v|^3} \right| + |\Delta_{2\theta}(r, \theta)| \leq d'_{1g_\theta} A \lambda r^{\lambda+1} + d'_{2g_\theta} A^2 \lambda^2 r^{2\lambda+2} \quad (\text{C.41})$$

for some λ dependent $d'_{1g}, d'_{2g}, d'_{1g_r}, d'_{2g_r}, d'_{1g_\theta}, d'_{2g_\theta} > 0$.

(iv) When $q(\theta) = 1$ and $\gamma = 0$, as $\theta \rightarrow \pm\alpha$,

$$|g(r, \theta)| \sim \frac{|Q|}{|\nabla v|^2} \sim 2A\lambda \frac{h}{|h'|^2} r^{\lambda+1} + A^2 \lambda^2 \frac{1}{|h'|^2} r^{2\lambda+2} \rightarrow 0, \quad (\text{C.42})$$

$$|g_r(r, \theta)| \sim A\lambda b'_{1g_r} \frac{h}{|h'|^2} r^\lambda + A^2 \lambda^2 b'_{2g_r} \frac{1}{|h'|^2} r^{2\lambda+1} \rightarrow 0, \quad (\text{C.43})$$

$$|g_\theta(r, \theta)| \sim A\lambda b'_{1g_\theta} \left(\frac{1}{|h'|} + \frac{h''h}{|h'|^3} \right) r^{\lambda+1} + A^2 \lambda^2 b'_{2g_\theta} \frac{h''}{|h'|^3} r^{2\lambda+2} \rightarrow 0, \quad (\text{C.44})$$

for some λ dependent $b'_{1gr}, b'_{2gr}, b'_{1g\theta}, b'_{2g\theta} > 0$. Thus, estimates in (C.39), (C.40) and (C.41) are all valid in this case.

Lemma 38. *In Ω_{r_0} , with $0 < r \leq r_0 \ll 1$ such that $|\nabla v| \gg 1$, and $\gamma \geq 0$, in either the $q(\theta) = \frac{1}{\bar{\kappa}h(\theta)} + \epsilon_0$ case or the $q(\theta) = 1$ case, we both have*

$$|g(r, \theta)| \ll 1. \quad (\text{C.45})$$

(Q can be either positive or negative, we set $|g(r, \theta)| \leq \frac{1}{2}$ for the later estimates). And then

$$\left(1 + \frac{Q}{1 + |\nabla v|^2}\right)^{-1/2} = 1 - \frac{Q}{2|\nabla v|^2} + \Delta_3(r, \theta), \quad (\text{C.46})$$

where

$$\Delta_3(r, \theta) = -\frac{1}{2}\Delta_2(r, \theta) + \int_0^{g(r, \theta)} \frac{3}{4(1+s)^{5/2}}(g(r, \theta) - s) ds. \quad (\text{C.47})$$

Moreover,

(i) when $q(\theta) = \frac{1}{\bar{\kappa}h(\theta)} + \epsilon_0$, $\gamma \geq 0$, and h', h'' are away from their singularities,

$$|\Delta_3(r, \theta)| \leq \frac{1}{2}|\Delta_2(r, \theta)| + \frac{9}{4}|g(r, \theta)|^2 \leq d_{1\Delta_3}Ar^{\lambda+5} + d_{2\Delta_3}A^2r^{2\lambda+2}, \quad (\text{C.48})$$

$$|\Delta_{3r}(r, \theta)| \leq \frac{1}{2}|\Delta_{2r}(r, \theta)| + \frac{9}{2}|g(r, \theta)||g_r(r, \theta)| \leq d_{1\Delta_{3r}}Ar^{\lambda+4} + d_{2\Delta_{3r}}A^2r^{2\lambda+1}, \quad (\text{C.49})$$

and

$$|\Delta_{3\theta}(r, \theta)| \leq \frac{1}{2}|\Delta_{2\theta}(r, \theta)| + \frac{9}{2}|g(r, \theta)||g_\theta(r, \theta)| \leq d_{1\Delta_{3\theta}}Ar^{\lambda+5} + d_{2\Delta_{3\theta}}A^2r^{2\lambda+2} \quad (\text{C.50})$$

for some λ dependent $d_{1\Delta_3}, d_{2\Delta_3}, d_{1\Delta_{3r}}, d_{2\Delta_{3r}}, d_{1\Delta_{3\theta}}, d_{2\Delta_{3\theta}} > 0$.

(ii) When $q(\theta) = \frac{1}{\bar{\kappa}h(\theta)} + \epsilon_0$ and $\gamma = 0$, as $\theta \rightarrow \pm\alpha$,

$$|\Delta_3(r, \theta)| \sim Ab_{1\Delta_3} \frac{1}{\bar{\kappa}h^2|h'|^2} r^{\lambda+5} + A^2b_{2\Delta_3} \frac{1}{\bar{\kappa}^2h^4} r^{2\lambda+2} \rightarrow 0, \quad (\text{C.51})$$

$$|\Delta_{3r}(r, \theta)| \sim Ab_{1\Delta_{3r}} \frac{1}{\bar{\kappa}h^2|h'|^2} r^{\lambda+4} + A^2b_{2\Delta_{3r}} \frac{1}{\bar{\kappa}^2h^4} r^{2\lambda+1}, \quad (\text{C.52})$$

$$|\Delta_{3\theta}(r, \theta)| \sim Ab_{1\Delta_{3\theta}} \frac{h''}{\bar{\kappa}|h'|^3h^2} r^{\lambda+5} + A^2b_{2\Delta_{3\theta}} \frac{h''}{\bar{\kappa}^2|h'|h^4} r^{2\lambda+2} \quad (\text{C.53})$$

for some λ dependent $b_{1\Delta_3}$, $b_{2\Delta_3}$, $b_{1\Delta_{3r}}$, $b_{2\Delta_{3r}}$, $b_{1\Delta_{3\theta}}$ and $b_{2\Delta_{3\theta}} > 0$. Thus, estimates in (C.48) and (C.49) are both valid, while, in this case, $|\Delta_{3\theta}(r, \theta)|$ tends to infinity. Fortunately, we do not need to worry about the estimate for $|\Delta_{3\theta}(r, \theta)|$ (see Remark 32).

(iii) When $q(\theta) = 1$, $\gamma \geq 0$, and h' , h'' are away from their singularities,

$$|\Delta_3(r, \theta)| \leq \frac{1}{2}|\Delta_2(r, \theta)| + \frac{9}{4}|g(r, \theta)|^2 \leq d'_{1\Delta_3}A\lambda r^{\lambda+5} + d'_{2\Delta_3}A^2\lambda^2r^{2\lambda+2}, \quad (\text{C.54})$$

$$|\Delta_{3r}(r, \theta)| \leq \frac{1}{2}|\Delta_{2r}(r, \theta)| + \frac{9}{2}|g(r, \theta)||g_r(r, \theta)| \leq d'_{1\Delta_{3r}}A\lambda r^{\lambda+4} + d'_{2\Delta_{3r}}A^2\lambda^2r^{2\lambda+1}, \quad (\text{C.55})$$

and

$$|\Delta_{3\theta}(r, \theta)| \leq \frac{1}{2}|\Delta_{2\theta}(r, \theta)| + \frac{9}{2}|g(r, \theta)||g_\theta(r, \theta)| \leq d'_{1\Delta_{3\theta}}A\lambda r^{\lambda+5} + d'_{2\Delta_{3\theta}}A^2\lambda^2r^{2\lambda+2} \quad (\text{C.56})$$

for some λ dependent $d'_{1\Delta_3}$, $d'_{2\Delta_3}$, $d'_{1\Delta_{3r}}$, $d'_{2\Delta_{3r}}$, $d'_{1\Delta_{3\theta}}$, $d'_{2\Delta_{3\theta}} > 0$.

(iv) When $q(\theta) = 1$ and $\gamma = 0$, as $\theta \rightarrow \pm\alpha$,

$$|\Delta_3(r, \theta)| \sim A\lambda b'_{1\Delta_3} \frac{h}{|h'|^4} r^{\lambda+5} + A^2 \lambda^2 b'_{2\Delta_3} \frac{h^2}{|h'|^4} r^{2\lambda+2} \rightarrow 0, \quad (\text{C.57})$$

$$|\Delta_{3r}(r, \theta)| \sim A\lambda b'_{1\Delta_{3r}} \frac{h}{|h'|^4} r^{\lambda+4} + A^2 \lambda^2 b'_{2\Delta_{3r}} \frac{h^2}{|h'|^4} r^{2\lambda+1} \rightarrow 0, \quad (\text{C.58})$$

$$\begin{aligned} |\Delta_{3\theta}(r, \theta)| &\sim A\lambda b'_{1\Delta_{3\theta}} \frac{1}{|h'|^3} r^{\lambda+5} + A\lambda b'_{2\Delta_{3\theta}} \frac{hh''}{|h'|^5} r^{\lambda+5} + A^2 \lambda^2 b'_{3\Delta_{3\theta}} \frac{h''}{|h'|^5} r^{2\lambda+6} \\ &\quad + A^2 \lambda^2 b'_{4\Delta_{3\theta}} \left(\frac{h}{|h'|^3} + \frac{h''h^2}{|h'|^5} \right) r^{2\lambda+2} \rightarrow 0 \end{aligned} \quad (\text{C.59})$$

for some λ dependent $b'_{1\Delta_3}$, $b'_{2\Delta_3}$, $b'_{1\Delta_{3r}}$, $b'_{2\Delta_{3r}}$, $b'_{1\Delta_{3\theta}}$, $b'_{2\Delta_{3\theta}}$, $b'_{3\Delta_{3\theta}}$ and $b'_{4\Delta_{3\theta}} > 0$. Thus, estimates in (C.54), (C.55) and (C.56) are all valid in this case.

Remark 32. When $q(\theta) = \frac{1}{\bar{\kappa}h(\theta)} + \epsilon_0$ and $\gamma = 0$, as $\theta \rightarrow \pm\alpha$, the asymptotics of $|g_\theta|$ and $|\Delta_{3\theta}|$ in (C.38) and (C.53), tend to infinity. Fortunately, in the later analysis, those terms will not appear alone, they accompany with other terms such that the desired property can be achieved.

Lemma 39. In Ω_{r_0} , with $0 < r \leq r_0 \ll 1$ such that $|\nabla v| \gg 1$, and $\gamma \geq 0$,

$$\frac{1}{(1 + |\nabla v|^2)^{1/2}} \left(1 + \frac{Q}{1 + |\nabla v|^2} \right)^{-1/2} = \frac{1}{(1 + |\nabla v|^2)^{1/2}} - \frac{Q}{2|\nabla v|^3} + \Delta(r, \theta), \quad (\text{C.60})$$

where

$$\Delta(r, \theta) = -\frac{Q}{2|\nabla v|^2} \Delta_1(r, \theta) + \frac{1}{|\nabla v|} \Delta_3(r, \theta) + \Delta_1(r, \theta) \Delta_3(r, \theta). \quad (\text{C.61})$$

Moreover,

(i) when $q(\theta) = \frac{1}{\bar{\kappa}h(\theta)} + \epsilon_0$, $\gamma \geq 0$, and h' , h'' are away from their singularities,

$$\begin{aligned} |\Delta(r, \theta)| &\leq \frac{|Q|}{2|\nabla v|^2} |\Delta_1(r, \theta)| + \frac{1}{|\nabla v|} |\Delta_3(r, \theta)| + |\Delta_1(r, \theta)| |\Delta_3(r, \theta)| \\ &\leq d_{1\Delta} A r^{\lambda+7} + d_{2\Delta} A^2 r^{2\lambda+4}, \end{aligned} \quad (\text{C.62})$$

$$\begin{aligned}
|\Delta_r(r, \theta)| &\leq \left(\frac{|Q_r|}{2|\nabla v|^2} + \left| \frac{Q|\nabla v|_r}{|\nabla v|^3} \right| \right) |\Delta_1| + \frac{|Q|}{2|\nabla v|^2} |\Delta_{1r}| \\
&\quad + \left| \frac{|\nabla v|_r}{|\nabla v|^2} \right| |\Delta_3| + \frac{|\Delta_{3r}|}{|\nabla v|} + |\Delta_{1r}| |\Delta_3| + |\Delta_1| |\Delta_{3r}| \\
&\leq d_{1\Delta_r} A r^{\lambda+6} + d_{2\Delta_r} A^2 r^{2\lambda+3},
\end{aligned} \tag{C.63}$$

and

$$\begin{aligned}
|\Delta_\theta(r, \theta)| &\leq \left(\frac{|Q_\theta|}{2|\nabla v|^2} + \left| \frac{Q|\nabla v|_\theta}{|\nabla v|^3} \right| \right) |\Delta_1| + \frac{|Q|}{2|\nabla v|^2} |\Delta_{1\theta}| \\
&\quad + \left| \frac{|\nabla v|_\theta}{|\nabla v|^2} \right| |\Delta_3| + \frac{|\Delta_{3\theta}|}{|\nabla v|} + |\Delta_{1\theta}| |\Delta_3| + |\Delta_1| |\Delta_{3\theta}| \\
&\leq d_{1\Delta_\theta} A r^{\lambda+7} + d_{2\Delta_\theta} A^2 r^{2\lambda+4}
\end{aligned} \tag{C.64}$$

for some λ dependent $d_{1\Delta}, d_{2\Delta}, d_{1\Delta_r}, d_{2\Delta_r}, d_{1\Delta_\theta}, d_{2\Delta_\theta} > 0$.

(ii) When $q(\theta) = \frac{1}{\bar{\kappa}h(\theta)} + \epsilon_0$ and $\gamma = 0$, as $\theta \rightarrow \pm\alpha$,

$$\begin{aligned}
|\Delta(r, \theta)| &\leq \frac{|Q|}{2|\nabla v|^2} |\Delta_1(r, \theta)| + \frac{1}{|\nabla v|} |\Delta_3(r, \theta)| + |\Delta_1(r, \theta)| |\Delta_3(r, \theta)| \\
&\sim Ab_{1\Delta} \frac{1}{\bar{\kappa} h^2 |h'|^3} r^{\lambda+7} + A^2 b_{2\Delta} \frac{1}{\bar{\kappa}^2 h^4 |h'|} r^{2\lambda+4} \rightarrow 0,
\end{aligned} \tag{C.65}$$

$$\begin{aligned}
|\Delta_r(r, \theta)| &\leq \left(\frac{|Q_r|}{2|\nabla v|^2} + \left| \frac{Q|\nabla v|_r}{|\nabla v|^3} \right| \right) |\Delta_1| + \frac{|Q|}{2|\nabla v|^2} |\Delta_{1r}| \\
&\quad + \left| \frac{|\nabla v|_r}{|\nabla v|^2} \right| |\Delta_3| + \frac{|\Delta_{3r}|}{|\nabla v|} + |\Delta_{1r}| |\Delta_3| + |\Delta_1| |\Delta_{3r}| \\
&\sim Ab_{1\Delta_r} \frac{1}{\bar{\kappa} h^2 |h'|^3} r^{\lambda+6} + A^2 b_{2\Delta_r} \frac{1}{\bar{\kappa}^2 h^4 |h'|} r^{2\lambda+3} \rightarrow 0,
\end{aligned} \tag{C.66}$$

$$\begin{aligned}
|\Delta_\theta(r, \theta)| &\leq \left(\frac{|Q_\theta|}{2|\nabla v|^2} + \left| \frac{Q|\nabla v|_\theta}{|\nabla v|^3} \right| \right) |\Delta_1| + \frac{|Q|}{2|\nabla v|^2} |\Delta_{1\theta}| \\
&\quad + \left| \frac{|\nabla v|_\theta}{|\nabla v|^2} \right| |\Delta_3| + \frac{|\Delta_{3\theta}|}{|\nabla v|} + |\Delta_{1\theta}| |\Delta_3| + |\Delta_1| |\Delta_{3\theta}| \\
&\sim Ab_{1\Delta_\theta} \frac{h''}{\bar{\kappa} |h'|^4 h^2} r^{\lambda+7} + A^2 b_{2\Delta_\theta} \frac{h''}{\bar{\kappa}^2 |h'|^2 h^4} r^{2\lambda+4} \rightarrow 0
\end{aligned} \tag{C.67}$$

for some λ dependent $b_{1\Delta}$, $b_{2\Delta}$, $b_{1\Delta_r}$, $b_{2\Delta_r}$, $b_{1\Delta_\theta}$ and $b_{2\Delta_\theta} > 0$. Thus, estimates in (C.62), (C.63) and (C.64) are all valid in this case.

(iii) When $q(\theta) = 1$, $\gamma \geq 0$, and h' , h'' are away from their singularities,

$$\begin{aligned}
|\Delta(r, \theta)| &\leq \frac{|Q|}{2|\nabla v|^2} |\Delta_1(r, \theta)| + \frac{1}{|\nabla v|} |\Delta_3(r, \theta)| + |\Delta_1(r, \theta)| |\Delta_3(r, \theta)| \\
&\leq d'_{1\Delta} A \lambda r^{\lambda+7} + d'_{2\Delta} A^2 \lambda^2 r^{2\lambda+4},
\end{aligned} \tag{C.68}$$

$$\begin{aligned}
|\Delta_r(r, \theta)| &\leq \left(\frac{|Q_r|}{2|\nabla v|^2} + \left| \frac{Q|\nabla v|_r}{|\nabla v|^3} \right| \right) |\Delta_1| + \frac{|Q|}{2|\nabla v|^2} |\Delta_{1r}| \\
&\quad + \left| \frac{|\nabla v|_r}{|\nabla v|^2} \right| |\Delta_3| + \frac{|\Delta_{3r}|}{|\nabla v|} + |\Delta_{1r}| |\Delta_3| + |\Delta_1| |\Delta_{3r}| \\
&\leq d'_{1\Delta_r} A \lambda r^{\lambda+6} + d'_{2\Delta_r} A^2 \lambda^2 r^{2\lambda+3},
\end{aligned} \tag{C.69}$$

and

$$\begin{aligned}
|\Delta_\theta(r, \theta)| &\leq \left(\frac{|Q_\theta|}{2|\nabla v|^2} + \left| \frac{Q|\nabla v|_\theta}{|\nabla v|^3} \right| \right) |\Delta_1| + \frac{|Q|}{2|\nabla v|^2} |\Delta_{1\theta}| \\
&\quad + \left| \frac{|\nabla v|_\theta}{|\nabla v|^2} \right| |\Delta_3| + \frac{|\Delta_{3\theta}|}{|\nabla v|} + |\Delta_{1\theta}| |\Delta_3| + |\Delta_1| |\Delta_{3\theta}| \\
&\leq d'_{1\Delta_\theta} A \lambda r^{\lambda+7} + d'_{2\Delta_\theta} A^2 \lambda^2 r^{2\lambda+4}
\end{aligned} \tag{C.70}$$

for some λ dependent $d'_{1\Delta}, d'_{2\Delta}, d'_{1\Delta_r}, d'_{2\Delta_r}, d'_{1\Delta_\theta}, d'_{2\Delta_\theta} > 0$.

(iv) When $q(\theta) = 1$ and $\gamma = 0$, as $\theta \rightarrow \pm\alpha$,

$$\begin{aligned}
|\Delta(r, \theta)| &\leq \frac{|Q|}{2|\nabla v|^2} |\Delta_1(r, \theta)| + \frac{1}{|\nabla v|} |\Delta_3(r, \theta)| + |\Delta_1(r, \theta)| |\Delta_3(r, \theta)| \\
&\sim A \lambda b'_{1\Delta} \frac{h}{|h'|^5} r^{\lambda+7} + A^2 \lambda^2 b'_{2\Delta} \frac{h^2}{|h'|^5} r^{2\lambda+4} \rightarrow 0,
\end{aligned} \tag{C.71}$$

$$\begin{aligned}
|\Delta_r(r, \theta)| &\leq \left(\frac{|Q_r|}{2|\nabla v|^2} + \left| \frac{Q|\nabla v|_r}{|\nabla v|^3} \right| \right) |\Delta_1| + \frac{|Q|}{2|\nabla v|^2} |\Delta_{1r}| \\
&\quad + \left| \frac{|\nabla v|_r}{|\nabla v|^2} \right| |\Delta_3| + \frac{|\Delta_{3r}|}{|\nabla v|} + |\Delta_{1r}| |\Delta_3| + |\Delta_1| |\Delta_{3r}| \\
&\sim A \lambda b'_{1\Delta_r} \frac{h}{|h'|^5} r^{\lambda+6} + A^2 \lambda^2 b'_{2\Delta_r} \frac{h^2}{|h'|^5} r^{2\lambda+3} \rightarrow 0,
\end{aligned} \tag{C.72}$$

$$\begin{aligned}
|\Delta_\theta(r, \theta)| &\leq \left(\frac{|Q_\theta|}{2|\nabla v|^2} + \left| \frac{Q|\nabla v|_\theta}{|\nabla v|^3} \right| \right) |\Delta_1| + \frac{|Q|}{2|\nabla v|^2} |\Delta_{1\theta}| \\
&\quad + \left| \frac{|\nabla v|_\theta}{|\nabla v|^2} \right| |\Delta_3| + \frac{|\Delta_{3\theta}|}{|\nabla v|} + |\Delta_{1\theta}| |\Delta_3| + |\Delta_1| |\Delta_{3\theta}| \\
&\sim A \lambda b'_{1\Delta_\theta} \left(\frac{1}{|h'|^4} + \frac{h''h}{|h'|^6} \right) r^{\lambda+7} + A^2 \lambda^2 b'_{2\Delta_\theta} \frac{h^2 h''}{|h'|^6} r^{2\lambda+4} \rightarrow 0
\end{aligned} \tag{C.73}$$

for some λ dependent $b'_{1\Delta}, b'_{2\Delta}, b'_{1\Delta_r}, b'_{2\Delta_r}, b'_{1\Delta_\theta}$ and $b'_{2\Delta_\theta} > 0$. Thus, estimates in (C.68), (C.69) and (C.70) are all valid in this case.

Using the results from Lemma 36 - Lemma 39, (C.12) becomes

$$Nw = Nv + \frac{1}{r} \left\{ \left[\frac{A\lambda q(\theta)r^\lambda}{(1 + |\nabla v|^2)^{1/2}} \right]_r + \left[\frac{Aq'(\theta)r^{\lambda-1}}{(1 + |\nabla v|^2)^{1/2}} \right]_\theta \right\} \\ - \frac{1}{2r} \left\{ \left[(rv_r + A\lambda q(\theta)r^\lambda) \frac{Q}{|\nabla v|^3} \right]_r + \left[\left(\frac{1}{r}v_\theta + Aq'(\theta)r^{\lambda-1} \right) \frac{Q}{|\nabla v|^3} \right]_\theta \right\} + \xi_1,$$

where

$$\xi_1 = \frac{1}{r} \left\{ \left[(rv_r + A\lambda q(\theta)r^\lambda) \Delta(r, \theta) \right]_r + \left[\left(\frac{1}{r}v_\theta + Aq'(\theta)r^{\lambda-1} \right) \Delta(r, \theta) \right]_\theta \right\}$$

and $\Delta(r, \theta)$ is defined in (C.61). In details,

$$\xi_1 = (hr^{-3} + A\lambda^2qr^{\lambda-2}) \Delta + (-hr^{-2} + A\lambda qr^{\lambda-1}) \Delta_r \\ + (h''r^{-3} + Aq''r^{\lambda-2}) \Delta + (h'r^{-3} + Aq'r^{\lambda-2}) \Delta_\theta.$$

$$\frac{1}{r} \left\{ \left[\frac{A\lambda q(\theta)r^\lambda}{(1 + |\nabla v|^2)^{1/2}} \right]_r + \left[\frac{Aq'(\theta)r^{\lambda-1}}{(1 + |\nabla v|^2)^{1/2}} \right]_\theta \right\} = A\lambda(\lambda + 2) (h^2 + h'^2)^{-1/2} q(\theta)r^\lambda \\ + A \left[(h^2 + h'^2)^{-1/2} q'(\theta) \right]_\theta r^\lambda + \xi_2,$$

where

$$\xi_2 = A\lambda^2qr^{\lambda-2}\Delta_1 + A\lambda qr^{\lambda-1}\Delta_{1r} + Aq''r^{\lambda-2}\Delta_1 + Aq'r^{\lambda-2}\Delta_{1\theta}.$$

$$-\frac{1}{2r} \left[(rv_r + A\lambda q(\theta)r^\lambda) \frac{Q}{|\nabla v|^3} \right]_r = -A\lambda(\lambda + 2)h^2 (h^2 + h'^2)^{-3/2} q(\theta)r^\lambda \\ + A(\lambda + 2)h'(\theta)h(\theta) (h^2 + h'^2)^{-3/2} q'(\theta)r^\lambda + \xi_3,$$

where

$$\begin{aligned}\xi_3 &= \frac{1}{2}(2\lambda + 3)A^2\lambda^2h (h^2 + h'^2)^{-3/2} q^2r^{2\lambda+1} + \frac{1}{2}(2\lambda + 3)A^2h (h^2 + h'^2)^{-3/2} (q')^2r^{2\lambda+1} \\ &+ (2\lambda + 3)A^2\lambda^2h (h^2 + h'^2)^{-3/2} q^2r^{2\lambda+1} - (2\lambda + 3)A^2\lambda h' (h^2 + h'^2)^{-3/2} qq'r^{2\lambda+1} \\ &- \frac{1}{2}(3\lambda + 4)A^3\lambda^3 (h^2 + h'^2)^{-3/2} q^3r^{3\lambda+2} - \frac{1}{2}(3\lambda + 4)A^3\lambda (h^2 + h'^2)^{-3/2} q(q')^2r^{3\lambda+2}.\end{aligned}$$

$$\begin{aligned}-\frac{1}{2r} \left[\left(\frac{1}{r}v_\theta + Aq'(\theta)r^{\lambda-1} \right) \frac{Q}{|\nabla v|^3} \right]_\theta &= A\lambda \left[h(\theta)h'(\theta) (h^2 + h'^2)^{-3/2} q(\theta) \right]_\theta r^\lambda \\ &- A \left[(h')^2 (h^2 + h'^2)^{-3/2} q'(\theta) \right]_\theta r^\lambda + \xi_4,\end{aligned}$$

where

$$\begin{aligned}\xi_4 &= -\frac{1}{2}A^2\lambda^2 \left[h' (h^2 + h'^2)^{-3/2} q^2 \right]_\theta r^{2\lambda+1} - \frac{1}{2}A^2 \left[h' (h^2 + h'^2)^{-3/2} (q')^2 \right]_\theta r^{2\lambda+1} \\ &+ A^2\lambda \left[h (h^2 + h'^2)^{-3/2} qq' \right]_\theta r^{2\lambda+1} - A^2 \left[h' (h^2 + h'^2)^{-3/2} (q')^2 \right]_\theta r^{2\lambda+1} \\ &- \frac{1}{2}A^3\lambda^2 \left[(h^2 + h'^2)^{-3/2} q^2q' \right]_\theta r^{3\lambda+2} - \frac{1}{2}A^3 \left[(h^2 + h'^2)^{-3/2} (q')^3 \right]_\theta r^{3\lambda+2}.\end{aligned}$$

Moreover,

(i) when $q(\theta) = \frac{1}{\bar{\kappa}h(\theta)} + \epsilon_0$, $\gamma \geq 0$, and h' , h'' are away from their singularities,

$$|\xi_1| \leq d_{1\xi_1}Ar^{\lambda+4} + d_{2\xi_1}A^2r^{2\lambda+1} \quad \text{and} \quad |\xi_2| \leq d_{\xi_2}Ar^{\lambda+4}, \quad (\text{C.74})$$

$$|\xi_3| \leq d_{\xi_3}A^2r^{2\lambda+1} \quad \text{and} \quad |\xi_4| \leq d_{\xi_4}A^2r^{2\lambda+1} \quad (\text{C.75})$$

for some λ dependent $d_{1\xi_1}, d_{2\xi_2}, d_{\xi_2}, d_{\xi_3}, d_{\xi_4} > 0$.

(ii) when $q(\theta) = \frac{1}{\bar{\kappa}h(\theta)} + \epsilon_0$, $\gamma = 0$, as $\theta \rightarrow \pm\alpha$, $\xi_1, \xi_2, \xi_3, \xi_4 \rightarrow 0$. Thus, in this case, the estimates in (C.74) and (C.75) are still valid.

(iii) when $q(\theta) = 1$, $\gamma \geq 0$, and h' , h'' are away from their singularities,

$$|\xi_1| \leq d'_{1\xi_1} A \lambda r^{\lambda+4} + d'_{2\xi_1} A^2 \lambda^2 r^{2\lambda+1} \quad \text{and} \quad |\xi_2| \leq d'_{\xi_2} A \lambda r^{\lambda+4}, \quad (\text{C.76})$$

$$|\xi_3| \leq d'_{\xi_3} A^2 \lambda^2 r^{2\lambda+1} \quad \text{and} \quad |\xi_4| \leq d'_{\xi_4} A^2 \lambda^2 r^{2\lambda+1} \quad (\text{C.77})$$

for some λ dependent $d'_{1\xi_1}, d'_{2\xi_1}, d'_{\xi_2}, d'_{\xi_3}, d'_{\xi_4} > 0$.

(iv) when $q(\theta) = 1$, $\gamma = 0$, as $\theta \rightarrow \pm\alpha$, $\xi_1, \xi_2, \xi_3, \xi_4 \rightarrow 0$. Thus, in this case, the estimates in (C.76) and (C.77) are still valid.

Combining the above together, and replacing $\xi_1, \xi_2, \xi_3, \xi_4$ by η_1 and η_2 , when $q = \frac{1}{\bar{\kappa}h(\theta)} + \epsilon_0$, and with $\gamma \geq 0$, we have

$$Nw = Nv + P_1(\theta)r^\lambda + \eta_1 + \eta_2, \quad (\text{C.78})$$

where

$$P_1(\theta) = A\lambda(\lambda+2)(h')^2 (h^2 + h'^2)^{-3/2} q(\theta) + A(\lambda+2)h'(\theta)h(\theta) (h^2 + h'^2)^{-3/2} q'(\theta) \quad (\text{C.79})$$

$$+ A\lambda \left[h(\theta)h'(\theta) (h^2 + h'^2)^{-3/2} q(\theta) \right]_\theta + A \left[h^2 (h^2 + h'^2)^{-3/2} q'(\theta) \right]_\theta, \quad (\text{C.80})$$

and

$$|\eta_1| \leq d_{\eta_1} A r^{\lambda+4} \quad \text{and} \quad |\eta_2| \leq d_{\eta_2} A^2 r^{2\lambda+1} \quad (\text{C.81})$$

for some λ dependent $d_{\eta_1}, d_{\eta_2} > 0$. In addition, when $\gamma = 0$, as $\theta \rightarrow \pm\alpha$, $P_1(\theta) \rightarrow 0$, and $\eta_1, \eta_2 \rightarrow 0$. The estimates above are all still valid.

When $q(\theta) = 1$ and with $\gamma \geq 0$, following a similar calculation as above, we obtain

$$Nw = Nv + P_1(\theta)r^\lambda + \eta_1, +\eta_2, \quad (\text{C.82})$$

where

$$P_1(\theta) = A\lambda(\lambda + 2)(h')^2 (h^2 + h'^2)^{-3/2} + A\lambda \left[h(\theta)h'(\theta) (h^2 + h'^2)^{-3/2} \right]_{\theta}, \quad (\text{C.83})$$

hence, there exists some constant $c_{P_1} > 0$,

$$|P_1(\theta)r^\lambda| \leq c_{P_1}A\lambda r^\lambda. \quad (\text{C.84})$$

and

$$|\eta_1| \leq d'_{\eta_1}A\lambda r^{\lambda+4} \quad \text{and} \quad |\eta_2| \leq d'_{\eta_2}A^2\lambda^2 r^{2\lambda+1} \quad (\text{C.85})$$

for some λ dependent $d'_{\eta_1}, d'_{\eta_2} > 0$. In addition, when $\gamma = 0$, as $\theta \rightarrow \pm\alpha$, $P_1(\theta) \rightarrow 0$, and $\eta_1, \eta_2 \rightarrow 0$. The estimates above are all still valid.

The results we obtained in (C.78) - (C.85) are consistent with Miersemann's [45, 46].

C.3 Computation of $\nu \cdot Tw$ on the Boundary Σ_{r_0} , where $w(r, \theta) = v(r, \theta) + Aq(\theta)r^\lambda$

In this section, we present the detailed calculation of the expansion of $\nu \cdot Tw$, where $w(r, \theta)$ has form $w(r, \theta) = v(r, \theta) + Aq(\theta)r^\lambda$ on the wall (boundary) Σ_{r_0} with small $r_0 > 0$ and the contact angle $\gamma \geq 0$, ν denotes the outward normal of Σ_{r_0} . Two cases will be discussed with different assumptions imposed, respectively.

- (1) When $q(\theta) = \frac{1}{\bar{\kappa}h(\theta)} + \epsilon_0$, for some small $\epsilon_0 > 0$, we assume $Ar^{\lambda+1} \ll 1$, $A > 0$ and $\lambda \geq 1$.
- (2) When $q(\theta) = 1$, we assume $0 < A\lambda \leq K_0$ for some $K_0 > 0$ and require $A > 0$, $0 < \lambda < 1$ (λ is sufficiently small).

We consider the $\theta = \alpha$ case (similar for the $\theta = -\alpha$ case with only a sign difference), and have

$$\nu \cdot Tw = \frac{\frac{1}{r}w_\theta}{\sqrt{1 + |\nabla w|^2}} \quad \text{at } \theta = \alpha, \quad (\text{C.86})$$

Next, we expand $\nu \cdot Tw$ at $\theta = \alpha$ for different choices of $q(\theta)$. Using the results from Lemma 36 - Lemma 39 in Appendix C.2, (C.86) turns into

$$\begin{aligned}\nu \cdot Tw &= \frac{\frac{1}{r}v_\theta + Aq'(\theta)r^{\lambda-1}}{(1 + |\nabla v|^2)^{1/2}} \left(1 + \frac{Q}{1 + |\nabla v|^2}\right)^{-1/2} \\ &= \frac{\frac{1}{r}v_\theta + Aq'(\theta)r^{\lambda-1}}{(1 + |\nabla v|^2)^{1/2}} - \left(\frac{1}{r}v_\theta + Aq'(\theta)r^{\lambda-1}\right) \frac{Q}{2|\nabla v|^3} + \hat{\xi}_1\end{aligned}$$

where

$$\hat{\xi}_1 = \left(\frac{1}{r}v_\theta + Aq'(\theta)r^{\lambda-1}\right) \Delta(r, \theta).$$

In details,

$$\frac{\frac{1}{r}v_\theta + Aq'(\theta)r^{\lambda-1}}{(1 + |\nabla v|^2)^{1/2}} = \frac{\frac{1}{r}v_\theta}{(1 + |\nabla v|^2)^{1/2}} + A(h^2 + h'^2)^{-1/2} q'(\theta)r^{\lambda+1} + \hat{\xi}_2,$$

where $\hat{\xi}_2 = Aq'r^{\lambda-1}\Delta_1(r, \theta)$, and $\Delta_1(r, \theta)$ is defined in Lemma 36 in Appendix C.2.

$$\begin{aligned}- \left(\frac{1}{r}v_\theta + Aq'(\theta)r^{\lambda-1}\right) \frac{Q}{2|\nabla v|^3} &= A\lambda h(\theta)h'(\theta) (h^2 + h'^2)^{-3/2} q(\theta)r^{\lambda+1} \\ &\quad - A(h')^2 (h^2 + h'^2)^{-3/2} q'(\theta)r^{\lambda+1} + \hat{\xi}_3,\end{aligned}$$

where

$$\begin{aligned}\hat{\xi}_3 &= -\frac{1}{2}A^2\lambda^2h'(\theta) (h^2 + h'^2)^{-3/2} q^2r^{2\lambda+2} - \frac{1}{2}A^2h'(\theta) (h^2 + h'^2)^{-3/2} (q')^2r^{2\lambda+2} \\ &\quad + A^2\lambda h (h^2 + h'^2)^{-3/2} qq'r^{2\lambda+2} - A^2h' (h^2 + h'^2)^{-3/2} (q')^2r^{2\lambda+2} \\ &\quad - \frac{1}{2}A^3\lambda^2 (h^2 + h'^2)^{-3/2} q'q^2r^{3\lambda+3} - \frac{1}{2}A^3 (h^2 + h'^2)^{-3/2} (q')^3r^{3\lambda+3}.\end{aligned}$$

Moreover,

(i) when $q = \frac{1}{\bar{\kappa}h(\theta)} + \epsilon_0$, with $\gamma > 0$, at $\theta = \alpha$, we have

$$|\hat{\xi}_1| \leq d_{1\hat{\xi}_1} Ar^{\lambda+5} + d_{2\hat{\xi}_1} A^2 r^{2\lambda+2}, \quad |\hat{\xi}_2| \leq d_{\hat{\xi}_2} Ar^{\lambda+5}, \quad \text{and} \quad |\hat{\xi}_3| \leq d_{\hat{\xi}_3} A^2 r^{2\lambda+2}$$

for some λ dependent $d_{1\hat{\xi}_1}, d_{2\hat{\xi}_1}, d_{\hat{\xi}_2}, d_{\hat{\xi}_3} > 0$.

(ii) when $q = 1$, with $\gamma > 0$, at $\theta = \alpha$, we have

$$|\hat{\xi}_1| \leq d'_{1\hat{\xi}_1} A \lambda r^{\lambda+5} + d'_{2\hat{\xi}_1} A^2 \lambda^2 r^{2\lambda+2}, \quad \hat{\xi}_2 = 0, \quad \text{and} \quad |\hat{\xi}_3| \leq d'_{\hat{\xi}_3} A^2 \lambda^2 r^{2\lambda+2}$$

for some λ dependent $d'_{1\hat{\xi}_1}, d'_{2\hat{\xi}_1}, d'_{\hat{\xi}_3} > 0$.

After the simplification, replacing $\hat{\xi}_1, \hat{\xi}_2, \hat{\xi}_3$ by $\hat{\eta}_1$ and $\hat{\eta}_2$, in the $q = \frac{1}{\bar{\kappa}h(\theta)} + \epsilon_0$ case, with $\gamma > 0$, we have

$$\nu \cdot Tw = \frac{\frac{1}{r} w_\theta}{(1 + |\nabla w|^2)^{1/2}} = \nu \cdot Tv + G_1(\theta) r^{\lambda+1} + \hat{\eta}_1 + \hat{\eta}_2,$$

where

$$G_1(\theta) = A \lambda h(\theta) h'(\theta) (h^2 + h'^2)^{-3/2} q(\theta) + A h^2 (h^2 + h'^2)^{-3/2} q'(\theta),$$

hence, there exists some constant $c_{G_1} > 0$ at $\theta = \alpha$ and

$$|\hat{\eta}_1| \leq d_{\hat{\eta}_1} Ar^{\lambda+5} \quad \text{and} \quad |\hat{\eta}_2| \leq d_{\hat{\eta}_1} A^2 r^{2\lambda+2}$$

for some λ dependent $d_{\hat{\eta}_1}, d_{\hat{\eta}_2} > 0$. In addition, when $\gamma = 0$, as $\theta \rightarrow \alpha$, $G_1(\theta) \rightarrow 0$, and $\hat{\eta}_1, \hat{\eta}_2 \rightarrow 0$. So, $\nu \cdot Tw = \nu \cdot Tv = 1$, the contact angle condition is met exactly.

When $q(\theta) = 1$, with $\gamma > 0$, following a similar calculation as above, we obtain

$$\nu \cdot Tw = \nu \cdot Tv + G_1(\theta) r^{\lambda+1} + \hat{\eta}_1 + \hat{\eta}_2,$$

where

$$G_1(\theta) = A\lambda h(\theta)h'(\theta) (h^2 + h'^2)^{-3/2}.$$

From Property 6, if $\gamma > 0$, there exists some constant $c_{G_1} > 0$ such that

$$G_1 \geq c_{G_1} \quad \text{at } \theta = \alpha. \tag{C.87}$$

And

$$|\hat{\eta}_1| \leq d'_{\hat{\eta}_1} A\lambda r^{\lambda+5} \quad \text{and} \quad |\hat{\eta}_2| \leq d'_{\hat{\eta}_2} A^2 \lambda^2 r^{2\lambda+2}$$

for some λ dependent $d'_{\hat{\eta}_1}, d'_{\hat{\eta}_2} > 0$. In addition, when $\gamma = 0$, at $\theta = \pm\alpha$, $G_1(\theta) \rightarrow 0$, and $\hat{\eta}_1, \hat{\eta}_2 \rightarrow 0$. $\nu \cdot Tw = \nu \cdot Tv = 1$, the contact angle condition is met exactly.